



UNIVERSITY *of the*
WESTERN CAPE

Effluent water treatment utilising a combination of hydrodynamic-shear and flotation technology for the specific application of wastewater from the oil and gas industry.

by

Bradley Robert Cerff

**A thesis submitted in fulfilment of the requirements for the degree of
Doctor of Philosophy in Chemistry, Faculty of Natural Sciences,
University of the Western Cape.**

Supervisor: Prof. Bernard Bladergroen

November 2022

Abstract

Water plays an important role in the petrochemical production and refining processes. The wastewaters released by these processes are often rich in petroleum pollutants, that requires significant treatment prior to disposal. Of particular importance is the processing of oil in water (o/w) emulsions. The processing and treatment of oil emulsions is focussed on breaking the emulsion and separation into the aqueous and oil phases for further appropriate disposal. The general approach is to optimise the processing to achieve relatively clean water, that can be recycled or discharged into the environment, whereas the oil is disposed of or recycled appropriately. The use of chemical coagulants and flocculants results in the degradation of the oil phase forming sludges as well as toxicity issues when using aluminium based coagulants.

This research investigates the use of hydrodynamic shear with air flotation, without the use of coagulants and flocculants to destabilise and separate laboratory prepared stable o/w emulsions. The phenomenon whereby the hydrophobic nature of air is likely facilitating oil to oil droplet aggregation, specifically in a high shear environment, was researched. Previous studies have demonstrated the impact of the application of shear and air flotation on o/w emulsions, however to date very little research has been done to evaluate the overall efficiencies of such processes. The focus of the research is aimed at demonstrating flotation treatment techniques that are effective in processing stable o/w emulsions utilising shear with the minimum use of chemicals, such as coagulants. A hybrid technology solution utilising shear flocculation and flotation is proposed as a practical and efficient method to treat and process stable prepared o/w emulsions.

The hydrodynamic shear is achieved through high energy mixing utilising a high-speed homogeniser. Stable surfactant and emulsifier free o/w emulsions were prepared utilising olive oil and two grades of Sasol lubricating engine oils, with chemical oxygen demand (COD) of between 411 to 1572 mg/L. The study is limited to the processing of surfactant and emulsifier free oil in water emulsions utilising shear and two specific flotation techniques, namely IAF and DAF.

A laboratory scale induced air flotation (IAF) cell was assembled with a shear mixer and a pilot scale dissolved air flotation (DAF) unit was designed and fabricated with a shear mixer integrated into the DAF unit. Turbidity, zeta (ζ) potential, electrical conductivity, droplet size

distribution (DSD) and COD, were measured pre and post emulsion treatment, to determine the overall effect of IAF and DAF on the emulsion stability.

For both the IAF and DAF systems micro bubbles were observed, that contributed to the overall effectiveness of the flotation process. For the IAF system, without the addition of any chemical coagulants, a treatment efficiency (the efficiency of oil removal from the o/w emulsion) from the emulsion ranging from 16.7% to 59.1% was observed, dependent on the respective oil used in the o/w emulsions. For the DAF system, using only one type of oil in a shear treatment, an efficiency of 46.5% was obtained. Using the same oil, DAF with chemical coagulation resulted in a maximum treatment efficiency of 69.8%.

It is evident that subjecting an emulsion to appropriate levels of hydrodynamic shear can induce the process of shear flocculation, that in turn leads to oil droplet coalescence and the destabilisation of the o/w emulsion. The destabilised emulsion when subjected to flotation results in a practical and efficient method to process and separate an o/w emulsion into aqueous and oil phases. In the DAF treatment experiments, the oil phase was analysed utilising a fatty acid methyl ester (FAMES) profile to assess the degree of oil degradation in the treated o/w emulsion samples. The oily sludge collected from the treatment of DAF with shear had the least degradation, with a FAMES profile result of 12.87 g/100 g of sample, whereas DAF utilising coagulants had more degradation with a FAMES profile result of 5.68 g/100 g of sample.

The overall treatment efficiencies for shear with flotation without coagulation and flocculation are lower than that for the proven technologies of flotation and coagulation, however the IAF and DAF systems with shear produced results that demonstrate flotation with shear is a viably beneficial process for the separation and processing of o/w emulsions without the use of hazardous chemicals.

Keywords

Oil-in-water emulsion

Oily wastewater

Emulsion

Emulsion separation

Emulsion processing

Demulsification

Coagulation

Flocculation

Shear separation

Shear flocculation

Emulsion stability

Flotation

Air flotation



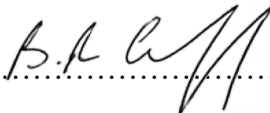
Declaration

I declare that, “**Effluent water treatment utilising a combination of hydrodynamic-shear and flotation technology for the specific application of wastewater from the oil and gas industry.**”, is my own work, it has not been submitted for any degree or examination at any other academic institution and that all the resources that have been quoted and used have been indicated and acknowledged by means of complete references.

Bradley Robert Cerff

November 2022

Signed:



Acknowledgements

I would like to thank the staff and my colleagues at the South African Institute for Advanced Materials Chemistry (SAIAMC) and the Faculty of Science of the University of the Western Cape for giving me this opportunity to develop this research project.

Sincere gratitude and appreciation to my supervisor, Prof Bernard Bladergroen, for his constant support, guidance and mentorship. Thank you so much for being so generous with your time and knowledge. This project and the resulting research would not have been a success without your direction.

Thank you to Mr Pieter Jansen and the staff of Abrimix for giving technical guidance, practical experience and assistance with on the ground solutions related to flotation technology. Thank you to SASOL for funding the project through the Sasol University Collaboration program and a special thank you to Dr Sitabule for his guidance on the suitability of this technology for industrial applications.

In particular, I would like to acknowledge and thank Prof David Key for his years of academic guidance, the insightful discussions, his many valued inputs, data interpretations and the scrutiny of results throughout this research process. Poor is the pupil who does not surpass his master.

To Mr David Vlotman, thank you very much for being available to listen to new ideas, for sharing your knowledge as well as providing input and guidance when I needed it most.

I am also thankful to Dr Stanford Chidziva and Mr Yaseen Arend for all their assistance in making sure the laboratory work could be completed accordingly. Thank you to Mr Kader Pool for his valued assistance with the planning, design and fabrication of the high shear and dissolved air flotation system. A special thank you to Prof Vladimir Linkov and Prof Sivakumar Pasupathi for giving their time and valuable academic assistance when available.

To Mr Darrin Arendse, thank you for the time and years of friendship. Our time spent to discuss work, life and spiritual matters has been a source of much reflection, inspiration as well as motivation to pursue the extraordinary and journey the road less travelled.

As special acknowledgement and recognition to my entire family for the love, care, prayers, and support throughout this process.

To a special friend, Dr Carl J. Firmin, who passed away suddenly during the final stages and completion of this thesis. You were an unbelievable friend that inspired this journey and walk with me to complete this work, thank you.

I owe a debt of gratitude to my parents, who have sacrificed and put aside their comforts for the sake of my education and overall wellbeing. Robert and Denise, your constant love, discipline and belief in traditional values have made boys the men they are today. To my brother, Andre thank you for the support and understanding that the pursuit of knowledge and education is a defining moment.

To my children, Jenna, Chelsea and Nina, who always believed that I can accomplish whatever I set out to do.

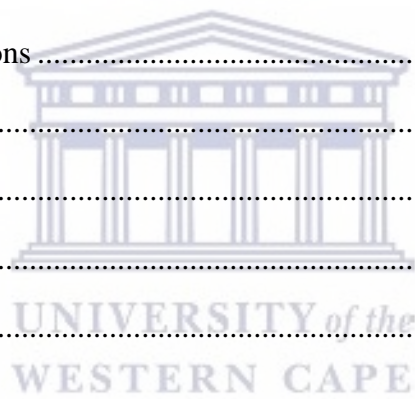
I am thankful for an incredible support system and my deepest gratitude to my wife, Cindy Lee, for her patience, for sacrificing her time to listen to me when no else would and who always encouraged me through this journey.

Thank God for his gifts and blessings granted to me that words can't describe. Blessings come in different ways and often missed. To those I missed and forgot to thank, it is for you that I pray a special prayer and I pray that God will bless you as much as you've blessed me.

Table of Contents

Abstract.....	i
Keywords	iii
Declaration.....	iv
Acknowledgements.....	v
Table of Contents.....	vii
List of Figures	xiii
List of Tables	xvii
List of Equations	xviii
List of Abbreviations	xix
List of Symbols.....	xxii
Research Output.....	xxiii
Chapter 1 Background and Introduction.....	1
1.1. Introduction.....	1
1.2. Problem statement.....	6
1.3. Purpose of the study.....	9
1.4. Thesis statement.....	9
1.5. Research questions.....	10
1.6. Aims and objectives.....	10
1.7. Thesis Delimitation.....	11
1.8. Significance of the Study	12
1.9. Thesis structure	13
Chapter 2 Literature Review	15
2.1. Use of relevant databases.....	15

2.2. Oil contamination in water.....	17
2.2.1. Free oil	17
2.2.2. Dispersed oil	17
2.2.3. Emulsified oil.....	18
2.2.4. Dissolved oil	18
2.3. Oily wastewater processing	18
2.4. Emulsion properties and parameters	21
2.4.1. Origin of charge on emulsion droplets.....	25
2.4.2. Rheology	26
2.4.3. Droplet size distribution.....	27
2.4.4. Zeta Potential	28
2.5. Emulsion droplet interactions	31
2.5.1. Flocculation.....	32
2.5.2. Creaming.....	33
2.5.3. Sedimentation	33
2.5.4. Phase inversion	33
2.5.5. Ostwald ripening.....	34
2.5.6. Coalescence.....	34
2.6. Forces related to droplet interactions	36
2.6.1. Van der Waals Interaction	37
2.6.2. Electrostatic Interaction	37
2.6.3. DLVO model	40
2.6.4. Non-DLVO Model.....	41
2.6.4.1. Non-DLVO forces resulting from polymer addition	42
2.6.4.2. Depletion attraction.....	43
2.6.4.3. Steric repulsion	44
2.6.5. Pickering emulsions	44



2.7. Principles of emulsion processing	45
2.7.1. Coagulation	47
2.7.1.1. Coagulation mechanisms	47
2.7.1.2. Chemical coagulation.....	49
2.7.1.3. Electrocoagulation	53
2.7.2. Flocculation as a process	55
2.7.3. Hybrid methods of oil separation.....	57
2.7.4. Coagulation / flocculation.....	58
2.7.5. Coagulation / flocculation / flotation	59
2.7.6. Flotation systems	63
2.7.6.1. Induced gas flotation.....	65
2.7.6.2. Dissolved gas flotation.....	66
2.7.6.3. Electroflotation	70
2.7.7. Shear flocculation flotation.....	72
2.7.7.1. Hydrodynamic shear	73
2.7.7.2. The effect of shear on emulsions	75
2.7.7.3. Reynolds number	78
2.7.7.4. Shear induced flocculation and flotation	78
 Chapter 3 Experimental Detail.....	 80
3.1. Chemicals and Materials.....	80
3.2. Experimental Design.....	80
3.2.1. Preparation of emulsions.....	82
3.2.2. Preparation of 0.0035 M Na ₂ CO ₃ dilution solution	83
3.2.3. Preparation of 0.01 M HCl dilution solution	83
3.2.4. Preparation of alum solution.....	83
3.2.5. Preparation of emulsion aliquots for analysis	83

3.2.6. Laboratory scale IAF experiments	84
3.2.6.1. Calculation of Reynolds number	85
3.2.6.2. Experimental settings for the laboratory scale IAF setup	87
3.2.6.3. Analysis of emulsions.	88
3.2.7. Hybrid DAF shear wastewater treatment unit	89
3.2.7.1. Preparation of emulsion for DAF shear unit.....	95
3.2.7.2. Coagulation test of emulsions	96
3.2.7.3. DAF with shear unit experimental procedure	97
3.2.7.4. Emulsions treated with DAF with coagulation.....	99
3.2.7.5. Emulsions treated with DAF with shear	99
3.2.7.6. Emulsions treated by DAF with coagulation and shear	100
3.2.7.7. Emulsions treated with DAF without coagulation and shear.....	100
3.2.8. Emulsion analysis and characterisation	100
3.2.8.1. Visual character	100
3.2.8.2. Microscopy	101
3.2.8.3. Turbidity	102
3.2.8.4. Bubble size analysis.....	103
3.2.8.5. Droplet size distribution (DSD)	104
3.2.8.6. Chemical Oxygen Demand	104
3.2.8.6.1. COD sample preparation.....	105
3.2.8.6.2. COD sample digestion and measurements	105
3.2.8.7. pH.....	106
3.2.8.8. Electrical conductivity	106
3.2.8.9. Zeta potential	110
Chapter 4 Results and Discussion.....	111
4.1. Analysis.....	111

4.2. Calculation of theoretical COD of prepared emulsions	112
4.2.1. Theoretical COD of olive oil emulsion.....	112
4.2.2. Theoretical COD of Sasol lubricating engine oil emulsions	113
4.2.3. Sasol lubricating engine multigrade oil	113
4.2.4. Sasol lubricating monograde engine oil.....	114
4.3. IAF shear experiments	116
4.3.1. Bubble sizes analyses of IAF shear experiments.....	116
4.3.2. Visual comparison of treatment on pure water	121
4.3.3. Properties of prepared emulsions prior to treatment.....	121
4.3.4. Emulsions exposed to shear	122
4.3.5. Effect of treatment on zeta potential	123
4.3.6. Effects of treatment on DSD.....	124
4.3.7. Effect of treatment on conductivity	130
4.3.8. Effect of treatment on turbidity.....	133
4.3.9. Effects of treatments on COD.....	135
4.4. Coagulation - jar test results	137
4.5. Experiment using DAF combined with and without coagulation and shear	140
4.5.1. DAF Bubble size analysis.....	141
4.5.2. Properties of emulsions prior to treatment.....	144
4.5.3. Effects of DAF treatment on conductivity.....	146
4.5.4. Effects of DAF treatment on zeta potential	147
4.5.5. Effects of DAF treatment on turbidity	148
4.5.6. Effects of DAF treatment on COD	149
4.6. Analysis of free and treated oil post the DAF treatments	151
Chapter 5 Conclusions	154
5.1. Overview.....	154

5.2. Laboratory scale IAF treatments.....	155
5.3. DAF treatment	156
Chapter 6 Future Work	158
References.....	159
Chapter 7 Annexures.....	191
A1. DAF shear system description	191
A2. DAF shear system start up procedure	195
A3. DAF unit emergency shut down procedure	198
B. DAF shear system tank sizes and volumes	200



List of Figures

Figure 1.1. Historical global primary energy source with projection to 2040. Adapted from [34].	3
Figure 1.2. Droplet size distributions of tight, medium and loose emulsions. Adapted from [54,83].	5
Figure 1.3. The effect of shear on emulsion droplets.	5
Figure 1.4. Forms of oil in wastewater and potential processing techniques.	7
Figure 2.1. Graphical depiction of various types of emulsions. Adapted from [78].	24
Figure 2.2. A plot of the ζ potential of a sample measured as a function of pH.	30
Figure 2.3. Diagrammatic representation of the oil in water emulsion separation process. Adapted from [78].	32
Figure 2.4. Process of Ostwald ripening. Adapted from [239].	34
Figure 2.5. Process of droplet flocculation and coalescence for droplets in a o/w emulsion. Adapted from [176].	35
Figure 2.6. Schematic representation of the Electrostatic and Van der Waals forces. Adapted from [228].	36
Figure 2.7. Diagrammatic representation of the electrical double layer. Adapted from [232].	38
Figure 2.8. Energy interaction for stable dispersions as per the classical DLVO theory. Adapted from [228].	40
Figure 2.9. Forms of non-DVLO forces developed through the addition of polymers.	43
Figure 2.10. Process of droplet approach and coalescence. Adapted from [120].	46
Figure 2.11. Schematic representation of the mechanisms of charge neutralisation and micro floc formation during coagulation in a colloidal suspension.	48
Figure 2.12. Schematic representation of the mechanisms of charge neutralisation and micro floc formation during coagulation in a colloidal suspension.	52
Figure 2.13. Schematic representation of polymer bridging flocculation.	56
Figure 2.14. Schematic representation of charge patch flocculation.	56
Figure 2.15. Wastewater treatment utilising DAF with coagulation and flocculation as pretreatment.	59
Figure 2.16. Schematic representation of the interaction of hydrophobic and hydrophilic particles with gas bubbles.	63
Figure 2.17. Graphical depiction of a mechanical IGF system. Adapted from [354].	66

Figure 2.18. Graphical depiction of a DGF system utilising air. Adapted from [379].	67
Figure 2.19. Schematic representation of shear forces in a fluid. Adapted from [396].	74
Figure 2.20. Schematic representation of a rotor stator mechanism for droplet break.	74
Figure 3.1. Experimental design for the IAF hybrid system.	81
Figure 3.2. Experimental design for the DAF hybrid system.	81
Figure 3.3. High-speed homogeniser emulsifying mixer and small hole rotor stator.	82
Figure 3.4. Specially designed and configured shear induced air flotation setup.	84
Figure 3.5. Position of rotor stator in the glass beaker.	85
Figure 3.6. Graphical depiction and assembly of the rotor stator unit of the high-speed homogeniser emulsifying mixer.	86
Figure 3.7. P&ID diagram for the DAF shear wastewater treatment system.	89
Figure 3.8. Hybrid DAF shear unit.	90
Figure 3.9. Top view of the hybrid DAF shear unit.	91
Figure 3.10. Photograph of the hybrid DAF shear unit wastewater system.	92
Figure 3.11. Photograph of the hybrid DAF shear unit, highlighting the floc tanks and the DAF flotation tank unit.	92
Figure 3.12. Photograph of the hybrid DAF shear unit, highlighting the control panel, bumble pump generator, shear unit.	93
Figure 3.13. Photograph of the hybrid DAF shear unit control panel.	93
Figure 3.14. Shear unit assembly attached to an electric motor with a drive belt.	94
Figure 3.15. Internal structure of the shear unit assembly.	94
Figure 3.16. Photo of the DAF shear unit.	95
Figure 3.17. Photograph of the VELP Scientific jar test apparatus utilised for the jar tests.	96
Figure 3.18. COD digester oven and AQ3140 COD colorimeter utilised for the COD measurements.	106
Figure 3.19. Set up of the conductivity instrument and probe during conductivity measurements of the emulsions pre and post treatment.	108
Figure 3.20. Set up of the conductivity instrument and probe during conductivity measurements of the emulsions pre and post treatment.	109
Figure 4.1. Examples of molecule structures of typical hydrocarbon molecules present in lubricating base oils: (a) paraffin (C ₁₅ H ₃₂); (b) branched paraffin (C ₂₀ H ₄₂); (c) naphthenic (C ₁₆ H ₃₂); (d) aromatic (C ₁₄ H ₂₂). Adapted from [455].	113

Figure 4.2. (A) olive oil and water mixture prior to emulsification process. (B) Olive oil emulsion highlighting free oil layer.	115
Figure 4.3. (A) Sasol multigrade oil and water mixture prior to emulsification process. (B) Sasol multigrade oil emulsion highlighting free oil layer.	116
Figure 4.4. Picture of the bubble swarm generated in pure water during the IAF process.	117
Figure 4.5. Picture of the area of interest below the rotor stator selected for bubble analysis.	118
Figure 4.6. Area of interest enhanced by the ImageJ software to highlight the bubbles in pure water during the IAF process, bubbles are white in colour with the water matrix in black.	118
Figure 4.7. Area of interest enhanced by the ImageJ software to highlight the bubbles in pure water during the IAF process, the bubbles and bubble groups are represented as areas with black outlines with the bubble counts in red.	119
Figure 4.8. Histogram of bubble sizes identified within the area of interest for pure water.	119
Figure 4.9. Histogram of bubble sizes identified within the area of interest for an olive oil o/w emulsion.	120
Figure 4.10. Visual comparison of the treatments on pure water, with (A) picture showing the result of air through the water, (B) picture showing the result of hydrodynamic shear, and (C) picture showing the effect of air and hydrodynamic shear.	121
Figure 4.11. Plot of ζ potential as a function of rpm of emulsions.	122
Figure 4.12. Graph of ζ potential readings of emulsions pre and post treatments.	124
Figure 4.13. Graph of the DSD of the emulsions pre and post treatment.	125
Figure 4.14. DSD curve of a prepared stable olive oil o/w emulsion.	128
Figure 4.15. DSD curve of the olive oil o/w emulsion sparged with air.	129
Figure 4.16. DSD curve of the olive oil emulsion exposed to shear.	129
Figure 4.17. DSD curve of the olive oil emulsion sparged with air while exposed to shear.	130
Figure 4.18. Graph of conductivity measurements of the emulsions pre and post treatments.	132
Figure 4.19. Regression analysis plot of conductivity as a function of DSD measurements of the emulsions post treatments.	133

Figure 4.20. Graph of turbidity measurements of the emulsions pre and post treatments.	134
Figure 4.21. Graph of COD measurements of the emulsions pre and post treatments.	135
Figure 4.22. Plot of turbidity as a function of coagulant concentration of jar test results.	138
Figure 4.23. Plot of ζ potential as a function of coagulant concentration of jar test results.	139
Figure 4.24. Plot of conductivity as a function of coagulant concentration of the jar test results.	140
Figure 4.25. Picture of the bubble swarm generated in pure water during the DAF process.	141
Figure 4.26. Area of interest enhanced by the ImageJ software to highlight the bubbles in pure water during the DAF process, A) bubbles are represented in white with the water matrix in black, B) the bubbles are represented as circles with the bubble counts in red.	142
Figure 4.27. Histogram of bubble sizes identified within the area of interest for pure water in the DAF unit.	143
Figure 4.28. Histogram of bubble sizes identified within the area of interest for the olive oil o/w emulsion in the DAF unit	144
Figure 4.29. Graph of conductivity measurements of the emulsions pre and post the DAF treatments.	146
Figure 4.30. Graph of the ζ potential of the emulsions pre and post the DAF treatments.	147
Figure 4.31. Graph of the turbidity measurements of the emulsions pre and post DAF treatments.	148
Figure 4.32. Graph of COD measurements of the emulsions pre and post DAF treatment.	149
Figure 7.1. P&ID, highlighting the components of the modified DAF treatment unit.	191
Figure 7.2. P&ID, highlighting the components of the DAF shear integrated treatment unit highlighting the two units.	194

List of Tables

Table 2.1. Forms of oil in wastewater and potential processing techniques.	20
Table 2.2. Types of colloidal suspensions. Adapted from [179].	22
Table 2.3. Schematic representation of the electrical double layer. Adapted from [221].	29
Table 2.4. A comparison between IGF and DGF. Adapted from [16,62].	69
Table 3.1. Source and purity of chemicals used.	80
Table 3.2. Rotor stator dimensions.	86
Table 3.3. Calculated Reynolds numbers for the high-speed homogeniser emulsifying mixer with a simplified geometry and without air.	87
Table 3.4. Particulars of experiments conducted utilising the modified IAF system.	88
Table 4.1. Comparison of theoretically calculated COD of emulsions versus measured results.	115
Table 4.2. Properties of the prepared untreated emulsions.	122
Table 4.3. Percentage increase of the DSD for the various treatments from the untreated emulsion.	126
Table 4.4. Normalised percentage increase of the DSD for the various treatments.	127
Table 4.5. Conductivity measurements of the oils and prepared emulsions at 20 °C.	131
Table 4.6. Treatment efficiency percentage of treatments based on changes in turbidity.	134
Table 4.7. Treatment efficiency percentage of treatments based on COD.	136
Table 4.8. Jar test results of the prepared emulsions used in the DAF experiments.	138
Table 4.9. Parameters of the prepared olive oil emulsion samples prior to treatment used in the DAF experiments.	145
Table 4.10. Summary of the emulsion turbidity data utilised in the ANOVA analysis.	145
Table 4.11. One way ANOVA analysis results based on the turbidity.	145
Table 4.12. Treatment efficiency with DAF treatments on the olive oil emulsions. Treatment efficiency percentage of treatments based on COD.	150
Table 4.13. FAMES profile analysis of olive oil samples analysed by Microchem laboratories.	152
Table 4.14. Summary of the FAMES profile analysis of olive oil samples	152
Table 5.1. Summary of results obtained for the laboratory scale IAF treatments.	155
Table 7.1. DAF unit emergency shut down procedure.	198

List of Equations

$\Delta G = (\gamma A) - (T\Delta S),$	Equation 2.1	24
$v_s = 2gr^2(\rho_2 - \rho_1)/9\eta,$	Equation 2.2	26
$V_T = V_{vdw} + V_{elec}$	Equation 2.3	40
$w = (i \cdot t \cdot M) / (Z \cdot F),$	Equation 2.4	54
$2H_2O + 2e^- \rightarrow H_2(g) + 2OH^-(aq), E^\circ = -0.83V,$	Equation 2.5	54
$Al(s) \rightarrow Al(aq)^{3+} + 3e^-, E^\circ = 1.662V,$	Equation 2.6	54
$Al^{3+} + H_2O \rightarrow Al(OH)^{2+} + H^+,$	Equation 2.7	54
$Al(OH)^{2+} + H_2O \rightarrow Al(OH)_2^+ + H^+,$	Equation 2.8	54
$Al(OH)_2^+ + H_2O \rightarrow Al(OH)_3 + H^+$	Equation 2.9	54
$2H_2O(l) + 2e^- \rightarrow H_2(g) + 2OH^-(aq),$	Equation 2.10	71
$2H_2O(l) \rightarrow O_2(g) + 4H^+(aq) + 4e^-,$	Equation 2.11	71
$2H_2O(l) \rightarrow 2H_2(g) + O_2(g),$	Equation 2.12	71
$N_R = D^2\eta\rho/\mu,$	Equation 2.13	78
$\text{data value} = (\text{value} - \text{minimum}) / (\text{max} - \text{minimum}) * 100$	Equation 4.1	111
$\text{Treatment efficiency, (TE)} = (C_0 - C_{pt}) / C_0 * 100,$	Equation 4.2	111
$C_{88}H_{164}O_{10} + 124 O_2 \rightarrow 88 CO_2 + 82 H_2O,$	Equation 4.3	112
$C_{15}H_{42} + C_{16}H_{32} + 49.5 O_2 \rightarrow 31 CO_2 + 37 H_2O,$	Equation 4.4	114
$C_{20}H_{42} + C_{14}H_{22} + 50 O_2 \rightarrow 34 CO_2 + 32 H_2O,$	Equation 4.5	114

List of Abbreviations

A	amperes
alum	aluminium sulphate
ANOVA	analysis of variance
(aq)	aqueous phase
BTEX	benzene, toluene, ethyl-benzene and xylene
CC	chemical coagulation
cm	centimetre(s)
COD	chemical oxygen demand
DAF	dissolved air flotation
DGF	dissolved gas flotation
DLVO	Derjaguin, Landau, Verwey and Overbeek
DSD	Droplet size distribution
EC	Electrocoagulation
EDL	electrical double layer
EIA	energy information administration
FAMES	fatty acid methyl ester
g	gram(s)
(g)	gaseous phase
g/mol	grams per mole
GDP	gross domestic product
h	hour(s)
Hz	hertz
IAF	induced air flotation
IBC	intermediate bulk container
IEP	isoelectric point
IGF	induced gas flotation
(l)	liquid phase
L	litre(s)

L/h	litre(s) per hour
L/m	litres per minute
m	metre
M	Molarity
m ³	cubic metre
max	maximum
mg	milligram(s)
mg/L	milligram(s) per litre
min	minute
mins	minutes
mL	millilitre(s)
mm	millimetres
mol	mole
mV	millivolts
NPD	naphthalene, phenanthrene and dibenzothiophene
NTU	nephelometric turbidity unit
o/w	oil in water
o/w/o	oil in water in oil
P&ID	piping and instrumentation diagram
PAC	poly aluminium chloride
ppm	parts per million
rpm	revolutions per minute
s	second(s)
SAIAMC	South African Institute for Advance Material Chemistry
SPE	society of petroleum engineers
SS	suspended solids
SSF	shear separation flotation
TDS	total dissolved solids
TOC	total organic content
TSS	total suspended solids

US	United States
UWC	University of the Western Cape
vdW	van der Waals
w/o	water in oil
w/o/w	water in oil in water



List of Symbols

μ	micro
η	nano
μm	micro meter
$\mu\text{S/cm}$	microsiemens per centimetre
ηm	nano meter
ζ	zeta potential
%	percentage



Research Output

Patent Filed

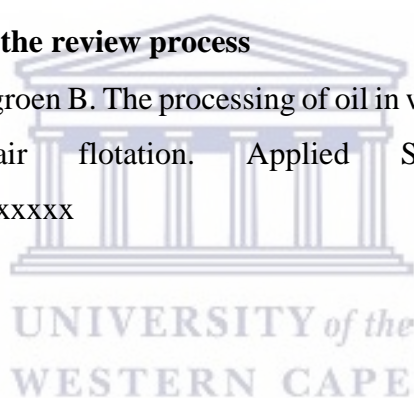
- **Cerff B**, Bladergroen B and Jansen P, Recovery of uncontaminated oils from emulsions based on mechanically induced flocculation of stable emulsions, 2022. Filed with the University of the Western Cape Technology Transfer Office, 15 November 2022. South African Provisional Patent Application No. 2022/12418

Publication

- **Cerff B**, Key D, Bladergroen B. A Review of the Processes Associated with the Removal of Oil in Water Pollution. *Sustainability*. 2021; 13(22):12339. <https://doi.org/10.3390/su132212339>

Publication submitted and in the review process

- **Cerff B**, Key D, Bladergroen B. The processing of oil in water emulsions utilizing shear flocculation and air flotation. *Applied Science*. 2022; 12, x. <https://doi.org/10.3390/xxxxx>



CHAPTER 1 BACKGROUND AND INTRODUCTION

This chapter provides background information on oil pollution and the contamination of water with specific reference to oil in water emulsions. It serves to introduce the topic of waste oil emulsions and their associated impacts on the environment and processing techniques. This chapter defines the problem statement, the research statement, research questions, aims and objectives following which, the research approach, delimitation and the thesis overview are described.

1.1. Introduction

Clean water is a necessity for life on earth. With the growth in the global human population and increased industrialisation in the last 100 years, clean fresh water has become one of the scarcest natural resources on the planet [1].

The contamination of water by oil is a chronic problem, caused by a number of industries, particularly from health, safety and environmental perspectives [1–3]. A small quantity of oil at very low concentrations can pollute a large quantity of water and significantly impact onshore and offshore environments [1–6].

Oil contaminated water, often referred to as oily wastewater, is generated in large quantities by a variety of industrial processes. [7–9]. Oily wastewater is produced by petroleum extraction and refining, food processing, printing, dyeing and many other industries [8,10–13]. Oil in water may be dispersed, emulsified or soluble in concentrations up to as much as 1000 mg/L [14–16]. The release of untreated oily wastewater into the environment, even at very low concentrations of oil contaminants, can affect the quality of groundwater, seawater, drinking or potable water and cause air pollution by the evaporation of volatile oil components into the atmosphere [1,2,4–6,17]. In some cases, the pollution may manifest itself many years after the initial discharge [2,18]. The chemical and physical properties of oily wastewater vary significantly and are a function of the industry and the associated processing parameters [18–20].

The petroleum industry is considered a water intensive sector, based on the high volumes of water used and wastewater produced in the extraction and refining processes [21]. The presence

of petroleum hydrocarbon contaminants in soil and water poses a substantial hazard to the environment [2,4–6].

In the upstream phase of the petroleum value chain, the production of oil and gas from hydrocarbon bearing formations in the earth, produce large quantities of water [22,23]. The water originating from underground geological formations, also referred to as formation water, is brought to the surface along with petroleum hydrocarbons during upstream production operations [6,24–26]. The extraction of unconventional petroleum resources, which include shale gas, coal bed methane and heavy oil are all associated with the use of large quantities of water [27–31].

The downstream phase of the petroleum value chain, includes petroleum refining where large quantities of water are utilised during distillation, thermal cracking, catalytic and treatment processes to generate refined products [6,17,32]. It is estimated that the refining process generates approximately 1.5 times the volume of wastewater for each barrel of crude oil processed [33].

On a global perspective, the United States (US), Energy Information Administration (EIA) reports, for the period from 1990 up to 2040, that the renewable sector will contribute the most to future growth in the energy sector, with some growth in natural gas, with little to no growth in conventional oil and coal sources [34]. **Error! Reference source not found.**, indicates that renewables will continue to grow, natural gas surpasses coal, while coal usage levels off by 2030. Petroleum and other liquid fuel maintain their its leading position and global market share into the foreseeable future [34].

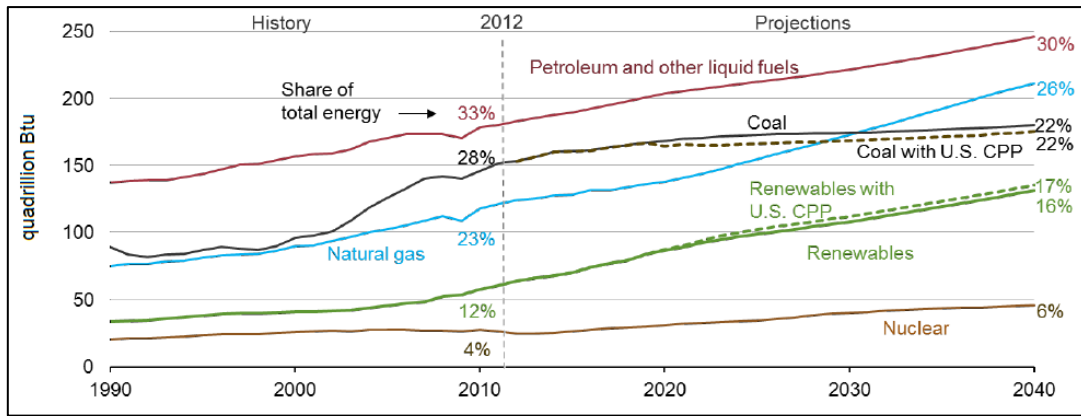


Figure 1.1. Historical global primary energy source with projection to 2040. Adapted from [34].

According to a number of reports, there is a clear relationship between real gross domestic product (GDP) growth and energy consumption [35–37]. It is evident that petroleum and other liquid fuel products play a significant role in the global economy currently and will remain very relevant into the future.

The use of petroleum products and the reliable supply of electricity are considered necessary requirements for economic and social development. With the forecasted increase in global economic development and the continued use of petroleum products, oil pollution will continue to be a major problem in the foreseeable future [1,24,38,39].

The contamination of water and soil with petroleum hydrocarbons is one of the most common environmental pollutants, arising either accidentally or operationally, wherever petroleum products are produced, transported, stored or used in industrial processes [5,39–41]. Wastewater containing petroleum pollutants poses a significant challenge for most industries as well as for conventional treatment plants, which often do not adequately process and remove the hazardous oil pollutants [1,2,21,33,42].

Various methods are used to process and remove oil pollution from water [7,22,43–45]. The methods can be categorised as chemical, electrochemical, physical, physiochemical and biological [41,46,47]. The processing techniques for the removal of oil emulsions have a number of associated problems, which include limited applicability, high cost, as well as oil degradation causing further contamination of the water from the resulting chemicals [48].

Of particular importance and interest is the treatment of dispersed oil and the associated emulsions generated by the petroleum and other industrial sectors [43,49,50]. Emulsified oil droplets of the order of a few micrometres in diameter are resistant to spontaneous coalescence into larger droplets. Oil emulsion separation by traditional techniques is a difficult time-consuming process as well as being energy intensive [51–54].

The conventional technologies for the treatment of oil in water contamination have several technology gaps in terms of applicability and efficiency. Of particular interest has been the use of flotation technology for the processing of oily wastewater [55–57]. The interaction of hydrophobic and hydrophilic colloidal particles with gas bubbles, is a method that has been developed and used for a number of decades in mineral processing operations to remove fine particles from a suspension [58–61]. It has been reported in the literature, that gas bubbles need to be smaller than the droplet or particle being floated out of solution, which results in a more efficient flotation process [62,63]. It has also been demonstrated by Lim *et al.* [64], that microbubbles in particular enhances separation of oil in water contamination as compared to larger bubbles. Therefore, the emphasis for emulsion processing has been on the destabilisation of the emulsion to allow for aggregation, flocculation and coalescence of droplets to make larger droplets in order to increase the efficiency of the flotation technology. There are a number of processes associated with destabilisation of emulsions, which result in the flocculation and coalescence of oil droplets, however one process that has caught the interest of a number of researchers is that of shear induced flocculation [65–67].

According to literature reports, Warren in 1975 first reported the aggregation of fine particles of scheelite with the application of shear energy [68–70]. The formation of aggregates under shear conditions is commonly referred to as shear flocculation [69–73]. Shear flocculation is the aggregation of fine particles by an appropriate shearing regime. For an emulsion, too much shear has a negative impact on the separation efficiency and results in smaller droplets being formed, generating a tighter emulsion with high kinetic stability [74–79].

Emulsions can be classified based on their degree of kinetic stability which is a function of the droplet size distribution (DSD) as per the following categories [54,80–82]:

- Loose emulsions are those that separate in a few minutes (mins).

- Medium emulsions, these will separate in hours or more.
- Tight emulsions, tend to separate (sometimes only partially) in a matter of hours or even days.

As highlighted in **Figure 1.2** below, the droplet size distribution in an emulsion determines the extent of stability of the emulsion and should be taken into account in the selection of an optimum treatment process and technology [39,54,79].

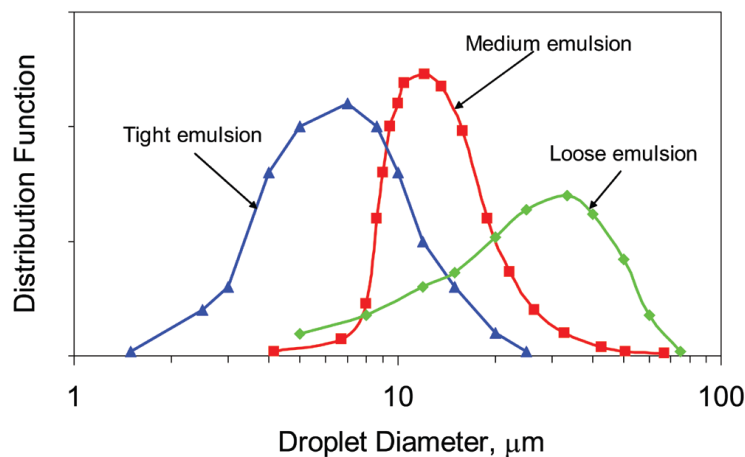


Figure 1.2. Droplet size distributions of tight, medium and loose emulsions. Adapted from [54,83].

High shear force is used in the emulsification process, where droplet breakage is the dominant process, where larger oil droplets are broken into smaller ones [77,84–86]. At relatively low shear force, the reverse is observed and oil droplets aggregate, flocculate and coalesce into larger droplets [87–90]. This process is depicted in **Figure 1.3**, below.

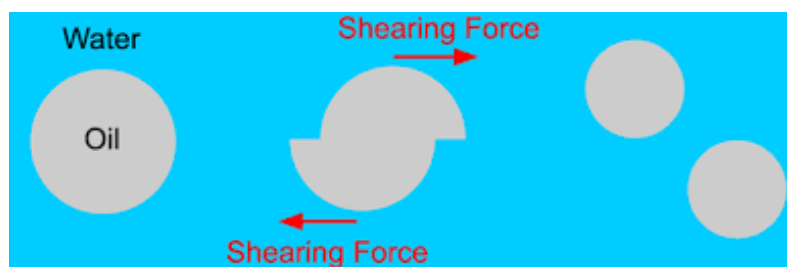


Figure 1.3. The effect of shear on emulsion droplets.

The process of shear-induced droplet aggregation, flocculation and coalescence has been reported in the literature [85,89,91,92]. The mechanism is a function of inter-droplet forces, hydrodynamic shear and the rupture of the thin film between neighbouring droplets [91]. Based on the initial reports, it is evident that low shear force could be a viable and efficient method for the processing of emulsions [93–95].

During industrial processing there are many possible sources of shear, for example electrical pumps, chokes and control valves which create turbulence and varying degrees of shear. The difference in velocity of fluid layers moving adjacent to each other generates hydrodynamic shear forces in the liquid [96,97]. For example, when an emulsion is in motion, hydrodynamic shear stresses develop as a result of the droplets in the emulsion moving relative to one another [77].

The use of shear and flotation together has however not been investigated and the intent of this work is to review this process and evaluate its suitability as a viable method to process oil in water emulsions and optimise the emulsion separation efficiencies.

1.2. Problem statement

The high demand for fresh water resources and growing environmental awareness has engendered a continual search for processes and technologies that recycle and reuse water [38,46,98]. Whatever the technology used to process wastewater, the main aim is always to clean the water to an appropriate level and dispose of it in an environmentally responsible and cost-effective manner [99–104].

Oily wastewater, can be classified into four categories, namely free oil, dispersed oil, dissolved oil and emulsified oil [21,62,105,106]. These categories are defined according to their physical and chemical properties and are discussed in more detail in the Chapter 2, the Literature Review [16,38,105].

The treatment of oily wastewater is generally split into three categories called primary, secondary and tertiary processing techniques. Within the literature there tends to be small differences of opinion regarding what is included in each category; however, all researchers tend to agree on the basic principles of separating oil from water. The basic premise is that the

processing and treatment of oily waste and the eventual separation of the oil from water is a function of the oil DSD.

Primary treatment methods focus on removing free oil and includes water strippers, separators sedimentation, flotation and centrifugation related techniques. Water stripping is a physical separation process where a vapour stream is utilised to remove one or more components from a liquid stream [107]. Secondary treatment methods remove dispersed oil and are used to break oil emulsions. Tertiary treatment includes ultrafiltration, biological treatment chemical oxidation and carbon adsorption. A summary of the forms of oil in wastewater and associated treatment techniques are presented in **Figure 1.4**.

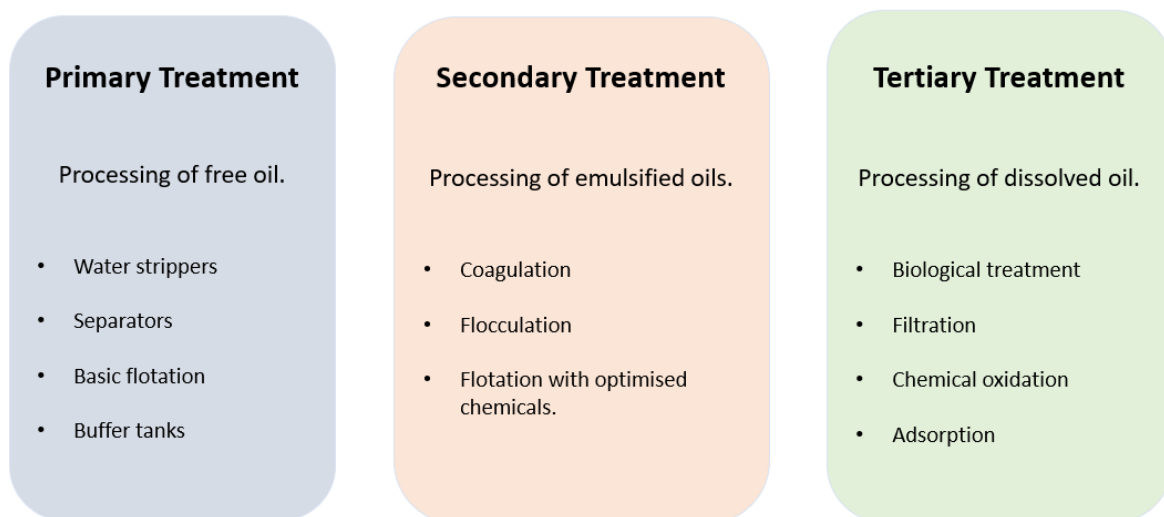


Figure 1.4. Forms of oil in wastewater and potential processing techniques.

Although emulsions are thermodynamically unstable, some emulsions, depending on the stabilisation parameters and properties, are kinetically stable and remain stable for long periods of time. The processing of oil in water emulsions is a key problem associated with high cost and low effectiveness using most current technologies.

Water treatment technologies are continually being researched, developed and implemented in order to limit and control environmental pollution by petroleum products [4,39,44,108,109]. Considerable amounts of effort and resources are deployed by research institutions, companies and governments from around the world to process and remove oily pollutants from wastewater [21,23,50,110].

The discharge of oily wastewater into the environment, is toxic and hazardous to life and thus manifests itself as significant environmental issue and concern [2,18,111,112]. Oily wastewaters have a number of reported adverse impacts on the environment, which include air pollution caused by the evaporation of oil and hydrocarbon solvents into the atmosphere as well as affecting groundwater, seawater and drinking water [1–3,17,18,111]. As much as possible, the concentrations of petroleum products in wastewater is monitored as they can cause serious environmental damage [47,113–115]. Wastewater containing petroleum pollutants such as oil and grease are a significant problem for conventional effluent treatment plants, which often do not adequately remove these pollutants [40,57,114,116].

To limit petroleum product pollution and improve discharge water quality, more efficient wastewater treatment technologies are continually being researched, developed and implemented [2,4–6,39,108]. Oil in water emulsions when present in wastewater, may affect treatment efficiency and influence the quality of the effluent produced and the amount of oil recovered [1,2,17,18].

Oil in water emulsions are defined as a liquid-liquid colloidal systems where the oil phase exists in water in the form of very small droplets [22,117]. Emulsions are stabilised by a balance of competing inter droplet forces, that act to repel the droplets making up the emulsion [114,118–120]. Demulsification enhancement is based on the premise that droplets must collide with each other and following the collision they aggregate, coalesce to form larger droplets and free oil, which can then be separated and processed.

Various oily wastewater treatment processes have developed from practices without a clear understanding of the underlying chemical and physical properties of the processing method [114]. The chemicals utilised in the breaking of the emulsions tend to degrade the oil to such an extent that the waste oil cannot be used in any other process and typically the waste oil is disposed of in landfills as solid waste [21,121–123].

This research study aims at demonstrating treatment procedures that are more effective than those currently applied for effluent oily wastewater emulsion treatment. It is believed that a hybrid technology solution utilising shear flocculation and flotation can be a practical and cost-effective method to treat process oily wastewater emulsions. This research study is being

conducted to evaluate the processing of laboratory prepared surfactant and emulsifier free oil in water emulsions, utilising a hybrid technology process of shear flocculation with flotation.

1.3. Purpose of the study

The existing conventional technologies for the treatment of emulsions require large amounts of chemicals, that impact on the water quality and degrade the oil, producing large quantities of sludge, making the oil unsuitable for recycling [12,48,124–127]. The sludges are often toxic and need to be further processed [12,128–131].

A suitable technology that processes waste and generates clean water and oil that can be recycled would be a promising alternative option. Of particular significance is the processing of waste oil in water (o/w) emulsions. Conventional waste o/w emulsion processing and separation methods, which are discussed in more detail in Chapter 2, have several technology gaps and challenges in terms of applicability and efficiency [14,21,23,39,53]. The removal and effective processing of emulsions in oily wastewater is a costly problem. The processing and treatment of waste emulsions is focussed on separation of the emulsion into separate water and oil components for environmentally acceptable disposal [20,43].

The aim of this research is focused on developing and evaluation of a novel shear flocculation and flotation treatment method, for the processing of oil in water emulsions. Shear flocculation with flotation has successfully been used in processing mineral ores and has to a limited degree demonstrated its potential application to destabilise and separate oil in water emulsions [58,65,69,132,133]. The Shear flocculation and flotation technology has the potential to process emulsions without the use of large amounts of chemicals and produce a relatively clean water stream and an oil product that can be recycled. The use of pre-treatment chemicals degrades the oil phase as well as adding toxic components to the water phase [48,113–116]. As part of this research study a unique shear flotation pilot plant will be designed and fabricated with a micro bubble generator to generate micro-bubbles in order to treat the wastewater by flotation of the oil emulsions.

1.4. Thesis statement

Shear flocculation and flotation can be used as a viable separation method for the separation of oil from an oil in water emulsion. This method has the potential to destabilise tight o/w

emulsions without the requirement of pre-treatment and the need for large amounts of chemicals which degrade the oil phase.

1.5. Research questions

The following research questions will be addressed in this study and include:

- Can a surfactant and emulsifier free oil in water emulsion be processed utilising various levels of shear?
- What levels of shear are required to process and separate emulsions?
- Can shear alone separate surfactant and emulsifier free emulsions?
- Can shear be used in a hybrid method with coagulation, flocculation and flotation.
- What is the processing and separation efficiency of shear flocculation and flotation?
- Can a shear unit be integrated with a conventional flotation system?
- Can shear flocculation lead to a reduction in the use of treatment chemicals?
- Can shear separation be upscaled from a laboratory scale system to a pilot scale plant?

1.6. Aims and objectives

The aims of this research are the following:

- To investigate the viability of shear flocculation as a method to process emulsions.
- To evaluate the processing efficiency of shear flocculation as a method on its own and in conjunction with conventional pre-treatment technologies.
- To utilise a combination of shear flocculation and flotation technology to treat and process oily wastewater emulsions.
- To evaluate the processing efficiency of shear flocculation and flotation on standard oil in water emulsions at laboratory scale.
- To design a shear unit that can be integrated with a flotation unit.
- To design and fabricate a pilot scale plant effluent water treatment plant for the processing of emulsions.

To achieve the aims set out above, the following activities are also required:

- Evaluate the factors that influence and drive effluent water treatment in the petroleum industry.

- Define the process parameters and conditions for shear flocculation and flotation for the treatment of emulsions in wastewater.
- Design a laboratory scale shear flocculation and flotation reactor that allows for emulsions to be treated to an extent that allows them to be recycled, reused and returned to the environment safely.
- Define general operating procedures for a shear flocculation and flotation reactor and the appropriate conditions for its application.
- Evaluate opportunities and the potential of implementing shear flocculation and flotation technology in the various sectors of the petroleum industry.
- Evaluate the current treatment process performance and constraints associated with existing wastewater facility design and performance.
- Investigate the various factors, *i.e.*, pH, temperature, coagulation and flocculation, that influence the processing of emulsions.
- Define the process parameters and conditions for the shear flocculation and flotation system, *i.e.*, flow parameters of the flotation unit, bubble properties and impeller speed of shear mixer.
- Define general operating procedures for the shear flocculation and flotation system and the appropriate conditions for its applications.
- Add to the scientific understanding of the shear flocculation and flotation processes.
- Characterise wastewater pre and post treatment through the hybrid system.
- Investigate the flotation of oil from wastewater in a laboratory-scale dissolved air flotation unit.

1.7. Thesis Delimitation

The processing of oily wastewater and specifically emulsions have been studied in various degrees of detail by a number of researchers. This study is limited to the processing of surfactant and emulsifier free oil in water emulsions utilising coagulation, flocculation, shear flocculation and flotation. This study does not include the processing of oil in water emulsions via other techniques.

The following has also been excluded from this study, namely, the processing of water in oil emulsions, complex emulsions and o/w emulsion samples from industrial applications.

1.8. Significance of the Study

In this research study, a specific focus area will be o/w emulsions and their associated physical characteristics, chemical stability, separation and removal from water. It is generally known that the physical characteristics of o/w emulsions vary greatly with their formulation. An emulsion is an extremely complex disperse system which is thermodynamically unstable. Knowledge and understanding of the oil DSD of a specific o/w emulsion is an important factor in choosing the most effective and efficient wastewater treatment technology.

The utilisation of chemicals is the most common method of emulsion processing and treatment [7,78,134]. Typical emulsion treatment chemicals are a blend of solvents, coagulants and flocculants [135]. The chemicals used target the emulsifying agents and disrupt the stabilising effect, which are a balance of inter droplet forces, which act to repel the individual droplets giving the emulsion stability [114,118–120]. Some of the chemicals used have been reported to carry over with the processed water stream, which is then disposed of into the environment [12,130,136–138].

It is evident that shear flocculation in conjunction with flotation is a new and interesting method for the processing of emulsions [87–90]. It has been reported that a potential solution utilising shear flocculation with flotation can be utilised to treat and process oily wastewater emulsions, however this technology and associated processes is still not well understood [16,65,77]. This research is being conducted to evaluate the processing efficiency and the associated parameters of oil in water emulsions utilising a hybrid process of shear flocculation with flotation technology.

If successful, this method can address identified gaps in the current technologies and reduce the amount of chemicals utilised. It has the potential to produce a water phase with lower levels of toxicity and less sludge that needs to go to landfill. The oil phase has the potential to be recycled. The current driver in emulsion treatment is to produce clean water as well as for the oil to be recovered as a secondary product. If the oil is not degraded to sludge, it can be sold as a secondary product for recycling.

1.9. Thesis structure

This thesis is divided into six chapters including Chapter 1, the present chapter. The organisation of the rest of the thesis is as follows:

Chapter 2 provides an overview of relevant literature on oil contamination in water with a specific focus on o/w emulsions; it includes a literature review of the treatment of oil in water dispersions and emulsions. Thereafter, a comparative study is made of the current industry oil in water processing techniques in which technology gaps are highlighted. This chapter also reviews the mechanisms associated with oil in water emulsion separation processes, the forces associated with emulsion droplet interactions and specific methods for processing oily wastewater such as coagulation, flocculation and shear flocculation and flotation. A large portion of this chapter has been published as a review paper and is included in the repository of plagiarism detection software Turnitin [14]. Due to a high occurrence of self-referencing the Turnitin score appears to be high.

Chapter 3 provides the outlines of the experimental procedures used in this study, including the design and the set-up utilised during the experiments. The procedures followed and the analytical techniques used are described in detail for preparing, processing and analysing the emulsion samples.

All the materials and methods used are described including the experimental details of the methods used to evaluate shear flocculation and flotation. Variables investigated that were aimed at optimising suitable processing conditions are set out. Experimental details of the measurement of performance efficiencies of shear flocculation and flotation are described. This chapter also provides design details of laboratory scale shear flotation setup and of the fabricated pilot scale plant.

Chapter 4 includes and provides not only details of the results but also their respective interpretations, in particular the results of processing emulsions with coagulants, flocculants, shear flocculation and flotation. A comparison is also made between the COD, pH and turbidity parameters of the different processing methods. The optimal processing parameters and processing efficiencies for shear flocculation and flotation are presented. In addition, this Chapter also shows the validation assessments of the results obtained.

Chapter 5, this chapter provides definitive answers to the main research questions developed in Chapter 1. It presents the conclusions of this research study based on the results obtained.

Chapter 6 gives an insight into possible future work to be carried out on the basis of the overall results obtained. The implications of the research findings are assessed with reference to current theory and practice.



CHAPTER 2 LITERATURE REVIEW

2.1. Use of relevant databases

A literature review was conducted utilising the resources from the University of the Western Cape (UWC) library, Google Scholar as well as from the Society of Petroleum engineers (SPE). The purpose of the review was to survey the existing body of literature, clarify concepts, evaluate the research conducted to date and to identify the current technology gaps.

The resources utilised were limited to English language literature spanning from approximately 1980 to 2022, which included books journal articles and websites. It is acknowledged that this is a limitation, however based on the literature accessed, this is considered as a minor limitation in the overall context.

All literature database searches were limited to the English language and the English abstracts of non-English language articles published between 1980 and June 2022.

The following is a list of electronic databases that were accessed via the UWC library, that included:

- <http://uwc.worldcat.org/>
- <http://lib.uwc.ac.za/index.php/a-za-database.html>
- [:http://scholar.google.co.za/ezproxy.uwc.ac.za/schhp?](http://scholar.google.co.za/ezproxy.uwc.ac.za/schhp?)
- <http://repository.uwc.ac.za/xmlui/>
- <http://atoz.ebsco.com/ezproxy.uwc.ac.za/Titles/unwc?lang=en&lang.menu=en&lang.subject=en#74/1/all>
- SciFinder Scholar, database of chemistry literature, Chemical Abstracts.

In addition to the UWC research databases, additional sources and digital platforms were first accessed by registration then utilised accordingly for this research, these include:

- <https://www.academia.edu/>
- <https://scholar.google.com/>
- <https://www.spe.org/en/>
- <https://www.sciencedirect.com/>
- <https://www.semanticscholar.org/>

- <https://ssww.mendelev.com/>
- <https://www.semanticscholar.org/>
- <https://www.mendeley.com/>

In order to manage the references obtained from the above databases, a free reference manager was used. The reference manager used was Mendeley Reference Manager obtained from the following website <https://www.mendeley.com/reference-management/reference-manager/>:

Through the initial preliminary review, a broad list of research terms pertinent to wastewater systems for the removal of oil from wastewater was developed, which included the following key terms:

oil-in-water, separation efficiency, emulsion stability, demulsification mechanism, Surfactants, oil in wastewater separation, emulsion, demulsification, flotation, droplet coalescence- droplet aggregation, DAF, industrial wastewater contamination, Ostwald ripening water pollution; emulsion stability wastewater with dispersed and soluble oils, multiple emulsions, encapsulation, droplet breakup, emulsion stability, shear stress, conventional emulsion treatment techniques are either not meeting the discharge standards or are not feasible.

These terms were further processed to create keywords that could be used to search the electronic databases highlighted above. Some of the research keywords included:

Petroleum wastewater, oil dispersions, oil emulsions, demulsification, emulsification, oil in water emulsions, oil dispersions, flotation dissolved air flotation, oil in water emulsion, coagulation, flocculation, droplet coalescence, droplet aggregation, separation, centrifugation, colloid phenomena, petroleum

Excluded from the literature review were commentaries, editorials and non-scientific publications. A similar screening process as highlighted above, was used for literature found through website searching. Material from websites, less formal, interpretive descriptions of a study or investigation that may be published on a web page that may or may not be linked to the report document were excluded.

This thesis is focussed on oily wastewater and specifically oil in water emulsions hence the literature review was focussed accordingly.

2.2. Oil contamination in water

Oil contaminated water, often referred to as oily wastewater, is generally classified into four categories, namely free oil, dispersed oil, emulsified oil and dissolved oil [21,62,105,106]. These categories are defined according to the wastewater's physical and chemical properties, with a key parameter being the droplet size distribution (DSD) [16,38,105]. It is often reported that oil in water may be dispersed, emulsified or soluble in concentrations of up to 1000 mg/L [14–16].

2.2.1. Free oil

Free oil physically separates from water and floats to the surface under calm conditions due to its lower specific gravity compared to that of water [139]. The free oil droplets present in wastewater generally range in size from a few millimetres to large droplets. The non-dispersed oil droplets coalesce relatively easily and float to the surface of the water. Free oil is usually cleaned up and collected using skimmers, booms, chemicals and various other techniques to remove it from the water surface [21,31,62,111,140–142].

2.2.2. Dispersed oil

Dispersed oil is defined as oil in water in the form of small droplets, the DSD is typically in the range of a hundred to several hundreds of microns [105,139]. Dispersed oils form when mixtures of oil and water move through pumps or pipelines, oily wastewater splashing in vessels, through natural phenomena like wave action, agitation or processes that break up free oil and disperse the oil droplets [22,31,103,143,144].

The oil droplets in the dispersion can either coalesce over time to form free oil or can be stabilised, leading to the formation of emulsions. For the separation of dispersed oils, gravity separation, gas flotation and filtration based technologies are commonly used techniques [56,145–147].

The separation efficiency of any processing technique utilised depends on a number of factors, which include oil droplet size, density of the oil, viscosity and density of the water phase, water pH, flow rate as well as temperature [79].

2.2.3. Emulsified oil

Dispersed oils can be stabilised leading to the formation of emulsions [148]. Oil emulsions that are formed from dispersed oils can be classified as mechanically or chemically stabilised emulsions [149].

Mechanically stabilised emulsions are formed by the development of surface electrical charge on the oil droplets in the water, which prevents their coalescence [84]. Chemically stabilised emulsions form similarly to mechanical emulsions; however, they have additional stability due to interactions of chemical agents at the oil droplet and water interface [150]. Chemical emulsions contain detergents, soaps or other additives that enhance the prevention of coalescence [54,105,149]. Depending on the formation conditions and relative proportions of the oil and water constituents, multiple emulsions of oil in water (o/w), water in oil (w/o), as well as complex oil in water in oil (o/w/o) multiple emulsions may be formed [78]. In the petroleum, pharmaceutical and food production industries the o/w and w/o simple emulsions are generally more common than the complex emulsions [76,78,151,152].

2.2.4. Dissolved oil

Dissolved oil occurs when oil dissolves in water such that there are no oil droplets present. In general, aliphatic hydrocarbons have low solubility in water; however, aromatic hydrocarbons, such as the single-ring compounds benzene, toluene, ethylbenzene and xylene (BTEX), as well as two-ring naphthalenes, along with phenols and organic acids are more soluble and usually form the largest component of dissolved oil [21,48,139,148,149].

Dissolved oil cannot be removed from water by physical treatment and is typically removed by adsorption in activated carbon, chemical adsorbents, chemical oxidation and biological treatment [48,103,110,139]. Gravity, filtration and flotation based separation methods are ineffective for dissolved oil separation and processing [105].

2.3. Oily wastewater processing

Oily wastewater causes a serious pollution problem, arising from wastewater generated by a wide range of industries [8,10–13]. Various methods are used to process and remove oil polluting contamination from water [7,22,43–45]. The methods are categorised as chemical, electrochemical, physical, physiochemical and biological [17,38,41,43,46,47,103,105,153,154]. The basic premise is that the processing and treatment

of oily water and the eventual separation of the oil from water is a function of the oil DSD [155].

Some of the more specific techniques include:

- Gravity [49,105,147],
- Air / gas flotation [55,56],
- Filtration [156,157],
- Absorption and adsorption [105],
- Chemical / oxidation [17,158], and
- Biological [17,38].

The steps in the process of removing oil from wastewater are firstly methods to remove the free and dispersed oil [49,52,53,159–162]. For example, in a gravity separator, with time and quiescence, most free oil droplets will rise to the surface where they are skimmed off, while the emulsified oil remains in the wastewater [159,160].

Once the free and dispersed oils are removed, the emulsified oil is processed and finally the dissolved oil is removed from the wastewater [17,18,108,163,164]. Depending on the characteristics and nature of oily wastewater, treatment methods are classified into primary, secondary and tertiary processes, which are a function of the specific type of oil pollution in the water [39,43,49,50,103].

The treatment methods are summarised and presented in **Table 2.1** below.

Table 2.1. Forms of oil in wastewater and potential processing techniques.

Oil in water form	Droplet size	Description	Processing Techniques
Free oil	> 100 μm	<ul style="list-style-type: none"> • Low specific gravity, relatively easy to process, separate and float • Separate oil droplets of a sufficient droplet size • The buoyancy force causes the oil to float to the water surface • The free oil is relatively easily removed by decanting the floating surface oil 	<ul style="list-style-type: none"> • Essentially, coalescence and decantation • Techniques include the following: <ul style="list-style-type: none"> ○ API and Parallel Plate Interceptor gravity separators [100] ○ Long residence time skim tanks ○ Corrugated plate interceptors [165–167]
Dispersed oil	> 20 μm	<ul style="list-style-type: none"> • Oil in the form of small droplets in water • Oil droplets are not stable enough to form an emulsion • The coalescence and surfacing time of the free oil depend on the DSD • Larger droplets with greater buoyancy rise faster than smaller ones 	<ul style="list-style-type: none"> • Secondary techniques, designed to encourage coagulation and coalescence to form free oil • Techniques include the following: <ul style="list-style-type: none"> ○ Hydrocyclone [146,147] ○ Air flotation [56] ○ Centrifugal separation
Emulsified oil-	5 – 20 μm	<ul style="list-style-type: none"> • Emulsion forms as a result of mechanical action such as mixing, valve throttling, shearing and wave action 	<ul style="list-style-type: none"> • Secondary techniques, designed to destabilise droplets of emulsions and to form free oil • Techniques include the following: <ul style="list-style-type: none"> ○ Coagulation [168,169] ○ Flocculation [129,170] ○ Air flotation - with optimised chemicals [62,171] ○ Hydrocyclones [139] ○ Centrifuges [15,172]
	< 5 μm	<ul style="list-style-type: none"> • Emulsion forms as a result of chemical action such as surfactants 	
Dissolved oil		<ul style="list-style-type: none"> • Oils that have solubility in water Emulsion forms as a result of chemical action such as surfactants • Typically removed by adsorption, membranes, chemical oxidation 	<ul style="list-style-type: none"> • Tertiary techniques designed to meet very stringent discharge limits • Tertiary techniques <ul style="list-style-type: none"> ○ Biological treatment [48,110,139] ○ Filtration with sand ○ Activated carbon ○ Membrane methods separation [78,173]

		and/or biological treatment	<ul style="list-style-type: none"> ○ Reverse osmosis ○ Chemical oxidation
--	--	-----------------------------	---

Most industrial oily wastewaters contain oil emulsions as the major contaminants [81,128,174]. Emulsions tend to remain stable as a result of electrostatic repulsion between droplets, preventing them from coalescing into larger droplets, making processing by conventional methods a difficult and time consuming process [51–54].

The specific focus of this research is on o/w emulsions and their associated physical characteristics, chemical stability, processing, separation and removal from water. It is generally understood that the physical characteristics of o/w emulsions vary greatly based on the preparation parameters and formulation [38,175,176].

The methods and techniques, both conventional and the more novel, of emulsion treatment are reviewed and presented in the subsequent sections. However, in order to understand the principles of how the various processing techniques work it is of importance to firstly understand the physical properties and parameters of emulsions.

2.4. Emulsion properties and parameters

Emulsions are defined as liquid-liquid multiphase heterogeneous colloidal systems, consisting of two or more immiscible liquids, where the dispersed phase exists in the form of droplets in a continuous phase of a different composition [22,117,177]. A colloidal system contains at least one of the phases in the form of very small particles and in the case of an emulsion, as droplets [22].

British scientist, Thomas Graham, in 1861 defined the term “colloid”, from the Greek word “kola”, meaning glue [178]. Colloidal dispersions, or simply, colloids, comprise a collection of small particles, droplets, or bubbles of one phase dispersed in a second phase [179]

Colloidal particles are larger than atoms and ions, however they are usually small enough not to be visible to the naked eye [180]. They range in size from 0.001 to 10 μm resulting in a very small ratio of mass to surface area. The consequence of very small particles is that they have a large surface area relative to their overall mass and the following resulting properties:

- gravitational effects are negligible,

- particle surface phenomena dominate, and
- particles assume electrical charges with respect to their surrounding environment.

Colloids can be gases, liquids, or solids and examples of each are listed in **Table 2.2**.

Table 2.2. Types of colloidal suspensions. Adapted from [179].

Continuous (External) Phase	Dispersed (Internal) Phase	Colloidal System	Examples
Gas	Liquid	Aerosol of liquids	Fogs, clouds, mists, fine insecticide sprays
Gas	Solid	Aerosol of solids	Smoke, volcanic dust, haze
Liquid	Gas	Foam or froth	Soap lather. Lemonade froth, foam, whipped cream, soda water
Liquid	Liquid	Emulsions	Milk, emulsified oils, medicines
Liquid	Solid	Sols	Most paints, starch in water, proteins, gold sol, arsenic sulphide sol, ink
Solid	Gas	Solid foam	Pumice stone, styrene rubber, foam rubber
Solid	Liquid	Gels	Cheese, butter, boot polish, jelly, curd
Solid	Solid	Solid sols (coloured glass)	Ruby glass, some gemstones and alloys

Colloidal particles in aqueous media have the tendency to adsorb ions from the surrounding medium that impart to the colloids an electrostatic charge relative to the bulk of the continuous phase. In pure water however, it is due to the orientation and charge of the water molecules at the surface of the colloidal oil particle [181].

The developed electrostatic repulsive forces prevent the colloidal particles from aggregating and consequently contribute to the overall stability of the colloidal suspension. The forces interacting on oil droplets in an emulsion are generally categorised according to the Derjaguin,

Landau, Verwey and Overbeek (DLVO) theory [182]. This model was developed in the 1940's and is a simple visualisation tool of the balance of forces of a variety of systems in a quantitative manner in terms of the distance between the colloidal particles [182,183]. The stability of colloids has been explained by the DLVO theory, which is discussed in more detail in subsequent sections.

Small particles are subject to constant Brownian motion, which is a thermally caused phenomenon and is directly related to the temperature of the solution [184]. Thermal motion is an essential factor keeping small particles homogeneously distributed in a solution. The diffusion rate of a colloidal particle further depends on the viscosity of the solvent and the particle size and shape. For spherical particles, the diffusion rate rapidly increases with decreasing particle radius. Sedimentation under gravitational forces is slower for small particles compared to larger ones. At sufficiently small particle sizes, rapid diffusion compensates for gravity and prevents particles from settling.

Emulsions are distinguished from other types of mixtures and colloidal suspensions by several distinctive properties and are classified on the basis of a number of factors; however, the most commonly used are the mode of dispersion, droplets characteristics and thermodynamic stability [78,79,185,186]. Droplet parameters that are important include size, the concentration, charge, rheological behaviour and droplet interactions [79,187,188]. The DSD of oil droplets is an important parameter of an o/w emulsion, that affects the overall stability, rheology and appearance of the emulsion [21,79].

Emulsions constitute a wide variety of products and are formed and produced in many processes of industrial relevance [78,79,185,186]. Despite some of the environmental issues associated with oil in water emulsions, emulsions have special properties that make them very useful in many diverse fields such as food technology, pharmaceuticals, agriculture, lubricants, cosmetics, laundry and cleaning agents [189–191]. Most lubricants, paints, cosmetics and many food products are emulsions [102,192].

As highlighted in the previous section, oil dispersions under the appropriate conditions may result in the formation of emulsions, which are classified based on the mode of emulsification. The emulsions can include o/w, w/o as well as multiple and complex emulsions, as depicted in **Figure 2.1** below [78].

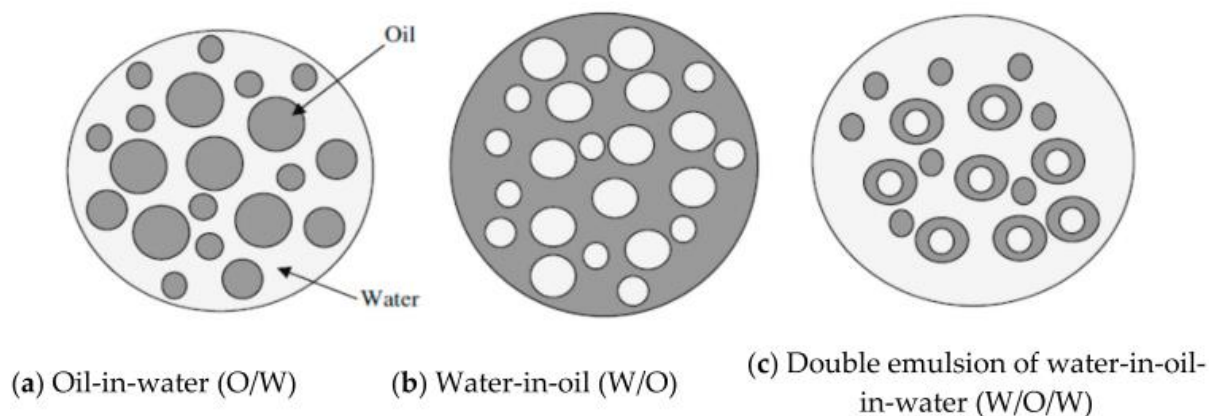


Figure 2.1. Graphical depiction of various types of emulsions. Adapted from [78].

An o/w emulsion consists of water as the continuous phase and the oil as the dispersed phase. Complex emulsions are those where the droplets of continuous phase are suspended in larger droplets of dispersed phase, which in turn is dispersed in the continuous phase. Emulsification is the process of formation of emulsions [21,79].

Emulsions are described as thermodynamically unstable and kinetically stable [120,193,194]. The theoretical stability and thermodynamics of an emulsion can be expressed by a derivation of the Gibbs free energy as per Equation 2.1.

$$\Delta G = (\gamma A) - (T\Delta S), \quad \text{Equation 2.1}$$

where, γ = interfacial tension, A = interfacial area, T = temperature, ΔS = mixing entropy

The magnitude of ΔG gives an indication of the thermodynamic stability of an emulsion. If ΔG is greater than zero, then the emulsion is relatively unstable and will result in separation. If ΔG is less than zero, then the emulsion is stable and no separation will take place [194].

The kinetic stability is a direct result of the DSD and the presence of an interfacial layer between the water and the oil droplet. When this interfacial film between the droplets thins and ruptures, the process of droplet coalescence occurs [195]. The kinetic stability of an emulsion can be increased with surfactants or emulsifiers, often referred to as stabilising agents [51]. The

addition of stabilising agents slows phase separation by lowering the interfacial free energy through adsorption and the provision of additional electrostatic or steric stabilisation at the interface [176,195,196]. The stabilisers suppress the separation mechanisms in emulsions. These types of stabilised emulsions are referred to as microemulsions [152,197–199].

Oil in water emulsions can remain stable for substantial lengths of time, which according to Tansel *et al.* [175], is a function of the compositional materials and processing parameters, droplet surface charge, specific gravity, surface tension and solubility characteristics relative to the water phase. Eventually, over time, the emulsion will separate into oil and water and are referred to as nanoemulsions [152,186,191,197,200,201]

2.4.1. Origin of charge on emulsion droplets

Experimental evidence has demonstrated that oil droplets in water move toward the anode in the presence of an electric field in electrophoresis experiments, implying that they develop a natural negative charge [202,203]. This experimental observation has served as the confirmation of the negative charge, but its origin has been a matter of debate for a number of years [203]. Based on this observation, there are a number of conflicting interpretations underlying the origins of the negative charge, however most researchers in the field attribute the charging mechanism to the process of selective adsorption and dissociation of surface ions [204–208].

The selective adsorption mechanism is the more common interpretation and is explained by the fact that negatively charged hydroxide ions (OH^-) adsorb and bind strongly to hydrophobic/water interfaces. It has been demonstrated that H^+ and OH^- have an effect on the droplet-water interfacial electrical charge. The ions originate from within the structure, where H_2O molecules prefer to donate and accept electrical charges from their neighbours via an interaction known as hydrogen bonding [209]. However, when they are close to the oil molecules at the droplet surface, they no longer find enough water neighbours to hydrogen bond with and this results in the water molecules donating their imbalanced electrical charges to the oil molecules at the droplet surface [207,208]. This charging mechanism implies that the water-oil interaction occurs via hydrogen bonding [203,209,210].

Hydroxide ions in water may not adsorb to hydrophobic interfaces, but rather react with traces of organic acids, which have been dissolved in the oil droplets and are present at the droplet/water interface [206]. In addition the molecules, making up the oil droplet may themselves undergo dissociation and release H⁺ ions into the medium resulting in the development of a negative charge on the oil droplet. [205,206].

It has also been demonstrated that bubbles in water also have a negative charge via similar mechanisms to those described above [211].

It is clear that the properties of colloidal dispersions are dependent on the electrical charge of the particles and the properties, parameters and characteristics of emulsions will be discussed in the subsequent sections.

2.4.2. Rheology

Rheology is defined as the science of the flow and deformation of materials and is the study of the interaction between shear stress, shear strains and time [193,212]. The flow properties of emulsions are physical attributes that significantly affect the overall stability of emulsions [85,213,214].

According to a derivation of Stokes law, the stability of an emulsion, made up of immiscible liquids with different densities, is influenced by the DSD and viscosity of the emulsion [120,187].

$$v_s = \frac{2gr^2(\rho_2 - \rho_1)}{9\eta}, \quad \text{Equation 2.2}$$

where, v_s = settling velocity, r = radius of the droplet, g = acceleration due to gravity, ρ_2 = density of the sphere, ρ_1 = density of continuous phase and η = viscosity of the continuous phase.

From Equation 2.2, a derivation of Stokes law, if emulsion droplets are denser than the fluid ($\rho_2 > \rho_1$), then v_s will be greater than zero and the droplets will fall to the bottom resulting in sedimentation. If the droplets are less dense compared to the fluid ($\rho_2 < \rho_1$) then v_s less than zero and the droplets will float to the surface.

For an emulsion, we can assume the droplets are spheres and that v_s is an indicator of the rate of separation. Equation 2.2, infers that v_s is inversely related to the viscosity of the water phase. This implies that the rate at which an oil droplet will move through the continuous phase increases as the viscosity decreases. It implies that more viscous emulsions are more stable than less viscous ones. This has been confirmed by a number of authors in industrial and pharmaceutical applications of emulsions [150,151,215].

Stoke's law demonstrates the importance and significance of droplet size on phase separation of a colloidal suspension. It is therefore beneficial to destabilise the emulsion and increase the DSD in order for gravity separation to be practical. By way of an example, two oil droplets in an emulsion with different size will have a different rise velocity. An oil droplet of 10 μm in size, with a density of 877 kgm^{-3} has a rise velocity of $6 \times 10^{-6} \text{ ms}^{-1}$, as compared to a smaller droplet of 1 μm in size of the same oil has a rise velocity of about $6 \times 10^{-8} \text{ ms}^{-1}$. Based on the above, the 1 μm droplet will take 93 hours (h) to rise 2 cm as opposed to 0.9 h for a 10 μm droplet to rise and travel the same distance. When the Reynolds number is less than 1.0, Stokes Law is applicable with the premise that the particle, droplet, is a spherical shape [216].

Parameters that affect and influence the emulsions rheological properties include, chemical composition of the continuous phase, droplet characteristics, *i.e.* size distribution, concentration, deformability, viscosity and droplet-droplet interactions, the volume fraction of the dispersed phase and the overall viscosity [187].

2.4.3. Droplet size distribution

Several factors determine the DSD of an emulsion. These include bulk properties of the oil and water, presence of solid material, nature of emulsifying agents and interfacial tension [84,105,176,185]. The DSD in an emulsion determines, to a certain degree, the stability of the emulsion and is an important parameter in considering the most suitable processing technique [39,54,89].

According to Stoke's law, the DSD of an emulsion is a factor that affects the stability of the emulsion [54,83].

2.4.4. Zeta Potential

The zeta (ζ) potential is also often referred to as electrokinetic potential and is a parameter applicable to all solid-liquid and liquid-liquid colloidal systems, including emulsions [202,217,218].

The origin of the ζ potential is the electric double layer (EDL), which results from the electrostatic charge of the oil droplet in water. The ζ potential is the measure of the difference in electrical potential between the bulk fluid in which a droplet is dispersed and the layer of fluid containing oppositely charged ions that is associated with the droplets surface [219]. In general, most particles or droplets dispersed or dissolved in water, naturally possess a negative surface charge [176,187,193]. Similarly for an emulsion, it is generally accepted that the surface of emulsion droplets are negatively charged [220].

The magnitude of the ζ potential gives an indication of the stability of the emulsion and the sign of the ζ potential gives an indication of the surface charges of the droplet [217,221,222]. It is generally accepted that emulsions with ζ potential values greater than ± 30 millivolts (mV) are indicative of stable emulsions [221,223]. A lower-magnitude ζ potential is indicative of a less stable emulsion, where droplets will tend to aggregate or flocculate [221,224]. Emulsions with ζ potentials greater than ± 60 mV have excellent stability, where particles with ζ potential values of between -5 mV and $+5$ mV, will experience rapid agglomeration, unless they are chemically stabilised.

For oil in water emulsions, the ζ potential is an important parameter that describes the surface properties of the droplet and is a measure of the magnitude of electrostatic potential, which determines the force of repulsion between droplets [217,221,222].

The most important factor that affects the ζ potential is the pH of the medium [221,225]. Other factors include ionic strength, the concentration of any additives and temperature. Important factors to consider when analysing ζ potential include:

- pH— H^+ ions can cause the build-up of positive charge on a particle's surface while OH^- will add negative charge thus altering the ζ potential. Functional groups at the particle surface may become protonated or deprotonated.

- Electrical conductivity — conductivity is inversely proportional to electrophoretic mobility. An increase in carrier conductivity in an applied electric field will yield a decrease in the average droplet velocity.
- Carrier viscosity — viscous mediums inhibit electrophoretic mobility, which is proportional to the ζ potential.
- Temperature — affects kinetic energy and carrier viscosity.

In summary, the ζ potential is a key indicator of the stability of a colloidal dispersion and emulsions, which correlates to the particles ability to repel each other electrostatically [202,217,221,226]. Its measurement brings detailed insight into the causes of dispersion, aggregation or flocculation and can be used to improve the formulation of emulsions. In general, when the ζ potential of an emulsion is high, the repulsive forces exceed the attractive forces, resulting in a relatively stable system [223]. The sign of the ζ potential gives an indication whether positive or negative charges are dominant at the surface of the droplet [221]. If two adjacent particles have sufficiently high ζ potentials of the same sign, they will not agglomerate due to repulsive electrostatic forces between particles with like charges.

Empirically, it is generally accepted that emulsions with absolute ζ potential values higher than ± 40 mV are indicative of stable emulsions [221]. **Table 2.3** gives an indication of the stability of emulsions in relation to their ζ potentials.

Table 2.3. Schematic representation of the electrical double layer. Adapted from [221].

ζ potential (mV)	Colloid stability
0 to ± 5	Unstable rapid agglomeration
± 10 to ± 30	Developing stability
± 30 to ± 40	Moderate stability
± 40 to ± 60	Good stability
Greater than ± 60	Excellent stability

Another possibility to modulate the electrostatic repulsive force is via the surface charge of the droplet [227]. The higher the surface charge, the stronger the electrostatic repulsion. At the isoelectric point (IEP) or point of zero charge, the number of negative and positive charges are

balanced, the electro static double layer collapses and the total surface charge becomes neutral [228,229]. By adjusting the pH to the IEP, the surface can be gradually reduced to initiate particle assembly and flocculation [230].

Figure 2.2, depicts a plot of the ζ potential of a sample measured as a function of the pH. In this example, the isoelectric point of the sample is at pH 5.8. In addition, the plot can be used to predict the pH ranges of emulsion stability. It can be seen that the sample should be stable at both extremes of pH.

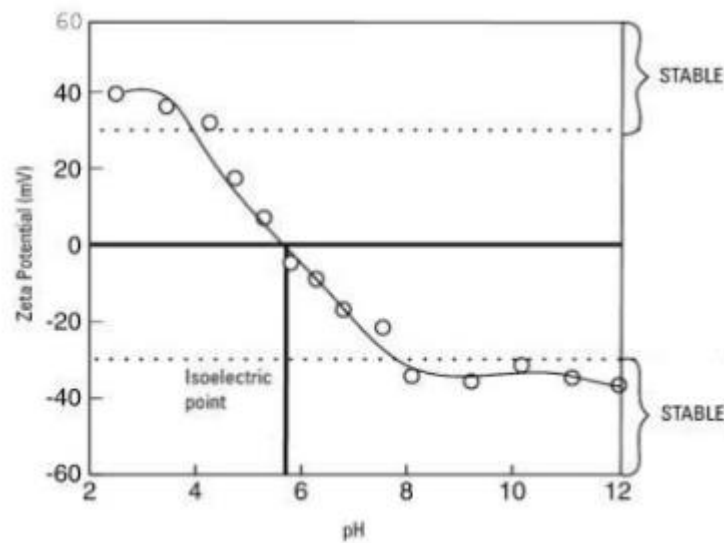


Figure 2.2. A plot of the ζ potential of a sample measured as a function of pH.

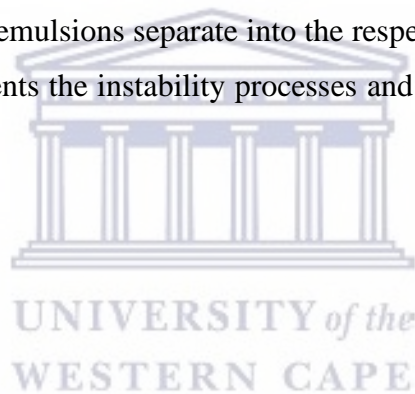
At pH values less than 4, there is significant positive charge present. In addition, at pH values greater than 8, there is significant negative charge present. At these extremes of pH, the forces resulting from this electrostatic repulsion should be sufficient for the sample to resist flocculation.

Understanding an emulsion's isoelectric point can assist in assessing stability and the possible processing technique to be utilised [231]. Similarly, the ζ potential of a colloidal system also demonstrates a dependence on pH.

2.5. Emulsion droplet interactions

Emulsions are stabilised by a balance of competing inter droplet forces resulting in inter droplet repulsion between the droplets making up the emulsion [114,118–120]. The concept of demulsification is based on the premise that droplets need to collide with each other and following the collision they aggregate, coalesce forming larger droplets and free oil. Three different transport mechanisms are at play which facilitate potential droplet collision, namely Brownian diffusion, fluid convection and interparticle interactions [22,117,185].

During the separation process, oil-in-water emulsions can proceed via several mechanisms which cause separation into the respective phases [54,193]. To date, the following mechanisms have been identified and extensively discussed in the literature, as key steps in the demulsification process, which consist of flocculation, creaming, sedimentation, Ostwald ripening, coalescence and phase inversion [78,193,200]. Demulsification is also described as an instability process whereby emulsions separate into the respective phases [51,129]. **Figure 2.3**, below, schematically presents the instability processes and mechanisms of o/w emulsion phase separation.



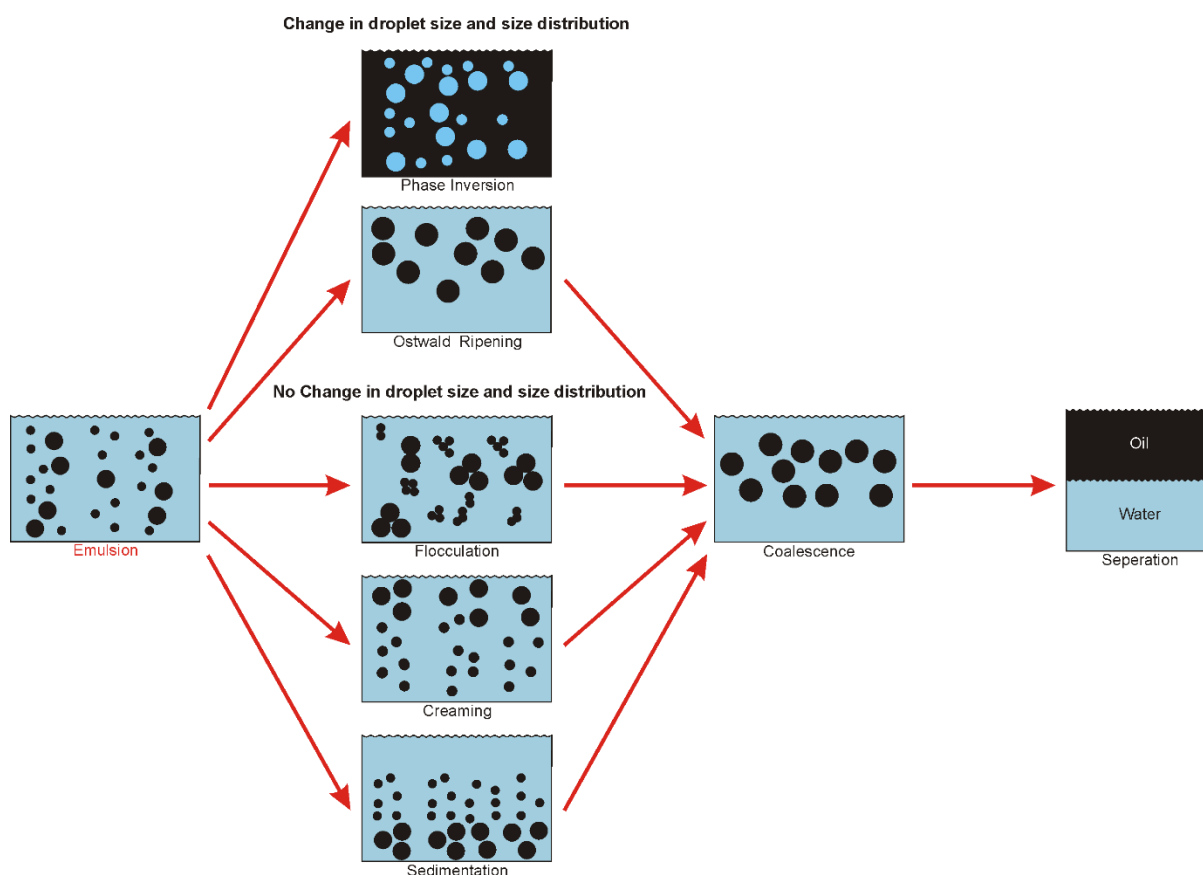


Figure 2.3. Diagrammatic representation of the oil in water emulsion separation process. Adapted from [78].

Of particular significance, that should be highlighted, is that for flocculation, creaming and sedimentation there is no definitive change in the associated droplet size and DSD [228,232]. However, with coalescence, phase inversion and Ostwald ripening there is a distinct change in the droplet size and DSD of the emulsion, as shown in **Figure 2.3**.

The section below provides a short description of different demulsification processes.

2.5.1. Flocculation

Flocculation is the process where individual droplets in the emulsion aggregate to form flocs [129]. Although the droplets aggregate and even make contact, they do not coalesce and they retain their individual droplet characterisation. During flocculation the emulsion structure changes, however, the DSD remains unaltered [233].

The rate of flocculation, depends on various factors such as temperature, pH, viscosity and density of the aqueous phase [234,235]. To increase and accelerate the process of flocculation, coagulants and flocculants can be added to the emulsion [124,160,175,236–238].

2.5.2. Creaming

Creaming is a process where, the less dense phase migrates to the surface to form a layer on the denser phase [54]. The creaming phenomenon occurs frequently in o/w emulsions, where the droplets move up to the surface because of the lower density of the oil droplets. During creaming the emulsion structure changes; however, the DSD typically remains unchanged [150].

2.5.3. Sedimentation

Sedimentation is the process that occurs when the denser-dispersed phase forms a layer of droplets at the bottom of the continuous phase. During sedimentation, the emulsion structure changes, however, the DSD typically remains unchanged [22,212].

The phenomena involved in each process highlighted above, is relatively complex and requires a detailed understanding of the droplet interactions and associated forces. It should be noted that the processes can take place simultaneously rather than consecutively, which adds to the overall complexity of the process of demulsification [193].

2.5.4. Phase inversion

Phase inversion occurs when the continuous phase of the emulsion changes to the dispersed phase. This occurs when an o/w emulsion becomes a w/o emulsion. This instability process can also occur when an emulsifier develops solubility in the dispersed phase rather than the continuous phase [198]. Phase inversion can often occur by altering the temperature or increasing the concentration of ionic solutes in the aqueous phase [193].

Phase inversion can be considered as instability of the emulsion system, it can also be used as an energy efficient method to prepare a stable emulsion by the formation of a micro emulsion using a minimum of mechanical energy. Phase inversion in a micro emulsion of very small droplets occurs readily, due to the interfacial tension between phases being extremely low at the inversion temperature.

2.5.5. Ostwald ripening

Ostwald ripening of an emulsion is the process in which smaller droplets in an emulsion dissolve into the bulk phase and deposit their material onto larger droplets. It reflects the theory that larger droplets are thermodynamically more stable as the surface area to volume ratio is lower [195]. Alternatively, one may view the process purely in terms of the reduction in free energy of the system through the lowering of the interfacial area [195]. Overall, the effect is an increase in the average radius of the emulsion droplets with time as number of smaller droplets decreases. Ostwald ripening is the growth of larger emulsion droplets at the expense of smaller ones and leads to an increase in DSD with time, as highlighted in **Figure 2.4** [193].

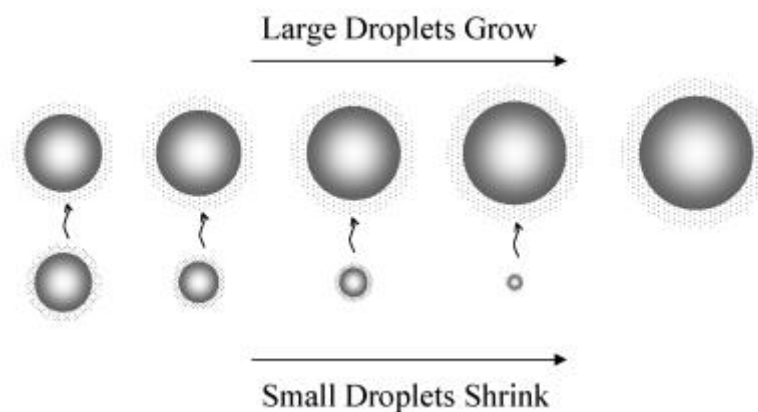


Figure 2.4. Process of Ostwald ripening. Adapted from [239].

Ostwald ripening also occurs in o/w emulsions where small oil droplets diffuse through the aqueous phase and add their material to the larger droplets [193,195,239]. With Ostwald ripening, the droplets do not need to be in close proximity to each other, because the process occurs by transport of small droplets through the dispersion medium [194,195]. Over time, this causes emulsion instability and eventually phase separation. In the literature it has also been referred to as isothermal distillation or molecular diffusion [195,228,232].

2.5.6. Coalescence

Droplet coalescence is a process in which two droplets merge to form a larger droplet, as highlighted in **Figure 2.5**.

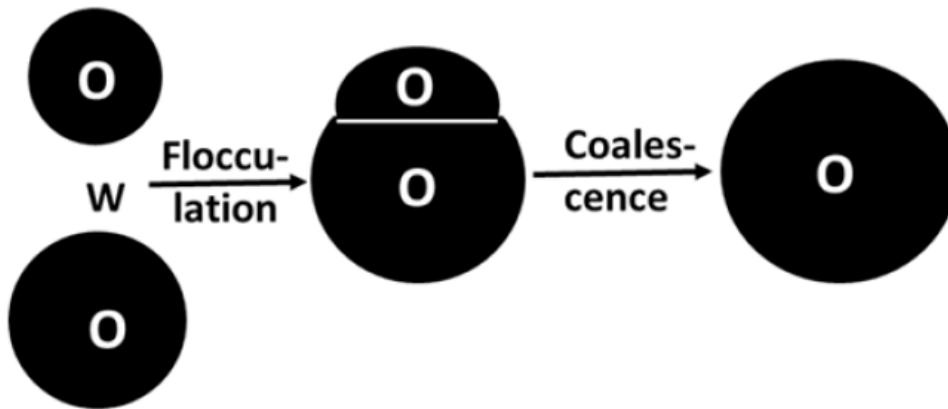


Figure 2.5. Process of droplet flocculation and coalescence for droplets in a o/w emulsion.
Adapted from [176].

In order for two oil droplets to coalesce into one larger droplet, the film of liquid trapped between them must drain away [85]. As the drainage proceeds, the film between the droplets becomes thin enough for the attractive inter-droplet forces to dominate and to form a thin capillary link between the droplets. This link grows and the droplets coalesce [176,193].

Without the influence of additional emulsifying forces, coalescence can be considered as an irreversible process, which is enhanced by a high rate of flocculation, creaming and sedimentation, the absence of mechanically strong films, high interfacial tension, low viscosities and high temperatures [54,193]. An understanding of the conditions associated with droplet coalescence is important for the design of emulsion separation processes. The coalescence between droplets in an immiscible liquid medium, or between a droplet and its own bulk phase occurs in three stages [176,240]. In the first stage, the droplets approach each other and are separated by a thin film of the continuous phase. The second stage involves the thinning of this film to reduce the interfacial area which is affected by the capillary pressure. The third stage occurs when the film reaches a certain critical thickness, any significant disturbance or instability will cause it to rupture and coalescence occurs [120].

The physical phenomena involved in each process highlighted above and associated with emulsion stability is not trivial and requires a detailed analysis of the various surface forces involved [193]. The disturbance of the initial emulsion equilibrium can be achieved with additives such as acids, bases, electrolytes, ligand stripping agents or non-solvents. Another possibility is the use of non-additive triggers such as temperature, irradiation or mechanical

methods such as centrifugation or ultrasonication. The difficulty in the destabilisation step lies in finding suitable triggers, which increase the overall attraction sufficiently and act uniformly over the entire volume.

The destabilising processes of emulsions has been extensively studied. However, a number of questions still remain unanswered in terms of the overall interaction of these forces on the processing of emulsions. The interaction of these forces on emulsion droplets will be discussed in more detail in the next section.

2.6. Forces related to droplet interactions

Emulsions are stabilised by a balance of competing inter droplet forces, which either act to repel or attract the individual droplets making up the emulsion [114,118–120]. The interaction of the forces in the emulsion play a crucial role in determining the properties of the emulsion as well as being highly relevant to a range of industrial and environmental protection processes [176,178,186,213].

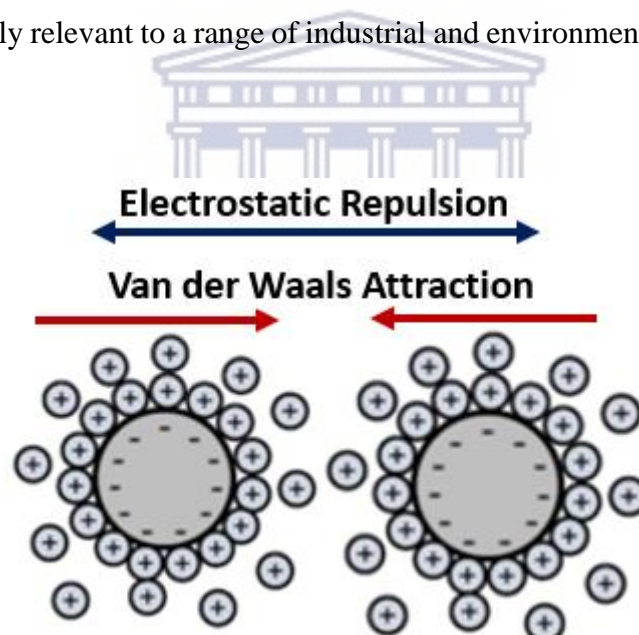


Figure 2.6. Schematic representation of the Electrostatic and Van der Waals forces. Adapted from [228].

It is generally accepted, as presented in **Figure 2.6**, there are two fundamental intermolecular forces that act on an emulsion droplet and in turn affect the stability of an emulsion, these include:

- Van der Waals forces, which are short-range attractive interactions and dominate when the separation distance between the droplet surfaces is small,

- Electrostatic forces, also known as Coulombic forces, which are repulsive forces, acting between the negatively charged oil droplets.

When the attractive forces are weaker than the repelling forces, the droplets remain dispersed, resulting in the emulsion being stable.

2.6.1. Van der Waals Interaction

The van der Waals (VdW) forces exist between atoms, molecules and colloidal particles including emulsion droplets [241]. These forces originate from the electric dipoles in the atoms and molecules [220]. These electric dipoles develop from oscillations in the electron clouds of atoms and molecules. The VdW interaction is a universal force and is present in every system. As mentioned in the previous section, the VdW force between similar particles in a medium is always attractive. Droplets further away from each other are also affected by the VdW force, however the force is relatively weak [227,242]. The VdW force increases rapidly with decreasing distance between droplets and results in irreversible droplet aggregation in the absence of any repulsive forces [183].

In stable emulsions, it is accepted that a counteracting repulsive force is present that prevents flocculation, creaming, sedimentation and eventual coalescence, this electrostatic interaction is a result of the charge on the particle surfaces and can be explained via the electrical double layer model.

2.6.2. Electrostatic Interaction

The electric double layer (EDL) model is an important concept in understanding the mechanism of the electrostatic interaction, which is associated with the stabilisation of colloids and emulsions [220,243,244]. In general, most particles and oil droplets dispersed in water have a negative surface charge and this results in the EDL [220,245].

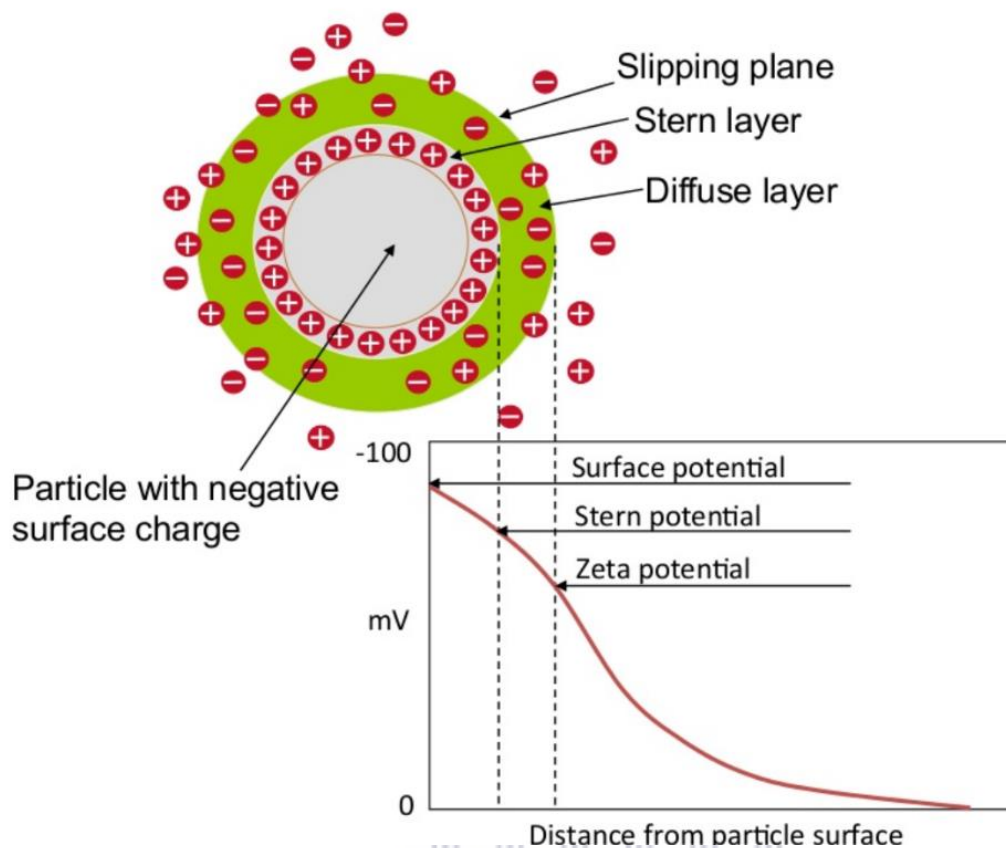


Figure 2.7. Diagrammatic representation of the electrical double layer. Adapted from [232].

The EDL is electrically neutral and consists of the following distinct parts around the droplet or particle, which is depicted in **Figure 2.7** and is described below:

Surface charge - The droplets initially have a negative charge (see section 2.4.1 above)

Stern layer - The negatively charged droplets attract positively charged ions that attach firmly to the charged droplet, forming a rigid layer around the droplet.

Diffuse layer – Outward from the Stern layer there is a concentration of free counter-ions. This region is called the diffuse layer and together both layers are referred to as the EDL [228].

Slipping plane – Is the boundary layer that develops as the colloidal particle moves in the medium and consists of the surrounding liquid close to the particle.

The electrical potential decreases with an increase in distance from the surface of the droplet. The ζ potential is the electric potential at the slipping plane and is an important parameter in

the theory and measurement of interaction between colloidal particles [219]. The electrical potential is at its maximum value on the droplet surface.

The approach of two charged oil droplets closer to the thickness of the double layers results in electrostatic interactions and the generation of an electrostatic force between the droplets [244]. It is this electrostatic repulsive force that prevents the droplets from aggregating and consequently contributes to the stability of the emulsion [246,247].

As highlighted in the previous section, the forces interacting on oil droplets in an emulsion can be categorised according to the DLVO theory [182]. The DLVO theory was developed in the 1940's and is named after the Russian scientists B. Derjaguin and L. Landau with Dutch scientists E. Verwey and J. Overbeek. The theory represents the cornerstone of the understanding of interactions between colloidal particles and their associated aggregation behaviour [182,183].

The theory, however, has its limitations and the existence of non-DLVO forces has also been proposed and observed [114,244,246–248], and will be discussed in more detail in the ensuing sections.

Non-DVLO forces described in the literature includes following:

- Hydration sphere repulsion
- Hydrophobic attraction

When polymers are added to the emulsion the following forces are present:

- Depletion attraction
- Bridging attraction
- Steric repulsion

The DVLO and non-DVLO forces are described in more detail in the following sections.

2.6.3. DLVO model

The DLVO model represents the basis of colloidal particle interactions and their associated aggregation behaviour [120]. The DLVO theory of emulsions is based on the following assumptions, which include the following:

- The dispersion is dilute
- The droplets of the emulsion have the same charge [220,241]
- The charge is distributed uniformly over the droplet surface
- Only two forces act on the emulsion droplet, these are van der Waals (V_{dW}) and electrostatic forces
- The distribution of ions in solution is a function of the electrostatic force and Brownian motion

The total energy interaction (V_T) between two droplets is the resultant force of the sum of the attractive (V_{VdW}) and repulsive (V_{elec}) force, which in simplistic terms can be described by Equation 2.3,

$$V_T = V_{VdW} + V_{elec} \quad \text{Equation 2.3}$$

The total energy interaction (V_T), between two oil droplets, is obtained by Equation 2.3 and can be plotted as a function of interparticle distance.

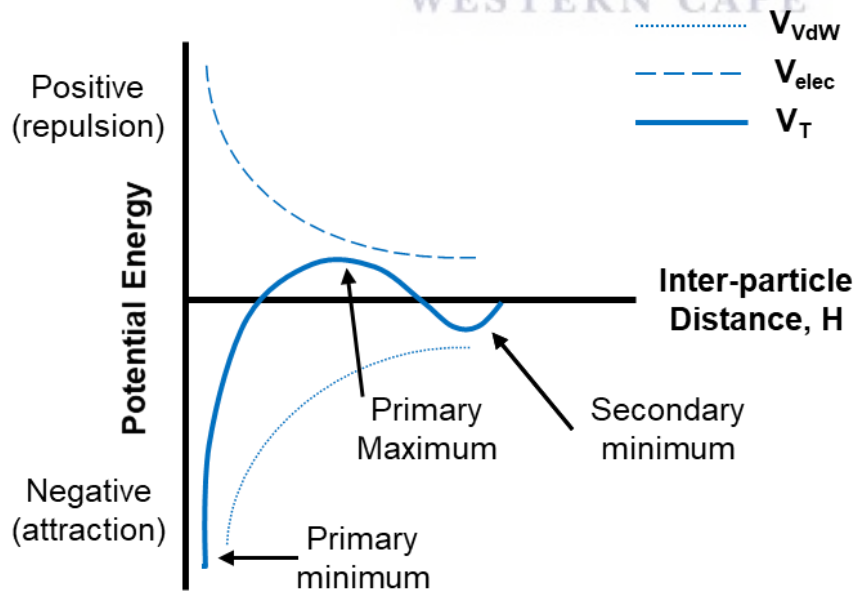


Figure 2.8. Energy interaction for stable dispersions as per the classical DLVO theory. Adapted from [228].

A typical interaction of stable dispersions as per the classical DLVO theory with distance is depicted in **Figure 2.8**.

The primary minimum is the lowest-energy state of an emulsion and this is where the droplets are expected to reside in a completely phase separated emulsion [183]. The primary maximum is the energy barrier that must be overcome for coalescence to occur. The secondary minimum is generally seen as the flocculated state, the droplets will only coalesce when they overcome the primary maximum and reach the primary minimum energy state [182].

When two droplets in an emulsion collide, the following outcomes are potentially possible:

- The droplets collide, do not aggregate but bounce off each other
- They aggregate, flocculate but do not coalesce
- The droplets collide and coalesce. This only happens when the droplets collide with enough energy to surpass the primary maximum state

DLVO theory suggests that the stability opposing aggregation in an emulsion is a function of van der Waals attraction and electrostatic repulsion [182]. However, these two forces do not represent a full account of all the interactions that may occur in colloidal systems [118]. The additional forces and interactions include steric repulsion, depletion attraction, hydration sphere repulsion and hydrophobic interactions, oscillatory surface forces and other forces [246]. These forces, often referred to as non-DLVO forces, will be discussed in more detail in Section 2.6.4

2.6.4. Non-DLVO Model

As highlighted in the previous sections, the interaction and behaviour of droplets in an emulsion is of significance for a quantitative understanding of the overall stability of the emulsion. For situations where the DLVO theory disagrees with experimental measurements, the model has been extended and referred to as non-DLVO forces [230,246,249].

These additional forces can be much stronger than the DLVO forces at small separation distances and can be repulsive, attractive and oscillatory. The following interactions, namely, hydrogen bonding and the hydrophobic effect, hydration force, non-charge transfer Lewis acid

base interactions and steric interactions are not considered by the traditional DLVO model [118,210,250]

The non-DVLO forces of repulsion, which act between droplets in an emulsion include:

- Steric forces, originating from hydrophilic molecules, which get attached to the surface of oil droplets [118]
- Depletion repulsive forces, are a result of hydrophilic macromolecules dissolved in an aqueous phase [250]
- Hydration forces are observed at small distances between droplets and result in the surfaces repelling each other [251]

The non-DVLO forces of attraction, which act between droplets in an emulsion include:

- The hydrophobic effect, which describes the attraction between hydrophobic molecules and surfaces that draws them together [210,220,252,253]
- Depletion attraction forces occur in emulsions that have a combination of large and small droplets. According to the literature, the small droplets push the larger droplets toward each other when the separation distance between the larger droplets is less than the size of the small droplets [250,254]

Of particular importance in the understanding of emulsion stability and processing has been research associated with the role of polymers either to stabilise the emulsion or to destabilise it for processing [118,255].

2.6.4.1. Non-DLVO forces resulting from polymer addition

Polymers are widely used as emulsion stabilisers in a number of industries and in particular protein polymers are used in the food and pharmaceutical industries [255]. The addition of polymers to an emulsion can facilitate the breakage of oil droplets during emulsification, by lowering the oil–water interfacial tension, as well as stabilising the droplets against coalescence during emulsification as well as during storage of the formed emulsions [118].

The non-DVLO forces, which arise from the addition of polymers to an emulsion as depicted in **Figure 2.8** include:

- Depletion attraction

- Steric depletion, and
- Bridging flocculation

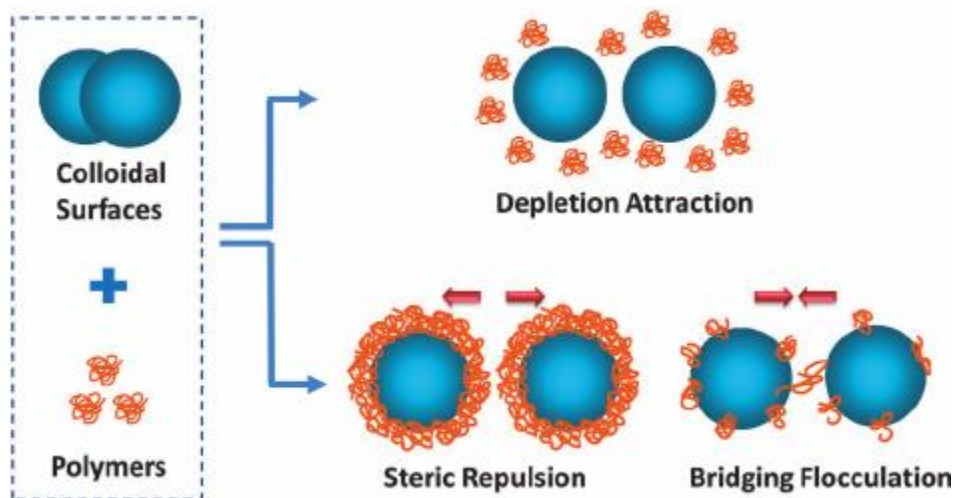


Figure 2.9. Forms of non-DVLO forces developed through the addition of polymers.

The efficiency of polymer agents depends on the density and structure of the polymer's adsorption layers on the droplet surface [223,250,256,257]. The quantity of polymer adsorbed and the structure of the adsorbed polymers is a function of a number of factors, which include the polymer and electrolyte concentration, pH, pre-heating of the polymer solutions and type of the polar phase [256,258,259]. It should be noted these effects are still not well understood and require additional research in the field.

2.6.4.2. Depletion attraction

Depletion interaction processes have been widely used and reported on in colloid chemistry since the theory was first proposed in the 1950's by Asakura *et al.* [193,242,254]. The theory describes the presence of an attractive force appearing between two bodies immersed in a solution of macromolecules, *i.e.* polymers. The magnitude of the force varies with concentration, shape and charge of the polymers [250,257]. The depletion interaction is an entropic interaction that occurs in a mixture of large and small colloids [223]. This force functions as an attractive interaction between droplets and is schematically presented in the top half of **Figure 2.9** [254].

2.6.4.3. Steric repulsion

Steric repulsions are forces between emulsion droplets that result from adsorption of polymer chains on emulsion droplets and are defined quantitatively in terms of the free energy change during that adsorption process. [118]. The stabilising role of the adsorbed polymers is explained by their effect on the surface forces, e.g., by modifying the electrical potential of the droplet surface and the Van der Waals interactions or by creating a steric barrier to droplet coalescence. The most important type of steric interaction is repulsive in nature and the phenomenon is often described as a volume restriction effect [260]. It is commonly referred to as steric or overlap repulsion and is schematically illustrated in the bottom half of **Figure 2.9**.

The physical basis of the steric repulsion is a combination of (i) a volume restriction effect arising from the decrease in possible configurations in the region between the two surfaces and (ii) an osmotic effect due to the relatively high concentration of adsorbed polymers in the region between the two surfaces as they approach one another. It is assumed here that the particles themselves are impenetrable.

The polymer adsorption layers result in the stabilisation of the emulsion films formed between neighbouring droplets against rupture. The detailed molecular mechanisms for emulsion stabilisation by adsorbed polymers are still only poorly understood and are constantly being investigated to gain a better understanding.

2.6.5. Pickering emulsions

Solid particles added to an oil-in-water emulsion may attach to droplets and impart stability for significant periods, which could last for weeks or even months [261–263]. Particle stabilised emulsions, also known as Pickering emulsions, have garnered interest in recent years and in particular the process by which particles alter the stability of an emulsion [264]. The particles stabilise the emulsion preventing processes such as flocculation and coalescence [262].

Conventional Pickering stabilisers include rigid micro or nano sized particles of highly cross-linked polymers, which include compounds such as polystyrene polymethylmethacrylate and amorphous solids like silica [213]. Particle stabilised oil droplets may have applications as drug delivery or formulations may attach to droplets and impart kinetic stability for significant periods, namely weeks or even months [261–263,265].

Softer particles like proteins have been used effectively for the stabilisation of emulsions [213,264]. Predicting the lifetime of an emulsion and the processes by which it destabilises remains challenging, even for surfactant and Pickering stabilised emulsions [165,261–263,265,266].

2.7. Principles of emulsion processing

The technologies and processes associated with breaking and separating emulsions into the phases of oil and water can be induced chemically, electrically and physically [101,112,139,147,156]. This process of breaking and separating emulsions is called demulsification. Technologies for treating emulsions of oily wastewater include gravity separation, microfiltration and ultrafiltration, membrane separation, activated carbon adsorption, dissolved air flotation, induced air flotation, electro flotation, column flotation, biochemistry, coagulation, coalescence, hydrocyclonic separation as well as many novel and hybrid systems [81,101,112,114,139,147,156,267,268].

In order to initiate the separation of the emulsion, droplets need to collide, aggregate and coalesce to form larger droplets and eventually free oil. Droplets can collide under the influence of three different transport mechanisms, namely Brownian diffusion, fluid convection and droplet interactions [269].

In summary, the process of emulsion separation can be understood as follows:

1. The oil droplets in an emulsion are negatively charged
2. All of the oil droplets take on the same charge
3. Droplets need to collide to aggregate, flocculate and coalesce to form free oil
4. In a pure oil-in-water emulsion, particularly with a small DSD, the electrostatic repulsive force between droplets prevents the droplets from aggregating, flocculating and coalescing; implying their ζ potential is too strong and Brownian diffusion is not sufficient as a transport mechanism to overcome electrostatic repulsion

Different results may occur when two droplets collide depending on the droplet size and the possible presence of surfactants as schematically represented in **Figure 2.10**:

- (i) the droplets can rebound;

- (ii) they can flocculate if the intermolecular repulsive forces are sufficiently strong to hold the droplets separated at a small equilibrium distance;
- (iii) they can coalesce if the film ruptures.

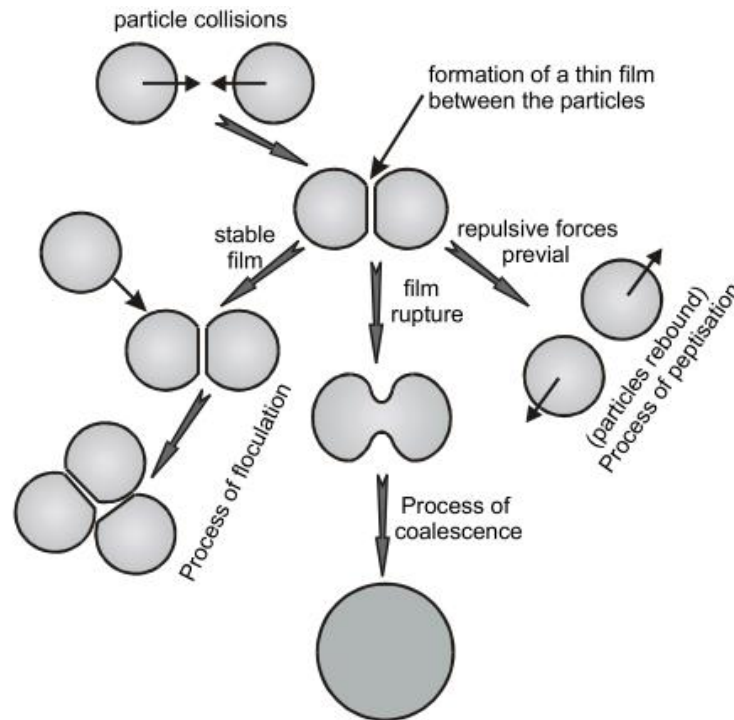


Figure 2.10. Process of droplet approach and coalescence. Adapted from [120].

Taking into account the above, one of the key processes always considered in emulsion treatment is charge neutralisation and electrical double layer compression of the individual droplet [270,271]. This reduces the repulsive potential of the droplets and allows them to approach each other in closer proximity, potentially forming microflocs. This process of charge neutralisation and electrical double layer compression of the individual droplets is known as coagulation [41,259].

The neutralised surface charge and electrical double layer compression directly impacts and lowers the ζ potential of the emulsion, which then allows droplet interactions causing droplet aggregation [272]. Despite coagulation being a very simple process arising from droplet charge neutralisation, it is often confused with flocculation. The difference between the two processes will be further explained in the following sections.

2.7.1. Coagulation

Coagulation is an essential process in wastewater treatment [168,169]. As reported in the literature, coagulation is one of the most widely applied processes for water and wastewater treatment to remove suspended particles, decrease turbidity, remove colour and remove pathogens [9,47,122,124,125,168,273–275].

Coagulation is a process that is considered to alter the nature of droplet interactions [276–278]. In the treatment of emulsions, the coagulation process disrupts the electrostatic stability of the emulsion and in particular assists with enhancing the collision of emulsion droplets [7,279]. The droplet interactions during coagulation are enhanced due to charge neutralisation resulting in aggregation and the formation of microflocs or free oil [125].

The efficiency of coagulation depends on a number of factors such as temperature, pH, dose and type of coagulant material, the size and distribution of the particles, total dissolved solids (TDS) and the concentration the colloidal particles in the suspension. With these parameters, the molecular and chemical characteristics of the pollutants need to be taken into account before selecting and applying the process of coagulation.

2.7.1.1. Coagulation mechanisms

In the literature, four mechanisms of coagulation are generally referred to, which include, charge neutralisation, adsorption, bridging and sweep [276–278]. **Figure 2.11**, depicts graphically the coagulation mechanisms.

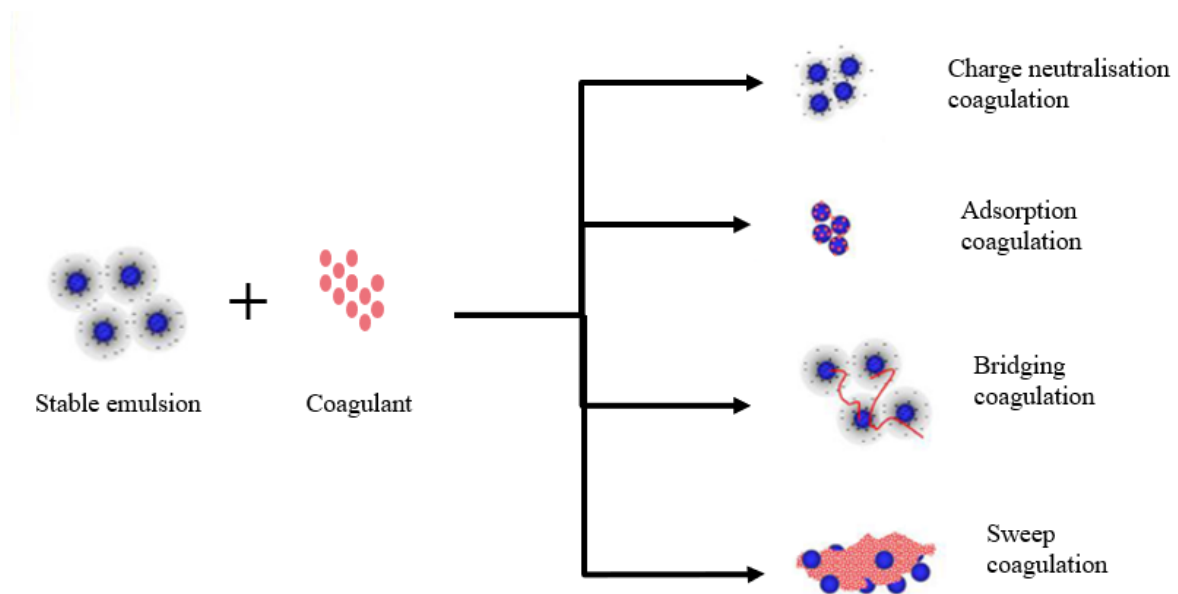


Figure 2.11. Schematic representation of the mechanisms of charge neutralisation and micro floc formation during coagulation in a colloidal suspension.

Charge neutralisation coagulation also often referred to as electrical double layer compression, occurs when the coagulants added to an emulsion result in increasing the concentration of positively charged ions in the diffuse layer around the droplets [278]. This results in the compression of the diffuse double layer and lessens the electrostatic repulsive forces between approaching droplets [41,259,280].

Adsorption coagulation takes place with the addition of coagulant which results in cations species being adsorbed onto the surfaces of the oil droplets, which neutralises their surface charge [272,281].

Bridging coagulation, also referred to as inter droplet bridging coagulation, dominates the coagulation process, especially when chemical polymers are used as the coagulant [279,281]. The polymer adsorbs onto the droplet surface and causes charge neutralisation as well as bringing the droplets into close proximity to each other. Polymers possess chain structures that bind the particles into larger and compact agglomerates. Polymers with high molecular weight are frequently more effective due to their longer chain lengths [279,281].

Sweep coagulation, also known as colloidal entrapment or enmeshment, occurs when a metal salt is added to wastewater at concentrations sufficiently high to cause precipitation of

amorphous metal hydroxides, where droplets can be enmeshed in these precipitates [126,275,276,282]. It is the formation of these precipitates that instigate the sweep coagulation, however these precipitates, combined with oil droplets, result in the formation of sludges [12,48,124–127]. These sludges may be toxic and often require further processing. [12,128–131]. This mechanism consumes coagulants in excess of that predicted by the stoichiometry.

Coagulation is the primary treatment process used in the production of clean drinking water treatment, it involves the addition of iron or aluminium, usually added as ferric sulphate or aluminium sulphate, which are readily soluble in water, however other chemicals, such as lime (Ca oxide or hydroxide), are also employed [245,283]. At low coagulant dosages, adsorption and charge neutralisation are possibly the dominant mechanism of coagulation [276,284]. However, at high doses of coagulant sweep coagulation is the dominant coagulation mechanism [276,285].

In practice, coagulation can be achieved by chemical and electrical means and will be reviewed in the subsequent sections in more detail [286,287]. Chemical coagulation (CC) and to a lesser extent, electrocoagulation (EC), are used in wastewater treatment processes for suspended particle removal [236,288,289]. Even though both, CC and EC are used for similar applications, they specifically differ in the dosing method. With EC the coagulant is added by electrolytic oxidation of an appropriate anode material, while in CC dissolution of a chemical coagulant is used [123,288]. These different methods operate different physical and chemical regimes, which impact the mechanism of coagulation and the formation of the flocs [245].

In summary, chemical coagulation utilises chemicals to achieve coagulation while electrocoagulation technology is a treatment process involving the application of electrical current, to produce the metal coagulants at the anode [154]. Coagulation is one of the most common pre-treatment processes for a number of wastewater treatment applications, which include flotation, biological treatment, filtration and membrane methods [56,125,290–292].

2.7.1.2. Chemical coagulation

Chemical coagulation (CC) is the use of specific chemicals, called coagulants, to drive the coagulation of colloidal suspensions [286,293]. As highlighted in the previous section, the key function of the coagulant is to disrupt the forces of electrostatic repulsion, between the colloidal

particles, which in turn disrupts stability of the colloidal suspension, resulting in the formation of microflocs [169,294]. Coagulation processes utilising coagulants, are among the most widely applied processes for water and wastewater treatment [286,293]. Coagulants are typically solutions of salts with high ionic strength or polymers, which attract the colloidal particles or oil droplets causing them to agglomerate forming larger particles [295].

In the area of water treatment, clarification of water with coagulating chemical agents, coagulants, has been practiced since ancient times, using a variety of substances, with the most notable being crushed seeds. The clarification of water with coagulants has been practiced by the Egyptians, from as early as 2000 BC, using crushed almonds smeared around the inside of a vessel to clarify water [274,294,296]. The most common and commercially available coagulants are the metal salts of aluminium and iron, which include aluminium sulphate, $\text{Al}_2(\text{SO}_4)_3$, also known as alum, poly aluminium chloride (PAC), $\text{Al}_2\text{Cl}(\text{OH})_5$, ferric sulphate and ferric chloride [47,125,138,293,294,297]. Aluminium sulphate, also known as alum, has been used as a coagulant in water treatment in England for the treatment of public water supplies since 1881 [274].

In recent years, various types of coagulants have been developed and researched for emulsion separation, which include inorganic, organic, synthetic and natural polymers, biomaterial as well as combinations of materials [233,290,296]. Aluminium based coagulants such as alum and PAC are commonly used to treat drinking water to enhance the removal of particulate and colloidal material. Iron and aluminium form many different cationic species in the pH range normally used in water treatment works (7 to 8, but sometimes lower), which help destabilise the natural particles by compressing the electrical double layer and/or eliminating the negative surface charge on the particles. Many other salts and materials may be used to add cations into the water. Iron and aluminium, when added at a high enough concentration, readily precipitate in different forms of iron (III) hydroxide and aluminium (III) hydroxide.

When added to water, the aluminium and iron salts dissociate and hydrolyse to form soluble polymeric and monomeric hydrolysed metal species, which form positively charged metal complexes and interact with the negatively charged droplets prior to precipitation. Mattson in 1928 concluded that the hydrolysis products of the coagulant species is responsible for the reduction in the turbidity and colour during water treatment [271,298].

The following Al hydrolysis products may be involved:

- five monomers (Al^{3+} , $\text{Al}(\text{OH})^{2+}$, $\text{Al}(\text{OH})_2^+$, $\text{Al}(\text{OH})_3$ and $\text{Al}(\text{OH})_4^-$)
- three polymeric species ($\text{Al}_2(\text{OH})_2^{4+}$, $\text{Al}_3(\text{OH})_4^{5+}$ and $\text{Al}_{13}\text{O}_4(\text{OH})_{24}^{7+}$)
- as well as solid precipitate $\text{Al}(\text{OH})_3$

It should be noted that the above Al hydrolysis species do not exist as free ions in water, but will always be hydrated with varying numbers of water molecules.

Several other formulae for polymeric Al species have been reported in literature, which include, $\text{Al}_{13}\text{O}_4(\text{OH})_{24}^{7+}$, often denoted by Al_{13} , which is the most effective and stable Al species in wastewater treatment [299]. As highlighted previously and reported extensively by Sillanpää *et al.*, [125] for Al-based coagulant, the mechanism is the positive Al hydrolysis products and specifically Al-based precipitates that act as the drivers of emulsion destabilisation. The destabilisation process occurs through adsorptive deposition resulting in the charge neutralisation of the negatively charged particles. The positively charged Al-based precipitates neutralise dissolved anionic organic compounds and promotes precipitation. An example of this is with the carboxylic and phenolic functional groups in organic compounds, which can be neutralised by the hydrolysis products of alum [125].

Fe(III) hydrolysis products are considered to be:

- five monomers, Fe^{3+} , $\text{Fe}(\text{OH})^{2+}$, $\text{Fe}(\text{OH})_2^+$, $\text{Fe}(\text{OH})_3$ and $\text{Fe}(\text{OH})_4^-$
- a dimer $\text{Fe}_2(\text{OH})_2^{4+}$
- a trimer $\text{Fe}_3(\text{OH})_4^{5+}$
- and a solid precipitate $\text{Fe}(\text{OH})_3$

It should be noted that the above Fe hydrolysis species do not exist as free ions in water, but will always be hydrated with varying numbers of water molecules.

As highlighted in **Figure 2.12**, the metal salts increase the concentration of positively charged ions in the diffuse layer around the particle, resulting in the compression of the EDL, reduction of the electrostatic repulsive forces between droplets and the formation of microflocs. [280]. The microflocs formed during coagulation are usually small, compact and extremely fragile.

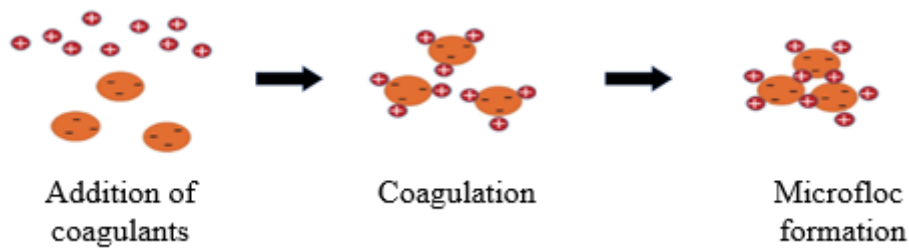


Figure 2.12. Schematic representation of the mechanisms of charge neutralisation and microfloc formation during coagulation in a colloidal suspension.

The extensive use and application of Al based coagulants in recent years have been a function of cost, where overall availability and efficiency to reduce turbidity are the main reasons for the prolonged application of Al based salts. It has also been reported that Al coagulants resulted in higher removal of organic content from wastewater as compared to other coagulants [237,300].

The toxicity issues of Al-based coagulants can possibly be attributed to monomeric aluminium ions, which are more available to living organisms than polymeric aluminium [115,263]. The residual aluminium concentration in the treated water was also found to be lower with PAC compared to using other aluminium based coagulants. The ancillary pollution generated from the addition of chemicals is considered the main drawback of the CC process. Lately, the application of ferric coagulants is gaining ground over the aluminium counter parts mainly due to the suspected health risks associated with residual aluminium and the better separation and removal capacities of ferric coagulants [130,136,302].

Determining the correct coagulant concentration and dosing process are important parameters and determine the overall treatment efficiency. It has been reported that coagulant overdosing results in a significant increase in the quantity of sludge generated and a decrease in pH [277,303]. An incorrect coagulant may also result in residual coagulant metals remaining in the treated water, hence the need for a closely regulated coagulation process [2,130,300]. According to reports, alum specifically produces significant amounts of sludge, but with a lower solids content, as compared with ferric chloride, which produces relatively smaller volumes of sludge [277,296].

As highlighted previously, the pH is also an important parameter to be optimised to establish an efficient coagulation process. In this regard, when the reaction pH is above the pH at which the coagulant solubility is minimal, 5.8 and 6.3 for ferric chloride and aluminium chloride respectively, high molar mass polymers species are generated [283]. When the pH is below the pH at which the coagulant solubility is minimal, medium mass polymers or monomers are produced. The higher pH is preferred because of higher solubility of the coagulant.

The selection of the coagulant for a specific emulsion is probably the most important initial process parameter and this is typically done through a jar test [304]. According to literature, the main operating conditions and parameters affecting the overall efficiency of any coagulation process are pH, the coagulant type and dosage [44,296,305,306]. Rapid mixing is required for proper dispersion of coagulant chemicals, to promote particle collisions and micro floc formation [307].

2.7.1.3. Electrocoagulation

Electrocoagulation (EC) technology is a wastewater treatment process that applies an electrical current to treat and remove wastewater contaminants [154,286,308–310]. EC is an alternative to classical chemical coagulation, as it reduces the need for chemicals. The anodic electrodes deliver the coagulant directly into the suspension electrochemically [169,245,311].

The most basic EC reactor consists of an electrolytic cell with an anode and a cathode [312,313]. EC uses iron or aluminium metal sheet electrodes that are arranged in anode and cathode pairs [314]. When electrochemically oxidised, the anodes generate the most commonly used ionic coagulants namely, Fe^{3+} (the initially formed Fe^{2+} is rapidly oxidised in air to Fe^{3+}) and Al^{3+} [278]. As with CC, the dissolved Al^{3+} or Fe^{3+} ions are hydrolysed to form polymeric coagulant species [123,311,315].

Over the last few decades EC has become recognised as an efficient technology for various wastewater treatment applications, including organic matter removal and emulsion processing [7,38,286,316–318].

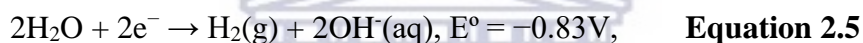
The dissolution of coagulant into solution is governed by Faraday's Law, as depicted by Equation 2.4 [303]:

$$w = (i \cdot t \cdot M) / (Z \cdot F), \quad \text{Equation 2.4}$$

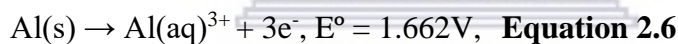
w = metal dissolving (g/cm²), i = current intensity (A/cm²), t = time (s), M = molecular weight of metal (g/mol), Z = number of electrons involved in the oxidation/reduction reaction, F = Faraday's constant = 9.64×10^4 coulombs per mole.

For EC the active coagulant species are generated in situ by electrolytic oxidation of an appropriate anode material, therefore differing from the direct application of chemical coagulants such as metal salts or polymers and polyelectrolytes. The electrochemical half reactions occurring in the EC cell, utilising an aluminium anode and their corresponding standard electrode potentials, illustrated by Equations 2.5 and 2.6, are:

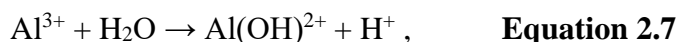
Cathode:



Anode:



$\text{Al}(\text{aq})^{3+}$ species produced by electrolytic dissolution of the anode (Equation 2.6) immediately undergo spontaneous hydrolysis reactions, which generate various monomeric species according to the following sequence (omitting co-ordinated water molecules for convenience):



Hydrolysis reactions, illustrated by Equations 2.7– 2.9 make the anode vicinity acidic. Conversely, hydrogen evolution at the cathode (Equation. 2.5) makes the electrode vicinity alkaline. Cationic hydrolysis products of aluminium then react with OH^- ions to transform finally in the bulk solution into amorphous $\text{Al}(\text{OH})_3(\text{s})$ [319].

In EC, as opposed to in CC, no negative counter ions besides OH^- are added. Cl^- or SO_4^{2-} ions can influence the aluminium hydrolysed species, because they can replace the hydroxyl ions and their absence in EC may affect the coagulation mechanisms.

The overall efficiency of the EC processes is a function of the duration of the electrolysis, the value of the electrical current, concentrations of the targeted contaminants, pH and conductivity of the aqueous phase. To date, several studies have investigated the use of EC to improve the separation of emulsions; these have also included the use of EC in combination with other technologies like centrifugation, filtration, heating and chemical treatment [320]. In the literature, EC is also often referred to as electro-coalescence [154,320–322].

High commercial electricity consumption is one of the disadvantages in the operation of lengthy electrocoagulation processes. To alleviate this problem, an integrated photovoltaic-electrocoagulation system has been demonstrated and used in treating oil palm mill effluent [323].

In wastewater treatment, in order to increase the overall efficiency, coagulation is almost always utilised as a pre-treatment process followed by processes such as flocculation, filtration or flotation. It should be noted that coagulation and flocculation are distinctly different processes and phenomena. A number of literature reports incorrectly use the term coagulation and flocculation interchangeably, coagulation is correctly defined as the electrostatic disruption and destabilisation of colloidal particles [14,129,238]. Flocculation describes the process in which the destabilised particles are induced to make contact leading to the formation of larger aggregates. Flocculation is a physical process, requiring gentle mixing in which the charge neutralised suspended colloidal particles clump together into a floc. In modern water treatment, coagulation is a fundamental process and often used as a pre-treatment process in combination with other treatment technologies [219,286,287].

2.7.2. Flocculation as a process

Flocculation is defined as a process that is used in water treatment to aggregate colloidal material after charge neutralization by coagulants, or by the use of flocculants to form floccules (flocs), which can then be removed from the solution [129,324]. Flocs can be described as loosely held aggregations of small particles or in the case of emulsions droplets.

The flocculants are typically high molecular weight synthetic polymers; however, in recent years natural environmentally friendly and biodegradable flocculants, like chitosan, tannin, various agricultural gums and resins have increasingly been used [237].

The two basic mechanisms of flocculation are particle bridging and charge patch interactions. Polymer-induced bridging occurs when droplets are adsorbed onto long-chain polymers with high molecular weight and low charge density [237,268]. The adsorption is considered to be due to hydrogen bonding between hydroxyl groups in the polymer and hydroxylated sites on particle surfaces [256]. After adsorption and attachment of the droplets, the polymers create bridges from one droplet to other droplets, forming a three-dimensional matrix, as depicted in **Figure 2.13**.

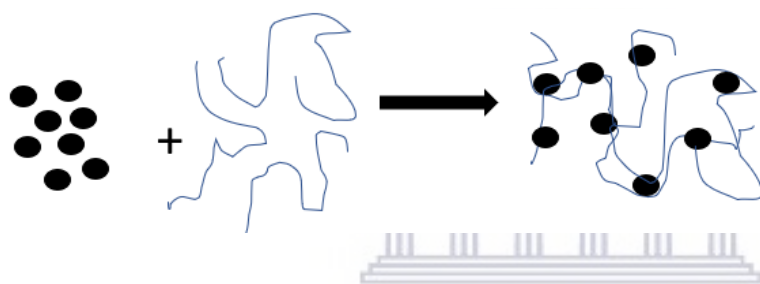


Figure 2.13. Schematic representation of polymer bridging flocculation.

Charge patch flocculation occurs when positively charged regions of a low-molecular-weight polymer adsorb colloidal particles due to their negatively charged surfaces. It is also called 'electrostatic patch' due to the formation of cationic 'patches' along the polymer chain, as depicted in **Figure 2.14**.

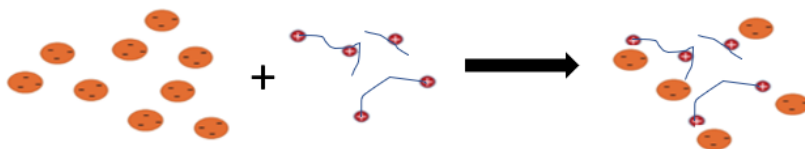


Figure 2.14. Schematic representation of charge patch flocculation.

In contrast to the process of coagulation, manipulation of the electric charge of the particle is not the dominant mechanism of flocculation. Flocculation is, in principle, all about collisions between the flocculants and the particles. The flocculation process is generally classified into two types, perikinetic and orthokinetic [324]. Perikinetic flocculation refers to collisions of droplets due to Brownian motion [325–327]. Orthokinetic flocculation is a result of bulk fluid motion, such as stirring, which results in the collisions [325–327].

Flocculation can occur as a result of the reduced surface charge of the particles and hence a decrease in electrical repulsion force between colloidal particles, which allows the VDW force of attraction to stimulate initial aggregation of colloidal and fine suspended materials.

The process of flocculation and floc formation generally involves the following steps, which occur sequentially:

- Mixing and dispersion of the flocculant,
- Adsorption of the particles onto the flocculant,
- Aggregation of the combined particle /flocculant species,
- The development of larger and stronger flocs.

Flocs are fragile with various internal structures and in recent years researchers have focused on the floc breakage and regrowth process to better understand floc characteristics and formation mechanisms [306,328]. The rate of floc formation is a balance between breakage and formation, with the process eventually reaching a steady state either peri- or orthokinetically. The parameters that still need clarification include the number of bonds, location of attachment points and internal attractive and repulsive forces within the structure. Better flocculants can be developed on the basis of improved understanding of the flocculation mechanism.

Flocculation combined with other treatment processes can be more efficient than flocculation as a process on its own [329].

2.7.3. Hybrid methods of oil separation

It is evident that based on the scale and complexity of oil pollution in water, there is not one technique that can be considered the silver bullet for treating and processing oily wastewaters

and emulsions [7,271,330,331]. It is evident that the integration of various technologies, processes and methods to obtain the most optimised configuration and methodology is essential and a necessity for efficiently processing oily wastewater [20,78,110,292,332].

A number of researchers have to date evaluated and reported on the basis and design of novel hybrid wastewater treatment systems and these have been successfully applied in a number of other industrial wastewater associated applications [46,113,192,332]. Multiple hybrid treatment technologies are currently being studied, including biodegradation, advanced oxidation processes, electrocoagulation and microbial fuel cell technology [62,169,245,311,333].

The next sections of this thesis, review the effectiveness of different coagulation-based hybrid treatment methods applied to oily wastewaters and emulsions.

2.7.4. Coagulation / flocculation

Coagulation followed by flocculation is one of the most widely used process combinations for the removal of suspended solids, colloidal material, organic matter and for emulsion processing [17,124,129,274,275]. It is a relatively simple and efficient method for wastewater treatment and has been extensively used for the treatment of various types of wastewater and widely employed in many industrial fields, including mining, oil extraction and paper production [160,237,334]. It is essential that the fundamentals of the processes are clearly understood in order to maintain the desired processing results.

The efficiency of coagulation / flocculation, depends on factors such as temperature, ionic strength, pH, type and dose of coagulant material, the size and distribution, TDS, concentration and properties of organic materials and colloidal particles in suspension.

Flocculants facilitate the agglomeration of the coagulated particles to form larger floccules and thereby hasten gravitational settling. In wastewater treatment, coagulation and flocculation are employed, to generate flocs following which, a solid separation process is employed to separate suspended solids from the aqueous phase [17,124,129,160,237,274,275,334]. Many researchers have added coagulants during wastewater treatment even though it was not necessary. When flocculation occurs after a coagulation process, the micro flocs created during

the coagulation process are further aggregated to form larger flocs utilising controlled levels of flocculants and mixing [237,268,329]. Coagulation–flocculation is a two-phase process designed at destabilising colloidal particles and aggregating the particles into larger flocs which is then followed by a separation process [286].

Flocculation is the second part of the hybrid process that results in the aggregation of coagulated particles and floc formation. Particle aggregation is contingent on the degree of destabilisation achieved during the coagulation process and on the rate of successful collision between the particles. According to the literature, flow system forces and the collision geometry will have a major impact the floc structure which varies significantly between different systems [286]. Coagulation with flocculation in sequential steps are common pre-treatment processes for a number of wastewater treatment applications such as flotation, biological treatment, filtration and membrane methods.

2.7.5. Coagulation / flocculation / flotation

Coagulation with flocculation, has most notably been used for the separation of oil from oil in water emulsions, as a pre-treatment method with other water treatment technologies such as dissolved air flotation (DAF) or membrane processes, as depicted in **Figure 2.15** [125,160,168,275].

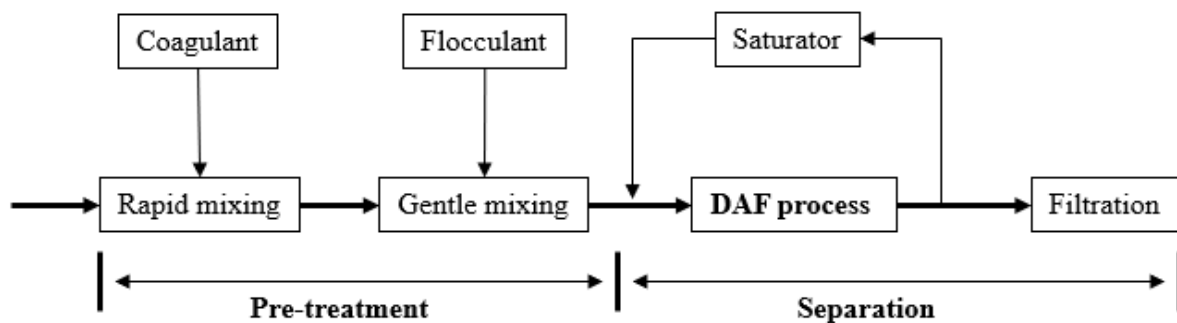


Figure 2.15. Wastewater treatment utilising DAF with coagulation and flocculation as pretreatment.

Gas flotation is a process whereby suspended particles are separated from the liquid bulk phase with the assistance of gas bubbles. These bubbles are introduced into the wastewater stream and adhere to the solid particles as they rise through the liquid phase [335,336]. The attached

bubble drastically improves the buoyancy of the particle and causes the particle to rise to the surface.

The general approach of the flotation process is to pre-treat the wastewater with coagulants and flocculants [337]. The gas bubbles, usually air, selectively attach to the flocculated solids and carry them to the surface of the liquid where they can be separated. The efficiency of the flotation process is a function of the probability of particle-bubble collision, particle-bubble attachment and particle-bubble detachment [338,339]. The flotation and separation of fine droplet emulsions usually requires, coagulants, flocculants, small bubbles and quiescent conditions in the separation zone of the flotation unit [62,336,340]. It is important to note that in order to increase the efficiency of the flotation process the bubbles preferably need to be (much) smaller than the particles to be floated. It is for this reason that coagulation and flocculation parameters need to be optimal in order to get the best flotation performance.

Gas flotation methods have been used for several decades in drinking water treatment as an alternative clarification method to sedimentation. During flotation, fine particles, oil droplets and other colloidal contaminants are removed from wastewater utilising the hydrophobic or hydrophilic properties of these contaminants, where the particle–bubble interaction is the fundamental process. However, the principles governing the interactions are not fully understood in detail.

Flotation as a wastewater treatment technique has been studied and reported in detail and has proved to be a cost-effective method to process oily wastewater and emulsions, which are not easily processed by other standard separation techniques [15,56,62,268,341]. By attaching gas bubbles to the oil droplets, both oil and associated solids can be floated to the surface. Separation of oily wastewater is enhanced by the rise velocity of the gas bubble being much higher than that of a comparably sized oil droplet, due to the higher specific gravity differential with water [329]. The mechanism of flotation for oil separation is a function of the forces in the bubble-droplet, the differences in density between the gas bubble, oil droplet aggregations and the aqueous phase [11,63,342].

Flotation is considered an effective process for oily wastewater treatment with the appropriate pre-treatment for increasing the DSD of the oil droplets or oil aggregates in the emulsion [57,340,343]. The other important aspect is that the oil droplet must be brought into contact

with the bubbles in order for the bubbles to attach to the droplet surface [62,145,335,344]. The principle is that if the bubbles and the droplets don't come into contact, flotation will not take place [268,338,345–347]. The floated oil droplets rise to the surface, while the processed water is removed from the bottom of the flotation tank. In order to remove dissolved organic compounds from the wastewater, post flotation treatment processes are implemented [103].

Efficient flotation can only be achieved if the surface properties of the oil droplets are thoroughly understood in order to create the conditions necessary for the optimal amounts of chemicals to be added, which has a direct impact on costs. With cost reduction and the utilisation of less chemicals, flotation technology could become more widely considered for emulsion treatment and processing. As observed in the literature, flotation is slowly becoming a technology of interest for processing and treating oily wastewater, specifically where the density of the oil is close to that of the aqueous phase [6,16,18,43,145].

Flotation processes for o/w emulsion separation is a function of the physicochemical properties of the aqueous phase, gas bubbles and the oil phase [257]. Understanding the physical and chemical properties of these parameters is a prerequisite to achieve an optimal and a functional flotation process [348]. The density and viscosity of the fluids, as well as the interfacial tensions between the fluids need to be carefully considered in order to design an efficient flotation process. Important parameters to consider include, size of bubbles generated, oil droplet size, the bubble droplet attachment as well as the bubble rise rate [349].

The use of chemicals, such as coagulants and flocculants is mostly utilised prior to the flotation process, however, the chemicals may contaminate the water and/or degrade the oil, which produces large quantities of potentially toxic water and sludge [125,136,158,296,350]. The sludge often requires further processing and dewatering, following which it is often disposed of at solid waste landfills where it is exposed to the environment [121,122,128,351]. The current drivers in oil in water emulsion treatment are to produce clean water and to recover the oil as a secondary product for reuse [127,174,352].

As reported in the literature, small gas bubbles can adhere and capture small oil droplets, while larger bubbles capture the larger oil droplets, implying that a range of gas bubble sizes is advantageous for optimal emulsion separation [340,348]. In addition to bubbles, chemical pre-treatment is usually required for effective emulsion treatment in order to ensure destabilisation,

the coalescence of oil droplets and phase separation. Gas bubbles and oil droplet collisions and adhesion is a crucial step in gas flotation, which can only be successfully achieved if this mechanism is understood.

The mechanism where gas bubbles and oil droplets interact, can be explained as the entrapment of gas bubbles by oil droplets to facilitate the rapid flotation and separation of the oil. Initially there must be a collision between the bubble and the oil droplet. Due to the fact that gas rises faster than oil, the flow pattern around the rising bubble could be reducing the possibility of attachment. Oily water flotation processes require the following important steps, which include [1,6]:

- Flocculation and coalescence of oil droplets,
- Collision of oil droplets and gas bubbles, the attachment of bubbles to oil droplets and the spreading oil droplets onto gas bubbles are required for successful flotation, and
- The rise and flotation of flocculated and coalesced oil droplets to the surface.

From an oily wastewater processing perspective, flotation as a technology has proved itself to be an established, feasible and practical method [162]. Depending on the parameters of the wastewater, coagulation and flocculation is often utilised as an essential pre-treatment process for efficient flotation. The flotation process depends strongly on the charge of the particles and bubbles with the maximum rate of flotation achieved when the ζ potential of the bubbles and particles are substantially different [60,353,354].

By increasing the collision frequency between bubbles and droplets and capture efficiencies, greater separation efficiencies can be achieved. Increasing the amount of gas utilised and reducing the bubble size in the flotation process, collision probability between bubbles and oil droplets can be increased. Through efficient coagulation and the generation and use of micro sized bubbles the adhesion efficiency can also be increased.

Flotation is considered a complex process, that is a function of thermodynamic and hydrodynamic forces associated with physicochemical interactions. The process of oil flotation is in essence different to mineral flotation in the fact that the oil droplets and the bubbles are elastic and have the same charge, which often results in them deforming each other rather than resulting in attachment. It is experimentally and theoretically clear that the flotation rate

increases with increasing particle size. Because of this, a number of techniques have been developed, which increase particle size. All of these techniques have the same feature; fine particles are induced to form flocs or aggregates [268]. A detailed review of the principles and associated mechanisms of flotation is described in the next sections.

2.7.6. Flotation systems

It is generally accepted that gas flotation as a separation process had its origins in mineral ore processing and separation [355]. In mineral processing, flotation is commonly referred to as froth flotation and is a process that selectively separates materials based upon their hydrophobic or hydrophilic character. During the flotation process stable froths are utilised to selectively separate different minerals from aqueous media [58,59,268,276,356–359]. The attachment of fine hydrophobic particles to gas bubbles results in the formation of lighter flocs that can be floated and removed at the water's surface, while hydrophilic materials remain in the liquid phase, as presented in **Figure 2.16**.

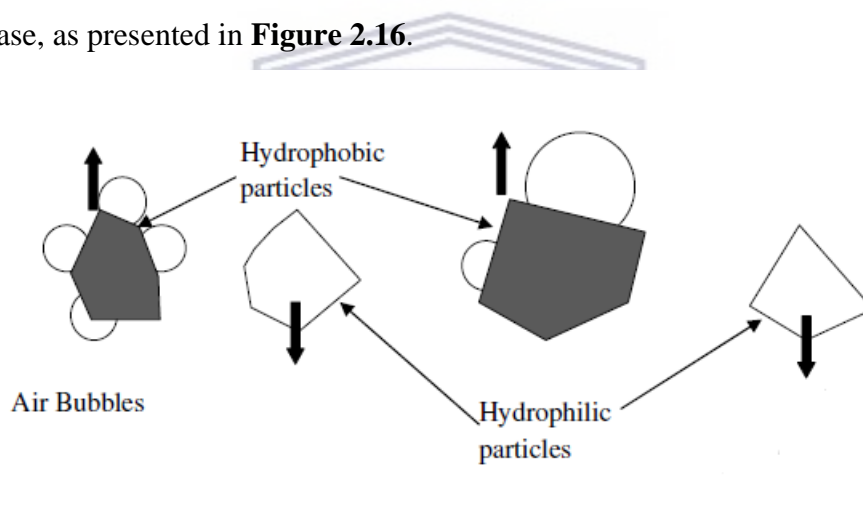


Figure 2.16. Schematic representation of the interaction of hydrophobic and hydrophilic particles with gas bubbles.

Gas flotation and sedimentation are often referred to as gravity based separation technologies and are widely used in wastewater treatment processes [56]. Flotation processes are often preferred over sedimentation techniques and systems due to the following key advantages [268]:-

- compact and smaller footprint
- retention times which are much shorter with higher loading rates
- higher effluent quality with the aid of coagulants and flocculants, and

- smaller and lighter particles have an enhanced separation efficiency

In flotation processes and systems, a variety of different gases are utilised with air being the most common [360]. In some instances, air is avoided due to the presence of oxygen, which could potentially lead to metal oxide precipitation. Carbon dioxide and nitrogen are also used as an alternative in some gas flotation applications.

Since its initial application, flotation has evolved and has become a fundamental process for oily wastewater treatment [16,62,216,335,343,361,362]. The attachment of droplets on a bubble is the result of a successful collision, attachment and the balancing of forces between the droplets and the bubble [363].

Within the relevant literature, four key steps of gas flotation treatment of oily wastewater treatment are often referred to and include:

- i. Gas bubbles generation: The quantity and size of the bubbles generated in relation to the oil droplets is essential in forming stable bubble-droplet aggregates. Low gas volumes and relatively large bubbles lead to poor droplet capture and separation efficiency [336].
- ii. Bubbles and oil droplets contact: frequent collisions between bubbles and oil droplets are required to promote bubble droplet attachment and adhesion [56].
- iii. Gas bubbles and oil droplet attachment: adhesion between oil droplets and bubbles is necessary to produce the required flotation buoyancy force. A low attachment efficiency results in ineffective separation.
- iv. Flotation of the oil aggregates and the removal of oil: the floated oil aggregates form an oil layer at the surface, which needs to be removed as part of the continuous flotation process.

The two most commonly used flotation methods for industrial applications are induced and dissolved gas flotation systems [145,307]. These systems are used in floating organic material, small suspended particles and hydrocarbons [323,364,365]. Reports in the literature have demonstrated that particles with size as small as 3 μm can be removed by flotation with coagulation and flocculation [56,291]. Gas flotation is a commonly used in processing technology for wastewater treatment, oxygenation of wine, fermentation and many other processes [58,358,366].

According to the literature, the gas bubbles need to be smaller than the particle or droplet being floated out of solution, which implies a larger surface charge and a more efficient flotation process [63,338,367]. It has also been demonstrated by Lim *et al.* [64], that microbubbles in particular enhances separation of oil in water contamination as compared to larger bubbles. In certain applications, the addition of “frothers” results in smaller bubbles with a narrower bubble size distribution [368,369]. Frothers work by preventing bubble coalescence and act in concert with gas dispersion devices to control bubble size [355,368–372]. Despite the advantages associated with using frothers, there are however some reported disadvantages which include, choosing the correct frother for the associated application, frother stability, the selectivity of the frothers in separation efficiencies as well as blends have proven to be more effective [355,370,373].

Microbubbles have a relatively high ζ potential and experimental evidence has shown that the strong negative charge of microbubbles limits their coalescence, where the bubble integrity is maintained at any depth and can remain stable for extended periods of time [343,374]. The charge of the particles, combined with higher concentration of microbubbles in the media improves separation efficiency in flotation processes by the increasing collision probability.[344,375].

The operating parameters of an IGF and DGF have been described extensively in the literature and specifically for the processing of oily wastewater and emulsions [11,16,134,171,216,307,357,362,376,377].

2.7.6.1. Induced gas flotation

IGF is often referred to in the literature as dispersed gas flotation, operates by dispersing and inducing gas bubbles into the aqueous influent [171,378]. The dispersion of gas can be achieved by mechanical or hydraulic methods.

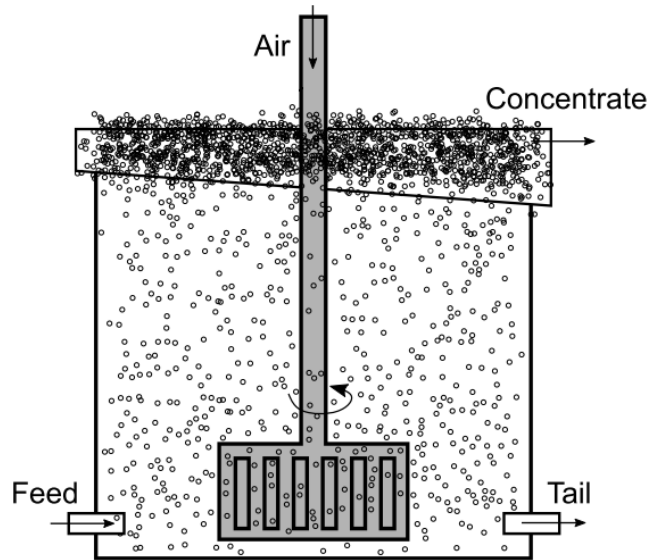


Figure 2.17. Graphical depiction of a mechanical IGF system. Adapted from [357].

As depicted in **Figure 2.17**, for mechanically based IGF, centrifugal pumps or high speed impellers are used to generate a vortex that mixes and disperses the gas into the aqueous stream which assists to generate gas bubbles [378]. For hydraulic IGF system a venturi is used to mix and entrain gas bubbles. In most systems the design requires that a portion of the processed effluent is recycled and delivered to the flotation chamber to deliver gas bubbles into the wastewater. The flotation mechanism post gas dispersion is the same for both mechanical and hydraulic IGF systems. The floated oil and other light aggregates, resulting from the bubble-droplet attachments, will rise to the surface of water where it will be skimmed off and removed.

IGF is the major flotation method for the processing of mineral ores. IGF, in terms of practical application has a number of advantages over DGF, which include a compact flotation system that can be easily setup at a laboratory scale [16,62,171]. However, due to the relative coarse bubbles produced during IGF it is less efficient than DGF, which has much smaller bubbles.

2.7.6.2. Dissolved gas flotation

DGF is a separation process for removing suspended particles from liquid by floating the particles to the surface of the liquid with gas bubbles, where the gas bubbles are formed and released into the liquid after having been dissolved in the liquid under pressure [56]. As a separation technique DGF is used to treat wastewater contaminated with microorganisms, particles and droplets with (an un-flocculated) size range of between 10 – 100 μm [379]. The

most common gas utilised is air, where air is dissolved at high pressure in a saturator, or, using a micro-bubble generating pump, and microbubbles are formed when water is released in the flotation unit at atmospheric pressure [343,380]. DAF as a process has been applied in many industries which include, wastewater treatment plants, in the mining and mineral processing industries to remove particles, as pre-treatment in desalination processes, for processing animal waste in the agricultural sectors, for wastewater at food processing plants and at crude oil refineries [343,379,381].

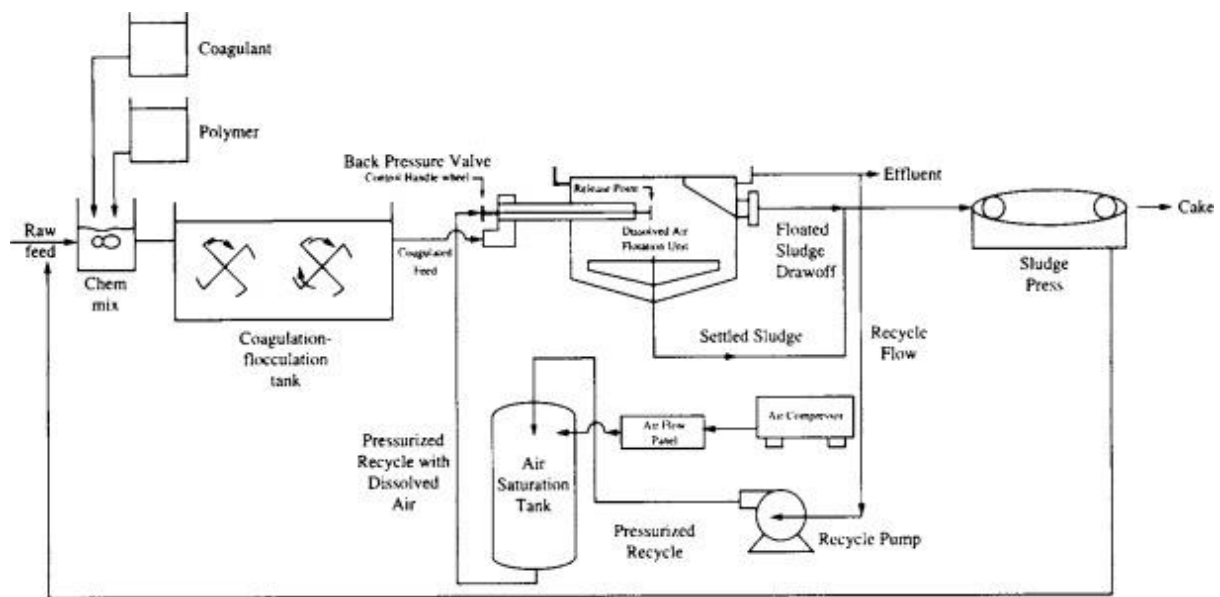


Figure 2.18. Graphical depiction of a DGF system utilising air. Adapted from [382].

As depicted in **Figure 2.18**, the water is saturated with air in a saturator at a pressure of between 1 and 5 bar [63,382]. The dissolved air in the air saturated water is released when the water is fed through a nozzle usually located at the bottom of the of the DAF tank. In the contact zone the rapid pressure reduction results in the formation and release of microbubbles [343,383].

DAF is usually considered for the clarification process when the raw source water contains low density contaminants [382]. This includes solids formed by adding inorganic aluminium or iron-based coagulants that form hydroxide flocs in alkaline solution, which on removal lower turbidity, colour and organic content.

Good coagulation is an important factor affecting flotation [160,277].

Three operating configurations have been described for DAF systems. These are:

- Full-flow pressure flotation, where the influent is pressurised and then released in the flotation tank where the bubbles are formed. This is commonly used for particles, which do not need flocculation but require large volumes of air bubbles.
- Split-flow pressure flotation, where part of the influent is pressurised and directly introduced into the flotation tank. This is employed in applications where suspended particles are susceptible to the shearing effects of pressure pump, also where suspended particles are at low concentration and thus have a low air requirement.
- Recycle-flow pressure flotation, where a portion of treated wastewater is pressurised and recycled to the flotation tank. This is generally employed where coagulation and flocculation are needed and the flocculated particles are mechanically weak. Recycle-flow pressure flotation is used more often than the others for applications, including oil removal.

As a process IAF has a number of operational advantages over DAF, which include lower retention times, less than 5 mins, and a more compact flotation unit. IAF can have airflow rates of 100% of the water stream as compared to DAF where airflows relatively low at between 5% and 6% [343]. Mechanically agitated flotation systems are commonly used in the mineral industry with tank sizes up to 250 cubic metres (m³) [16]. In addition, IAF systems have the advantage of large capacities, high aeration rates and vigorously turbulent particle/droplet-bubble contacting. However, a major disadvantage of IAF is that much coarser (and thus less efficient) bubbles are produced than in the case of DAF. Mechanically agitated flotation systems are used commercially for oil flotation, there is very little published studies on their overall flotation performance [16].

The attachment and spreading of oil on a bubble's surface is much easier for smaller gas bubbles. Flotation efficiencies can be improved significantly by coalescing the oil droplets and manipulating the concentration and size of gas bubbles. Oil droplet coalescence can be achieved through the addition of coagulants, resulting in larger aggregates with more efficient collision and adhesion frequencies with the bubbles.

It has been reported that the flotation process depends strongly on the charge of the particles and bubbles and that the maximum rate of flotation can be achieved when the ζ potential of the

particles is zero [14,22]. Chemical pre-treatment of oil–water emulsions to enhance, demulsification, is based on the addition of chemicals that destroy the protective action of the emulsifying agent, overcoming the repulsive effects of the electrical double layers to allow the micro sized oil droplets to form larger droplets through coalescence [23,24].

DAF requires high-pressure conditions to create a sufficient amount of dissolved air in water for the release of significant number of fine bubbles upon decompression. The emulsified oily wastewater is first pre-treated with appropriate coagulant and flocculant. Tiny bubbles, commonly between 10 -100 μm , are produced when the water flows through a pressure control valve (or patent pressure reduction nozzles) into an atmospheric pressure flotation tank. Gas solubility in a liquid is a function of pressure, which implies that larger amounts of microbubbles can be generated by increasing the saturator pressure. The gas saturated water is then released into the contact zone area of the flotation, where the bubble-droplet collisions and adhesions occur.

The most common commercial DGF system is the dissolved air flotation (DAF) system. DAF systems are primarily used as a drinking water and wastewater clarification process when the raw source water contains low density contaminants [340].

Table 2.4. A comparison between IGF and DGF. Adapted from [16,62].

Parameters	IGF	DGF
Bubble size	100–1000 μm	10–100 μm
Bubble generation process	Velocity based with dispersion of gas bubbles	Gas bubble formation upon depressurization of gas liquid
Bubble generation volume	High	Low (limited by saturation)
Operating environment	Turbulent multi-unit environment	Quiescent single unit environment.
Capital investment	Relatively low	Relatively high
Foot print	Relatively small and compact	Relatively large
Maintenance	Substantial; particularly associated with wear and tear in mechanical IAF systems	Relatively small, few moving parts

As highlighted in **Table 2.4**, there is a clear difference between the operating mechanisms of IAF and DAF, and a direct comparison between the process data is not always practically possible [56,62,160,336,340,362]. IAF and DAF have proved to be a viable technique for

processing oily wastewater and emulsions with dispersed oil droplets larger than 20 μm [14,57,62].

IAF, in terms of practical application, has a number of advantages over DAF, which include a compact flotation system that can be easily setup at a laboratory scale [16,171]. IAF utilises bubbles of greater than 100 μm in turbulent hydrodynamic conditions with relatively short retention times of less than 10 mins [377,384–386]. DAF on the other hand employs bubbles of less than 100 μm in size and quiescent environments. The smaller bubble sizes produced in DAF, ensures that the process is much more efficient in removing suspended solids as compared to IAF [377,387].

2.7.6.3. Electroflotation

An alternative and effective smaller scale flotation technique is electroflotation, which is also known as electrolytic flotation [268,388]. The basis for the bubble generation at the cathode is electrolysis of the aqueous solution, where large amounts of small bubbles (hydrogen in case of water as the liquid) are formed at the cathode with minimum turbulence. The gas production, residence time and the other operating conditions of electroflotation can be evaluated quickly and are generally easily controlled [278,338,389,390].

Applications of electroflotation at an industrial scale, have been mainly in the area of colloidal system removal such as emulsified oils, pigments, ink and fibres from water as well as effluents that previously would not have been considered suitable for treatment by flotation [391,392].

In general the electroflotation equipment is reliable and safe to operate since only low voltages in the range 5–20 Volts are utilised [388]. The relative quantities of gases produced are a function of current density and salinity of the solution. Electroflotation can be used in cases where air or other gases could be difficult to dissolve in a particular effluent. As highlighted previously, when a sacrificial iron or aluminium anode is utilised, the metal dissolves and produces coagulant ions implying electrocoagulation precedes flotation [319]. Electroflotation is an alternative to chemical treatment methods and can be implemented without adding chemicals [126,245].

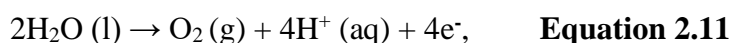
Throughout the process, fine bubbles nucleate at the cathode, detach and while rising to the water surface, attach to solid or liquid particles suspended in water [389]. The bubble-particle aggregates formed, float to the water surface and are collected by mechanical skimming [388].

In electrolysis of pure water using inert electrodes, the following redox reactions, as illustrated by Equations 2.10 to 2.12, occur.

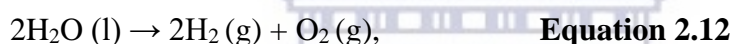
At the cathode electrode:



At the anode electrode:



The overall reaction:



These two gases, oxygen and hydrogen can be used either separately or together, or in combination with air bubbles in electroflotation [338]. The advantages reported in the literature include increased clarity of the treated wastewater and one of the disadvantages include low throughput volumes [366].

It has also been demonstrated by Lim *et al.* [64], that microbubbles in particular enhances the separation of oil in water contamination as compared to larger bubbles. As highlighted in this section, electroflotation produces small bubbles, however it has very little impact on the aggregation, flocculation and coalescence of oil droplets. As highlighted in previous sections, the emphasis for emulsion processing has been on the destabilisation of the emulsion to allow for aggregation, flocculation and coalescence of droplets to make larger droplets in order to increase the efficiency of the flotation technology. There are a number of reported processes associated with destabilisation of emulsions, which result in the flocculation, coalescence and flotation of oil droplets, however one flotation process that has caught the interest of a number of researchers is that of shear induced flocculation flotation [65–67].

2.7.7. Shear flocculation flotation

Shear flocculation flotation, also referred to as shear flocculation technology, has been recognised as a phenomenon applicable to fine minerals and coals beneficiation for nearly 30 years [69,70,73,393]. According to the literature, Warren in 1975 first reported and observed the aggregation of fine particles of scheelite with the application of hydrodynamic shear of sufficient magnitude [68,69]. Following this initial report, numerous authors from the mineral processing industry have reported the use of shear flocculation for the recovery of mineral fine particles, referred to as fines or slimes, which otherwise would have been discarded to tailings dumps [385,393,394].

The formation of aggregates under shear conditions is commonly referred to as shear flocculation or selective flocculation [69,71]. The fines represent a potential resource and the recovery of valuable minerals and is an additional income stream. The fines are generally difficult to separate by gravity separation and flotation alone. Through selective shear flocculation the fines are increased in size and are then floated as larger flocs.

The mechanisms of shear flocculation are generally believed to be as follows:

- an added collector molecule adsorbs onto a mineral surface, leaving an aliphatic chain pointing toward the bulk solution, which results in the particle having a hydrophobic surface;
- if a collision of sufficient momentum occurs, the kinetic energy of the particles is sufficient to overcome the surface repulsive force;
- the hydrocarbon chains come together and form a hydrophobic bond, resulting in floc formation.

The advantage of shear flocculation as reported in the literature, is the production of relatively stable hydrophobic flocs, which are strong and stable enough to withstand the turbulence in subsequent mineral processing operations [86,395]. The hydrophobic flocs can be separated from remaining hydrophilic dispersed particles by sedimentation or flotation. The importance of the shear flocculation in mineral processing has been increasing gradually since the initial report [393,396].

In addition to the hydrodynamic requirements, the mineral surface needs to adopt a hydrophobic surface, which usually requires the addition of surfactants that encourages aggregation at the particle-particle interface [69,385]. Selective adsorption of the hydrophobe or polymer onto the valuable particles is considered key and subtle effects of surface chemistry are involved in obtaining adequate selectivity [397]. Shear flocculation occurs when particles with hydrophobic surfaces collide at sufficient velocity to result in attachment. Flocs formed in this manner are smaller, but stronger than flocs formed with high molecular weight polymers.

Despite extensive research by various investigators, shear flocculation has not been widely adopted in the mineral processing industry. Shear flocculation was found to have a narrow window in which optimal floc size is obtained, although the size increase was found to be relatively modest. A complication in real systems is that the initial suspension is often naturally coagulated and needs to be dispersed before being selectively flocculated.

Following from the early reports, Bilgen *et al.* [69], reported in 1991 that highly charged particles in a suspension can be aggregated if they are hydrophobic and providing enough kinetic energy is applied to the system through agitation to overcome the energy barrier between the particles. It was this report, which led to several authors describing similar results, whereby shear is utilised to process and induce flocculation and coalescence of liquid - liquid dispersions [71,88,398].

2.7.7.1. Hydrodynamic shear

Shear stress is most commonly applied to solids and shear forces act tangentially to a surface of a solid body, which may cause an associated deformation [91]. In contrast to solids that can resist deformation, fluids lack this ability and flow under the action of the force [399].

When a fluid is in motion, shear stresses are developed due to the particles in the fluid moving relative to one another. For a fluid flowing in a pipe, fluid velocity will be zero at the pipe wall, the velocity will increase moving towards the centre of the pipe [399]. Shear forces are normally present because adjacent layers of the fluid move with different velocities compared to each other, as schematically depicted in **Figure 2.19** [399].

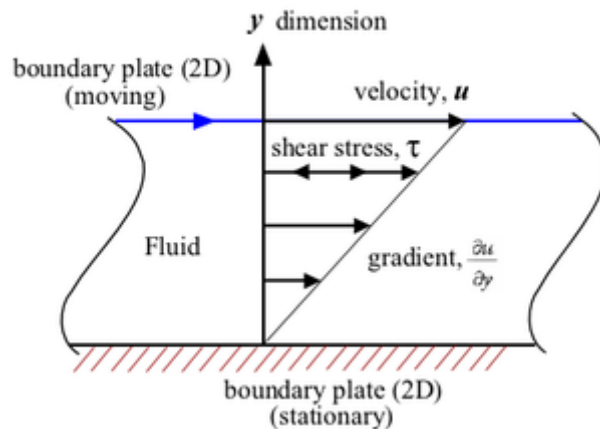


Figure 2.19. Schematic representation of shear forces in a fluid. Adapted from [399].

To generate large amounts of hydrodynamic shear rotor–stator mixers and high shear homogenisers are often utilised [400]. Shear forces are key in a rotor stator homogeniser in which a metal shaft (rotor) rotates inside a stationary casing (stator) [401]. The sample is drawn into the narrow space between the rotor and stator and the droplets are broken into smaller droplets as depicted in **Figure 2.20**.

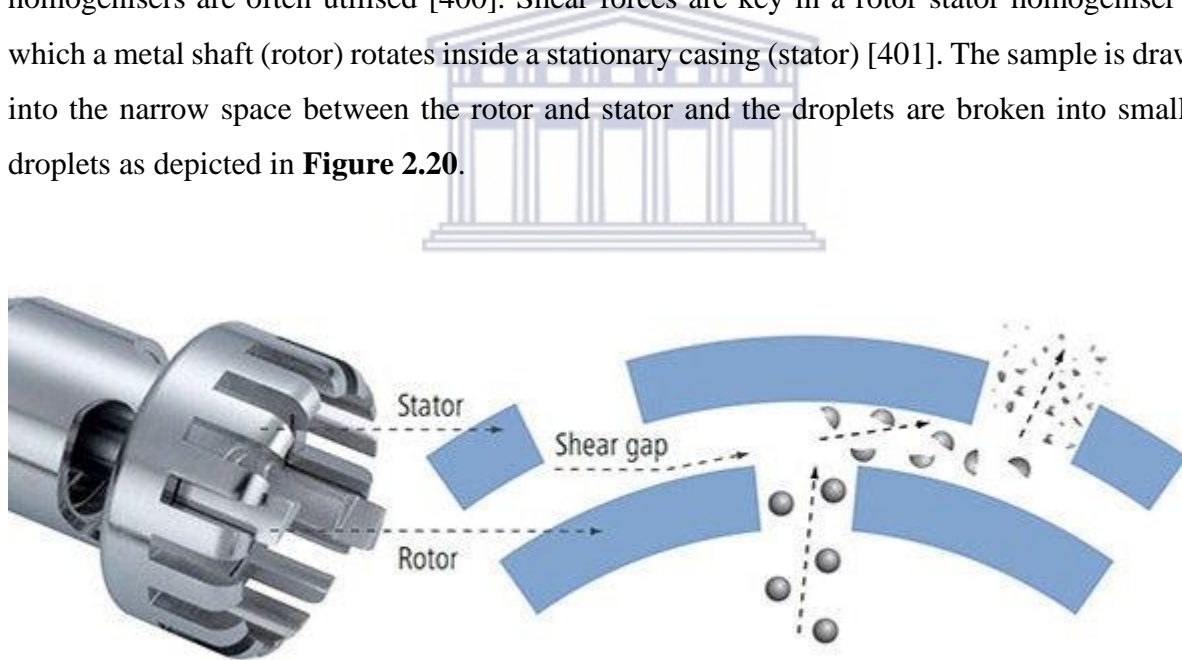


Figure 2.20. Schematic representation of a rotor stator mechanism for droplet break.

From the laws of fluid mechanics, the velocity of the fluid immediately adjacent to the rotor is the same as the velocity of the rotor [402]. It therefore follows that the velocity of the fluid directly adjacent to the stator is zero, which results in a high velocity gradient in the small gap between the rotor and stator and subjects the sample to high shear forces [403].

As highlighted in the previous sections as well by various literature reports, it is evident that there is not one technique that has the ability to effectively process all oily wastewaters. A hybrid technology of combining shear flocculation with flotation is a potential technique and has the possibility to yield exciting results in the field of emulsion processing. The process of shear flocculation for emulsion processing will be discussed in subsequent sections.

2.7.7.2. The effect of shear on emulsions

As highlighted in previous sections of this chapter, for an emulsion hydrodynamic shear forces affect both droplet break-up as well as droplet coalescence. The utilisation of high speed mixing is often associated with the formation of emulsions, where the oil is dispersed in the water phase and oil droplets are fragmented and broken into smaller droplets [151,404,405]. Smaller droplets take a longer time to separate and in presence of emulsifying agents they can form stable emulsions [151].

As discussed in the previous sections, for oil in water mixtures exposed to high shear environments, droplet break up is the dominant process and this results in the formation of emulsions with relatively small droplets, whereas in specific lower shear regimes, emulsion droplet aggregation and coalescence dominate [151,197,405].

If the energy dissipation rate is constant, shear forces acting on an emulsion balance the mechanism of coalescence and break-up, creating a stable range of droplet sizes existing in the flow. In general, the higher the energy dissipation rate and shear forces acting on the emulsion, the smaller the average DSD of the dispersed phase [74]. In an intermediate shear regime the balance between coalescence and breakup can shift either way [269]. The ratio between coalescence and break-up of droplets determines the droplet-size distribution in an oil-water mixture.

This emulsion separation process is often referred to as shear coagulation, shear flocculation or shear coalescence [87,88,91,196,261,269,394,406,407]. It should be noted that it is not correct to describe the process as shear coagulation as no charge manipulation is conducted during the shearing process, however a number of reports use this term incorrectly including Vanni *et al.*, Higashitani *et al.* and Bal [269,407,408].

When an emulsion is subjected to shear flow, droplet collisions increase because of the inter droplet relative motion increase induced by the velocity field of the medium. If there are no repulsive surface forces between droplets, every collision will lead to flocculation and eventual coalescence. At low shear rates, when the shear stresses are small compared to the interface stresses, coalescence is the dominant process, while breakup of droplets occurs at high shear stresses [197].

Based on the literature, shear separation can be described in terms of two principal mechanisms [409]. The first being an increase in temperature, which breaks the outer film of droplets, as described in Section 2.5, and reduces the viscosity of the emulsion. The other is molecular rearrangement resulting from the movement of ions around the oil droplets in the water, which impacts the ζ potential due to the rearrangement of electrical charges surrounding the associated water molecules [409]. A combination of the above processes results in separation of an emulsion without the addition of any chemical agents. Therefore, the oil recovered from an emulsion can be reused and secondary pollution from chemical coagulants and flocculants are non-existent.

In comparison to Brownian flocculation, based on the random motion of particles in the fluids, shear flocculation is due to the velocity gradient of the flow field. The mechanism of shear-induced droplet flocculation has been studied in detail by a number of researchers, the mechanism generally depends on the balance between the shear forces and inter-droplet forces, as well as the susceptibility of the thin film between adjacent droplets to rupture [91]. Several studies have investigated the impact of relatively low shear stress on the flocculation rate [95]. There have also been reports that have demonstrated an increase in particle size distribution as a result of increasing shear rate [93,94]. Similarly, it was shown that by increasing shear rate on an oil–water emulsion the rate of droplet growth is increased [410].

Shear induced flocculation can be described in terms of the DLVO theory [182]. Shear flocculation is a direct consequence of hydrodynamic shear, which plays an important role in the efficacy of the shear flocculation process [65,66,86,394]. Particle aggregation is a result of attractive force dominating, however it is accepted that droplets may require additional kinetic energy to overcome the energy barrier caused by repulsive forces [65,196,385]. Shear force has the potential to induce flocculation and droplet coalescence, despite unfavourable inter-droplet forces [91].

It is also known that in some cases, when hydrophobicity is sufficiently high, aggregation may occur in the absence of additional shear [14,51,129,397]. This is a result of transport mechanisms that facilitate droplet collisions, which include Brownian diffusion, fluid convection and interparticle interactions [14,78,129,193,233]. A number of studies have also reported that a specific amount of shear needs to be applied to an emulsion for shear flocculation to occur [87,91]. Shear-induced flocculation and coalescence with flotation has the potential to process emulsions with reduced amounts of chemicals and produce a relatively clean water stream and an oil product that can be recycled.

According to the literature the collision frequencies for Brownian motion and laminar shear are independent, however the effects are additive for a wide range of conditions [411]. Despite the above rule of thumb, it is also accepted that in high turbulent flow or high shear environments, the mechanism of droplet fragmentation and break up is also accompanied by some degree of droplet aggregation and coalescence [151]. The equilibrium of droplet fragmentation and aggregation is a function of the properties of the emulsion and the associated hydrodynamic shear force [197,412,413]. The shear induced droplet aggregation, flocculation and coalescence has been reported by a number of authors in various levels of detail [65,87,91,196,394,414,415]. The mechanism of droplet aggregation is a function of inter-droplet forces, the amount of applied shear, the ability of the thin film between adjacent droplets in an aggregation to rupture and result in droplet coalescence [91,196,269,409].

Despite this interest, very little work has been done to quantify the exact parameters associated with the phenomenon of shear aggregation and flocculation in emulsions. It is therefore the aim of this research to further develop and understand this process of shear induced aggregation and flocculation through which, it may be possible that the use of chemical coagulants and flocculants can be reduced.

The overall coalescence mechanism is driven by both hydrodynamic and thermodynamic factors. The rate of coalescence depends on parameters such as the viscosity of the droplet and of the continuous phase, the surface tension, the size of the droplets, type and intensity of flow. All of these parameters can be rearranged in a number of dimensionless parameters to describe the droplet deformation under flow and the kinetics of the coalescence process, with the Reynolds number being an important parameter describing the mixing of fluids.

2.7.7.3. Reynolds number

The Reynolds number is a key parameter of fluid mechanics, which is especially useful in conceptualising industrial fluids mixing [416,417]. The Reynolds number is used in describing the boundary point between laminar and turbulent flow. Laminar flow is fluid flow characterised by long, smooth flow currents, mainly in the same direction as the bulk of the flow [416].

In a closed mixing system, fluids with a laminar flow have Reynolds numbers less than 2,000 [416,418]. Turbulent flow, is a fluid flow in which the velocity at any given point varies erratically in magnitude and direction. In a closed mixing system, fluids with a turbulent flow have Reynolds numbers greater than 4,000. Mixing, where Reynolds numbers are from 2,000 to 4,000 is considered to be in the transitional zone, in-between laminar and turbulent flow regimes [419].

In wastewater treatment the Reynolds number can be calculated utilising Equation 2.13 below.

$$N_R = D^2 \eta \rho / \mu, \quad \text{Equation 2.13}$$

where N_R - Reynolds number, D - impeller diameter, η - revolutions per second, ρ - liquid mass density, μ - fluid dynamic viscosity.

For water the $\rho = 997 \text{ kg/m}^3$ and $\mu = 0.0091 \text{ poise}$ at $25 \text{ }^\circ\text{C}$

2.7.7.4. Shear induced flocculation and flotation

Shear flocculation with flotation has successfully been used in the processing of mineral ores and has been demonstrated to be a possible process of interest for the processing of o/w emulsions [92–95,240].

Concerning the mineral processing industry, there is a considerable body of experimental and theoretical evidence to indicate that shear has the ability to play an important role as a pre-treatment in the flotation process and on the overall flotation kinetics [65,69,72,385].

Studies have shown that low flotation efficiency in emulsion processing is mainly due to the low probability of bubble-droplet collision [335]. Efficient attachment of droplets to bubbles and improved flotation rate has been observed when a distribution of bubbles are produced, which includes bubbles in the range of 10 to 1000 μm , as described in Section 2.7.6. [23,161,335]. In an emulsion, the phase separation reaction kinetics are governed by the probability of droplet-droplet collisions [320,322]. It is therefore possible that the phase separation process can be enhanced by stimulating the interaction between the droplets, using external forces such as mechanical, electrostatic and chemical or a combination of these. For emulsion separation, it is experimentally and theoretically clear that the flotation rate increases with increasing DSD [338].

The use of shear to induce coalescence of oil in water emulsions followed by flotation has been reported by a number of authors, however the optimal parameters of the emulsion and of the conditions for coalescence and separation to occur still remain uncertain [87,88,91,261]. The shear rates used should be small enough such that droplet breakup is minimal and that coalescence due to Brownian motion is negligible. Also, the densities of the droplets and the continuous phase must be matched so that creaming-induced coalescence is insignificant. The increase in the overall DSD in the system, occurs due to shear-induced coalescence alone. The physicochemical properties of the two phases, particle characteristics and the nature of the interfacial layer will affect the shear rate at which these processes occur [200,328,420]. After a period of time, a steady state is reached between fragmentation and aggregation, which is marked by an aggregate size distribution that is constant and unique to the associated shear conditions of the system [286].

Taking into account the adverse effects of chemical processing, a number of authors have proposed that the utilisation of shear flocculation as a pre-treatment prior to flotation under the correct conditions could be a novel approach for emulsion processing [240,396,420]. The process has the potential to recover the oil from an emulsion, which can be reused and secondary environmental pollution caused by additional chemicals is avoided.

CHAPTER 3 EXPERIMENTAL DETAIL

3.1. Chemicals and Materials

This section presents the list of chemicals and materials used in the study. Analytical grade chemicals and solvents were used for all experiments and analyses as shown are in **Table 3.1**.

Table 3.1. Source and purity of chemicals used.

Chemical	Source	Purity
Aluminium Sulphate	Aqua Aero Vitae Pty Ltd	17% minimum
Olive oil	Sigma Aldrich	99.5%
Hydrochloric Acid	Kimix Chemical & Lab Supplies	37%
Sasol Multigrade L SAE 20W-50	Sasol (South Africa)	-
Sasol Monograde 40 SAE 40	Sasol (South Africa)	-
Sodium carbonate	Merck	99.5%

All chemicals were used as purchased and received without further purification. The water used in all the experiments was ultra-pure purified water prepared with a Milli-Q water purification system supplied by a system from Millipore (South Africa, with resistivity 18.2 MΩ cm and TOC 2 ppb).

3.2. Experimental Design

The research methodology and experimental design was developed to evaluate the use of hydrodynamic shear with flotation to destabilise a variety of oil in water emulsions.

The effect of shear and shear with air flotation on oil in water emulsions was studied in this research. Three different emulsions were selected; one based on olive oil, one based on Sasol multigrade and one based on Sasol monograde oil. Three emulsions were treated to demonstrate the effectiveness of the application on emulsions with varying chemical properties.

Experiments were designed to investigate the impact of shear and flotation on emulsion stability and processing efficiency. According to previous studies, the application of shear and air flotation to an emulsion has an impact on the overall stability of an emulsion, however to

date very little research has been done to compare the efficiencies of each process individually [65,151,413].

A laboratory scale IAF and a pilot scale DAF plant were designed and fabricated. With both the IAF and the DAF system a shear mixer unit was integrated as part of the overall system. Experiments and experimental procedures were designed and conducted to analyse and test various oil in water emulsions with the IAF and DAF systems. Turbidity, ζ potential, conductivity, DSD and COD were measured pre and post treatment to determine the overall effect of the treated water.

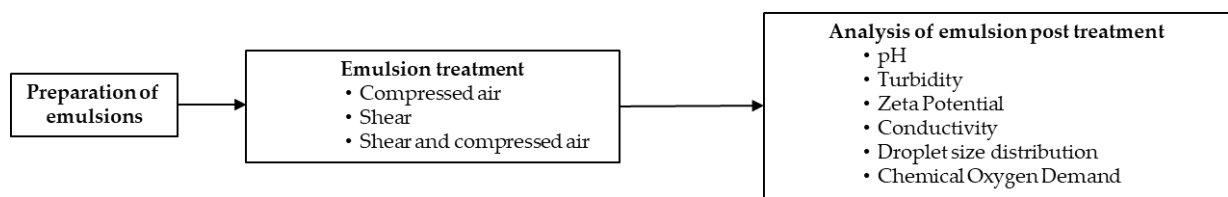


Figure 3.1. Experimental design for the IAF hybrid system.

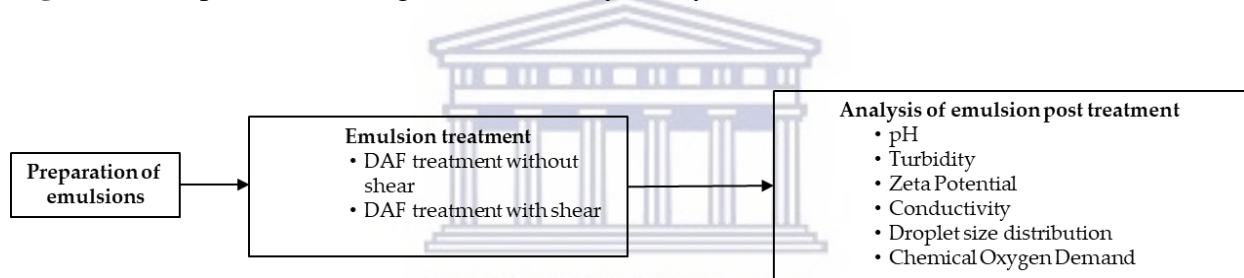


Figure 3.2. Experimental design for the DAF hybrid system.

Figure 3.1 and **Figure 3.2** highlight the experimental designs for the IAF and DAF system.

Desktop experiments were conducted in the wet chemistry laboratory at the SAIAMC building and once satisfactory results were achieved, similar emulsions were prepared and processed with the shear mixing and flotation unit located in the laboratory container at the SAIAMC Pilot Plant building.

The intention of the experiments at the laboratory container is to process larger volumes of emulsified wastewater utilising the novel hybrid system consisting of an industrial pilot DAF unit and a uniquely designed shear mixer. The aim of this system is to evaluate the use of shear mixing with flotation to break emulsions with the use of minimal chemical pre-treatment of coagulants and flocculants.

Treated water samples were preserved in opaque plastic sample jars at room temperature prior to analysis of each sample in triplicate, unless otherwise stated.

3.2.1. Preparation of emulsions

A homogeniser (JRJ300-I, solid/liquid powder emulsification mixer) was used to prepare the surfactant and emulsifier free oil in water emulsions for both the IAF and DAF shear experiments. The choice of homogeniser was based on availability in the market, practicality and ease of use.

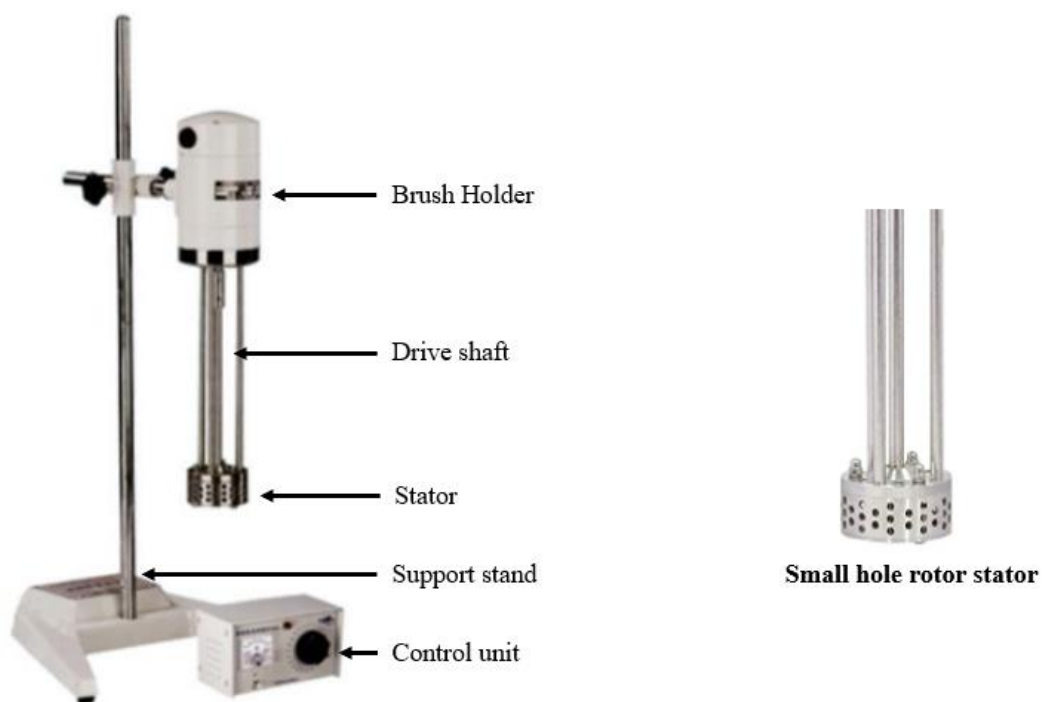


Figure 3.3. High-speed homogeniser emulsifying mixer and small hole rotor stator.

The oil in water emulsions were prepared utilising the following oils:

- olive oil (Sigma-Aldrich, South Africa),
- Sasol Multigrade L SAE 20W-50 (Sasol, South Africa),
- Sasol Monograde 40 SAE 40 (Sasol, South Africa).

The oil in water emulsions were prepared in the laboratory, with 500 mL deionised water with the addition of 20 mL, of the above oils. The water and oil were mixed in a 600 mL glass mixing beaker at ambient temperature at 6000 revolutions per minute (rpm) for 2 mins utilising

a high-speed homogeniser emulsifying mixer (JRJ300-1, China). The homogeniser has a mixing speed range of between 2000 and 11000 rpm. Various rpms were tested and the optimal rpm for a stable emulsification was established at 6000 rpm. The homogeniser was fixed in an upright position using a small hole rotor stator, the configuration is shown in **Figure 3.3**.

The use of shear homogenisers have been reported to promote the reduction of emulsion droplet diameter ensuring physical stability of the emulsion [421,422].

3.2.2. Preparation of 0.0035 M Na₂CO₃ dilution solution

1 g of Na₂CO₃ was diluted in 1000 mL with deionised water to produce a 0.0035 M solution with a pH of 11.4.

3.2.3. Preparation of 0.01 M HCl dilution solution

Concentrated (37%) HCl is 12 M. 0.83 mL of 37% HCl to 1 litre with deionised water to produce 0.01 M HCl solution with a pH of 2.

3.2.4. Preparation of alum solution.

A 5000 mg/L Alum solution was prepared by transferring 29.412 g of 17% Al₂(SO₄)₃ into a 1L volumetric flask. The solution was used as a stock solution to prepare 10 mg/L, 30 mg/L, 50 mg/L and 70 mg/L solutions which were then used in the jar test experiments.

3.2.5. Preparation of emulsion aliquots for analysis

The emulsion was prepared as per the procedure above and was allowed to stand for 10 mins, following which, a sample of 40 mL was taken at 5 cm below the water level using a syringe with a 1mm needle and transferred into a 60 mL sample vial. The pH, turbidity, conductivity and ζ potential were recorded immediately. Special care was taken to wipe the needle removing any trace of free oil in order to avoid contamination of the sample with the free oil floating on the surface of the jar or beaker.

3.2.6. Laboratory scale IAF experiments

Oil in water emulsions were prepared with three different types of oils. The stable emulsions of the oils were then subjected to treatments consisting of air and shear. The emulsions post-treatment were then analysed utilising the analytical techniques described above.

A specifically designed shear flotation setup, as illustrated in **Figure 3.4**, was used to study the effect of shear and air flotation on a stable oil in water emulsion. The shear flotation setup consisted of a modified high-speed homogeniser emulsifying mixer with air tube inlets directly inserted into the rotor stator in order to disperse and mix the air and to create small air bubbles through mechanical agitation. Three different treatment methods were employed, the emulsions were sparged with air, exposed to shear, sparged with air whilst being exposed to shear.

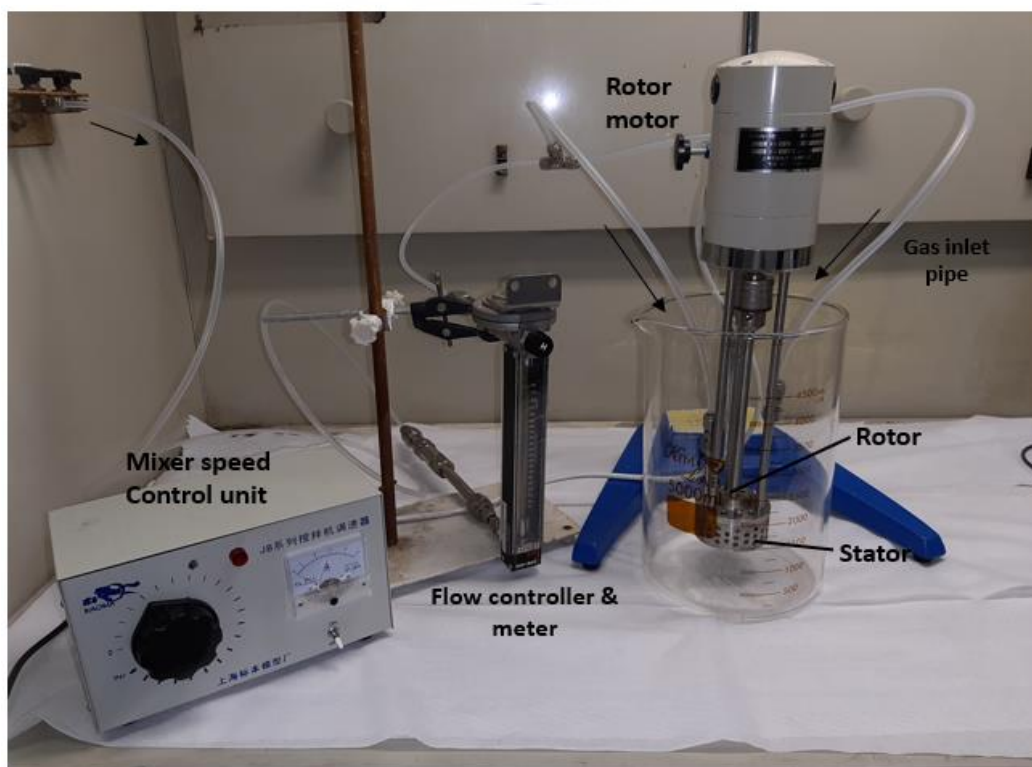


Figure 3.4. Specially designed and configured shear induced air flotation setup.

For all three emulsion treatment methods, the rotor stator was placed in the centre of the beaker, with the top of the rotor stator at a depth of 5 cm below the emulsion level, to ensure that the stator is fully submerged.

The placement of the rotor stator in the beaker and emulsion is illustrated in **Figure 3.5**.

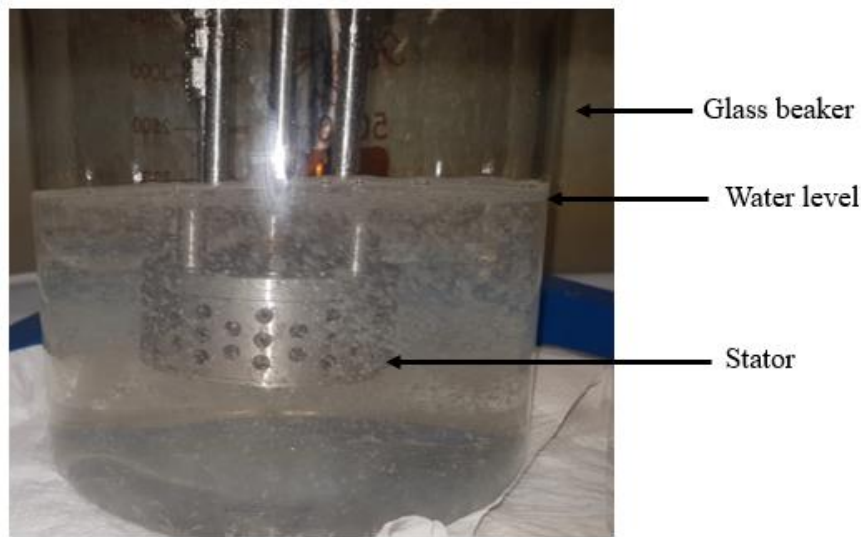


Figure 3.5. Position of rotor stator in the glass beaker.

3.2.6.1. Calculation of Reynolds number

The complicated shape of the rotor stator makes it virtually impossible to calculate the Reynolds numbers achieved during these experiments. Also, the fact that the experiment deals with multiphase mixtures of uncertain composition (as the residence time of the bubble in suspension and therefore the air-liquid concentration, viscosity and density are challenging to quantify). However, the Reynolds numbers for the rotor-stator setup, utilised in the experiments, (see **Figure 3.6**) were calculated assuming a stator without any holes. In such case the Reynolds number for each rpm can be calculated utilising Equation 2.13, presented in Section 2.7.7.4. In reality the Re number should be significantly higher taking into account that the stator wall has holes, which results in a turbulent flow regime [147,423].

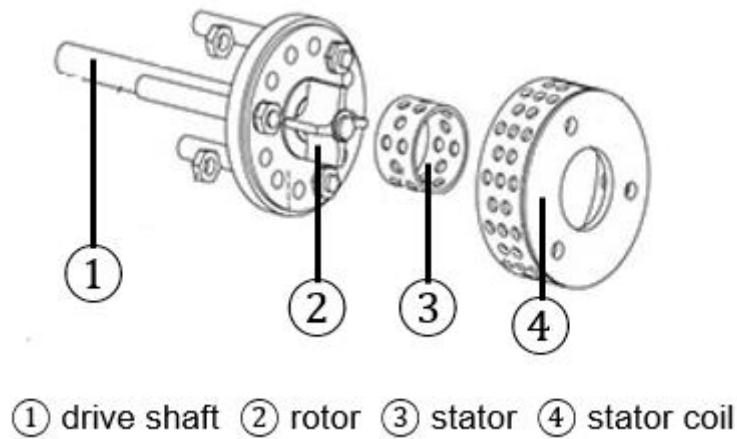


Figure 3.6. Graphical depiction and assembly of the rotor stator unit of the high-speed homogeniser emulsifying mixer.

The measurements of the rotor stator of the high-speed homogeniser emulsifying mixer depicted in **Figure 3.6**, is presented in **Table 3.2** below.

Table 3.2. Rotor stator dimensions.

Parameter	Outside diameter	Inside diameter	Height (mm)
	(OD) (mm)	(ID) (mm)	
Stator	31.2	28.0	19.6
Stator coil	68.5	65.0	27.2

The diameter of rotor was measured at 26.7 mm with the gap between rotor and stator was calculated at 1.3 mm. There are 18 holes in the in the stator all with a diameter of 5 mm in diameter.

Table 3.3. Calculated Reynolds numbers for the high-speed homogeniser emulsifying mixer with a simplified geometry and without air.

Revolutions per minute (rpm)	Reynolds number
1000	781,045
2000	1,562,090
3000	2,343,136
4000	3,124,181
5000	3,905,227
6000	4,686,272

Based on the results of the calculations it is evident that the flow produced by the mixing for the rpm's utilised in the experiments are all associated with turbulent flow, a flow in which the velocity at a given point varies erratically in magnitude and direction. The assumption is made that the Reynolds numbers for the more complex geometry are even higher, ensuring high shear rates which should be able to influence the destiny of emulsion droplets [87,147,423].

3.2.6.2. Experimental settings for the laboratory scale IAF setup

The emulsions were prepared as per the procedure above and were allowed to stand for 10 mins. Each of the prepared emulsions was divided into 4 batches. The first batch of each emulsion was left untreated and served as the control sample. The second batch was exposed only to air flow (1000 L/h) for 2 mins. The third batch was mixed with the high-speed mixer at 4000 rpm for 2 mins, without any air flow. The fourth batch of samples was mixed with the high-speed mixer at 4000 rpm for 2 mins, while a 1000 L/h air flow was introduced into the mixer. The treatment details of each emulsion batch are captured in **Table 3.4.**

Table 3.4. Particulars of experiments conducted utilising the modified IAF system.

No.	Experiment description	Emulsion	Air (L/h)	Shear (rpm)
1	Olive oil emulsion as prepared	Merck Olive Oil	0	0
2	Exposed to air		1000	0
3	Exposed to shear		0	4000
4	Exposed to air and shear		1000	4000
5	SAE 20W emulsion as prepared	Sasol Multigrade L SAE 20W-50	0	0
6	Exposed to air		1000	0
7	Exposed to shear		0	4000
8	Exposed to air and shear		1000	4000
9	SAE 40 emulsion as prepared	Sasol Monograde SAE 40	0	0
10	Exposed to air		1000	0
11	Exposed to shear			4000
12	Exposed to air and shear		1000	4000

3.2.6.3. Analysis of emulsions.

Droplet size distribution samples were taken immediately after the treatment and all other tests were carried out after the solutions were allowed to stand for 10 mins.

For all experiments, a sample of 40 mL of 5 cm below the water level was transferred into a 60 mL sample vial. The pH, turbidity and conductivity were recorded immediately. **Table 3.7**, provides a summary of the experiments conducted utilising the IAF system.

3.2.7. Hybrid DAF shear wastewater treatment unit

A pilot scale 3 L/min hybrid DAF shear wastewater unit was designed, fabricated and commissioned at the University of the Western Cape, specifically for this project. The system was designed utilising a conventional DAF treatment unit with the integration of a hydrodynamic shear mixer. The piping and instrumentation diagram (P&ID) of the DAF shear hybrid unit is depicted in **Figure 3.7** and was drafted utilising Microsoft Office Visio Professional 2003. A detailed explanation of the entire system, the associated start-up procedure and an emergency shut down procedure is provided in Appendix A1, A2 and A3 respectively.

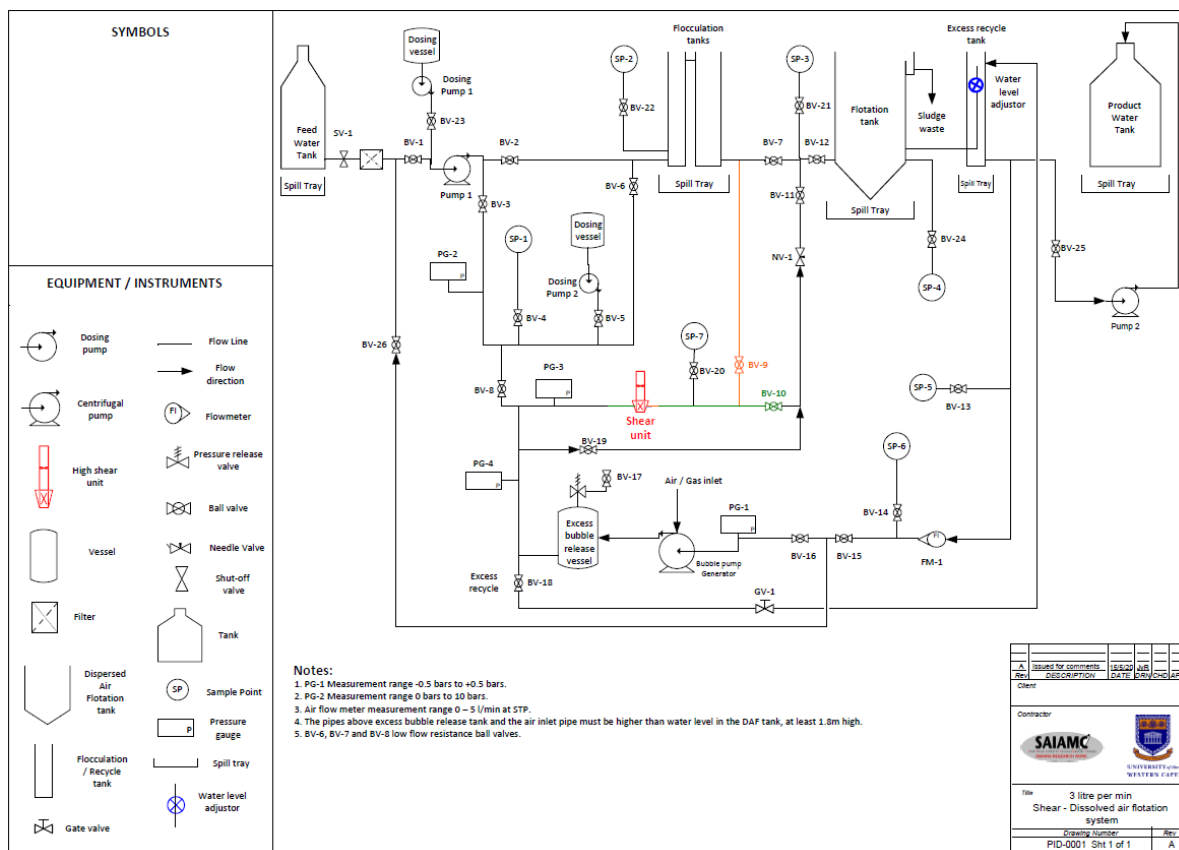


Figure 3.7. P&ID diagram for the DAF shear wastewater treatment system.

The unit consisted of intermediate bulk containers (IBC) flocculation tanks, a stainless-steel flotation tank, a recycle tank, an excess bubble release vessel, an Ozone Green Plant micro-bubble generation pump, dosing vessels, dosing pumps, needle valve, gate valve, shut off valve, water level adjustor, flow meter, ball valves (BV-1 to BV-26), sample points (SP-1 to SP-7) and pressure gauges (PG-1 to PG-4).

The objective of the system is to study the extent to which oil emulsions can be broken and separated into their specific phases utilising hydrodynamic shear, coagulation, flocculation and flotation. The unit was designed to produce air saturated water at 3.5 bar pressure.

The unit, is graphically represented in **Figure 3.8** and **3.9** and photographs of the system are shown in **Figures 3.10, 3.11, 3.12** and **3.13**.

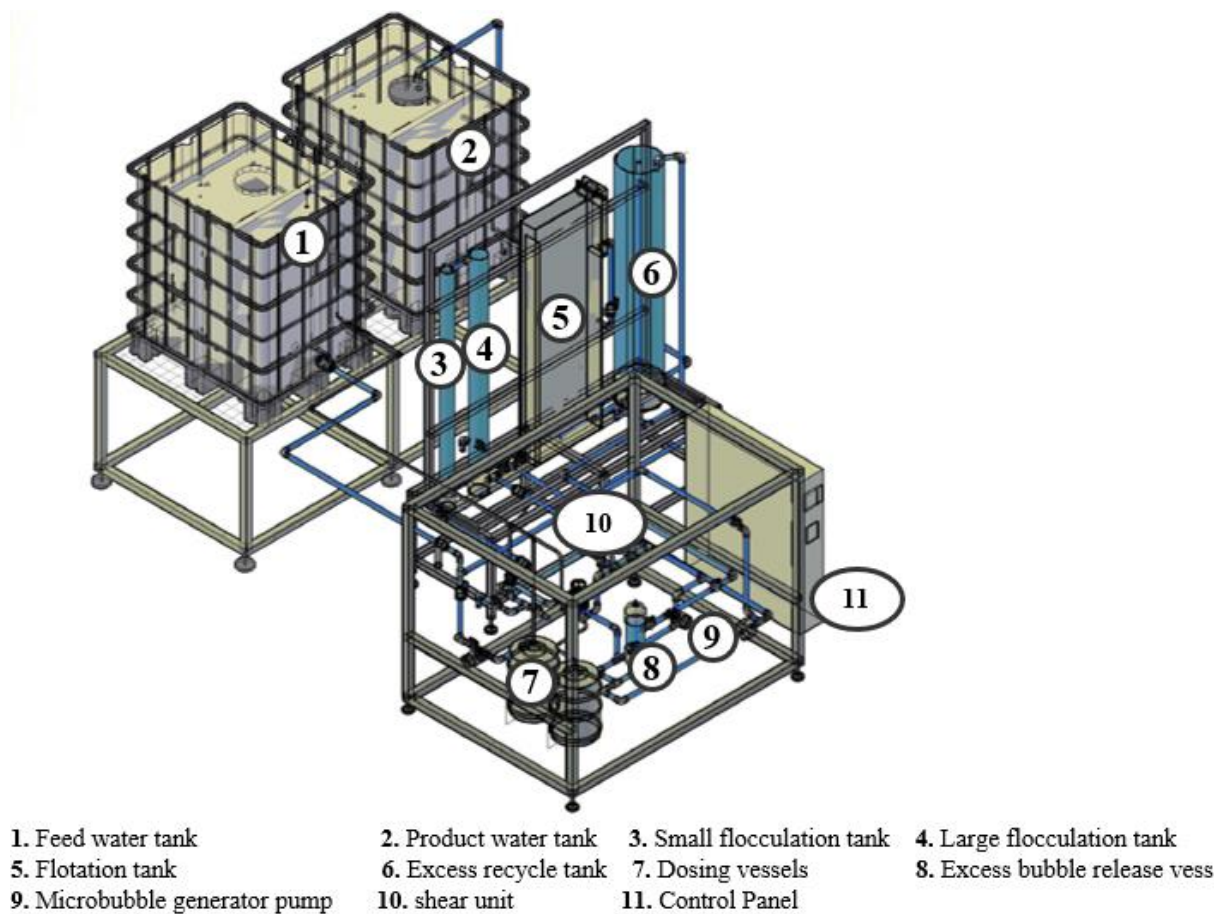
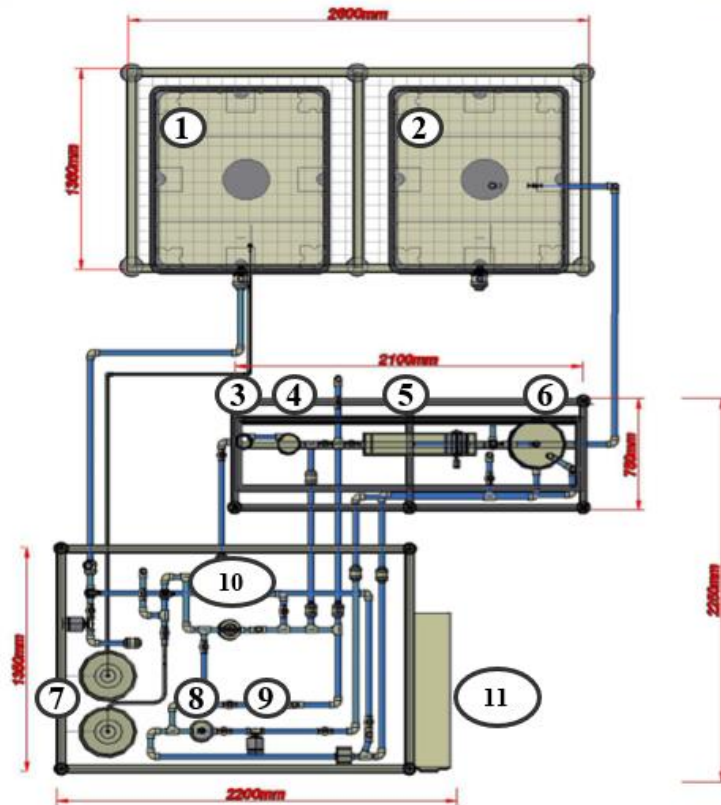


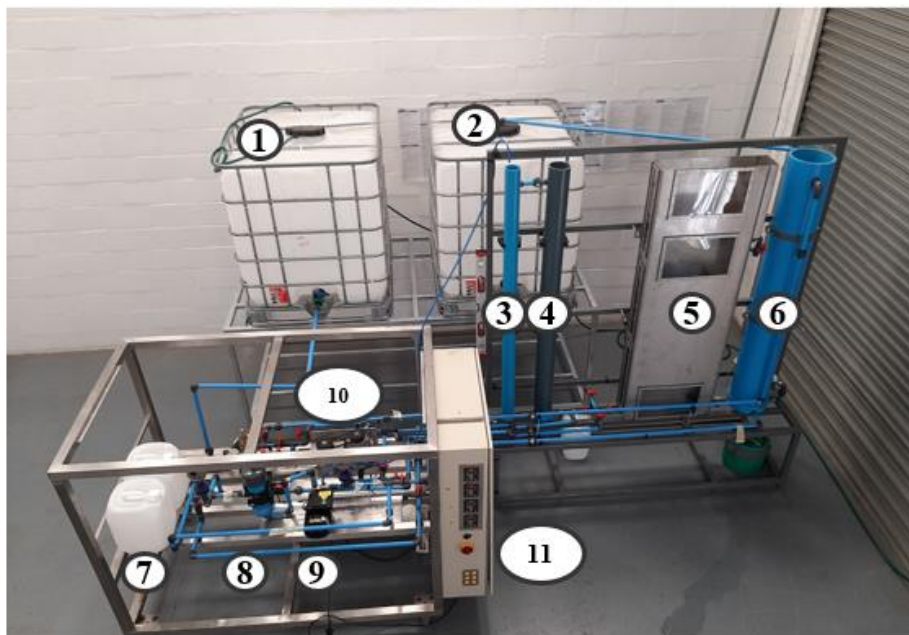
Figure 3.8. Hybrid DAF shear unit.



- | | | | |
|-------------------------------|------------------------|----------------------------|---------------------------------|
| 1. Feed water tank | 2. Product water tank | 3. Small flocculation tank | 4. Large flocculation tank |
| 5. Flotation tank | 6. Excess recycle tank | 7. Dosing vessels | 8. Excess bubble release vessel |
| 9. Microbubble generator pump | 10. shear unit | 11. Control Panel | |

Figure 3.9. Top view of the hybrid DAF shear unit.

UNIVERSITY of the



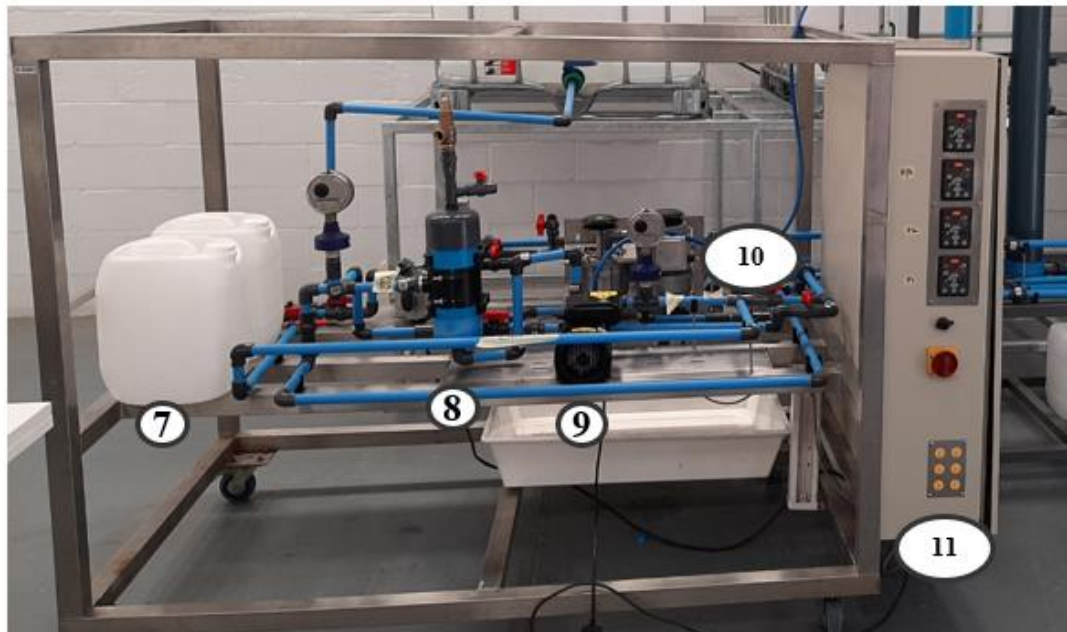
- | | | | |
|-------------------------------|------------------------|----------------------------|---------------------------------|
| 1. Feed water tank | 2. Product water tank | 3. Small flocculation tank | 4. Large flocculation tank |
| 5. Flotation tank | 6. Excess recycle tank | 7. Dosing vessels | 8. Excess bubble release vessel |
| 9. Microbubble generator pump | 10. shear unit | 11. Control Panel | |

Figure 3.10. Photograph of the hybrid DAF shear unit wastewater system.



- | | | |
|----------------------------|-----------------------|----------------------------|
| 1. Feed water tank | 2. Product water tank | 3. Small flocculation tank |
| 4. Large flocculation tank | 5. Flotation tank | 6. Excess recycle tank |

Figure 3.11. Photograph of the hybrid DAF shear unit, highlighting the floc tanks and the DAF flotation tank unit.



7. Dosing vessels 8. Excess bubble release vessel 9. Microbubble generator pump
 10. shear unit 11. Control Panel

Figure 3.12. Photograph of the hybrid DAF shear unit, highlighting the control panel, bubble pump generator, shear unit.



Figure 3.13. Photograph of the hybrid DAF shear unit control panel.

The shear unit was constructed out of steel sheets joined together to form a rigid outer structure with a rotating inner watertight unit as depicted in **Figures 3.14** and **3.15**. The multi-layered steel structure provides an elongated rotor-stator shear gap with an inlet and outlet for the wastewater.

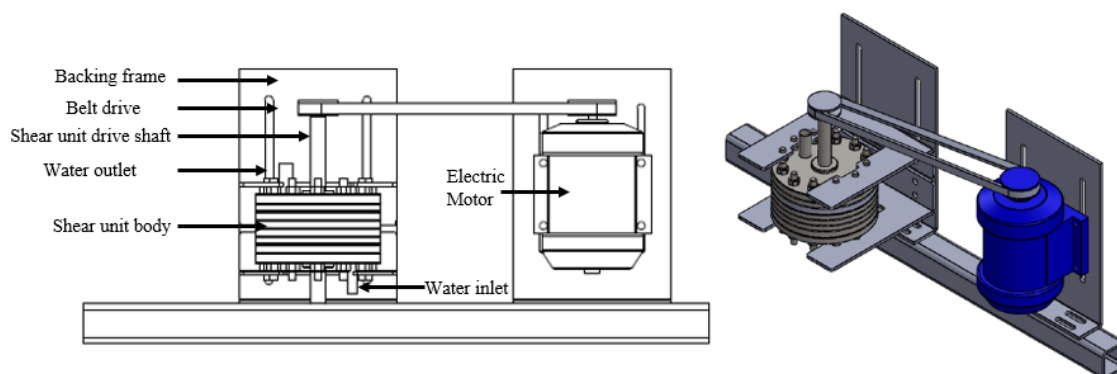


Figure 3.14. Shear unit assembly attached to an electric motor with a drive belt.

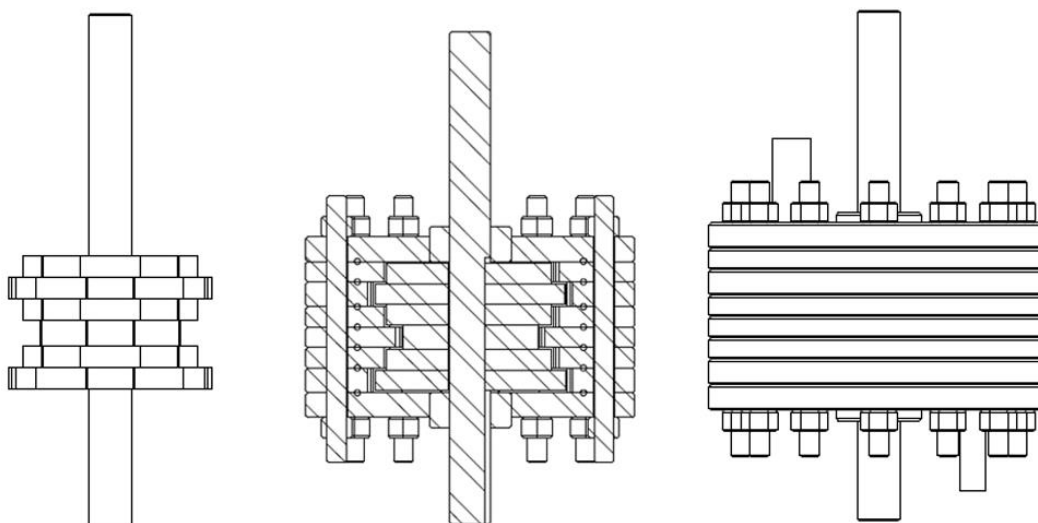


Figure 3.15. Internal structure of the shear unit assembly.

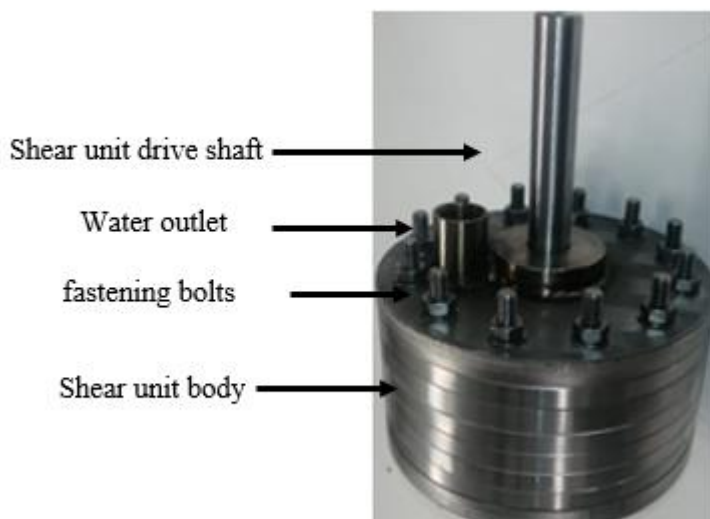


Figure 3.16. Photo of the DAF shear unit.

The sizes and volumes of the associated tanks of the DAF unit are presented in Appendix B.

3.2.7.1. Preparation of emulsion for DAF shear unit

For the DAF shear unit experiments only olive oil, surfactant and emulsion oil in water emulsions were prepared and processed.

The o/w emulsion for the DAF shear unit was prepared in 50 litre (L) batches, in a 50 L open top plastic drum, making up a 1% emulsion solution. Batches were prepared to a total volume of 900 L, which was added to the 1000 L IBC tank.

The oil in water emulsions were prepared, with deionised water with the addition of 1000 mL, of olive oil to 50 L of water. The water and oil were prepared and mixed in the 50 L plastic drum at ambient temperatures at 6000 rpm for 10 mins with a high-speed homogeniser emulsifying mixer. Following the emulsification process the 50 L emulsion was transferred into the IBC tank. Once the IBC container was filled to 900 L the entire IBC tank was stirred with an Ingo Mixer MX214008, 1400 W for approximately 30 mins and allowed to stand for 30 mins. A sample of 200 mL was taken at 30 cm below the water level and transferred into a 200 mL sample bottle.

The pH, turbidity, conductivity and ζ potential were recorded immediately whereas the COD analysis was sent to an external laboratory for analysis.

3.2.7.2. Coagulation test of emulsions

A VELP Scientific jar test (South Africa) with 76 x 25 mm flat paddle impellers was used to perform the jar tests with 600 mL of emulsion at a room temperature ($23 \pm 1.0^\circ\text{C}$) as depicted in **Figure 3.18**.

The aim of the jar tests was to determine the appropriate pH and amounts of coagulant to use in the DAF experiments, jar tests were initially carried out to determine the alum dosing concentration for the best coagulation dosage. The coagulation and flocculation experiments were conducted with a jar test apparatus (FC4S, Jar test, VELP Scientifica, South Africa) with 76 x 25 mm flat paddle impellers and 600 mL beakers to assess coagulation and flocculation of the emulsion samples.



Figure 3.17. Photograph of the VELP Scientific jar test apparatus utilised for the jar tests.

After flocculation and sedimentation, 200 mL of the supernatant aqueous zone from 3 cm below the water surface was taken for the various analysis and measurements.

Based on the turbidity of samples taken from the above initial investigations, the optimum conditions and the following jar test procedure was developed with the following steps:

- 500 mL of the emulsion samples were transferred into beakers and the pH was adjusted with a 0.0035 M Na_2CO_3 solution to between 7 and 8.
- Four different concentrations of the alum coagulant were used 10 ppm, 20 ppm, 30 ppm and 40 ppm, and added to the emulsions.
- The coagulant, alum, were added to the jars immediately after the start of rapid mixing.
- After adding the coagulant to the emulsified oily wastewater, the jar tests started with an initial rapid stirring at the maximum 200 rpm for 5 mins followed by slow stirring at 50 rpm for 2 mins and ended with a standing period of 3 mins.
- Each coagulation experiment was repeated three times with an average final result.
- The clarified water below the surface oil layer was collected using a syringe at a depth 3 cm below the water surface was collected for the measurement of emulsion parameters.

3.2.7.3. DAF with shear unit experimental procedure

Oil in water emulsions were prepared and processed with the unit. The unit was designed to perform various experiments, which included the processing of emulsions with:

- DAF with coagulation
- DAF with shear, and
- DAF with coagulation and shear

It should be noted that no chemical flocculants were used during the experiments. This was done in order to recover as much oil as possible and to not degrade the recovered oil.

The oily wastewater was pumped from the feed water IBC tank, through a filter into the DAF unit. During all experiments, the oily wastewater was first tested and pre-treated by adjusting the pH between a pH range of 5.5 -7.5 with the 0.0035 M solution of Na_2CO_3 .

With reference to the P&ID diagram, **Figure 3.7**, the following procedure was developed and utilised during the experimental runs. Downstream of the flocculation tanks, the wastewater passed through the flotation tank with the dissolved air bubbles, where the microflocs of oil droplets were allowed to float up and subsequently be removed at the top of the flotation tank.

Samples were taken at various points in the system to monitor chemical and physical processes in the system. The flotation tank was also designed with viewing windows at various levels in order to evaluate the bubble sizes and wastewater flows.

The unit allows for the following wastewater cycles post the flotation tank:

- Recycle back through the flocculation tanks back to the flotation tank
- Pump via a micro-bubble pump and back to the flotation tank to allow for flocs, which did not form to be recovered, improving wastewater processing
- Pumped via a micro-bubble pump and a shear mixer back to the flotation tank
- Remove processed wastewater via the bottom of the flotation tank and the excess recycle tank

The oil in water emulsion was prepared and pumped into the system from the feed water IBC via pump 1. The emulsion wastewater was circulated through the unit until the water level remained constant and the pressure constant at 2.5 bar as measured at pressure gauges (PG-4 and PG-3). This pressure was maintained throughout the treatment process. After circulation and when the water level and pressures were stable the micro-bubble pump was switched on to dissolve air into the water and the needle valve (NV-1) was opened allowing the air to come out of solution and the wastewater stream and the micro-bubbles to enter into the flotation tank.

After recirculation of approximately 30 mins the system became stable in terms of flow rate and water level. Processed and clarified water stream was routed and pumped (Pump 2) directly from the excess recycle tank into the product water IBC tank by opening ball valve BV-25. Samples of the processed water were collected directly from product water IBC tank and from sample point 7, by opening ball valve (BV-23).

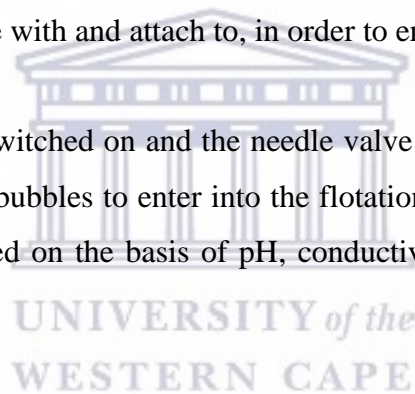
Each experiment was conducted for approximately 4 hours, which resulted in the feed water tank being completely empty after this duration. After a steady state was achieved for the unit, samples were collected at the sample points (SP-7, SP-4, SP-5) and were analysed.

The floated oil was removed and collected from the surface of the water at the flotation tank and analysed accordingly.

3.2.7.4. Emulsions treated with DAF with coagulation

The emulsions were prepared as per the procedure above and the feed wastewater in the IBC tank was pumped into the system with Pump 1. After circulation the wastewater stream was dosed with coagulant, alum, from the dosing vessel and dosing pump 2. The coagulant dosing was done for the entire duration of the experiment. Following from the coagulant dosing, the wastewater was pumped through the flocculation tanks to ensure adequately sized flocs to form for the micro-bubbles to collide with and attach to, in order to ensure efficient flotation.

The micro-bubble pump was switched on and the needle valve (NV-1) was opened allowing the recycle stream with micro-bubbles to enter into the flotation tank. Treated water samples were analysed and characterised on the basis of pH, conductivity, turbidity, ζ potential and COD.



3.2.7.5. Emulsions treated with DAF with shear

The emulsions were prepared as per the procedure above and the feed water in the IBC tank was pumped into the system with Pump 1. The DAF with shear experiments were conducted by diverting the wastewater through the shear unit by opening ball valve (BV-10) and closing ball valve (BV-9). During the shear process, the shear unit speed was adjusted from 1Hz to 10Hz on the control panel and kept constant at 10 Hz throughout the processing.

The micro-bubble pump was switched on and the needle valve (NV-1) was opened allowing the wastewater stream with micro-bubbles to enter into the flotation tank. Treated water samples were analysed and characterised on the basis of pH, conductivity, turbidity, ζ potential and COD.

3.2.7.6. Emulsions treated by DAF with coagulation and shear

The emulsions were prepared as per the procedure above and the feed water in the IBC tank was pumped into the system with Pump 1. The DAF with shear experiment was conducted by diverting the wastewater through the shear unit by opening ball valve (BV-10) and closing ball valve (BV-9). During the shear process, the shear unit speed was adjusted to 10 Hz (= rpm?) on the control panel and kept constant at this speed throughout the processing.

The bubble pump was switched on and the needle valve (NV-1) was opened allowing the wastewater stream with dissolved air to enter into the flotation tank.

Treated water samples were analysed and characterised on the basis of pH, conductivity, turbidity, ζ potential and COD.

3.2.7.7. Emulsions treated with DAF without coagulation and shear

The emulsions were prepared as per the procedure above and the feed wastewater in the IBC tank was pumped into the unit with Pump 1. No coagulant was dosed into the wastewater stream and the shear unit was by passed.

The micro-bubble pump was switched on and the needle valve (NV-1) was opened allowing the wastewater stream with micro-bubbles to enter into the flotation tank.

Treated water samples were analysed and characterised on the basis of pH, conductivity, turbidity, ζ potential and COD.

3.2.8. Emulsion analysis and characterisation

3.2.8.1. Visual character

Colloidal particles are so small that they may appear uniform even under a microscope. The droplets generated in the present investigation were however large enough to scatter light and due to this scattering, most emulsions appeared opaque or cloudy unless they were very dilute. A light beam can be seen as it passes through a colloidal suspension, which is known as the Tyndall effect. The Tyndall effect makes it possible to see the light beam coming from a projector in a smoke-filled theatre as well as the light beam from a cars headlights on a dusty road [179].

Due to the phenomenon of scattering of light at the oil/water interface, an emulsion generally looks opaque and muddy. In general, the colour will be lighter when the diameter of droplets is small, whereas it looks darker when the diameter of droplets are large [331]. The stability of an emulsion affects an emulsion's appearance and in most instances emulsion instability can be observed visually. According to the literature, visually observing an emulsion is the simplest, quickest and cheapest method to assess and evaluate emulsion stability without analytical equipment [8,144,199].

Depending on the interaction of light with the emulsion droplets, the size of droplets will affect the visual appearance of the emulsion, which can be opaque or optically transparent.

The separation processes most easily visually observed is creaming and sedimentation. By observing the thickness of the sedimentation or creaming layer of an emulsion, the extent of the destabilisation as a process can easily be evaluated. Other instability phenomena and processes such as Ostwald ripening, sedimentation, flocculation and coalescence are easily assessed by visual observation alone. To observe the first stage of emulsion instability analytical equipment is required to make an accurate determination [239].

3.2.8.2. Microscopy

Microscopy is also a visualisation tool, which can be used to examine emulsion droplets with sizes smaller than 100 μm , as well as observe processes that influence the stability of an emulsion. Different types of microscopes are available to characterise emulsions and its associated stability including properties which include, optical, electron, fluorescent and atomic force microscopy [187].

With the aid of microscopy, the distribution and dimensions of droplets can be observed providing valuable information on the origins of the emulsion systems stability. As an example, microscopy can identify if the droplets are homogeneously distributed, if the emulsion is flocculated or non-flocculated. As highlighted in Chapter 2, the flocculation and sedimentation processes of an emulsion can be observed when the droplets aggregate in close proximity to each other without coalescing into larger droplets. In this research a RS PRO USB Digital Microscope was used to observe and photograph the bubbles produced.

3.2.8.3. Turbidity

Turbidity and total suspended solids (TSS) are one of the most commonly used parameter of water quality. The visual appearance and water clarity is often considered an indicator of clean water [424]. Turbidity is an optical determined parameter and is often used to infer water quality based on clarity and for the determination of TSS [425]. Turbid water affects the physical look of the water making it appear murky or coloured and cloudy. Suspended solids and dissolved material may reduce water clarity by inducing a muddy, coloured or hazy, appearance.

The turbidity of a water sample is a function of the amount of light scattered by the droplets or particles in the water. The light scattered is dependent on the particles that are present, therefore turbidity and TSS are related. It should be noted that turbidity is not a direct measurement of the total suspended materials in water. Instead, as a measure of relative clarity, turbidity is often used to indicate changes in the total suspended solids concentration in water without providing an exact measurement of the solids. Turbidity and water clarity are both visual properties of water based on scattering and attenuation of light.

While turbidity and total suspended solids often overlap, there are a few outlying factors that only contribute to one or the other. Turbidity is determined by the amount of light scattered by these particles. While this measurement can then be used to estimate the total dissolved solids concentration, it will not be exact. Turbidity does not include any settled. In addition, turbidity measurements may be affected by dissolved organic matter. While this dissolved matter is not included in TSS measurements, it can cause artificially low turbidity readings as it absorbs light instead of scattering it.

Dissolved natural organic matter (NOM) is also sometimes referred to as humic stain, which refers to the tea colour produced from decaying organic material with the release of tannins and other molecules into the water. It should be noted that dissolved organic material can contribute to the turbidity reading. Turbidity is most often measured with a turbidity meter. Turbidity is measured in a unit called Nephelometric Turbidity Unit (NTU).

Total suspended solids, on the other hand, is a total quantity measurement of solid material per volume of water. This means that TSS is a specific measurement of all suspended solids,

organic and inorganic, by mass. TSS includes settleable solids and is the direct measurement of the total solids present in a water body. As such, TSS can be used to calculate the rate of sedimentation, while turbidity cannot be used [426].

Water turbidity is important from three aspects: aesthetic, filter blocking and disinfection. Excessive turbidity could show a defect in a purification system, and because of the relationship between turbidity and some features of microbial organisms, turbidity can be considered as an indirect parameter in determining the removal efficiency or the presence of these factors.

Turbidity was measured using a Hach TL2350 tungsten filament lamp turbidimeter supplied by Agua Africa CC (Hach, South Africa) utilising the nephelometric measurement method. The measurement range was between 0 - 10000 nephelometric turbidity units (NTU).

3.2.8.4. Bubble size analysis

As highlighted in Section 2.7.6, the efficiency of a flotation system is directly associated with the size of the bubbles generated [427]. The bubble size analysis was conducted utilising the ImageJ software for Windows. ImageJ is a public domain Java image processing program inspired by NIH Image, which is part of the National Institute of Health of the United States of America [428].

The software can display, edit, analyse, process, save and print 8-bit, 16-bit and 32-bit images as well as read images from various formats. It can measure distances and angles, which supports standard image processing functions such as contrast manipulation, sharpening, smoothing, edge detection and median filtering [428]. Spatial calibration is available to provide dimensional measurements, converting pixels in the image into various units of measurement making it possible to calculate the diameter of the bubbles in wastewater, which will be referred to as bubble size. High-definition pictures of the bubbles generated by the IAF and DAF units were analysed with the ImageJ software. The above photographic technique for bubble size measurements has also been reported by other research groups [340,429–431].

A threshold intensity was set to determine the segmentation so that each pixel in an image is matched with the set threshold. Next the scale of reference was entered as a known calibration,

after which, the 'Analyse tool' was employed to measure the area of the bubble. The effective bubble diameter was obtained by calculating the projected area of each bubble from images.

For the bubble size analysis for an area of interest below the rotor stator was selected to ensure that the smallest bubbles within the bubble swarm was analysed. For a representative sampling of bubbles in the areas of interest, several images were captured and analysed.

3.2.8.5. Droplet size distribution (DSD)

There are a number of particle and droplet sizing techniques commonly used, which include light scattering, ultrasonic spectrometry and electrical pulse counting [187,285,432]. These instruments are relatively easy to operate, can be fully automated and provide substantial information within a short period of time.

The light scattering technique measures the angle of backscattered light as well as the percentage of light when a beam of near-infrared monochromatic light is focussed on a sample. The larger percentage of backscattered light is indicative of higher droplet concentrations, while the droplet size distribution is associated with how the scattering pattern is observed through the number of scattering angles versus the associated light intensity. For light scattering instruments, samples with low droplet concentrations provides a more accurate result as it prevents the occurrence of multiple scattering effects [17].

The oil droplet size distribution (DSD) measurements of the emulsions were conducted with an Anton Paar particle size analyser model No. PSA 1190 (Anton Paar, South Africa) utilising a small volume unit for the analysis of small samples. The instrument utilises laser scattering for the measurement of droplet size. The P90 values of the emulsions were recorded and reported. The samples were measured in liquid mode using water as the carrier liquid. The measurements were performed without any sonication and stirring, to avoid any droplet breakage in the samples.

3.2.8.6. Chemical Oxygen Demand

The Chemical oxygen demand (COD) is the amount of oxygen that is required to oxidise organic materials in the water [44]. The COD is a measure of water and wastewater quality and an important measure of organic matter content [433]. The test has its widest application in

measuring waste loadings of treatment plants and in evaluating the efficiency of treatment processes.

The COD test uses a strong chemical oxidant in an acid solution and heat to oxidise organic carbon to CO₂ and H₂O. The COD is essentially the amount of oxygen consumed to chemically oxidise organic matter. The COD is often measured using excess of a strong oxidant, usually potassium dichromate, potassium iodate, or potassium permanganate, under acidic conditions [273].

In terms of process, a known amount of an oxidant is added to a sample. Once oxidation is complete, the concentration of organics in the sample is calculated by measuring the amount of oxidant remaining in the solution. The COD value gives an indication of the amount of oxygen consumed per litre of solution and is expressed in milligrams per litre (mg/L) [433]. COD is considered an important quality control parameter of effluent in wastewater treatment [434].

For the COD analysis a colorimeter method in water was utilised with a Thermo Scientific™ Orion™ AQUAfast™ AQ3140 COD colorimeter single parameter instrument. The AQUAfast AQ3140 COD colorimeter is used in sectors such as the food and beverage, pharmaceutical and agriculture for water analysis. The following procedure outlined below was utilised.

3.2.8.6.1. COD sample preparation

A COD high range digestion reagent vial was selected and 0.2 mL of the sample to be tested was added to the digestion vial. Similarly, a blank was also prepared by adding 0.2 mL of deionised water to the digestion vial. The blank is stable when stored in the dark and can be used for further measurements with vials from the same batch.

Following the addition of the sample to the digestion vials, the vials were slowly inverted several times, approx. 4-5 times to mix and ensure homogeneity of sample and reagent in the digestion vials.

3.2.8.6.2. COD sample digestion and measurements

The digester oven was preheated to 150°C for approximately 10 mins, following which, the prepared samples were placed in the preheated COD digester oven.



Figure 3.18. COD digester oven and AQ3140 COD colorimeter utilised for the COD measurements.

The vials were placed in the digester oven and heated for two hours, **Figure 3.18**. Following the heating, the digestion vials and its associated contents were inverted several times, while still warm to allow for mixing and allowed to cool to ambient temperature. Once cooled, the samples were tested using the colorimetric procedures.

3.2.8.7. pH

The pH of the samples was measured by means of a glass pH electrode and Martini instrument Mi 150 pH meter (Kimix Chemical & Lab Supplies CC, South Africa). The pH meter was calibrated utilising a pH 4, 7 and 10 standards.

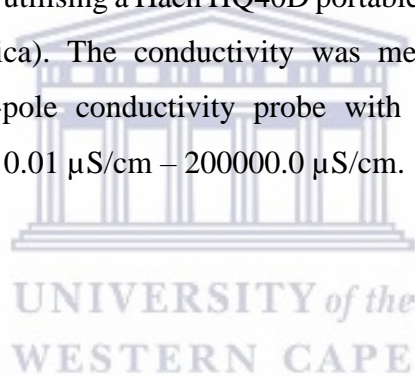
3.2.8.8. Electrical conductivity

Electrical conductivity, often referred to as conductivity is frequently used as a water quality parameter [435]. Conductivity is the measure of a material's capacity to conduct an electric charge. For a liquid and specifically for emulsions, this ability depends on the chemical

composition and in particular the dissolved ion concentrations, ionic strength and temperature [436]. The electrical conductivity of a colloidal suspension is a function of the continuous phase particle size, charge and volume fraction [435,437–439].

The conductivity of emulsion systems has also been studied and reported by a number of authors [435,440–445]. It has also been demonstrated that o/w emulsions have a higher electrical conductivity than w/o emulsions, implying that the emulsion type can be distinguished by measuring the electrical conductivity [442,445]. It is known that organic and petroleum oils are poor conductors of electricity, however they do exhibit some degree of electrical conductivity [443,446]. The electrical conductivity of an emulsion decreases with an increase in the oil volume fraction. Also, an o/w emulsion has a higher electrical conductivity as compared to that of w/o emulsions [437,441,447–450].

The conductivity was measured utilising a Hach HQ40D portable multi meter supplied by Agua Africa CC (Hach, South Africa). The conductivity was measured utilising an Intellical CDC401, digital, graphite, 4-pole conductivity probe with a temperature sensor and a measurement range of between 0.01 $\mu\text{S}/\text{cm}$ – 200000.0 $\mu\text{S}/\text{cm}$.



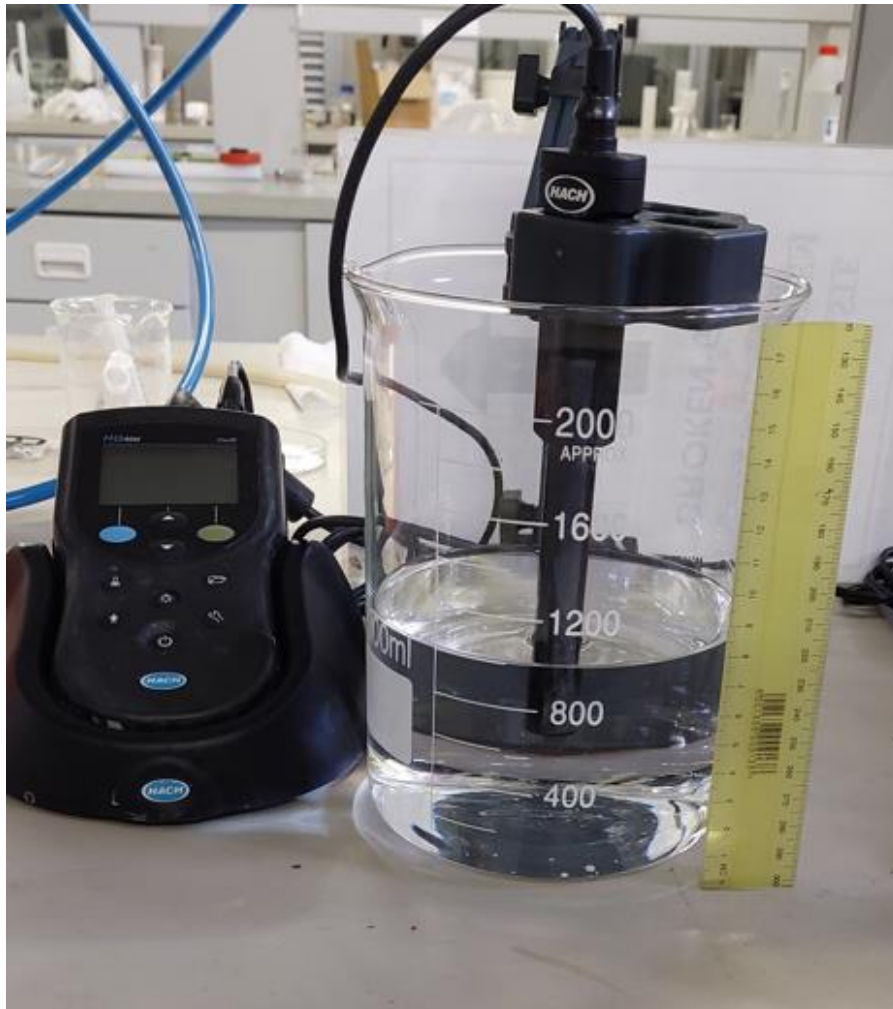


Figure 3.19. Set up of the conductivity instrument and probe during conductivity measurements of the emulsions pre and post treatment.

The conductivity measurements were recorded at 5 cm below the water surface as per **Figure 3.19**, depicting the setup and position of the conductivity probe. Every effort was made to ensure that conductivity measurements were taken at the same height below the water level, pre and post emulsion treatments.

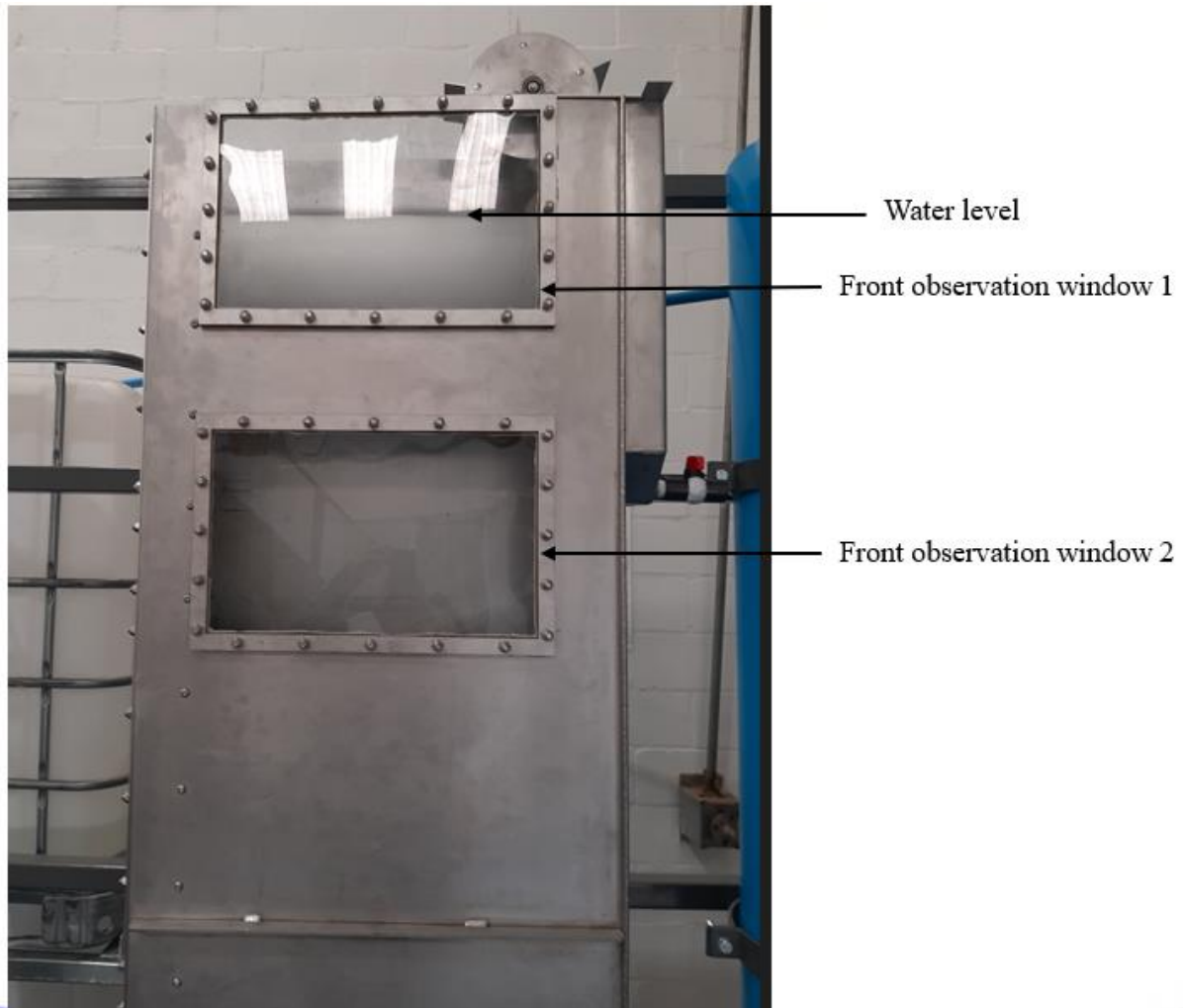


Figure 3.20. Set up of the conductivity instrument and probe during conductivity measurements of the emulsions pre and post treatment

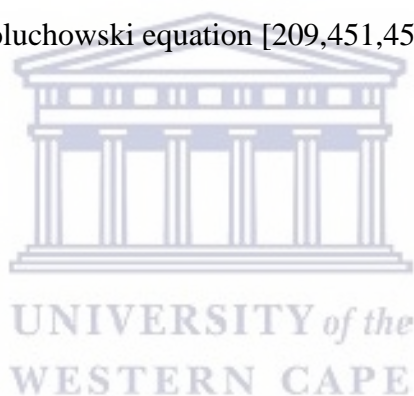
For the DAF experiments the conductivity measurements were recorded at 4.5 cm below the water surface as per **Figure 3.20**. Every effort was made to ensure that conductivity measurements were taken at the same height below the water level, pre and post emulsion treatments.

3.2.8.9. Zeta potential

The ζ potential measurements were performed immediately after emulsion preparation and emulsion treatment with IAF and DAF.

The capillary cells were rinsed with methanol and deionised water prior to use. In order to avoid the introduction of air bubbles into the capillary cells, the filling was done with a 1 mL syringe. The capillary cell was filled with the diluted sample and then inserted into the ζ potential instrument. For data analysis purposes, all measurements were reported as the average of three separate readings per sample.

The ζ potential measurements were conducted with a Malvern zetasizer Nano-ZS instrument (Malvern Instruments Ltd., South Africa) utilising folded capillary cells (DTS1070) and the universal dip cell kit (ZEN1002 – Serial Number MAL1050878). The ζ potential values were calculated by means of the Smoluchowski equation [209,451,452].



CHAPTER 4 RESULTS AND DISCUSSION

4.1. Analysis

All measurements and data points recorded are presented and expressed as the mean value and a standard deviation of at least three independent measurements.

Where variations in measurements were large, the data sets were normalised in order to identify and establish robust relationships between the data. The aim of the normalisation process was to make relational comparisons more informative between recorded measurements. The normalisation procedure utilised the minimum - maximum (max) process, normalising the new data value in the data set to a value between 0 and 100. The equation for the normalisation procedure is presented in Equation 4.1 below,

$$\text{data value} = (\text{value} - \text{minimum}) / (\text{max} - \text{minimum}) * 100 \quad \text{Equation 4.1}$$

In order to determine and establish trends and relationships between data sets regression analysis was performed. In this analysis as compared to other reports, R^2 values greater than 0.6 were considered significant and would imply a high level of correlation between data, whereas a measure below 0.4 would show a low correlation [56,453,454].

To determine statistical significance between datasets, Analysis of Variance (ANOVA) tests were conducted between data groups at a 95% confidence interval. Where applicable, one-way ANOVA tests were conducted and the null hypothesis assumed that there is no difference between the groups and equality between means. The alternative hypothesis tested was that there is a statistical difference between the groups and equality between means. Similar ANOVA statistical analysis were conducted by other researchers to evaluate the effects and relative importance of factors, interactions and performance associated with wastewater treatments [45,134,135,275,337,455].

The treatment efficiencies of the experiments were calculated utilising Equation 4.2.

$$\text{Treatment efficiency, (TE)} = (C_0 - C_{pt}) / C_0 * 100, \quad \text{Equation 4.2}$$

Where, C_0 is the initial measurement and C_{pt} the post treatment measurement with specific reference to turbidity and COD measurements before and after treatments, respectively.

The data was compiled, analysed and presented graphically using the Microsoft Excel 365 version and the Analysis ToolPak add-in.

4.2. Calculation of theoretical COD of prepared emulsions

Surfactant and emulsifier free oil in water emulsions were prepared utilising the following oils:

- Olive oil (Merck, South Africa),
- Sasol Multigrade L SAE 20W-50 (Sasol, South Africa),
- Sasol Monograde 40 SAE 40 (Sasol, South Africa).

The theoretical COD calculations are described below for each of the three oils used to prepare the o/w emulsions. It is assumed that the volumes of water and oil used are the same as those described in section 3.2.1. As described in the previous sections, the COD is a measure of the oxygen equivalent of the organic matter in an aqueous sample, which is oxidised by the addition of excess strong chemical oxidant.

4.2.1. Theoretical COD of olive oil emulsion

The theoretical COD of the olive emulsion was calculated utilising the following assumptions:

- Olive oil density = 0.92 g/mL
- Olive oil consists of fatty acids such as palmitic (C16:0), palmitoleic (C16:1), stearic (C18:0), oleic (C18:1), linoleic (C18:2) and linolenic (C18:3). Myristic (C14:0), heptadecanoic and eicosanoic acids are found in trace amounts with oleic acid consisting of between 55.0 - 83.0% [456].
- $C_{88}H_{164}O_{10}$, is the representative molecular formula for olive oil and has a molecular weight 1382.2 g/mol [457].

Utilising the density assumption, 20 mL of olive oil has a weight of 18.4 g. In 500 mL of H_2O the mass of oil per litre is 36800 mg/L.



Utilising the balanced reaction Equation 4.3, the theoretical COD was calculated to be 105645 mg/L.

4.2.2. Theoretical COD of Sasol lubricating engine oil emulsions

Most lubricating oils are of mineral origin and contain several different hydrocarbon species with mean molecular weights generally between about 300 g/mol and 600 g/mol [458].

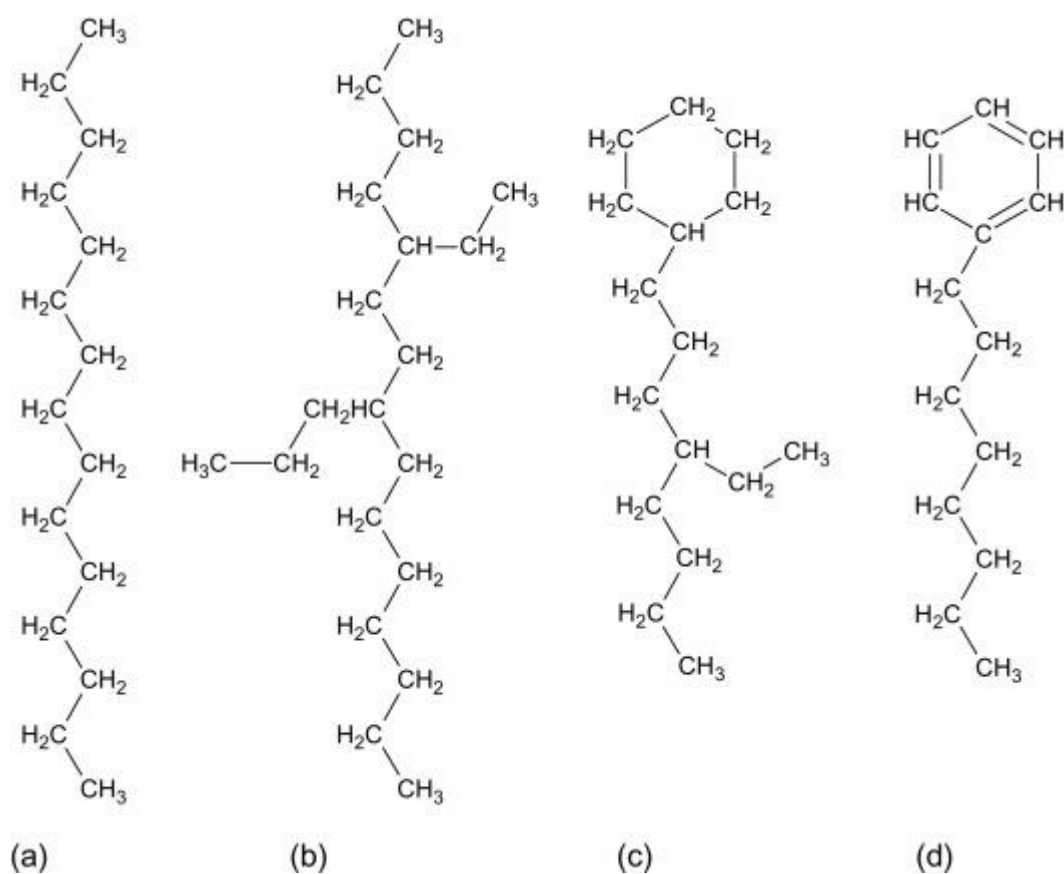


Figure 4.1. Examples of molecule structures of typical hydrocarbon molecules present in lubricating base oils: (a) paraffin ($C_{15}H_{32}$); (b) branched paraffin ($C_{20}H_{42}$); (c) naphthenic ($C_{16}H_{32}$); (d) aromatic ($C_{14}H_{22}$). Adapted from [458].

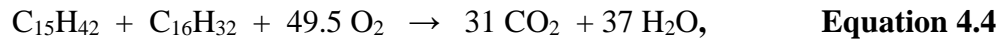
Examples of typical molecular structures of lubricating base oils are depicted in **Figure 4.1**.

4.2.3. Sasol lubricating engine multigrade oil

The theoretical COD of the Sasol multigrade engine oil emulsion was calculated utilising the following assumptions:

- Combination of paraffin (C₁₅H₃₂) and naphthenic (C₁₆H₃₂) compounds
- Density = 0.89 g/mL
- C₁₅H₃₂ and C₁₆H₃₂, combined molecular weight 436.84 g/mol [458].

Utilising the density assumption, 20 mL of Sasol monograde engine oil has a weight of 17.8 g. In 500 mL H₂O the mass per litre is 35600 mg/L.



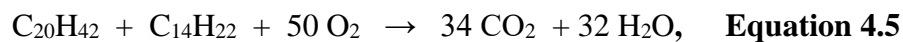
Utilising the balanced reaction Equation 4.4, the theoretical COD was calculated to be 129087 mg/L.

4.2.4. Sasol lubricating monograde engine oil

The theoretical COD of the Sasol monograde engine oil emulsion was calculated utilising the following assumptions:

- Combination of branched paraffin (C₁₅H₄₂) and aromatic (C₁₄H₂₂) compounds
- Density = 0.92 g/mL
- C₂₀H₄₂ and C₁₄H₂₂, molecular weight 472.87 g/mol [458].

Utilising the density assumption, 20 mL of Sasol monograde engine oil has a weight of 18.4 g. In 500 mL H₂O the mass per litre is 36800 mg/L.



Utilising the balanced reaction Equation 4.5, the theoretical COD was calculated to be 124516 mg/L.

Table 4.1. Comparison of theoretically calculated COD of emulsions versus measured results.

Emulsion	Theoretical calculated COD (mg/L)	Measured COD (mg/L)	Percentage of oil emulsified (%)
Olive Oil	105645	1572±82	1.5
Sasol Multigrade	129087	899±89	0.7
Sasol Monograde	124516	411±40	0.3

The theoretical calculated and actual COD measurements of the emulsions are presented in **Table 4.1**. Based on the comparison between the theoretical calculated and actual COD measurements, it is evident that with the emulsification procedure utilised, only approximately 1.5% to 0.3% of the oil was present in the aqueous continuous phase and emulsified or dissolved oil. The balance of the oil remained present in the aqueous continuous phase as free oil.

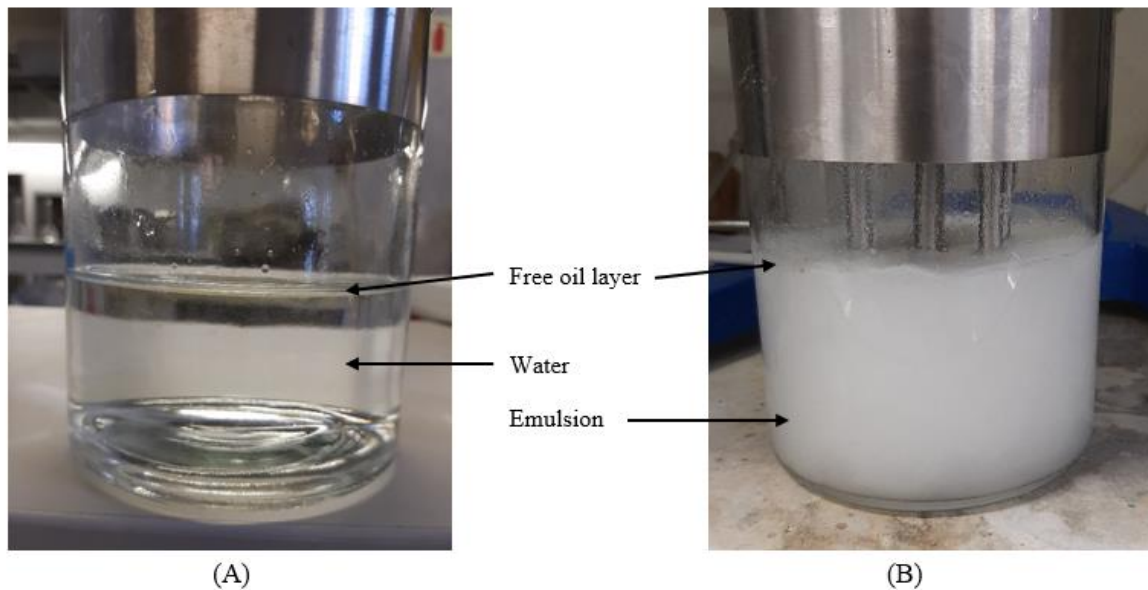


Figure 4.2. (A) olive oil and water mixture prior to emulsification process. (B) Olive oil emulsion highlighting free oil layer.

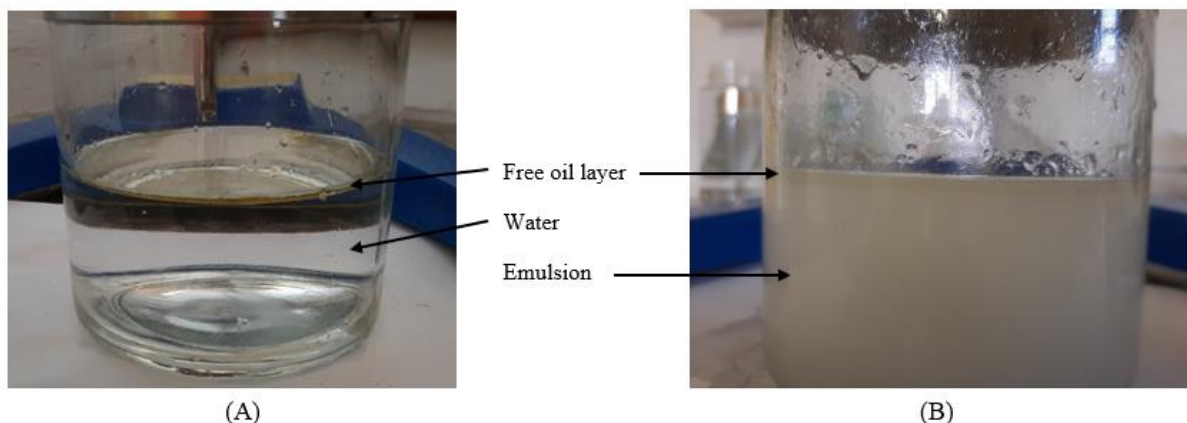


Figure 4.3. (A) Sasol multigrade oil and water mixture prior to emulsification process. (B) Sasol multigrade oil emulsion highlighting free oil layer.

Prior to the emulsification process the oils were added to the water and as observed in **Figure 4.2 A** and **Figure 4.3 A**, free oil was present on the surface of the water. During and after the emulsification process, free oil was also observed on the surface of the emulsion as highlighted in **Figure 4.2 B** and **Figure 4.3 B**, providing evidence that not all the oil was emulsified or dissolved during the emulsification process. Post the emulsification process, free oil was present and was observed on the surface of the emulsion, for all the prepared emulsions.

4.3. IAF shear experiments

The IAF shear experiments were conducted utilising the procedure described in Section 3.2.6.

4.3.1. Bubble sizes analyses of IAF shear experiments

As highlighted in Chapter 2, the bubble size, *i.e.* the bubble diameter, the hydrodynamic behavior are fundamental to the formation of bubble-droplet attachment, aggregation and the overall performance of flotation equipment and processes [62,159,336,340].

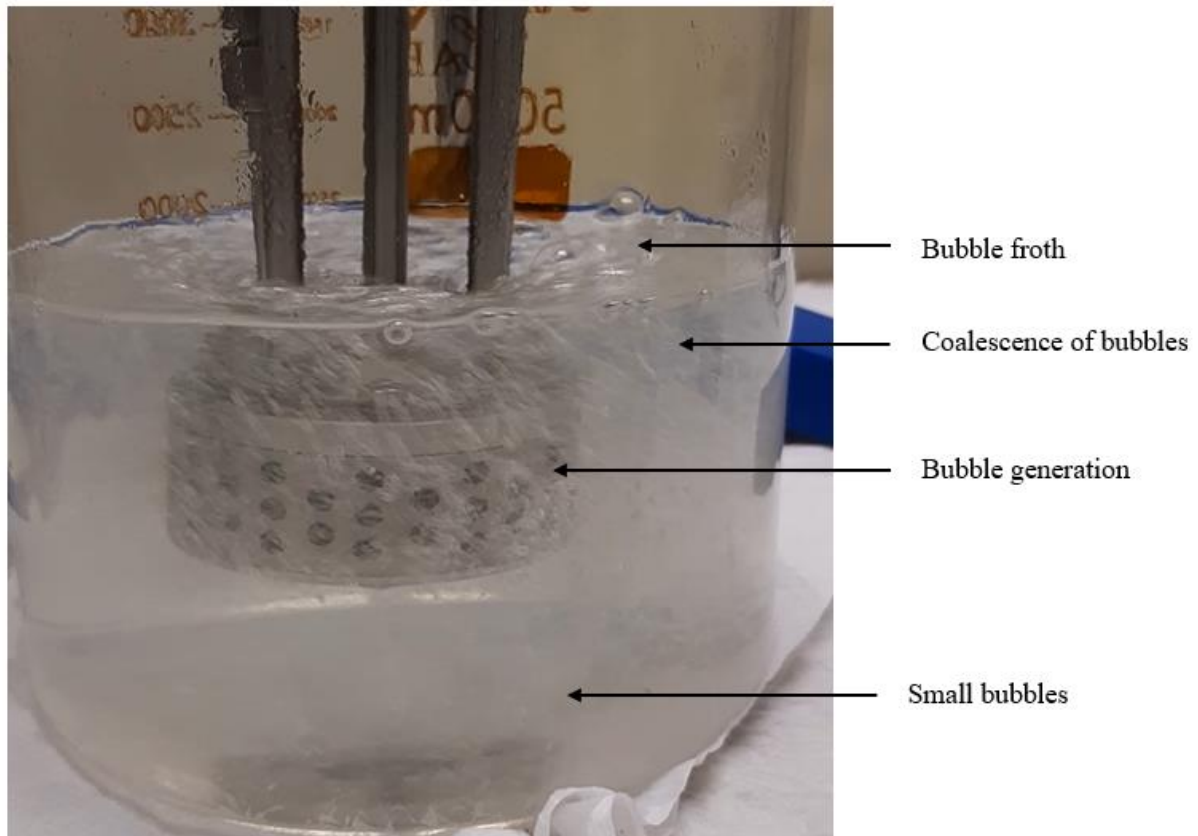


Figure 4.4. Picture of the bubble swarm generated in pure water during the IAF process.

Prior to the IAF emulsion treatments, experiments were conducted to assess the bubble size of the bubbles generated within the bubble swarm of the IAF experimental set up, as per the experimental procedure described in Section 3.2.8.4., and highlighted in **Figure 4.4**. The bubbles generated at 4000 rpm with air in pure water were analysed visually from photos in terms of approximate size within the bubble swarm [348].

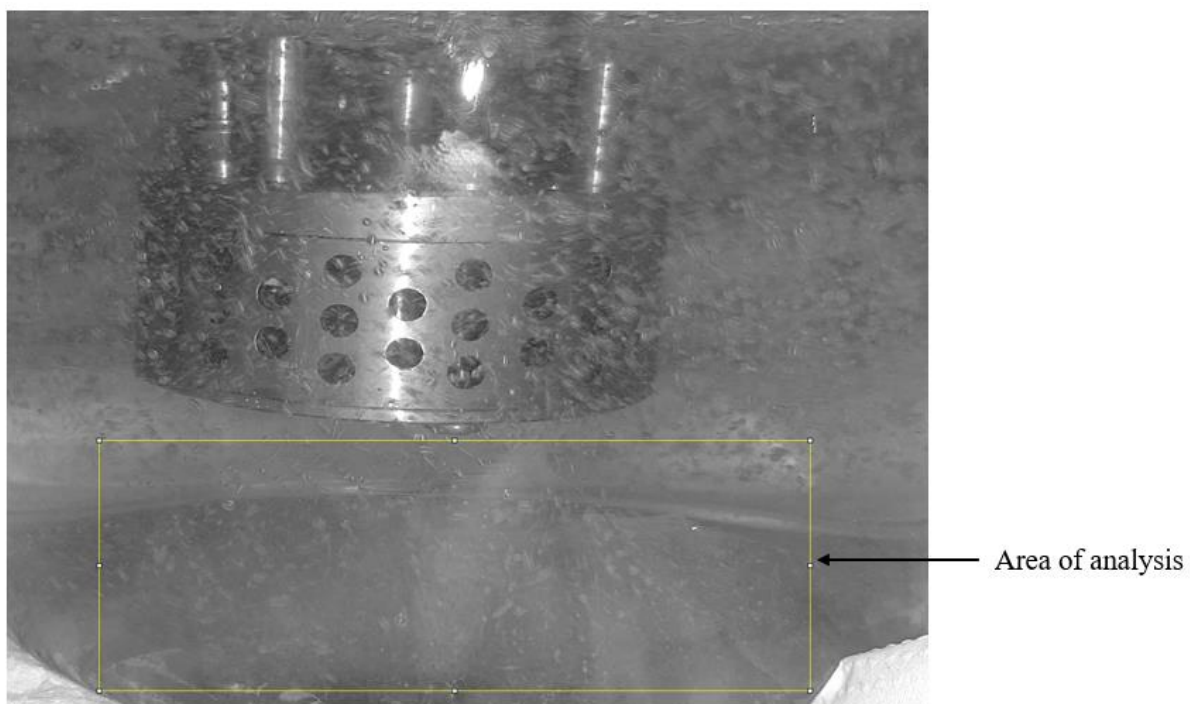


Figure 4.5. Picture of the area of interest below the rotor stator selected for bubble analysis.

For the bubble size analysis, an area of interest below the rotor stator was selected to ensure that the smallest bubbles within the bubble swarm were analysed as depicted in **Figure 4.5**.

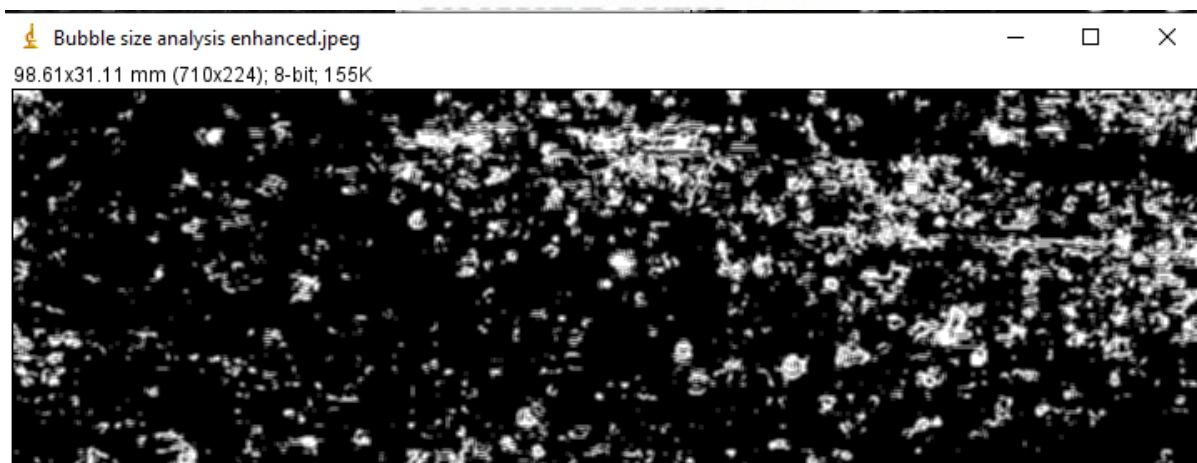


Figure 4.6. Area of interest enhanced by the ImageJ software to highlight the bubbles in pure water during the IAF process, bubbles are white in colour with the water matrix in black.

The photo of the area of interest was converted to an 8-bit image and further enhanced with the bubbles depicted in white and the background water in black, **Figure 4.6**.

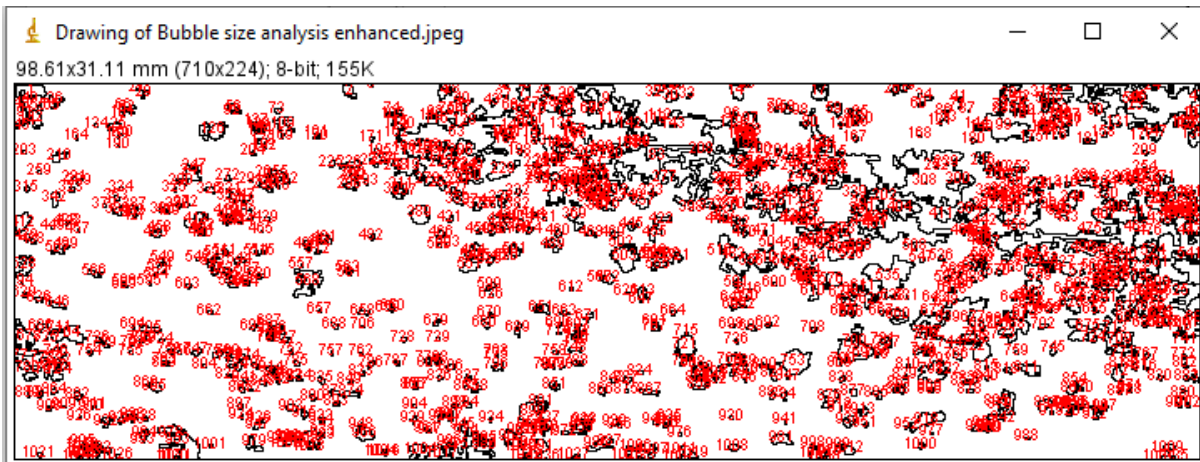


Figure 4.7. Area of interest enhanced by the ImageJ software to highlight the bubbles in pure water during the IAF process, the bubbles and bubble groups are represented as areas with black outlines with the bubble counts in red.

The bubbles within the area of interest were analysed in terms of the size, which for the specific image, **Figure 4.7**, 1038 bubbles were identified.

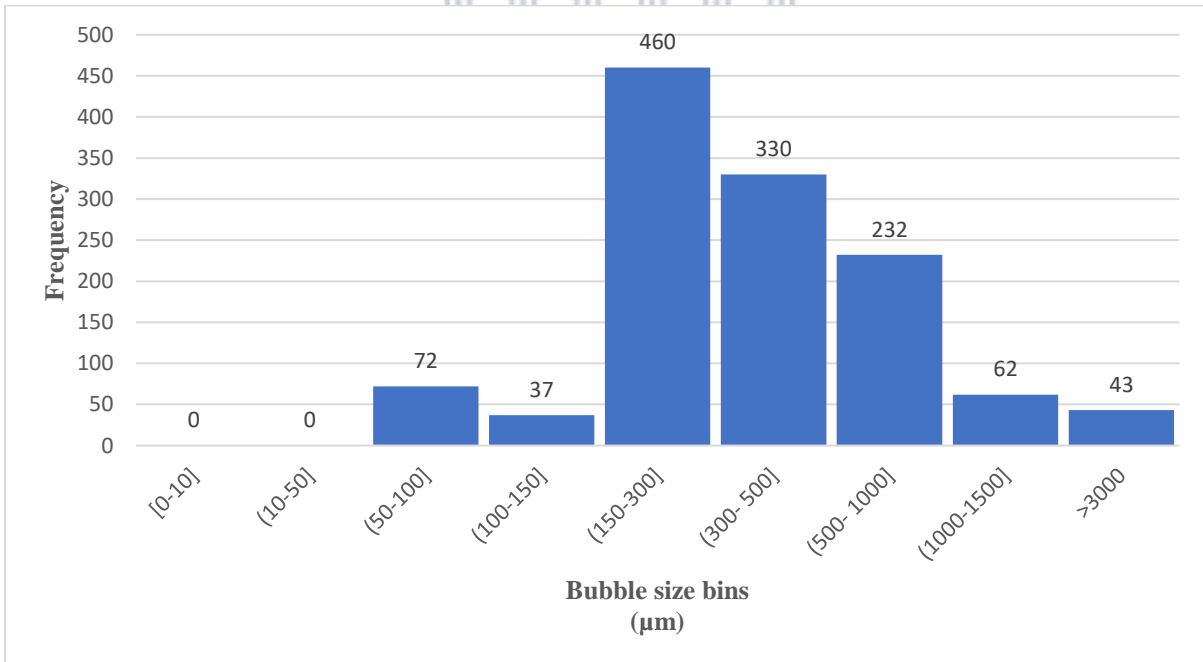


Figure 4.8. Histogram of bubble sizes identified within the area of interest for pure water.

Figure 4.8 depicts a positively skewed histogram of the bubble size versus frequency in the area of interest for pure water. As depicted in **Figure 4.8**, in the area of interest there were no

bubbles with a diameter of less than 50 μm , approximately 6 % of the bubbles observed had a diameter of between 50 μm and 100 μm , 3% of the bubbles had a diameter of between 100 μm to 150 μm and 37% of the bubbles had a diameter of between 150 μm to 300 μm , this implies that 50% of the bubbles were greater than 300 μm .

A similar procedure was followed to determine the spread of bubble sizes produced for the prepared emulsions exposed to IAF experiments.

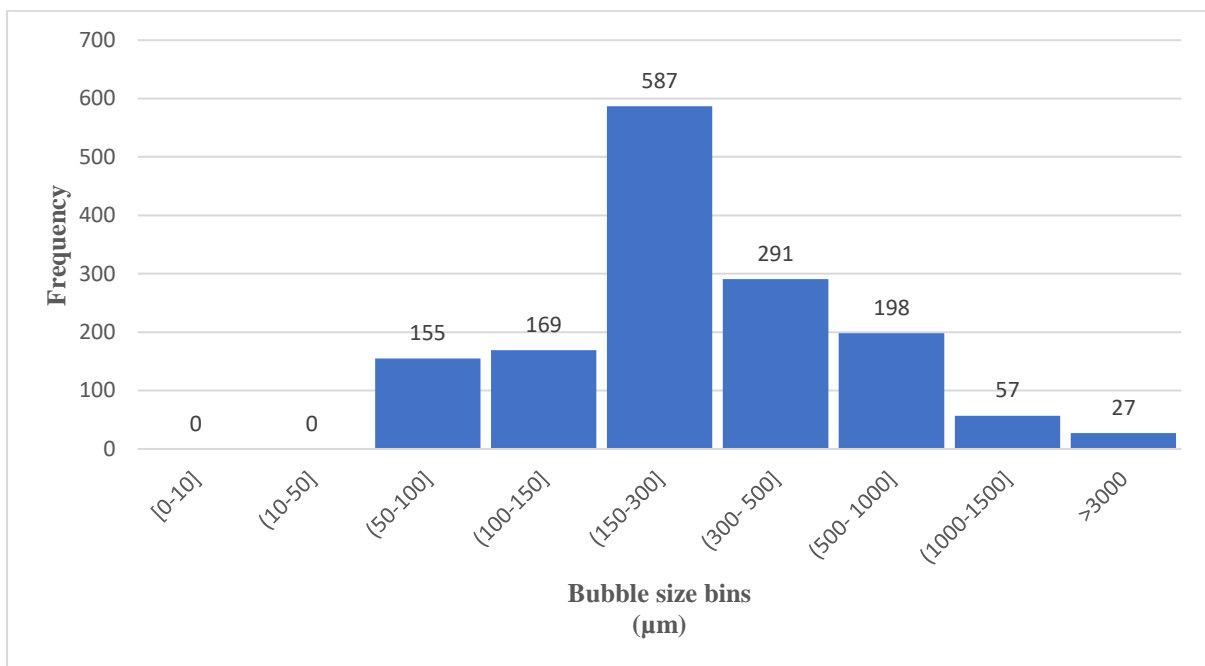


Figure 4.9. Histogram of bubble sizes identified within the area of interest for an olive oil o/w emulsion.

As with the pure water experiment, the bubbles produced for an olive oil o/w emulsion are depicted in **Figure 4.9** as a positively skewed histogram of the bubble size versus frequency. The results are similar to those for pure water. In the area of interest there were no bubbles with a diameter of less than 50 μm , approximately 10% of the bubbles observed had a diameter of between 50 μm and 100 μm , 11% of the bubbles had a diameter of between 100 μm to 150 μm and 39% of the bubbles had a diameter of between 150 μm to 300 μm , this implies that 38% of the bubbles were greater than 300 μm .

The results as depicted in **Figure 4.9**, are similar to the bubble sizes reported by other authors in the literature for IAF flotation systems [16,62,349,386,459].

4.3.2. Visual comparison of treatment on pure water

Prior to the treatments being performed on the emulsions, the treatments were conducted in pure water and the effects were compared visually.

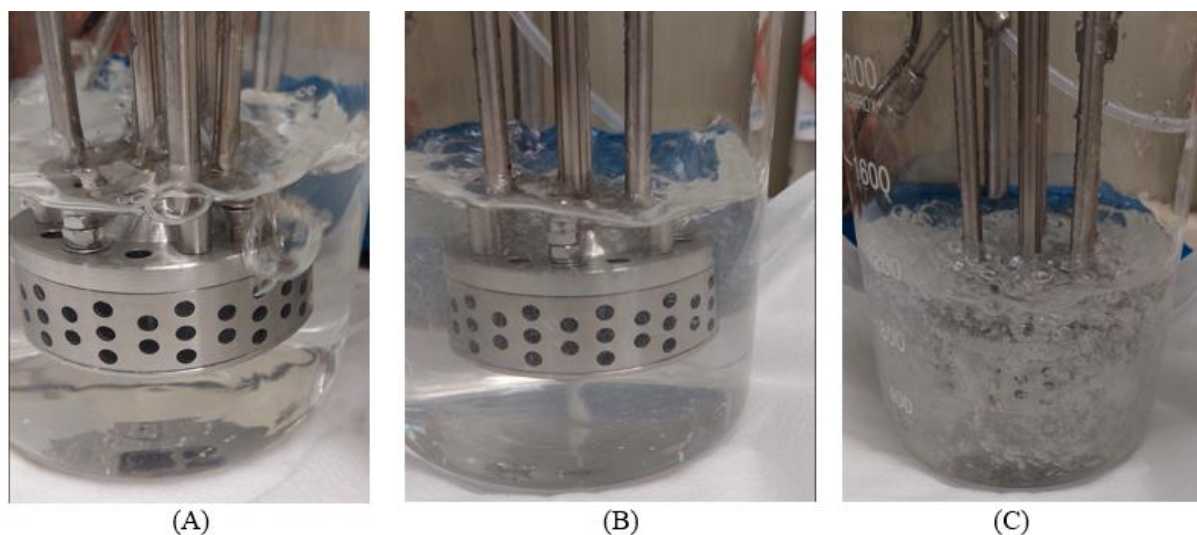


Figure 4.10. Visual comparison of the treatments on pure water, with (A) picture showing the result of air through the water, (B) picture showing the result of hydrodynamic shear, and (C) picture showing the effect of air and hydrodynamic shear.

The visual comparison and effects of the treatment on pure water are presented in **Figure 4.10** above. Exposing the water to air alone with no stirring produces air bubbles that are relatively large with no impact on the overall appearance of the water, **Figure 4.6(A)**. Exposing the water to hydrodynamic shear alone, at 4000 rpm, results in high-speed mixing of the water with the water appearance becoming more turbid with a small number of very small bubbles being produced, **Figure 4.6(B)**. Exposing the water to air and hydrodynamic shear produces a bubble swarm that consist of a large number of bubbles of various sizes. A large number of bubbles, small and large, rising through the liquid resulted in the formation of a short-lived foam or froth on the surface of the water, **Figure 4.6(C)**.

4.3.3. Properties of prepared emulsions prior to treatment

The physical properties of the prepared emulsions are presented in **Table 4.2**. All the prepared emulsions produced and utilised in the experiments had measurements of ζ potentials greater than -60 mV, turbidity values greater than 282 NTU, conductivity's greater than 24.48 $\mu\text{S}/\text{cm}$

and DSD of less than 20 μm . The parameters measured, are an indication of relatively stable oil in water emulsions, which were produced for all three oils used in the IAF experiments. The initial turbidity, conductivity and ζ potential measurements of the stable emulsion is associated with the typically small average oil droplet size in the continuous aqueous phase.

Table 4.2. Properties of the prepared untreated emulsions.

Emulsion	pH	DSD, D90 (μm)	ζ Potential (mV)	Turbidity (NTU)	COD (mg/L)	Conductivity ($\mu\text{S}/\text{cm}$)
Olive oil	7.2	2.7 \pm 0.02	-64.2 \pm 8	363 \pm 30	1572 \pm 82	61.7 \pm 3
Sasol multigrade oil	5.3	4.8 \pm 0.004	-82.9 \pm 4	282 \pm 42	899 \pm 89	57.2 \pm 2
Sasol monograde oil	6.2	18.1 \pm 0.6	-73.0 \pm 5	288 \pm 33	411 \pm 40	24.5 \pm 12

4.3.4. Emulsions exposed to shear

The ζ potentials of the associated o/w emulsions prepared from olive oil, Sasol multigrade and Sasol monograde oil, subjected to hydrodynamic shear over a rpm range of between 2000 to 6000 rpm are depicted in **Figure 4.11**.

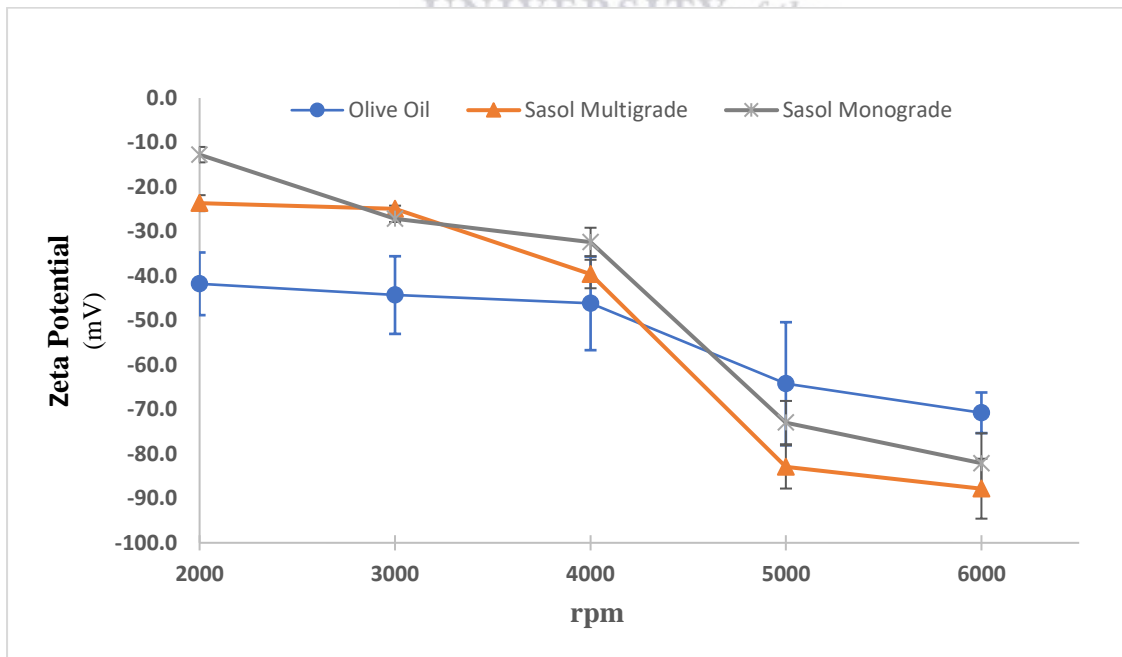


Figure 4.11. Plot of ζ potential as a function of rpm of emulsions.

Based on the results presented in **Figure 4.11**, it is evident that emulsions exposed to high rates of shear, *i.e.* rpm's greater than 4000 rpm, resulted in higher ζ potential values of between -60 mV and -87 mV, which are reflective of emulsions becoming more stable. The negative values of the ζ potential imply that oil droplets in the water are negatively charged over the studied pH range (5.3–7.2), which is consistent with literature reports [57,134,204].

This result was also observed by other authors, utilising various organic material and oily solvents to produce o/w emulsions, highlighting that high shear mixing in various emulsions including ointments, o/w emulsions, w/o emulsions and other colloids, results in the rupture of oil droplets, creating a smaller DSD and produces relatively more stable emulsions at higher rpms [74,151,405]. As highlighted in Chapter 2, it is evident that when shear rates are high enough, the droplet rupture phenomenon becomes preponderant, resulting in smaller droplets [460]. Based on the results obtained and presented in **Figure 4.10**, to avoid producing stable emulsions during the treatments all the shear treatments were conducted as to not exceed 4000 rpm. The amount of shear as well as the flow rate of air applied to the emulsions were kept constant at 4000 rpms and 1000 L/h respectively, where air and shear were applied during the treatments.

4.3.5. Effect of treatment on zeta potential

The ζ potentials of the emulsions pre and post treatments were measured as per the procedure in Section 3.2.8.9.

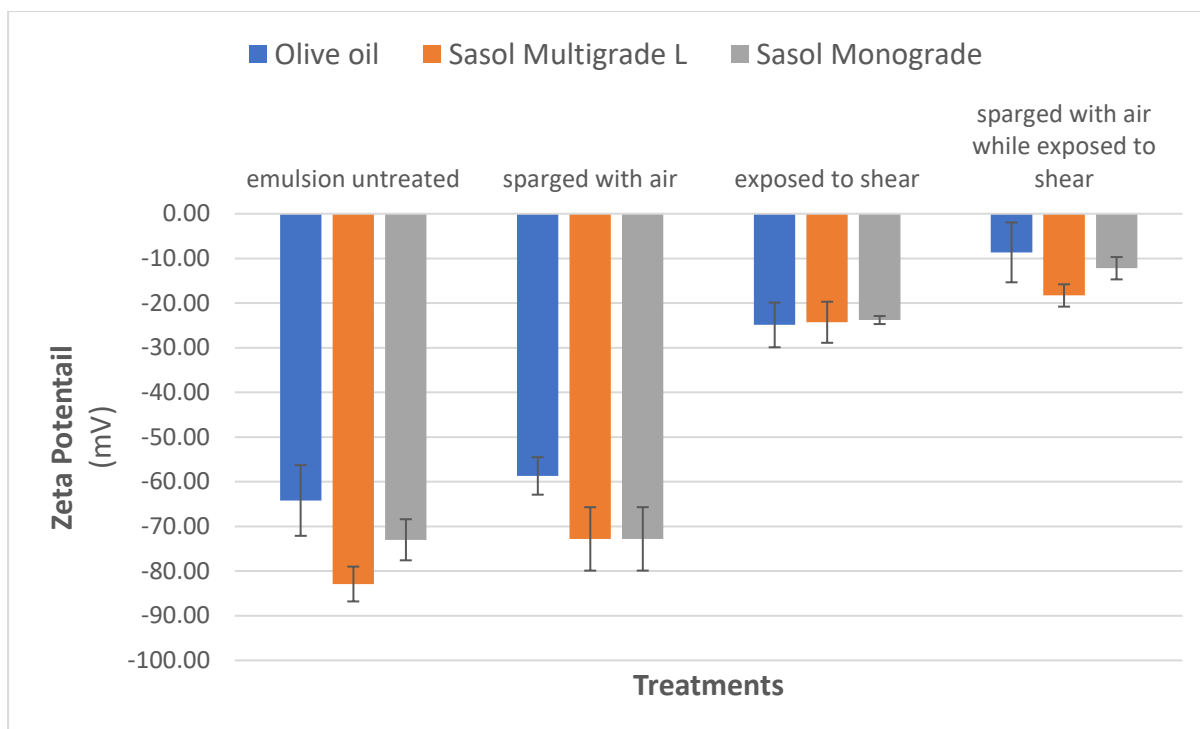


Figure 4.12. Graph of ζ potential readings of emulsions pre and post treatments.

Figure 4.12 shows the effect of various treatments on the ζ potential. The treatment sparged with air shows no significant change in the ζ potential of the treated emulsion, this result is evident for all three oil in water emulsions utilised in the study. This highlights the fact that this treatment had no impact on the overall stability of the three emulsions.

For the treatment exposed to shear only, and the treatment sparged with air and exposed to shear, the ζ potential of the emulsions are moving closer to 0. This change in ζ potential can be ascribed to a change in the stability of the emulsion with the specific treatments. It is evident that these treatments have a direct impact on the overall stability of the emulsions. As highlighted in Chapter 2, resultant ζ potentials below ± 30 mV for emulsions result in processes like aggregation, sedimentation and flocculation resulting in demulsification and phase separation of the emulsion [221,224].

4.3.6. Effects of treatment on DSD

For all DSD measurements, the D90 values are reported, which describe the diameter where ninety percent of the distribution of the sample analysed has a smaller particle size and ten percent has a larger particle size.

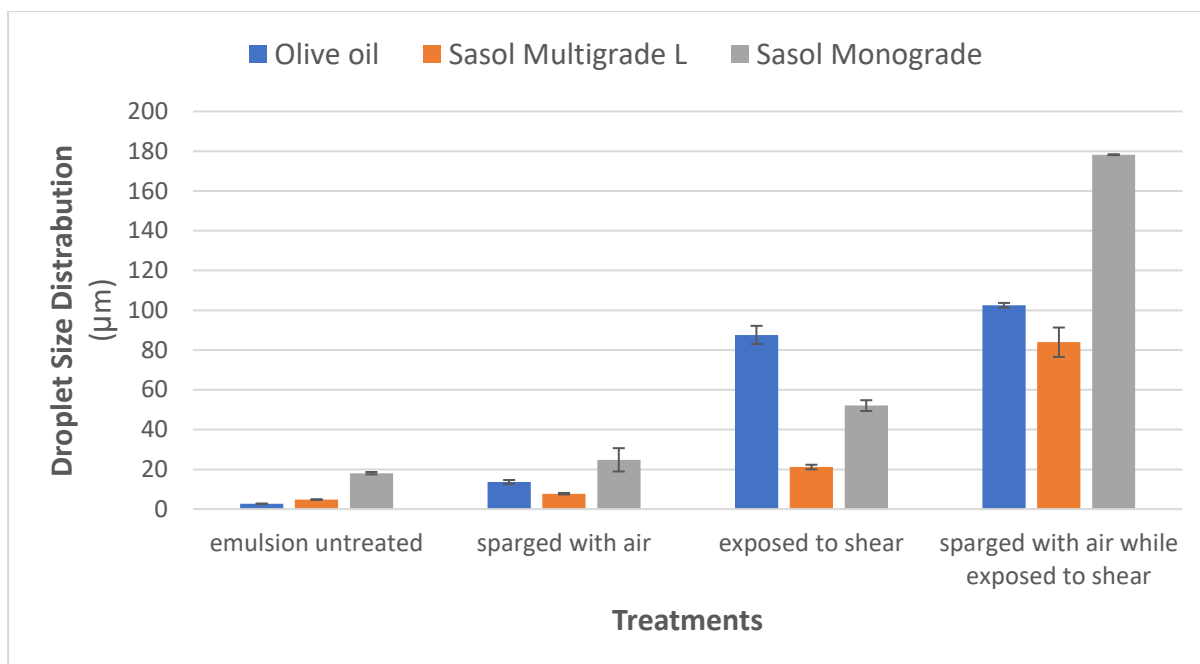


Figure 4.13. Graph of the DSD of the emulsions pre and post treatment.

Figure 4.13 shows the D90 DSD measurement values of the emulsions before and after each treatment. Measurements of DSD did not include those of free oil and every effort was made to ensure representative and homogenous samples from the emulsions and processed water were recorded, as described by the procedure in Section 3.2.8. The DSD results presented in **Figure 4.13**, indicate that the emulsions sparged with air showed only a minor increase in the overall DSD. For the olive oil emulsion, it increases from 2.7 µm to 13.7 µm, for Sasol Multigrade emulsion increased from 4.8 µm to 7.7 µm and for the Sasol Monograde from 18.1 µm to 24.8 µm. The DSD for all the emulsions sparged with air are all less than 25 µm indicating relative overall stability of the emulsions.

Table 4.3. Percentage increase of the DSD for the various treatments from the untreated emulsion.

Emulsion	sparged with air (%)	exposed to shear (%)	sparged with air while exposed to shear (%)
olive oil	406	3140	3693
Sasol Multigrade L	62	342	1654
Sasol Monograde	37	188	886

Table 4.3 presents the percentage increase of the DSD for the various treatments from the untreated emulsion. For the treatment, sparged with air while exposed to shear, there was a relatively large and significant percentage increase of DSD measurements. Due to fact that the increased change in DSD percentages were so large the dataset was normalised, utilising the procedure highlighted in Section 4.1, to give a clearer representation and presentation of the effect of various treatments on DSD.

As shown in the **Table 4.3**, there is also a relatively large percentage increase in the DSD for the olive oil emulsion exposed to shear, however only relatively small percentage increases in DSD's were observed for the other two shear treated emulsions. The olive oil emulsion measurement does not follow the same trend and this could be due to a number of factors including the olive oil chemical composition. Perhaps it is the limited ζ potential of olive oil, requiring less effort to force droplet aggregation. Further work would need to be carried out to explain this anomaly in more detail.

Table 4.4. Normalised percentage increase of the DSD for the various treatments.

Emulsion	sparged with air (%)	exposed to shear (%)	sparged with air while exposed to shear (%)
olive oil	10.08	84.87	100.00
Sasol Multigrade L	0.68	8.34	44.23
Sasol Monograde	0.00	4.13	23.23

The normalised percentage increase of the DSD for the various treatments, as presented in **Table 4.4** gives a clearer depiction of the overall DSD results. Based on the results, sparging of air had no significant effect on the overall DSD or on the overall stability of the emulsions.

For the treatments utilising exposure to shear alone as well as those sparging with air while exposure to shear, resulted in a relatively large increase in the measured DSD. Based on the results observed in **Figure 4.13**, it is evident that application of shear rate resulted in droplet aggregation and coalescence, which correlates with the decrease in ζ potential. The treatment, sparged with air while exposed to shear, resulted in the largest DSD increase and destabilisation with separation of the emulsions. This result is consistent with other reports where emulsions exposed to shear, which results in an increase in the DSD and phase separation is observed [16,87,196]. The air being introduced within the high shear environment is a historically a means to introduce bubbles into the destabilised emulsion which attach to flocs which will rise to the surface thereby separating oil droplets from the aqueous phase.

To the author's knowledge, there has been no reports in literature of the role air plays in a high shear environment and how it initiates coagulation, it is clear, based on this research, that it is not only used to float flocs to the surface. The measured DSD is derived from samples that are drawn from below the surface of the water where the free oil is floating. The oil that floated to the top as a result of its attachment to air bubbles is not the oil in the DSD sample. This possibly is indicative of another mechanism which is at play that creates larger particles. The hydrophobic nature of air is likely facilitating oil to oil droplet aggregation, specifically in a high shear environment. The air being introduced within the high shear environment is historically a means to introduce bubbles into the destabilised emulsion which attach to flocs which will rise to the surface thereby separating oil droplets from the aqueous phase. This

phenomenon whereby the hydrophobic nature of air is likely facilitating oil to oil droplet aggregation, specifically in a high shear environment, was researched in more detail and transformed in the registration of a South African provisional patent with application number, 2022/12418

The change in the DSD with the treatments may be explained as a result of flocculation and coalescence processes of the emulsion droplets associated with destabilisation and separation of the emulsion, as have been reported in the literature [193,461]. These observations are consistent with other reports associated with stable emulsions exposed to hydrodynamic shear [74,143,144,405].

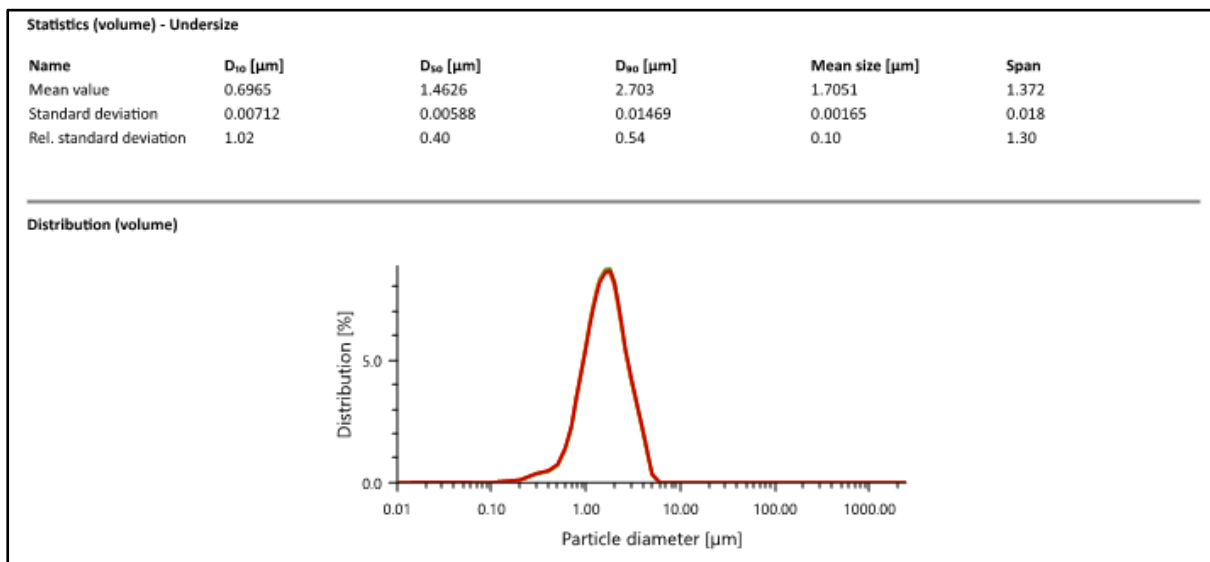


Figure 4.14. DSD curve of a prepared stable olive oil o/w emulsion.

The DSD of the prepared emulsions before treatments were observed to be relatively monodisperse with a consistent uniformity. **Figure 4.14**, shows an example of the monodisperse nature of the DSD curve with a consistent uniformity for the prepared olive oil emulsion with a D₉₀ DSD of 2.7 μm. For all the DSD results, three measurements of the same sample were recorded and are presented as a green, yellow and red curve on the DSD graph.

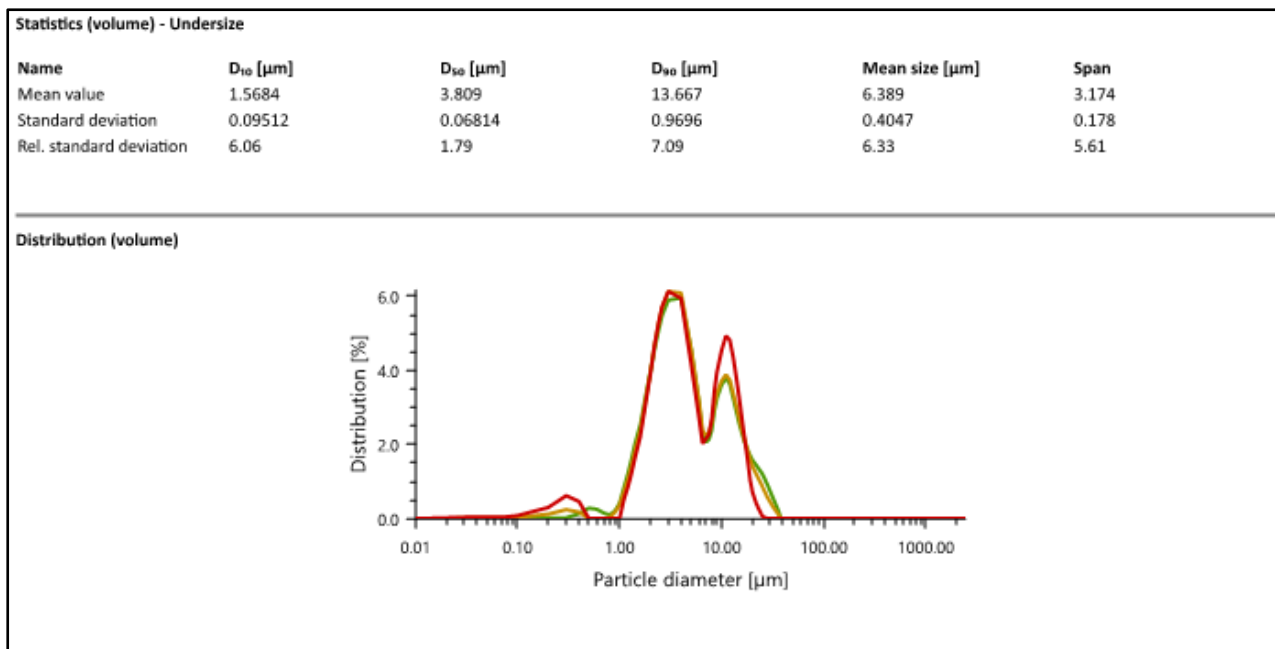


Figure 4.15. DSD curve of the olive oil o/w emulsion sparged with air.

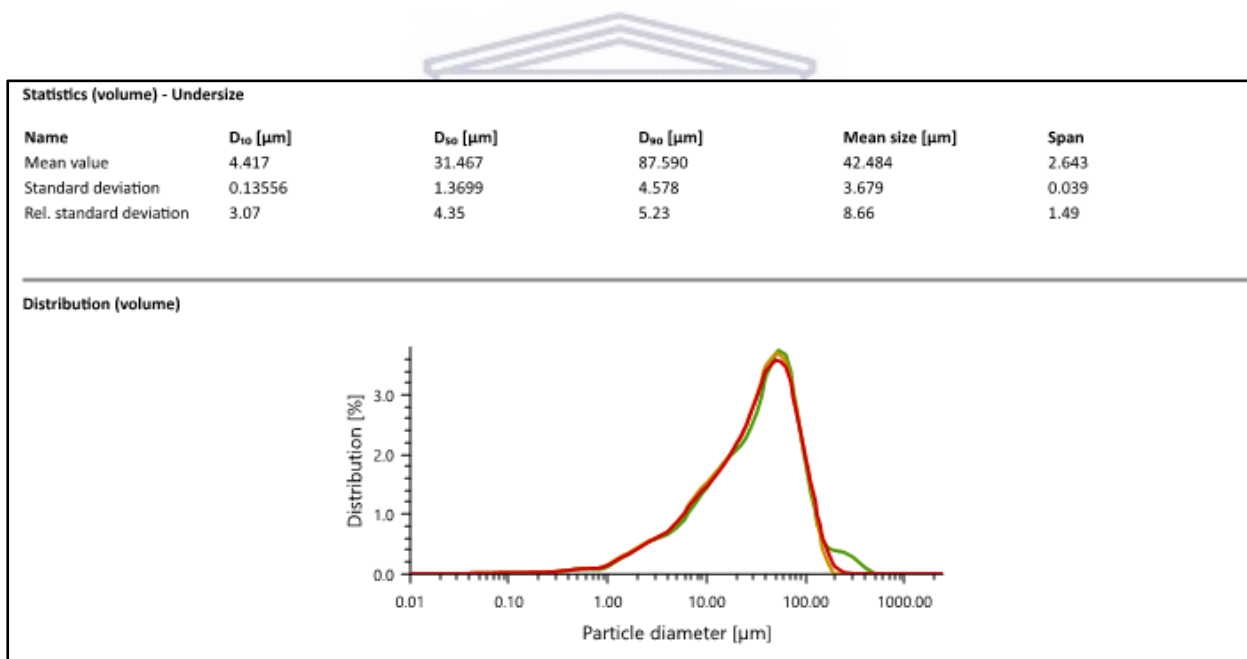


Figure 4.16. DSD curve of the olive oil emulsion exposed to shear.

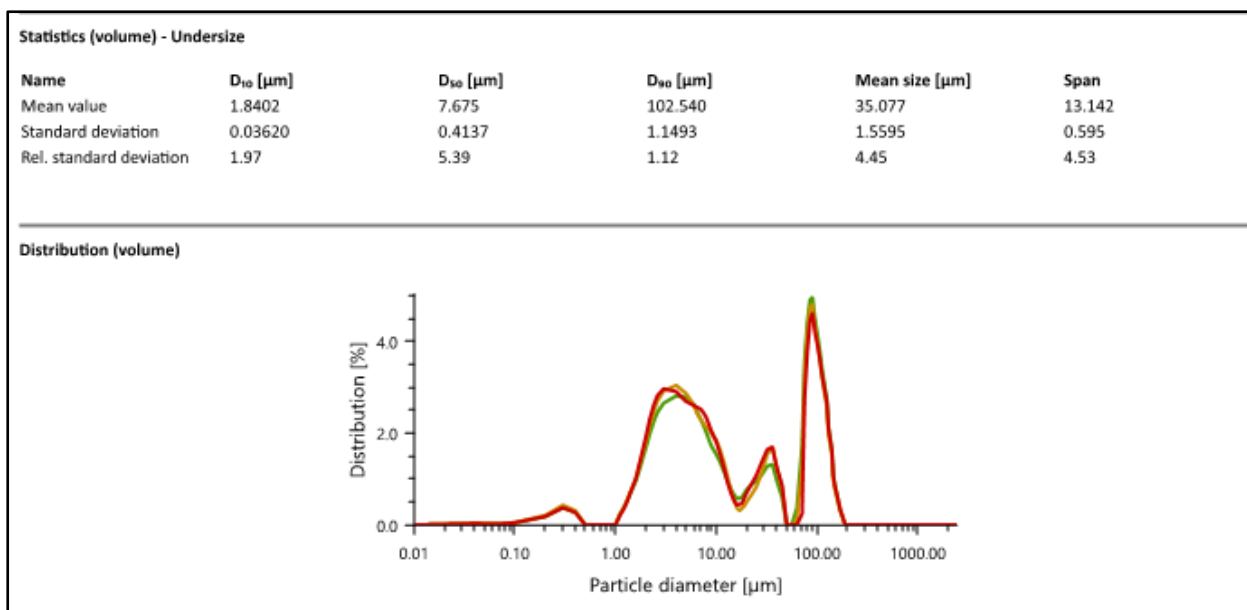


Figure 4.17. DSD curve of the olive oil emulsion sparged with air while exposed to shear.

In contrast to the monodispersed nature of the prepared olive oil emulsion prior to treatment, **Figures 4.15, 4.16 and 4.17**, shows the polydispersed nature of the olive oil emulsion post treatments. The polydispersed nature of the distribution curves post treatments are a result of emulsion destabilisation processes associated with the treatments. The results highlighted in **Figure 4.10** indicate that the DSD in the emulsion has a relatively wide range, from between 1.8 μm to 102 μm, implying that emulsion has become unstable with the DSD transforming from a relatively narrow range to a relatively wide range, associated with droplet flocculation and coalescence resulting in the formation of larger droplets [39,53,175,405,462].

4.3.7. Effect of treatment on conductivity

The conductivity of the oils used prior to the emulsification process and those of the prepared emulsions were recorded utilising the procedure presented in Section 3.2.8.8, and presented in **Table 4.5**. The conductivity of the water used for the emulsion preparation was recorded a 0.05 ± 0.01 μS/cm at 20 °C

Table 4.5. Conductivity measurements of the oils and prepared emulsions at 20 °C.

Oil	Pure bulk oil ($\mu\text{S}/\text{cm}$)	Emulsion ($\mu\text{S}/\text{cm}$)
Olive oil	0.11 \pm 0.7	61.68 \pm 2.75
Sasol multigrade oil	0.29 \pm 0.9	57.15 \pm 2.43
Sasol monograde oil	0.33 \pm 0.9	24.48 \pm 12.7

The results presented in **Table 4.5**, show there is an increase in the conductivity of the associated prepared emulsions, as compared to the original pure bulk oil. These results are consistent with literature reports for low concentration of o/w emulsions [445,446,450]. It has also been demonstrated that o/w emulsions, have a higher electrical conductivity than w/o emulsions, implying that the emulsion type can be identified through the measurement of its electrical conductivity [442,445]. It is generally accepted that organic and petroleum oils are bad conductors of electricity, however they do exhibit some degree of electrical conductivity [446]. The conductivity of oil is dependent on several factors, including the chemical composition of the base oil, additives and the associated polarity of the chemical compounds [443]. The increase in conductivity of the emulsion, as compared to that of the pure bulk oil and to that of the aqueous phase is associated with the physical properties of the oil making up the emulsion, which can include the size of the droplets, the associated charge of oil droplets, oil volume fraction and the dissolved ions in the continuous aqueous phase from the associated oils [440,441].

It has been reported extensively that the electrical conductivity of o/w emulsion is directly related to the oil volume fraction [441,449,450]. The electrical conductivity of an emulsion decreases with an increase in the oil volume fraction, as well as an o/w emulsions has a higher electrical conductivity as compared to that of w/o emulsions [437,447,448].

With respect to olive oil, it has been reported that it is rich in oleic fatty acid, which is known to act as an emulsifying agent, as well as being able to introduce protons from the carboxylic acid groups into the continuous phase [442,456,463]. For the Sasol oils, some degree of the conductivity increase can be attributed to the fact that the oils are zinc fortified. It has been demonstrated that the larger the concentration of metal-organic additives, the higher the

petroleum lubricant's conductivity as well as that of the resultant produced emulsion as ionic metal complex species become charge carriers in the continuous phase [464,465].

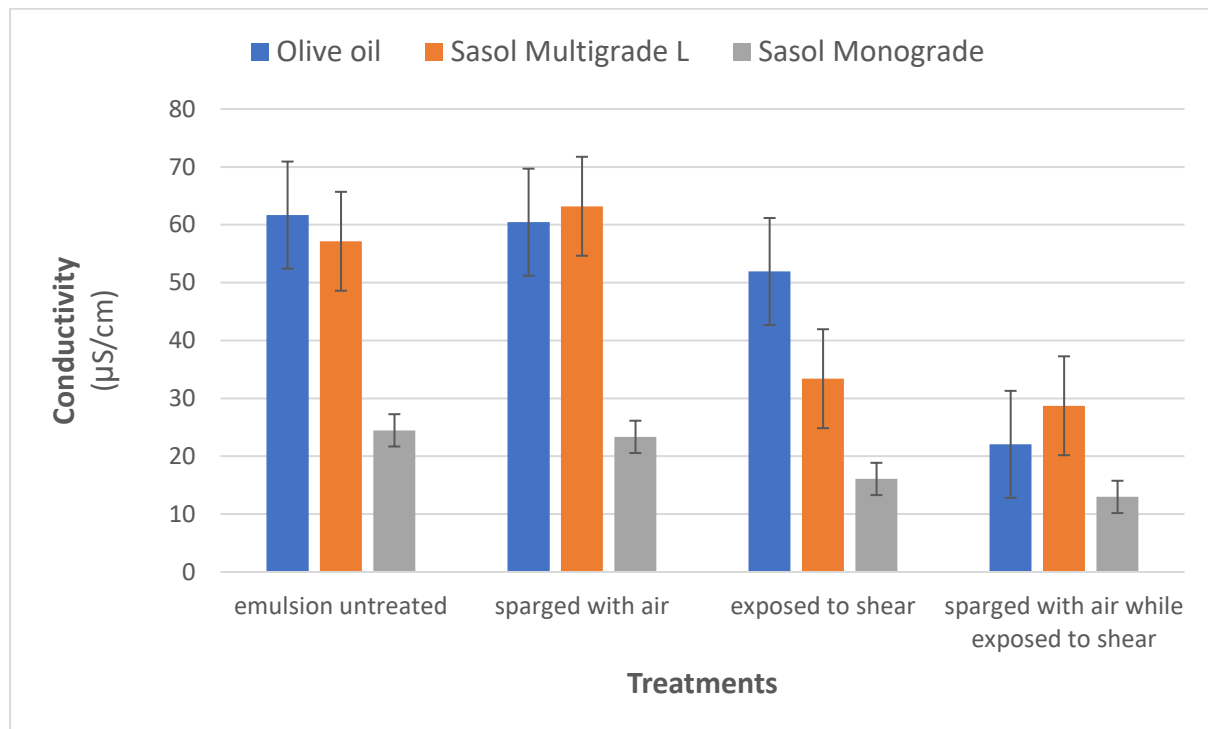


Figure 4.18. Graph of conductivity measurements of the emulsions pre and post treatments.

Figure 4.18 shows the effect of the treatments on the conductivity of the post treatment emulsion. The treatment, sparged with air, showed little change in conductivity, which is evident that sparging with air alone does not significantly affect the emulsion stability. Where the emulsion was exposed to shear and to shear combined with air sparging these treatments resulted in a decrease in the associated conductivity. This decrease in conductivity can be attributed to the increase in the amount of oil in the emulsion specifically at the level of the conductivity probe, located at 5 cm below the surface of the water. The decrease of the conductivity is a direct result of the increase in droplet size as pointed out in section 4.3.6. An increase in DSD constitutes a reduction of the total charge carrying droplet surface area, which is supported by the observed reduction of the ζ potential. This phenomena of emulsion destabilisation and coalescences during flotation IAF processes has been reported by a number of authors [268,466,467].

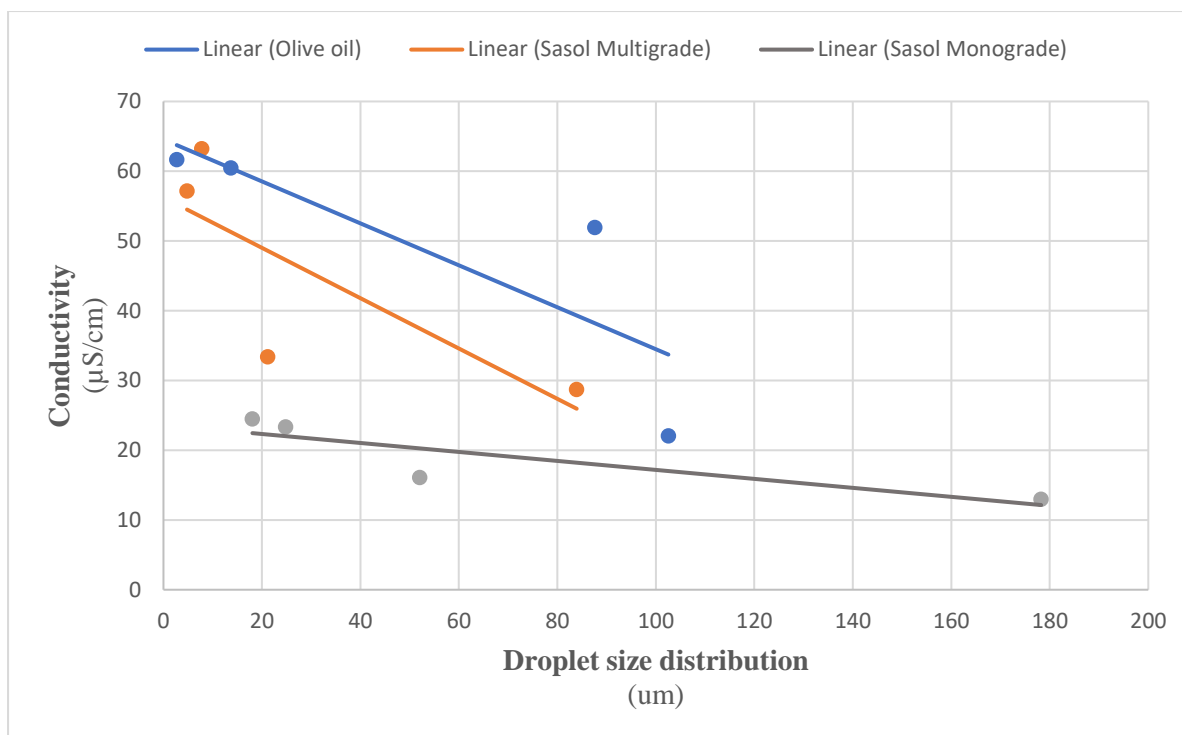


Figure 4.19. Regression analysis plot of conductivity as a function of DSD measurements of the emulsions post treatments.

Figure 4.19 shows a plot of DSD versus conductivity data for the emulsions post treatment. The R^2 for the olive oil emulsion is equal to 0.681, the R^2 for the Sasol multigrade oil emulsion was equal to 0.611 the R^2 for the Sasol multigrade oil emulsion was equal to 0.742. Taking into account the R^2 values for the correlations, all are greater than 0.6, which shows a fair correlation between DSD and conductivity data, which is in line with research reports [436,437]. The data shows that a decrease in conductivity with an increase oil droplet size, consistent with literature reports [436,437].

4.3.8. Effect of treatment on turbidity

The turbidity of the prepared emulsions was recorded utilising the procedure presented in Section 3.2.8.3.

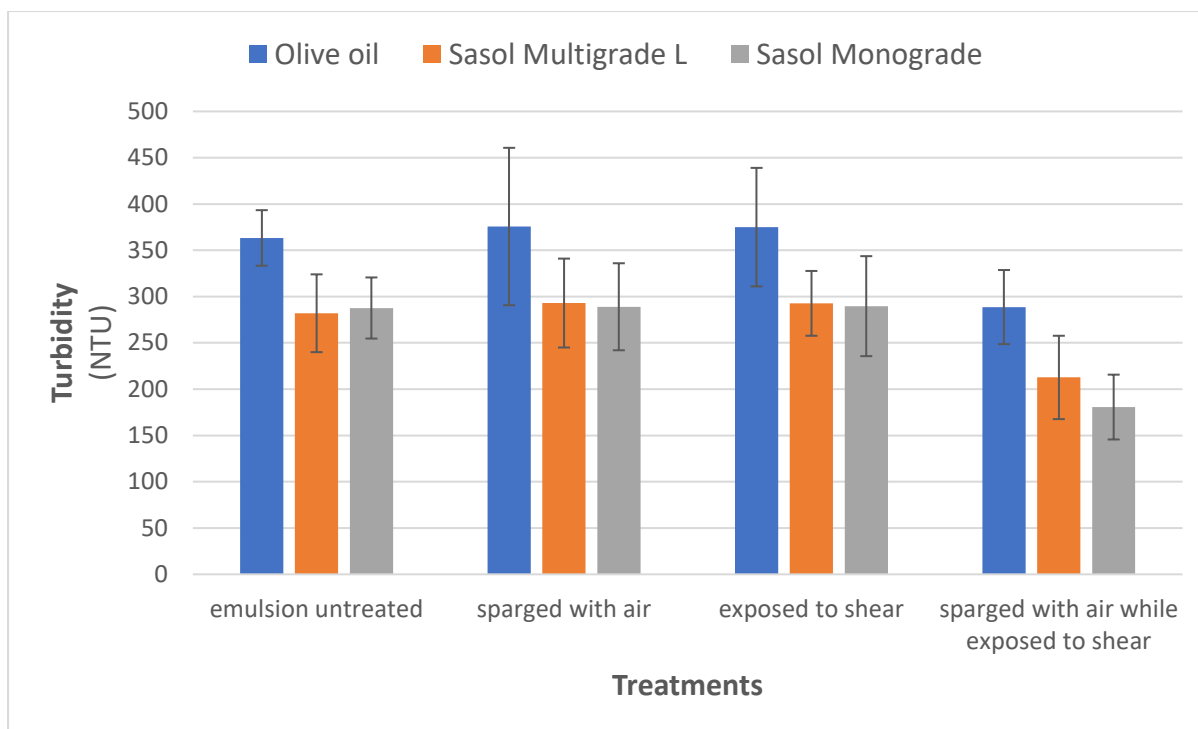


Figure 4.20. Graph of turbidity measurements of the emulsions pre and post treatments.

Figure 4.20 shows the effect of the treatments on the turbidity of the emulsions pre and post treatments.

Table 4.6. Treatment efficiency percentage of treatments based on changes in turbidity.

Emulsion	Treatment efficiency (TE)		
	Sparged with air (%)	Exposed to shear (%)	Sparged with air while exposed to shear (%)
Olive oil	-3.4	-3.2	20.6
Sasol multigrade oil	-3.9	-3.8	24.6
Sasol monograde oil	-0.5	-0.7	37.2

As per **Table 4.6**, the two treatments, sparged with air and exposed to shear showed no decrease in the turbidity, however a relatively small increase in turbidity was observed, all less than 4%. Turbidity is both a function of droplet size and droplet numbers. With shear treatment alone, a significant droplet size increase and also a reduction in the absolute ζ potential was observed.

However, the number of droplets were still significant, leading to a small increase rather than decrease of the turbidity. The treatment where the emulsion was exposed to shear combined with air sparging resulted in a significant decrease in turbidity of the emulsion all greater than 20%. It is suggested that this last treatment caused a higher degree of destabilisation leading to a larger number of droplets to coalesce to form free oil and as a result to remove itself from the sampling zone. Despite the increased size of the droplets within the sampling zone (as shown in section 4.6.3), the number of droplets must have been significantly less as the turbidity reading was reduced.

4.3.9. Effects of treatments on COD

The COD of the prepared emulsions were recorded utilising the procedure presented in Section 3.2.8.6.

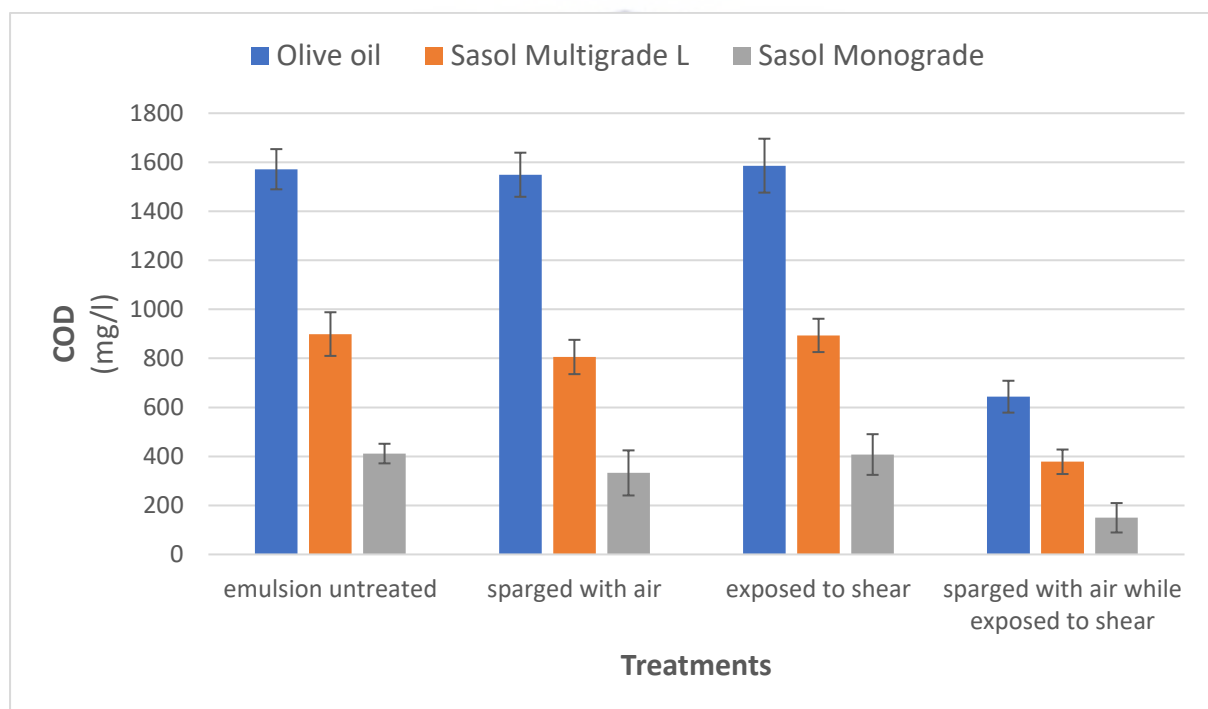


Figure 4.21. Graph of COD measurements of the emulsions pre and post treatments.

The results shown in **Figure 4.21** highlights the effect of the various treatments on the COD.

Sparging with air while exposed to shear had a treatment efficiency based on the COD of 51.9% for the olive oil emulsion, 33.2% for the Sasol multigrade oil and 16.7% for the Sasol monograde oil, as depicted in **Table 4.7**. The difference in treatment efficiency is a result of

the difference in physical properties and DSD of the respective emulsions. This is ascribed to destabilisation of the emulsions causing aggregation and flocculation followed by the resulting free oil rising to the surface of the water. Hence the oil content of the remaining emulsion decreases.

Table 4.7. Treatment efficiency percentage of treatments based on COD.

Emulsion	Treatment efficiency percentage		
	Sparged with air (%)	Exposed to shear (%)	Sparged with air while exposed to shear (%)
Olive oil	1.4	-0.9	59.1
Sasol multigrade oil	5.9	0.35	33.2
Sasol monograde oil	5.0	0.25	16.7

The treatments, sparging with air and exposed to shear resulted in a very small and insignificant change in the COD. A possible reason for the result obtained for sparging with air, is that the bubbles produced are large and hence were not effective in destabilising the emulsion. Similar findings, of bubble sizes have been described and reported by other authors [65,338,368,468]. The observed COD reduction, the increase of the average droplet size, the decrease of the absolute ζ potential, the decrease of turbidity and the decrease in conductivity are all providing a clear trend towards a reduced emulsion stability.

The reduction of turbidity in conjunction with an increased droplet size can only be explained when a significant number of droplets have been removed from the sampling zone as free oil. The obtained COD results correlate well with the decrease in turbidity and increased droplet size.

It is evident based on the results presented in **Figures 4.18, 4.20** and **Table 4.21** that the effect of shear combined with air sparging had a statistically significant impact on emulsion stabilisation, which resulted in a decrease in turbidity, conductivity, COD and an increase in droplet size of the treated emulsion. This change in the overall emulsion stability indicates the presence of the mechanism of shear flocculation and coalescence. Sparging with air while exposed to shear also generated small enough bubbles to make flotation possible and

demonstrates the effectiveness of the treatment, resulting in a treatment efficiency ranging from 16.7% to 51.9%.

Researchers have demonstrated that petroleum hydrocarbons with smaller molecular weights in general have higher solubility in water, which implies these compounds have higher tendency to be removed by bubbles as air is released from the water in comparison to those with higher molecular weights [162,469]. This process has been reported to occur through the accumulation of petroleum hydrocarbons within the bubble film and eventual transport to the surface in the water column [162,469]. A number of authors also observed that the processing of organic compounds from wastewater by bubble formation and release during DAF treatment of wastewater is significant [162,469].

To increase the oil removal efficiency, chemicals in combination with air sparging and shear could be used, however, the amount of chemicals required could probably be reduced as compared with that of using chemicals alone. The combined process would include the use of shear prior to chemical addition. This has not been demonstrated in the current research study and is work for future research.

4.4. Coagulation - jar test results

Coagulation jar test analyses were conducted on olive oil, o/w emulsions, utilising the procedure presented in Section 3.2.7.2. The olive oil emulsions were prepared as per the procedure in Section 3.2.1. Only olive oil emulsions were utilised in the jar test due to the fact that only olive oil emulsions were used in the DAF experiments.

Table 4.8. Jar test results of the prepared emulsions used in the DAF experiments.

Parameter	Pretreatment Emulsion Parameters	Jar test results			
		1	2	3	4
Coagulant dose (ppm)		10	20	30	40
pH	7.1	6.4	6.8	6.1	6.3
Turbidity (NTU)	368±10	349±8	290±11	169±10	287±11
Turbidity Treatment Efficiency (%)		6	21	56	23
Conductivity (uS/cm)	62±8	54.7±5	23.7±8	12.1±9	35.4±9
ζ potentials (mV)	-38.7±7.1	-25.7±0.4	-28.0±0.6	-4.4±0.9	-5.5±2.5

Based on the results of the jar tests conducted, shown in **Table 4.8**, all the coagulant dose concentrations resulted in a decrease in the turbidity, conductivity and the absolute value of the ζ potential of the emulsion, indicating a decrease in the overall stability of the emulsion with the addition of the alum coagulant. This destabilisation of the emulsion is a result of the addition of positively charged Al(III) ions from the alum coagulant, which neutralise the negative charges of the oil droplets in the emulsion system.

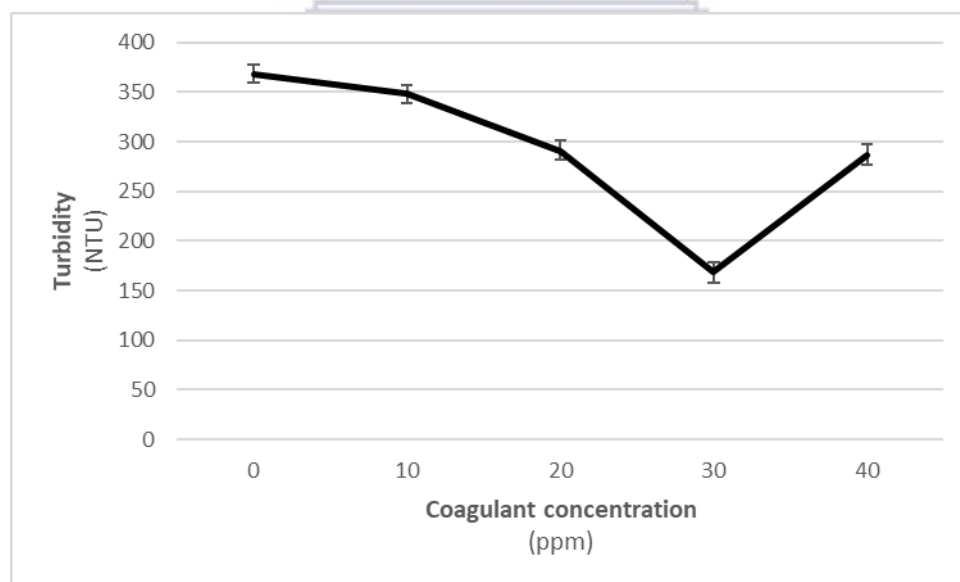


Figure 4.22. Plot of turbidity as a function of coagulant concentration of jar test results.

As per **Figure 4.22**, the turbidity decreases with an increase in coagulant concentration until 30 ppm. A further increase of the coagulant concentration, from 30 to 40 ppm, leads to a sharp increase of the turbidity from 169 to 287 NTU. The turbidity trajectory as a function of

coagulant concentration highlights that positive ions added to the system initially neutralise the negative charged oil drops of the emulsion. At a concentration of 30 ppm coagulant, it appears the surface is optimally neutralised, which correlates with the ζ potential results display in **Figure 4.23**.

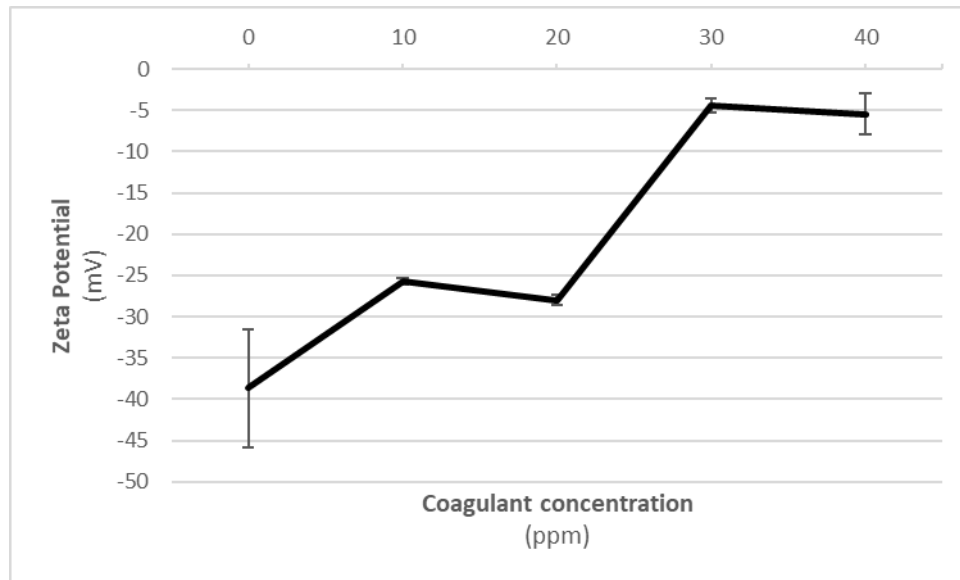


Figure 4.23. Plot of ζ potential as a function of coagulant concentration of jar test results.

With an increase in coagulant dosage concentration, from 10 to 30 ppm, the ζ potential changed from -38.7 mV to -4.4 mV, as presented in **Figure 4.23**, it is indicative of a decrease in the overall stability of the emulsion.

The decrease in emulsion stability resulted in a decrease in the conductivity. This decrease in conductivity is a direct result of the removal of the small oil droplets through droplet coalescence, a reduction of the overall droplet surface area and a neutralised droplet surface charge. This phenomenon of conductivity decrease with the increasing coagulant dose as well as with the increase in oil droplet size has been observed by other authors [437,470,471]. The increase in conductivity at 40 ppm can be explained by an excess Al(III) cations beyond the optimal coagulant dosage in solution.

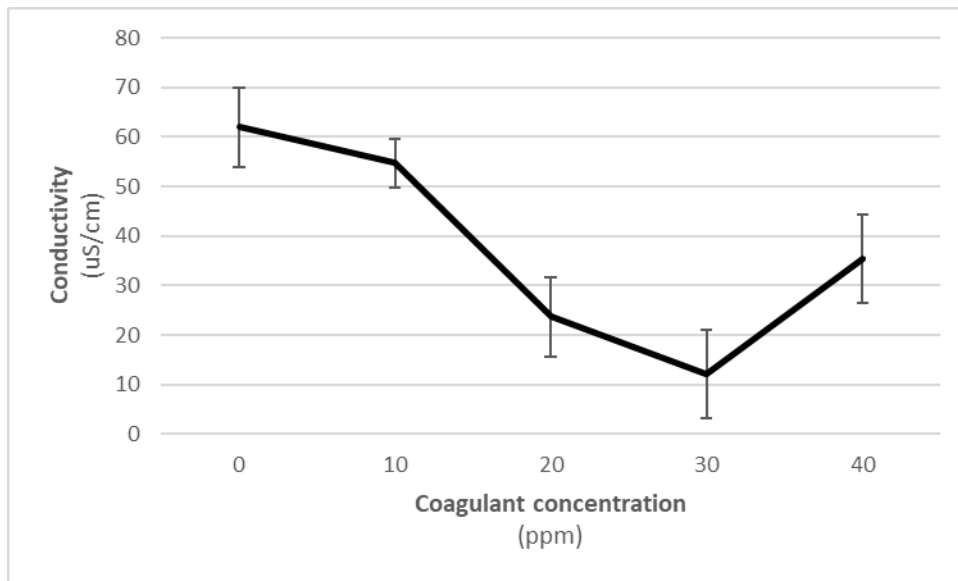


Figure 4.24. Plot of conductivity as a function of coagulant concentration of the jar test results.

Based on the results obtained and presented in **Table 4.8**, and the results presented in **Figures 4.22, 4.23** and **4.24** it is evident that alum as a coagulant, does impact the overall stability of the prepared olive oil emulsion. The impact on emulsion stability is a result of charge neutralisation and the electrical double layer compression, which in turn results in droplet coalescence, formation of larger oil droplets and eventually free oil.

The coagulant dose of 30 ppm resulted in the highest treatment efficiency of 56% based on the turbidity measurements. A coagulant dose concentration increase from 30 ppm to 40 ppm, resulted in a significant increase in turbidity and conductivity with a relatively small increase of the absolute ζ potential. Taking into account the above results a coagulant dose of 30 ppm was used in the DAF experiments.

4.5. Experiment using DAF combined with and without coagulation and shear

The effectiveness of DAF with and without coagulant and shear was investigated for the processing of olive oil o/w emulsions, utilising the experimental procedure described in Section 3.2.7. For the DAF experiments, only olive oil emulsions were prepared and utilised, to mitigate against the risk of hazard oil spills associated with this research at the UWC campus. The tests were conducted at room temperature, which was between 19 and 23°C.

4.5.1. DAF Bubble size analysis

Prior to the DAF emulsion treatments, experiments were conducted to assess the bubble size of the bubbles generated within the bubble swarm by the experimental set up, as per the experimental design procedure described in Section 3.2.8.3.

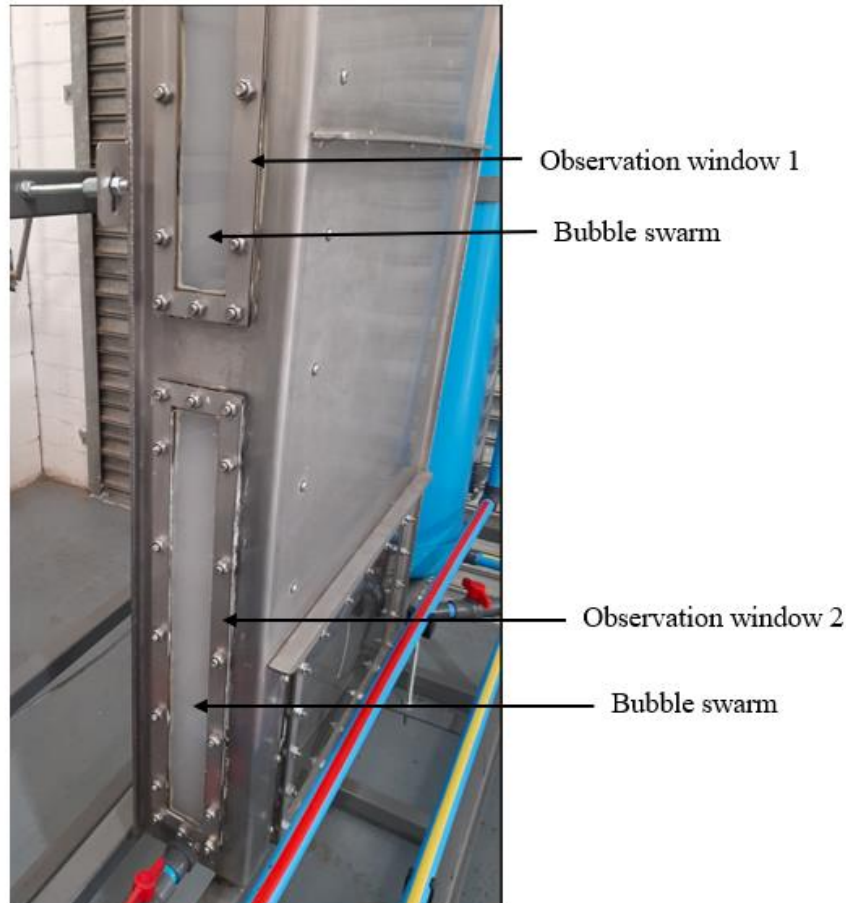


Figure 4.25. Picture of the bubble swarm generated in pure water during the DAF process.

The bubbles were analysed visually from photos in terms of approximate size and volume within the bubble swarm from observation window 1, located at the front side of the DAF unit. For the bubble size analysis an area of interest in observation window 2 was selected to ensure that the smallest bubbles within the bubble swarm were analysed as depicted in **Figure 4.25**. The bubbles in the observation window were located closest to the inlet and theoretically would have the smallest bubbles sizes.

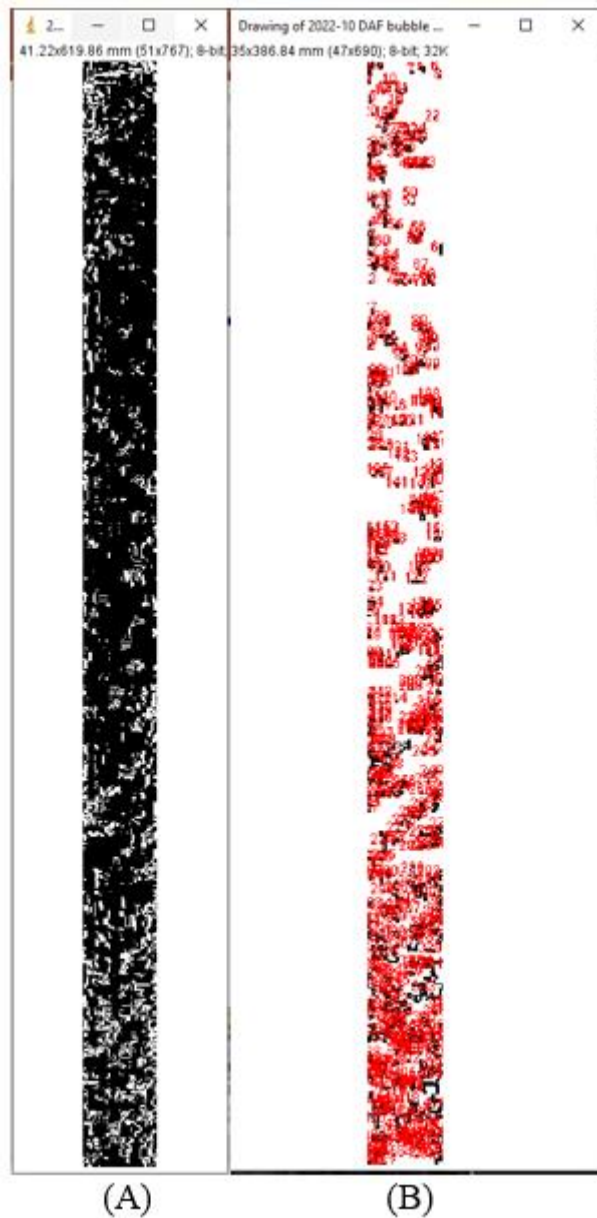


Figure 4.26. Area of interest enhanced by the ImageJ software to highlight the bubbles in pure water during the DAF process, A) bubbles are represented in white with the water matrix in black, B) the bubbles are represented as circles with the bubble counts in red.

The area of interest was converted to an 8-bit image and further enhanced with the bubbles enhances in white and the background water in black, **Figure 4.26 (A)**. From **Figure 4.26 (B)** 1236 bubbles were identified and analysed.

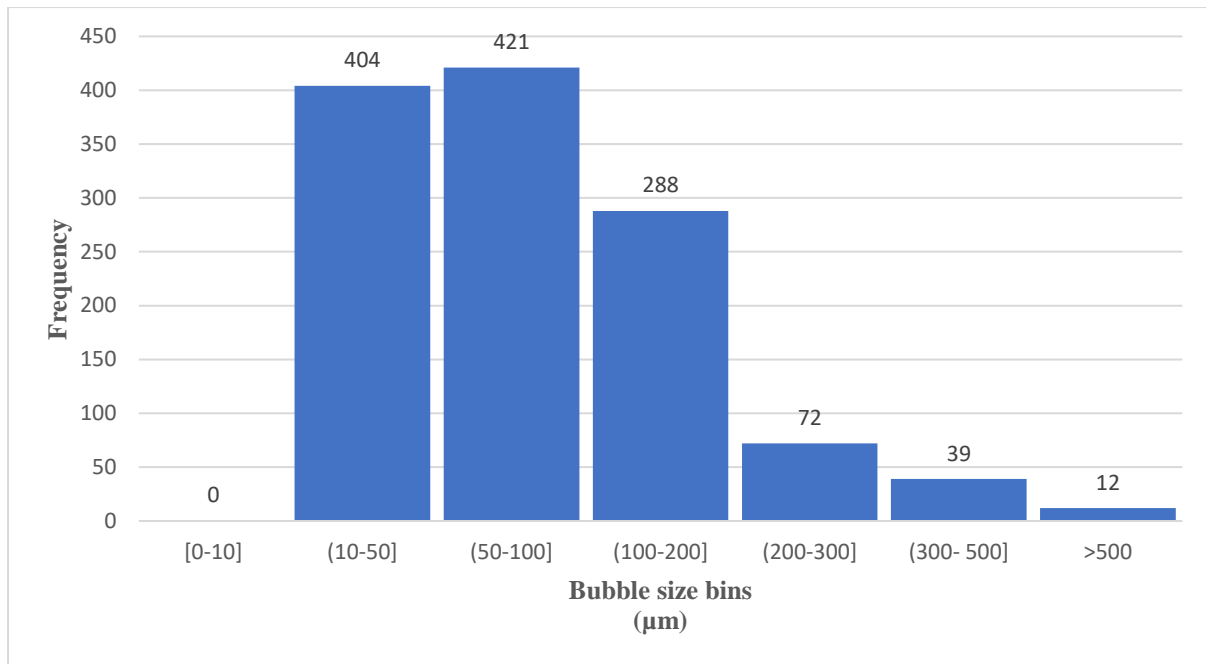


Figure 4.27. Histogram of bubble sizes identified within the area of interest for pure water in the DAF unit.

Figure 4.27 depicts a positively skewed histogram of the bubble size versus frequency for pure water within the DAF unit. As depicted in the **Figure 4.27**, in the area of interest there were no bubbles with a diameter of less than 10 μm, approximately 33% of the bubbles observed had a diameter of between 10 μm and 50 μm, 34% of the bubbles had a diameter of between 50 μm to 100 μm and 33% of the bubbles had a diameter greater than 100 μm.

A similar procedure was followed to determine the air bubble sizes produced in the prepared emulsions. As discussed in the Section 3.2.7, for the DAF unit, untreated water is recycled and pumped through the micro bubble generator.

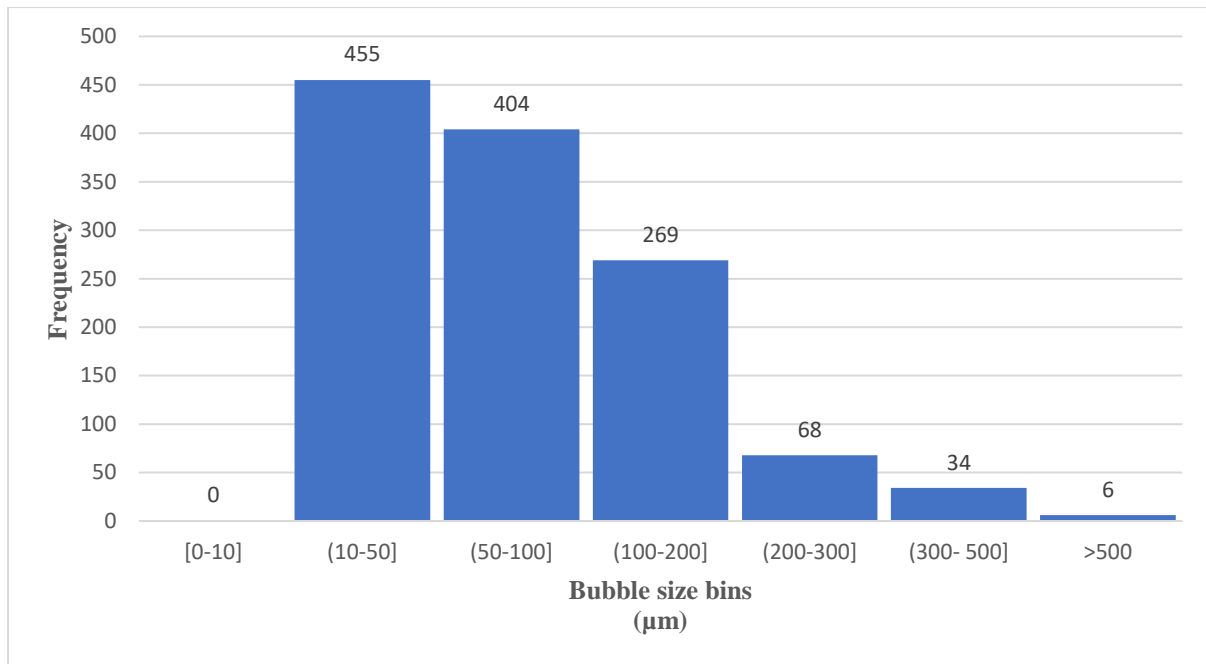


Figure 4.28. Histogram of bubble sizes identified within the area of interest for the olive oil o/w emulsion in the DAF unit

Figure 4.28 depicts a positively skewed histogram of the bubble size versus frequency within the olive oil o/w emulsion inside the DAF unit. As depicted in the **Figure 4.28**, in the area of interest there were no bubbles with a diameter of less than 10 μm, approximately 37% of the bubbles observed had a diameter of between 10 μm and 50 μm, 33% of the bubbles had a diameter of between 50 μm to 100 μm and 30% of the bubbles had a diameter were greater than 100 μm. This bubble size distribution result observed is also observed and reported by authors in the literature for DAF flotation systems [343,377,383,387].

4.5.2. Properties of emulsions prior to treatment

The physical parameters of the prepared o/w emulsions used in the experiments are presented in **Table 4.9**. Of particular significance and importance were the ζ potential measurements of greater than -58 mV and DSD P90 measurements of less than 6.5 μm, indicating relatively stable emulsions. The results presented in **Table 4.9** confirm the stability of the emulsions before each treatment.

Table 4.9. Parameters of the prepared olive oil emulsion samples prior to treatment used in the DAF experiments.

Samples to be treated	COD (mg/L)	DSD P90 (μm)	Conductivity ($\mu\text{S/cm}$)	Turbidity (NTU)	ζ potentials (mV)
Sample to be treated by DAF with coagulation	1589 \pm 86	4.7 \pm 1.2	56.20 \pm 2.3	374 \pm 7	-58.7 \pm 0.9
Sample to be treated by DAF with shear	1549 \pm 59	6.4 \pm 0.2	60.45 \pm 1.7	376 \pm 13	-66.6 \pm 0.2
Sample to be treated by DAF with coagulation and shear	1657 \pm 77	5.2 \pm 0.4	51.93 \pm 2.3	380 \pm 13	-70.4 \pm 0.6

To ensure the emulsions treated, were statistically the same, an ANOVA test was performed on the emulsions with the null hypothesis, that there is no difference between the emulsions. The summary of the data utilised and analysis of the results are presented in **Table 4.10** and **4.11** respectively.

Table 4.10. Summary of the emulsion turbidity data utilised in the ANOVA analysis.

Groups	Count	Sum	Average	Variance
Reading 1	3	1151	383.666	44.333
Reading 2	3	1105	368.333	9.3333
Reading 3	3	1136	378.666	180.333

Table 4.11. One way ANOVA analysis results based on the turbidity.

Source of Variation	SS	df	MS	F	P-value	Fcrit
Between Groups	366.88	2	183.44	2.351	0.176	5.143
Within Groups	468	6	78			
Total	834.88	8				

Where, SS is the sum of squares for each source of variation. df is the degrees of freedom for each source of variation, the df is indicative of the number of independent pieces of information

used to calculate each sum of squares. MS is the mean square corresponding to the sum of squares divided by its associated degrees of freedom. F is the F ratio, which measures if the means of different samples are significantly different or not. The P-value is the probability calculation which determines if the results are statistically significant. F_{crit} is the $F_{critical}$ determined by the ANOVA test.

Based on the results of the ANOVA test with P-value of 0.389, which is greater than 0.05, implies that there was no statistical difference between the three emulsions used in the DAF treatment experiments.

4.5.3. Effects of DAF treatment on conductivity

The conductivity of the emulsion pre and post treatment, was conducted as per the procedure described in Section 3.2.8.8.

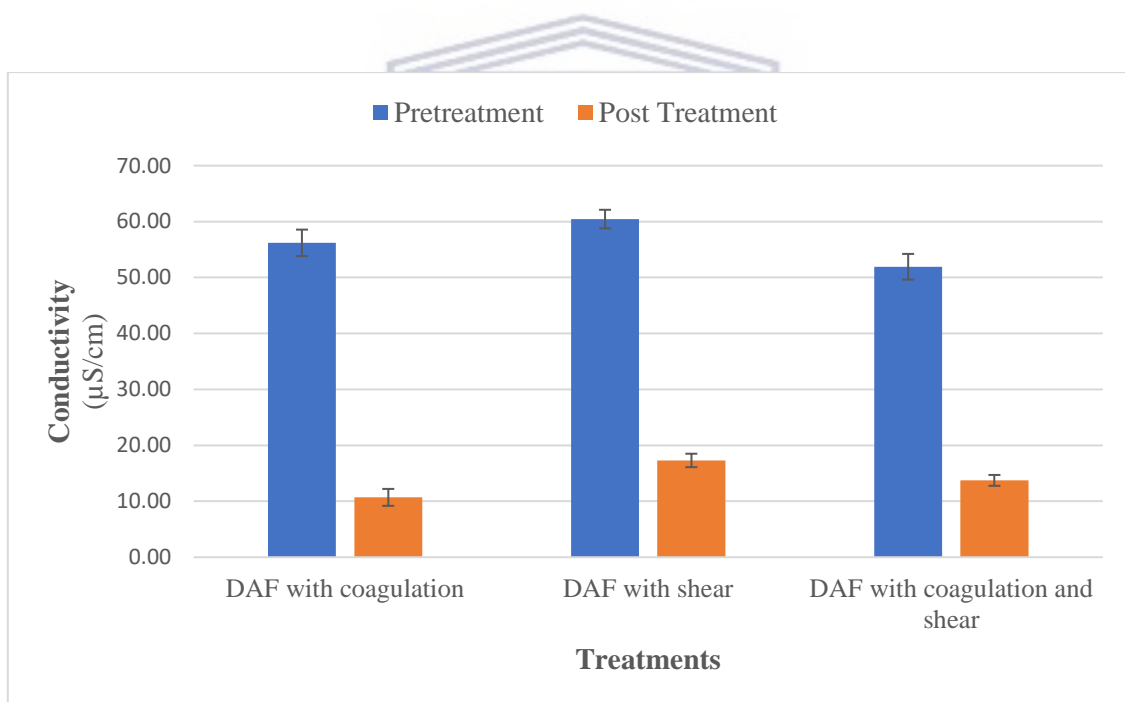


Figure 4.29. Graph of conductivity measurements of the emulsions pre and post the DAF treatments.

As with the IAF treatment, the decrease in conductivity associated with all three DAF treatments, shown in **Figure 4.29**, is a result of the destabilisation of the emulsions resulting in the coalescence of droplets and the increase of the oil droplet concentration in the surface region of the water where the conductivity readings were recorded. This result is consistent

with reports by other authors, especially where coagulants are utilised with DAF. [437,472]. The reduction of conductivity with DAF and shear is also noted indicating that the shear with bubbles and flotation has an impact on the overall stability of the emulsion resulting in separation and an increase in the concentration of oil droplets in the surface region of the water where the conductivity measurements were recorded. However, combining DAF with shear and coagulation did not significantly alter the conductivity reduction, caused by DAF with coagulation alone or with shear alone.

4.5.4. Effects of DAF treatment on zeta potential

The ζ potentials of the emulsions pre and post DAF treatments were measured as per the procedure in Section 3.2.8.9.

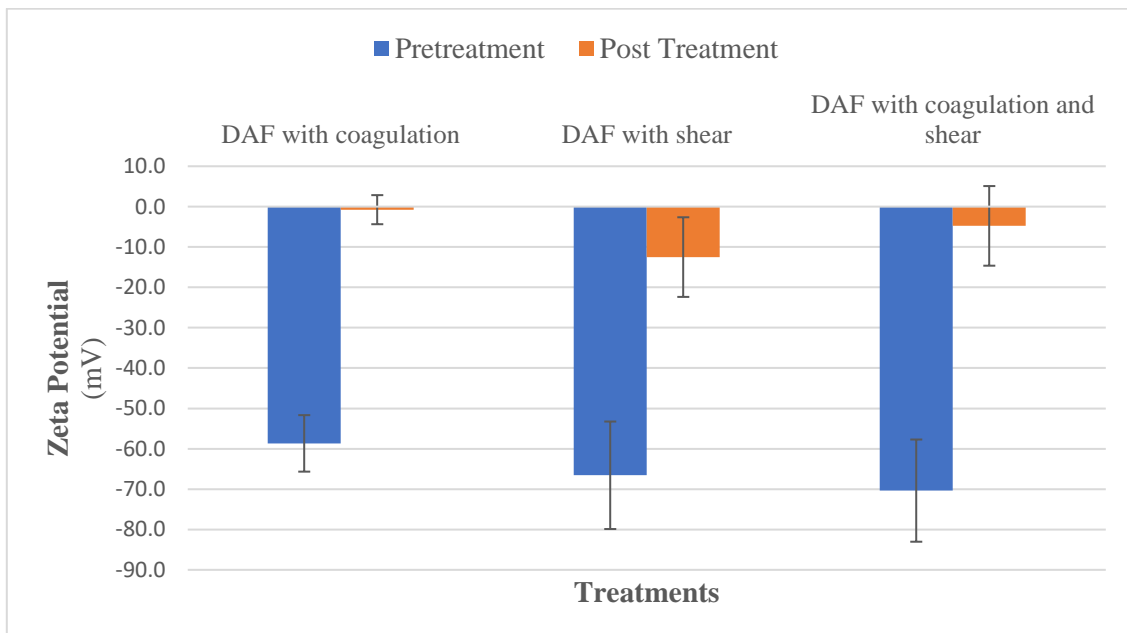


Figure 4.30. Graph of the ζ potential of the emulsions pre and post the DAF treatments.

For all the treatments there is a decrease of the absolute value of the ζ potential. This decrease of the absolute value of the ζ potential shown in **Figure 4.31** is a result of destabilisation of the emulsion through the addition of a coagulant, which results in the neutralisation of the droplet surface charge and electrical double layer compression of the oil droplets. The treatments, DAF with coagulation and DAF with coagulation and shear resulted in a reduction of the ζ potential to below -5 mV, with the DAF with shear had a final ζ potential of -12.5 mV. The most significant decrease in ζ potential was for the treatment of DAF with coagulation with a

decrease from -58 mV to -0.8 mV. Combining DAF with coagulation and shear showed a lower decrease in ζ potential than that of DAF with coagulation but without shear.

As described in Section 2.6, the oil droplet charge neutralisation and electrical double layer compression directly impact the emulsion stability and results in decreasing the absolute value of the ζ potential of the emulsion, which then allows droplet interactions causing droplet aggregation [183,272]. The treatment DAF with shear has a similar effect of ζ potential reduction, however the reduction in ζ potential is not as significant as with the addition of coagulants alone.

4.5.5. Effects of DAF treatment on turbidity

The turbidity of the prepared emulsions was recorded utilising the procedure presented in Section 3.2.8.3.

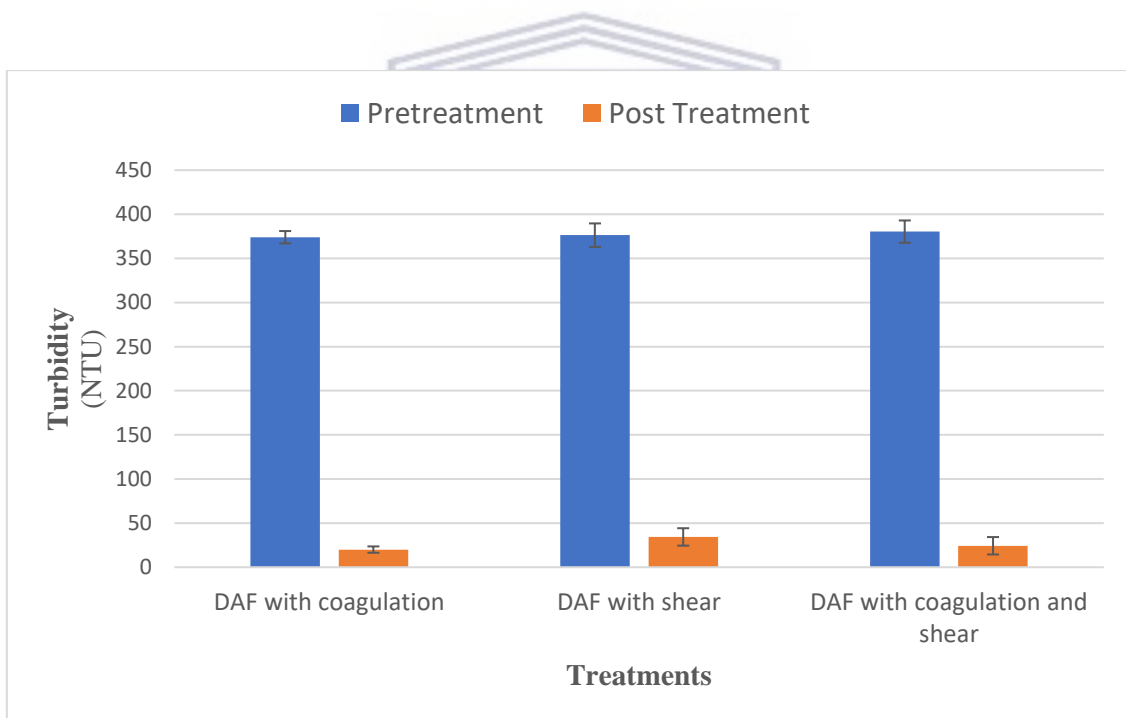


Figure 4.31. Graph of the turbidity measurements of the emulsions pre and post DAF treatments.

Figure 4.31 shows the effect of the DAF treatment on turbidity and for all the treatments there is a significant decrease in the turbidity. This decrease is a direct result of the efficiency of DAF with coagulation as a clarification process to decrease turbidity, which has been reported by a number of authors [334,343,377,425]. This decrease in turbidity with DAF and shear is a

result and evidence of shear flocculation in combination with the DAF unit. The process of shear flocculation has been described in detail in Chapter 2 whereby shear is utilised to induce flocculation and coalescence of liquid - liquid dispersions. Subsequently, with DAF, these flocs float to the water surface [71,88,398]. The results in **Figure 4.31** correlate well with the results in **Figure 4.30**.

4.5.6. Effects of DAF treatment on COD

The COD of the prepared emulsions were recorded utilising the procedure presented in Section 3.2.8.6.

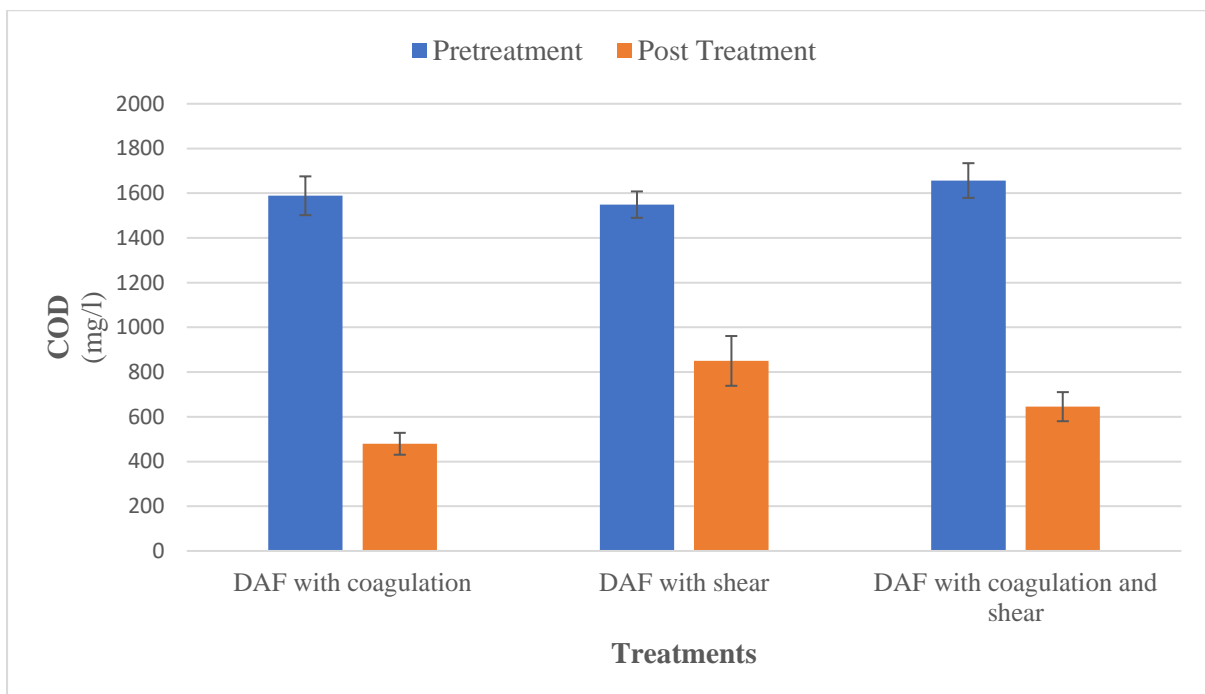


Figure 4.32. Graph of COD measurements of the emulsions pre and post DAF treatment.

The effect of the treatments on COD are presented **Figure 4.32**. For all the treatments there is a decrease in the COD measurements of the processed water. This decrease in COD is a result of the emulsion destabilisation, that leads to less oil content in the treated water. It should however be noted that the total amount of oil in the sample remains the same, but the sample volume taken for COD is from below the level of the free oil on the surface of the water resulting from demulsification. The DAF with coagulation treatment results in the largest decrease from 1589 mg/L to 528 mg/L.

The treatment efficiencies of the treatments conducted, based on the changes in COD and utilising Equation 4.2, were calculated. The results of the treatment efficiency results are presented in **Table 4.12** below.

Table 4.12. Treatment efficiency with DAF treatments on the olive oil emulsions. Treatment efficiency percentage of treatments based on COD.

Treatment	COD before treatment (mg/L)	COD post treatment (mg/L)	Treatment Efficiency (TE) (%)
DAF with coagulation	1589±86	479±49	69.8
DAF with shear	1549±59	850±111	46.5
DAF with coagulation and shear	1657±77	645±65	59.4

From **Table 4.12** the best treatment efficiency was obtained with DAF and coagulation with a 69.8% TE, followed by DAF with coagulation and shear and the least efficient being DAF with shear. From these results it is evident that coagulation is an important part of processing stable emulsions and DAF with shear alone results in separation efficiencies of 46.5%.

The measured treatment efficiency for DAF with coagulation, is comparable with the results achieved in similar experiments described in the literature [21,171,307,473]. It should be noted that in the literature reports, coagulation is almost always followed by flocculation whether it is necessary or not.

During the DAF process, for all the treatments described, oil droplet removal takes place via the interactions of coagulants or shear, oil droplets and air bubbles. As discussed in Chapter 2, the addition of coagulant reduces the electrostatic charge of the oil droplets and enhances the aggregation of the oil droplets. There is the school of thought, that the formed aggregations could be disintegrated under turbulence and shear forces, however other reports have suggested that shear and agitation have the potential to enhance the contact between oil droplets and air bubbles. Accordingly, the observed removal of oil with shear is consistent with results reported by Wells *et al.* [29].

The results of all the treatments, shown in **Figures 4.28, 4.29, 4.30, 4.31 and 4.32**, highlight a decrease in the conductivity, turbidity, COD and an increase in the ζ potential, highlighting that the treatments resulted in a destabilisation of the emulsion. Based on the results presented, it is observed that all the treatments had a relatively positive impact on the treatment of processing of the stable olive oil o/w emulsions.

4.6. Analysis of free and treated oil post the DAF treatments

The oil layer, usually referred to as the sludge or float layer, at the surface of the DAF unit was collected and analysed against the original olive oil utilised to produce the emulsions. A number of authors have reported that the presence of suspended solids and water has an impact on the stability of olive oils and may result in the degradation of the olive oil [474–476]. Coagulation applied in oily wastewater treatment has been reported to generate significant amounts of waste sludge and this has been identified as the main disadvantages of coagulation processes [109,216,283]. Waste sludge often requires additional treatment processes and/or needs to be disposed of as expensive, sometimes toxic, waste. As noted in Chapter 1 and Chapter 2, the processing of o/w emulsions is typically focussed on and optimised for the recovery of clean water with little regard for recovering the oil phase [15,22]. The available literature shows that the sludge is the result of oil degradation in aqueous media combined with the hydrolysis of coagulants that add to the sludge generation [121,172,283]. The sludge generated is a direct result of the degradation of the oil in the o/w emulsion, as well as the coagulant dose and pH [471].

The collected oils were analysed by means of the fatty acid methyl ester (FAMES) profile analysis to assess the quantity and degradation of fatty acids in the collected oil samples during the DAF treatment [477,478]. The profile comparisons is a common robust comparative method to measure the amount of degradation of the olive oils collected post the DAF treatments [479]. It is inferred that the lower the FAMES analysis measurements the more resultant degradation of fatty acids of the bulk oil has occurred during the processing.

The FAMES analyses were conducted by an independent third-party laboratory Microchem Lab Services (Pty) Ltd (Cape Town, South Africa).

Table 4.13 highlights the FAMES profile analysis of olive oil sludge collected samples, while **Table 4.14** presents the summary of the results of the measurements, post the DAF treatments.

Table 4.13. FAMES profile analysis of olive oil samples analysed by Microchem laboratories.

Sample ID	AT85145	AT85146	AT85147	AT85148	AT85149	AT85150
Description	Original bulk olive oil (g/100g per sample)	DAF with shear (g/100g per sample)	DAF with coagulation (g/100g per sample)	DAF with coagulation and shear (g/100g per sample)	DAF with shear (g/100g per sample)	DAF with coagulation and shear (g/100g per sample)
First Run						
Measurement 1	84.10	9.88	4.01	2.02	10.02	3.94
Measurement 2	95.85	12.10	3.25	1.06	20.45	3.56
FAT_Avg	89.98	10.99	3.63	1.54	15.25	3.75
Second Run						
Measurement 1			5.76	3.64	16.63	3.5
Measurement 2			9.71	4.1	8.16	5.12
FAT_Avg			7.74	3.87	12.39	4.31

Table 4.14. Summary of the FAMES profile analysis of olive oil samples

Treatment	FAT Avg g/100g per sample
Original bulk olive oil	89.98
DAF with coagulation	5.68
DAF with shear	12.87
DAF with coagulation and shear	3.37

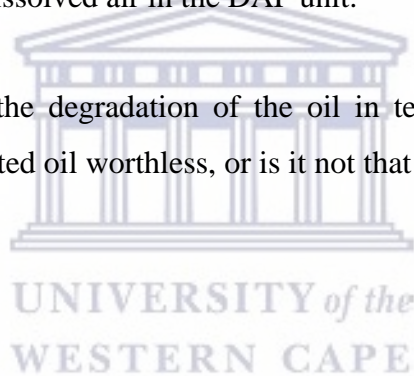
As shown in **Table 4.14**, the oily sludge collected post the treatment with coagulation, DAF with coagulation and DAF with coagulation and shear showed the most degradation from the bulk oil. This result corresponds well with the literature reports that the use of alum coagulants causes oil degradation and sludge formation during flotation [121,172,283]. It is observed that DAF with coagulation and shear resulted in most degradation, with a measurement of 3,37g/

100g, as compared to 5.68g/100g of sample using DAF and coagulation. This result could be ascribed to a more intense mixing process of the coagulant with the oil droplet in a high shear environment.

The oily sludge collected from the treatment of DAF with shear had the least degradation from the original bulk oil at 12.87g/100g of sample. The reason for this result can be explained by the fact that no coagulant was utilised. The fact that less degradation of the olive oil occurred during the DAF with shear process, is encouraging.

It should be noted that based on the results, as presented in **Table 4.14** all the treatments resulted in oil degradation as compared with the untreated olive oil. It can also be noted that only shear, without chemical addition, also lowered the FAMES levels substantially. This is a result of the oil droplets in the emulsion being exposed to agitation in an aqueous oxidising environment emanating from dissolved air in the DAF unit.

Question: How significant is the degradation of the oil in terms of SAMES reduction in industry? Does it make the floated oil worthless, or is it not that important?



CHAPTER 5 CONCLUSIONS

This chapter summarises the significance of the research findings related to the outlined aims and objectives described in Chapter 1. Further included herein is the overview elucidating the contribution to knowledge of the research.

5.1. Overview

As emphasised in Chapter 1 and Chapter 2, the processing of oily wastewater and specifically o/w emulsions, has been studied in various amounts of detail by a number of researchers [336,340,348]. The processing of o/w emulsions has been typically focussed on and optimised for the recovery of clean water with little emphasis on the recovery of the oil phase [15,22]. The current driver in emulsion treatment is to produce clean water as well as for the oil to be recovered as a secondary product. If the oil is not degraded to sludge, it can be recycled and sold as a secondary product. The available literature shows that sludge produced during the processing of o/w emulsions is the result of oil degradation in the aqueous media combined with the hydrolysis of coagulants and the pH of the emulsion [121,172,283,471].

This research is aimed at demonstrating flotation treatment techniques that are effective in processing o/w emulsions utilising shear with the minimum use of chemicals, such as coagulants. A hybrid technology solution utilising shear flocculation and flotation is proposed as a practical and efficient method to treat and process oily wastewater emulsions. This study is limited to the processing of surfactant and emulsifier free oil in water emulsions utilising shear and two specific flotation techniques, namely IAF and DAF.

Based on the results presented in Chapter 4, it is evident that both IAF and DAF can be used in conjunction with shear to destabilise and process o/w emulsions, although DAF proved to be significantly more efficient than IAF.

The results indicate that both the laboratory scale IAF and pilot scale DAF systems utilised in this research were able to produce micro sized bubbles necessary for the efficient flotation. In the IAF experiments there were no bubbles with a diameter of less than 50 μm , the produced bubbles sizes had a diameter of between 50 μm and greater than 300 μm . For the DAF experiments approximately a third of the bubbles observed in the area of interest had a diameter of between 10 μm and 50 μm with the balances of the bubble sizes greater than 100 μm .

5.2. Laboratory scale IAF treatments

For the laboratory scale IAF treatment three oils were used to prepare surfactant and emulsifier free oil in water emulsions utilising olive oil, Sasol Multigrade and Sasol Monograde oil and were subjected to three treatments, which included:

- sparged with air,
- exposed to shear, and
- sparged with air while exposed to shear.

Table 5.1. Summary of results obtained for the laboratory scale IAF treatments.

Treatments		
Sparged with air	Exposed to shear	Sparged with air while exposed to shear
<p>No micro bubbles generated.</p> <p>For all the emulsions, no statistically significant result was observed in:</p> <ul style="list-style-type: none"> • ζ potential • DSD • Conductivity • Turbidity, and • COD 	<p>No micro bubbles generated.</p> <p>For all the emulsions, no statistically significant change was observed in:</p> <ul style="list-style-type: none"> • Turbidity, and • COD <p>For all the emulsions a statistically significant result was observed for:</p> <ul style="list-style-type: none"> • ζ potential • DSD, and • Conductivity 	<p>Micro bubbles generated in the bubble swarm.</p> <p>For all the emulsions a statistically significant result was observed in:</p> <ul style="list-style-type: none"> • ζ potential • DSD • Conductivity • Turbidity, and • COD <p>Treatment efficiency based on COD was calculated at:</p> <ul style="list-style-type: none"> • Olive oil: 59.1% • Sasol Multigrade: 33.2% • Sasol Monograde: 16.7%

As shown in **Table 5.1**, the treatment sparged with air had no statistically significant impact on the overall stability of the emulsions. The treatment exposed to shear only impacted the

turbidity and COD of the emulsions. However, the treatment sparged with air while exposed to shear had a statistically significant impact on all the observed measurements. The above results imply that the treatment exposed to shear alone does have an impact on the overall stability of the emulsions resulting in droplet flocculation and coalescence. However, due to almost no bubbles being generated during shear, the treatment does not result in complete emulsion separation.

For the treatment sparged with air while exposed to shear the results show a complete destabilisation of the emulsions resulting in droplet flocculation, coalescence and the formation of free oil. As emphasised in Chapter 4, only micro bubbles were observed for the treatment sparged with air while exposed to shear. The micro bubbles generated resulted in making flotation possible and effective. Therefore, due to the generation of the micro bubbles, this treatment was ~~most~~ effective in processing the emulsions without any chemical coagulants and flocculants. This treatment resulted in a treatment efficiency ranging from 16.7% to 59.1% for the respective o/w emulsions.

The conclusion from this is that the laboratory scale IAF treatment combining sparged with air while exposed to shear is a successful method for o/w emulsions processing. This treatment process has the potential to be scaled up to a pilot plant scale, which in turn addresses an identified gap in the current technologies and reduces the amount of chemicals utilised. It has the potential to produce a water phase with lower levels of toxicity and less sludge that needs to go to landfill.

5.3. DAF treatment

For the DAF experiments a pilot scale DAF unit with a shear unit was designed, fabricated and utilised for treating olive oil emulsions. The treatments included:

- DAF with coagulation,
- DAF with shear, and
- DAF with coagulation and shear.

For all the DAF treatments the results show a complete destabilisation of the o/w emulsions resulting in droplet flocculation, coalescence and the formation of free oil. As presented in

Chapter 4, micro bubbles were observed for all the DAF treatments. For all the treatments, statistically significant results were observed for the measurements of:

- ζ potential
- Conductivity
- Turbidity, and
- COD

To the author's knowledge, there are very few reports available in the literature that have analysed and described emulsions pre and post treatments to this level of detail. All the treatments resulted in oil degradation as per the results of the FAMES analysis. As discussed in Section 4.6 the oil droplets in the emulsion are continuously being exposed to an aqueous oxidising environment emanating from dissolved air in the DAF unit. It is observed that DAF with coagulation and shear resulted in the highest degradation of the oil in the emulsion. The least degradation of oil was obtained for the DAF with shear treatment with a measurement of 12.87 g/100 g of sample.

The best treatment efficiency was obtained with DAF and coagulation with a 69.8% TE, followed by DAF with coagulation and shear with a TE of 59.4% and the least efficient being DAF with shear resulting in TE of 46.5%.

The conclusion from this is that hydrodynamic shear and DAF is a successful method for o/w emulsions processing, which based on the results confirms that this treatment results in the lowest oil degradation. Despite the relatively low processing efficiency compared to the other DAF treatments, the unique treatment DAF with shear has demonstrated that shear can replace chemical coagulants and can produce a water phase with lower levels of chemicals and relatively lower levels of sludge and degraded oil.

Taking into account the results obtained an invention and patent relating to a process for recovering uncontaminated oil from a stable o/w emulsion has been filed accordingly, South African provisional patent with application number, 2022/12418.

CHAPTER 6 FUTURE WORK

This chapter outlines recommendations for future research in the field of o/w emulsion processing utilising hydrodynamic shear and flotation technology. The research questions, aims and objectives raised in this thesis have been successfully addressed, however there are other interesting aspects, not within the scope of the study, which can be further researched. Based on the results and findings from this work, it is recommended further work to be undertaken in the following areas:

- The processing and analysis of surfactant and emulsifier stabilised o/w emulsions and more complex emulsions, such as w/o and w/o/w emulsions, employing IAF and DAF pilot scale systems
- The processing of other types of stable emulsions prepared from compounds frequently encountered in the petroleum, agricultural and pharmaceutical sectors
- The processing of typical industrial effluents, where lower oil contents and other contaminants, such as other organics and suspended solids, are present
- The use of inert (N_2), oxidising (O_2 , O_3), acidic (CO_2) or basic gasses (NH_3) instead of air
- The upscaling of the laboratory scale IAF system to a pilot scale, which is able to process larger quantities of water
- The evaluation of emulsion pre-treatments to increase associated treatment efficiencies and increase the recovery of the oil phase
- The degradation analysis of the oil phase associated with the processing of emulsions utilising flotation and other separation technologies

References

1. Council National Research *Oil in the Sea III*; National Academies Press: Washington, D.C., 2003; ISBN 978-0-309-08438-3.
2. Abdel-Shafy, H.I.; Mansour, M.S.M. A review on polycyclic aromatic hydrocarbons: Source, environmental impact, effect on human health and remediation. *Egypt. J. Pet.* **2016**, *25*, 107–123, doi:10.1016/j.ejpe.2015.03.011.
3. Wiese, F.K.; Ryan, P.C. The extent of chronic marine oil pollution in southeastern Newfoundland waters assessed through beached bird surveys 1984-1999. *Mar. Pollut. Bull.* **2003**, *46*, 1090–1101, doi:10.1016/S0025-326X(03)00250-9.
4. O'Hara, P.D.; Morandin, L.A. Effects of sheens associated with offshore oil and gas development on the feather microstructure of pelagic seabirds. *Mar. Pollut. Bull.* **2010**, *60*, 672–678, doi:10.1016/j.marpolbul.2009.12.008.
5. Nordborg, F.M.; Jones, R.J.; Oelgemöller, M.; Negri, A.P. The effects of ultraviolet radiation and climate on oil toxicity to coral reef organisms – A review. *Sci. Total Environ.* **2020**, *720*, doi:10.1016/j.scitotenv.2020.137486.
6. Santo, C.E.; Vilar, V.J.P.; Botelho, C.M.S.; Bhatnagar, A.; Kumar, E.; Boaventura, R.A.R. Optimization of coagulation-flocculation and flotation parameters for the treatment of a petroleum refinery effluent from a Portuguese plant. *Chem. Eng. J.* **2012**, *183*, 117–123, doi:10.1016/j.cej.2011.12.041.
7. Zhao, C.; Zhou, J.; Yan, Y.; Yang, L.; Xing, G.; Li, H.; Wu, P.; Wang, M.; Zheng, H. Application of coagulation/flocculation in oily wastewater treatment: A review. *Sci. Total Environ.* **2020**, 142795, doi:10.1016/j.scitotenv.2020.142795.
8. Linke, C.; Drusch, S. Turbidity in oil-in-water-emulsions — Key factors and visual perception. *Food Res. Int.* **2016**, *89*, 202–210, doi:10.1016/j.foodres.2016.07.019.
9. Kulkarni, S.J.; Goswami, A.K. A Review on Wastewater Treatment for Petroleum Industries and Refineries. *Int. J. Innov. Res. Sci. Eng. Technol.* **2015**, *1*, 280–283, doi:180/12.2014.
10. Borchate, S.S.; Kulkarni, G.S.; Kore, S. V; Kore, V.S. Application of coagulation flocculation for vegetable tannery wastewater. *Int. J. Eng. Sci. Technol.* **2012**, *4*, 1944–1948.
11. Meyssami, B.; Kasaeian, A.B. Use of coagulants in treatment of olive oil wastewater model solutions by induced air flotation. *Bioresour. Technol.* **2005**, *96*, 303–307, doi:10.1016/j.biortech.2004.04.014.
12. Teh, C.Y.; Budiman, P.M.; Shak, K.P.Y.; Wu, T.Y. Recent Advancement of Coagulation-Flocculation and Its Application in Wastewater Treatment. *Ind. Eng. Chem. Res.* **2016**, *55*, 4363–4389, doi:10.1021/acs.iecr.5b04703.
13. Islam, M.N.; Park, K.J.; Alam, M.J. Treatment of swine wastewater using sequencing batch reactor. *Eng. Agric. Environ. Food* **2011**, *4*, 47–53, doi:10.1016/S1881-8366(11)80020-0.
14. Cerff, B.; Key, D.; Bladergroen, B. A review of the processes associated with the removal of oil in water pollution. *Sustain.* **2021**, *13*, doi:10.3390/su132212339.

15. da Rosa, J.J.; Rubio, J. The FF (flocculation–flotation) process. *Miner. Eng.* **2005**, *18*, 701–707, doi:10.1016/j.mineng.2004.10.010.
16. Welz, M.L.S.; Baloyi, N.; Deglon, D.A. Oil removal from industrial wastewater using flotation in a mechanically agitated flotation cell. *Water SA* **2007**, *33*, 453–458, doi:10.4314/wsa.v33i4.52939.
17. Aljuboury, D.A.D.A.; Palaniandy, P.; Abdul Aziz, H.B.; Feroz, S. Treatment of petroleum wastewater by conventional and new technologies - A review. *Glob. Nest J.* **2017**, *19*, 439–452, doi:10.30955/gnj.002239.
18. Varjani, S.; Joshi, R.; Srivastava, V.K.; Ngo, H.H.; Guo, W. Treatment of wastewater from petroleum industry: current practices and perspectives. *Environ. Sci. Pollut. Res.* **2020**, *27*, 27172–27180, doi:10.1007/s11356-019-04725-x.
19. Lee, C.H.; Tiwari, B.; Zhang, D.; Yap, Y.K. Water purification: oil-water separation by nanotechnology and environmental concerns. *Environ. Sci. Nano* **2017**, *4*, 514–525, doi:10.1039/C6EN00505E.
20. Jamaly, S.; Giwa, A.; Hasan, S.W. Recent improvements in oily wastewater treatment: Progress, challenges, and future opportunities. *J. Environ. Sci. (China)* **2015**, *37*, 15–30, doi:10.1016/j.jes.2015.04.011.
21. Jafarinejad, S. Treatment of Oily Wastewater. In *Petroleum Waste Treatment and Pollution Control*; Elsevier: Oxford, 2017; pp. 185–267 ISBN 9780128092439.
22. Abdulredha, M.M.; Siti Aslina, H.; Luqman, C.A. Overview on petroleum emulsions, formation, influence and demulsification treatment techniques. *Arab. J. Chem.* **2020**, *13*, 3403–3428, doi:10.1016/j.arabjc.2018.11.014.
23. Rowland, G.; Walsh, J. Addressing Gaps in Water Treatment Technology. *J. Pet. Technol.* **2013**, *65*, 82–88, doi:10.2118/1013-0082-jpt.
24. Bakke, T.; Klungsøyr, J.; Sanni, S. Environmental impacts of produced water and drilling waste discharges from the Norwegian offshore petroleum industry. *Mar. Environ. Res.* **2013**, *92*, 154–169, doi:10.1016/j.marenvres.2013.09.012.
25. Denney, D. Offshore Water-Disposal Wells: Formation Damage and Treatment. *J. Pet. Technol.* **2013**, *65*, 172–175, doi:10.2118/1113-0172-jpt.
26. Schovsbo, N.H.; Gottfredsen, S.N.; Schmidt, K.G.; Jørgensen, T.M. Oil production monitoring and optimization from produced water analytics; a case study from the Halfdan chalk oil field, Danish North Sea. *IFAC-PapersOnLine* **2018**, *51*, 203–210, doi:10.1016/j.ifacol.2018.06.378.
27. Jackson, M.; Twine, T.; Potgieter, R.; Anderson, D.; Soobyah, L. Econometrix Karoo Shale Gas Report. **2012**, 76.
28. Vermulen, P. A South African perspective on shale gas hydraulic fracturing. *C.D. McCullough, M.A. Lund L. Wyse Int. Mine Water Assoc. Symp. Bunbury Aust.* **2012**, 149–156.
29. Bocora, J. Global Prospects for the Development of Unconventional Gas. *Procedia - Soc. Behav. Sci.* **2012**, *65*, 436–442, doi:10.1016/j.sbspro.2012.11.145.
30. Mohammad-Pajooch, E.; Weichgrebe, D.; Cuff, G.; Tosarkani, B.M.; Rosenwinkel, K.H.

- On-site treatment of flowback and produced water from shale gas hydraulic fracturing: A review and economic evaluation. *Chemosphere* **2018**, *212*, 898–914, doi:10.1016/j.chemosphere.2018.08.145.
31. Hashmi, K.; Canada, N.R. Treatment of Produced Water : A Challenge for Heavy Oil Production. **2016**.
 32. Coelho, A.; Castro, A. V.; Dezotti, M.; Sant'Anna, G.L. Treatment of petroleum refinery sourwater by advanced oxidation processes. *J. Hazard. Mater.* **2006**, *137*, 178–184, doi:10.1016/j.jhazmat.2006.01.051.
 33. Sun, P.; Elgowainy, A.; Wang, M.; Han, J.; Henderson, R.J. Estimation of U.S. refinery water consumption and allocation to refinery products. *Fuel* **2018**, *221*, 542–557, doi:10.1016/j.fuel.2017.07.089.
 34. US Energy Information Administration (EIA) Annual Energy Outlook 2016 With Projections To 2040. **2016**, Energy Information Administration, doi:doe/eia-0383(2016).
 35. Odularu, O.; Okonkwo, C. Does energy consumption contribute to economic performance? Empirical evidence from Nigeria. *J. Econ. Int. Financ.* **2009**, *1*, 44–58.
 36. Asif, M.; Muneer, T. Energy supply, its demand and security issues for developed and emerging economies. *Renew. Sustain. Energy Rev.* **2007**, *11*, 1388–1413, doi:10.1016/j.rser.2005.12.004.
 37. Eggoh, J.C.; Bangake, C.; Rault, C. Energy consumption and economic growth revisited in African countries. *Energy Policy* **2011**, *39*, 7408–7421, doi:10.1016/j.enpol.2011.09.007.
 38. El-Naas, M.H.; Alhaija, M.A.; Al-Zuhair, S. Evaluation of a three-step process for the treatment of petroleum refinery wastewater. *J. Environ. Chem. Eng.* **2014**, *2*, 56–62, doi:10.1016/j.jece.2013.11.024.
 39. Farid Benyahia; Mohamed Abdulkarim; Ahmed Embaby; Madduri Rao; F .Benyahia, A.; A. Embaby; M.Rao; Mohamed Abdulkarim and Ahmed Embaby Refinery wastewater treatment : a true technological challenge. *Seventh Annu. U.A.E. Univ. Res. Conf.* **2006**, *8*, doi:10.13140/RG.2.1.4642.8562.
 40. Ossai, I.C.; Ahmed, A.; Hassan, A.; Hamid, F.S. Remediation of soil and water contaminated with petroleum hydrocarbon: A review. *Environ. Technol. Innov.* **2020**, *17*, 100526, doi:10.1016/j.eti.2019.100526.
 41. Awaleh, O.M.; Soubaneh, D.Y. Waste Water Treatment in Chemical Industries: The Concept and Current Technologies. *J. Waste Water Treat. Anal.* **2014**, *05*, 1–12, doi:10.4172/2157-7587.1000164.
 42. Choudri, B.S.; Baawain, M. Petrochemicals. *Water Environ. Res.* **2013**, *85*, 1548–1566, doi:10.2175/106143013X13698672322543.
 43. Yu, L.; Han, M.; He, F. A review of treating oily wastewater. *Arab. J. Chem.* **2017**, *10*, S1913–S1922, doi:10.1016/j.arabjc.2013.07.020.
 44. Khader, E.; Mohammed, T.; Mirghaffari, N. Use of Natural Coagulants for Removal of COD, Oil and Turbidity from Produced Waters in the Petroleum Industry. *J. Pet. Environ. Biotechnol.* **2018**, *09*, doi:10.4172/2157-7463.1000374.

45. Rocha e Silva, F.C.P.; Rocha e Silva, N.M.P.; da Silva, I.A.; Ferreira Brasileiro, P.P.; Luna, J.M.; Rufino, R.D.; Santos, V.A.; Sarubbo, L.A. Oil removal efficiency forecast of a Dissolved Air Flotation (DAF) reduced scale prototype using the dimensionless number of Damköhler. *J. Water Process Eng.* **2018**, *23*, 45–49, doi:10.1016/j.jwpe.2018.01.019.
46. Tee, P.F.; Abdullah, M.O.; Tan, I.A.W.; Rashid, N.K.A.; Amin, M.A.M.; Nolasco-Hipolito, C.; Bujang, K. Review on hybrid energy systems for wastewater treatment and bio-energy production. *Renew. Sustain. Energy Rev.* **2016**, *54*, 235–246, doi:10.1016/j.rser.2015.10.011.
47. Dhote, J.; Ingole, S.P. Review on Waste Water Treatment Technologies. *Int. J. Eng. Res. Technol.* **2012**, *1*, 1~10.
48. Fakhru'l-Razi, A.; Pendashteh, A.; Abdullah, L.C.; Biak, D.R.A.; Madaeni, S.S.; Abidin, Z.Z. Review of technologies for oil and gas produced water treatment. *J. Hazard. Mater.* **2009**, *170*, 530–551, doi:10.1016/j.jhazmat.2009.05.044.
49. Kenawy, F.A.; Kandil, M.E. Comparative evaluation between a modified CFP separator and all other available oil-water separation techniques. *Soc. Pet. Eng. - SPE Int. Conf. Heal. Safety, Environ. Oil Gas Explor. Prod. 1998, HSE 1998* **1998**, doi:10.2523/46817-ms.
50. Radelyuk, I.; Tussupova, K.; Zhapargazinova, K.; Yelubay, M.; Persson, M. Pitfalls of wastewater treatment in oil refinery enterprises in Kazakhstan-a system approach. *Sustain.* **2019**, *11*, 1–20, doi:10.3390/su11061618.
51. Sunil, K.; Wingrove, M. Emulsion separation index: From laboratory to field case studies. *SPE Annu. Tech. Conf. Proc.* **2000**, 589–600, doi:10.2523/63165-ms.
52. A Issaka, S. Review on the Fundamental Aspects of Petroleum Oil Emulsions and Techniques of Demulsification. *J. Pet. Environ. Biotechnol.* **2015**, *06*, doi:10.4172/2157-7463.1000214.
53. Zolfaghari, R.; Fakhru'l-Razi, A.; Abdullah, L.C.; Elnashaie, S.S.E.H.; Pendashteh, A. Demulsification techniques of water-in-oil and oil-in-water emulsions in petroleum industry. *Sep. Purif. Technol.* **2016**, *170*, 377–407, doi:10.1016/j.seppur.2016.06.026.
54. Kokal, S. Crude-oil emulsions: A state-of-the-art review. *SPE Prod. Facil.* **2005**, *20*, 5–12, doi:10.2118/77497-PA.
55. Zhang, H.; Liu, J.; Wang, Y.; Cao, Y.; Ma, Z.; Li, X. Cyclonic-static micro-bubble flotation column. *Miner. Eng.* **2013**, *45*, 1–3, doi:10.1016/j.mineng.2013.01.006.
56. Aliff Radzuan, M.R.; Abia-Biteo Belope, M.A.; Thorpe, R.B. Removal of fine oil droplets from oil-in-water mixtures by dissolved air flotation. *Chem. Eng. Res. Des.* **2016**, *115*, 19–33, doi:10.1016/j.cherd.2016.09.013.
57. Abuhasel, K.; Kchaou, M.; Alquraish, M.; Munusamy, Y.; Jeng, Y.T. Oily Wastewater Treatment: Overview of Conventional and Modern Methods, Challenges, and Future Opportunities. *Water* **2021**, *13*, 980, doi:10.3390/w13070980.
58. Abd El-Rahiem, F.H. Recent Trends in Flotation of Fine Particles. *J. Min. World Express* **2014**, *3*, 63, doi:10.14355/mwe.2014.03.009.
59. Hadler, K.; Cilliers, J.J. The Effect of Particles on Surface Tension and Flotation Froth

- Stability. *Mining, Metall. Explor.* **2019**, *36*, 63–69, doi:10.1007/s42461-018-0020-z.
60. FAN, M.; TAO, D.; HONAKER, R.; LUO, Z. Nanobubble generation and its application in froth flotation (part I): nanobubble generation and its effects on properties of microbubble and millimeter scale bubble solutions. *Min. Sci. Technol.* 2010, *20*, 1–19.
 61. Calgaroto, S.; Azevedo, A.; Rubio, J. Separation of amine-insoluble species by flotation with nano and microbubbles. *Miner. Eng.* **2016**, *89*, 24–29, doi:10.1016/j.mineng.2016.01.006.
 62. Saththasivam, J.; Loganathan, K.; Sarp, S. An overview of oil-water separation using gas flotation systems. *Chemosphere* **2016**, *144*, 671–680, doi:10.1016/j.chemosphere.2015.08.087.
 63. Prakash, R.; Majumder, S.K.; Singh, A. Flotation technique: Its mechanisms and design parameters. *Chem. Eng. Process. - Process Intensif.* **2018**, *127*, 249–270, doi:10.1016/j.cep.2018.03.029.
 64. Lim, M.W.; Lau, E. V.; Poh, P.E. Analysis of attachment process of bubbles to high-density oil: Influence of bubble size and water chemistry. *J. Taiwan Inst. Chem. Eng.* **2016**, *68*, 192–200, doi:10.1016/j.jtice.2016.08.037.
 65. Forbes, E. Shear, selective and temperature responsive flocculation: A comparison of fine particle flotation techniques. *Int. J. Miner. Process.* **2011**, *99*, 1–10, doi:10.1016/j.minpro.2011.02.001.
 66. Murphy, D.D.; Bakker, M.G.; Spears, D.R. New insights into the mechanism of shear-flocculation of silica with fatty acids. *Miner. Metall. Process.* **1994**, *11*, 26–30, doi:10.1007/bf03403036.
 67. Quemada, D. Rheological modelling of complex fluids: II. Shear thickening behavior due to shear induced flocculation. *EPJ Appl. Phys.* **1998**, *2*, 175–181, doi:10.1051/epjap:1998170.
 68. Song, S.; Lopez-Valdivieso, A.; Reyes-Bahena, J.L.; Lara-Valenzuela, C. Floc flotation of galena and sphalerite fines. *Miner. Eng.* **2001**, *14*, 87–98, doi:10.1016/S0892-6875(00)00162-X.
 69. Bilgen, S.; Wills, B.A. Shear flocculation - A review. *Miner. Eng.* **1991**, *4*, 483–487, doi:10.1016/0892-6875(91)90148-O.
 70. Patil, D.P.; Andrews, J.R.G.; Uhlherr, P.H.T. Shear flocculation-kinetics of floc coalescence and breakage. *Int. J. Miner. Process.* **2001**, *61*, 171–188, doi:10.1016/S0301-7516(00)00036-3.
 71. Spicer, P.T.; Keller, W.; Pratsinis, S.E. The effect of impeller type on floc size and structure during shear-induced flocculation. *J. Colloid Interface Sci.* **1996**, *184*, 112–122, doi:10.1006/jcis.1996.0601.
 72. Spicer, P.T.; Pratsinis, S.E. Shear-induced flocculation: The evolution of floc structure and the shape of the size distribution at steady state. *Water Res.* **1996**, *30*, 1049–1056, doi:10.1016/0043-1354(95)00253-7.
 73. Somasundaran, P.; Das, K.K.; Yu, X. Selective flocculation. *Curr. Opin. Colloid Interface Sci.* **1996**, *1*, 530–534, doi:10.1016/s1359-0294(96)80123-3.

74. Silva, T.M.; Cerize, N.N.P.; Oliveira, A.M. The Effect of High Shear Homogenization on Physical Stability of Emulsions. *Int. J. Chem.* **2016**, *8*, 52, doi:10.5539/ijc.v8n4p52.
75. Walsh, J.M. The Effect of Shear on Produced Water Treatment. *Soc. Pet. Eng.* **2016**, *5*, 16–23, doi:10.2118/0216-0016-OGF.
76. Wang, Z.; Lin, X.; Rui, Z.; Xu, M.; Zhan, S. The role of shearing energy and interfacial Gibbs free energy in the emulsification mechanism of waxy crude oil. *Energies* **2017**, *10*, doi:10.3390/en10050721.
77. Luhede, L.; Wollborn, T.; Fritsching, U. Stability of multiple emulsions under shear stress. *Can. J. Chem. Eng.* **2020**, *98*, 186–193, doi:10.1002/cjce.23578.
78. Saad, M.A.; Kamil, M.; Abdurahman, N.H.; Yunus, R.M.; Awad, O.I. An overview of recent advances in state-of-the-art techniques in the demulsification of crude oil emulsions. *Processes* **2019**, *7*, 1–26, doi:10.3390/pr7070470.
79. Canselier, J.P.; Poux, M. Emulsion preparation: Theoretical notions and practical aspects. *PharmaChem* **2004**, 16–21.
80. Okereke, U.; Ohia, N.; Obah, B. Effects of Demulsifiers on the Droplet Size and Ashphaltene Content of an Oil Tight Emulsion. *Int. Res. J. Adv. Eng. Sci.* **2018**, *3*, 152–156.
81. Chen, G.; He, G. Separation of water and oil from water-in-oil emulsion by freeze/thaw method. *Sep. Purif. Technol.* **2003**, *31*, 83–89, doi:10.1016/S1383-5866(02)00156-9.
82. Pan, L.L.; Chen, Y.; Chen, D.; Dong, Y.Q.; Zhang, Z.T.; Long, Y.X. Oil removal in tight-emulsified petroleum waste water by flocculation. *IOP Conf. Ser. Mater. Sci. Eng.* **2018**, *392*, doi:10.1088/1757-899X/392/4/042005.
83. Raya, S.A.; Mohd Saaid, I.; Abbas Ahmed, A.; Abubakar Umar, A. A critical review of development and demulsification mechanisms of crude oil emulsion in the petroleum industry. *J. Pet. Explor. Prod. Technol.* **2020**, *10*, 1711–1728, doi:10.1007/s13202-020-00830-7.
84. Maindarkar, S.; Dubbelboer, A.; Meuldijk, J.; Hoogland, H.; Henson, M. Prediction of emulsion drop size distributions in colloid mills. *Chem. Eng. Sci.* **2014**, *118*, 114–125, doi:10.1016/j.ces.2014.07.032.
85. Al-Mulla, A.; Gupta, R.K. Droplet coalescence in the shear flow of model emulsions. *Rheol. Acta* **2000**, *39*, 20–25, doi:10.1007/s003970050003.
86. Berre, F. Le; Chauveteau, G.; Pefferkorn, E. Shear induced aggregation/fragmentation of hydrated colloids. *J. Colloid Interface Sci.* **1998**, *199*, 13–21, doi:10.1006/jcis.1997.5308.
87. Shardt, O.; Derksen, J.J.; Mitra, S.K. Simulations of droplet coalescence in simple shear flow. *Langmuir* **2013**, *29*, 6201–6212, doi:10.1021/la304919p.
88. Korobko, A. V.; Van Den Ende, D.; Agterof, W.G.M.; Mellema, J. Coalescence in semiconcentrated emulsions in simple shear flow. *J. Chem. Phys.* **2005**, *123*, 1–11, doi:10.1063/1.2121627.
89. Pathak, J.A.; Davis, M.C.; Hudson, S.D.; Migler, K.B. Layered droplet microstructures in sheared emulsions: Finite-size effects. *J. Colloid Interface Sci.* **2002**, *255*, 391–402,

- doi:10.1006/jcis.2002.8608.
90. Caserta, S.; Sabetta, L.; Simeone, M.; Guido, S. Shear-induced coalescence in aqueous biopolymer mixtures. *Chem. Eng. Sci.* **2005**, *60*, 1019–1027, doi:10.1016/j.ces.2004.09.076.
 91. Whitby, C.P.; Fischer, F.E.; Fornasiero, D.; Ralston, J. Shear-induced coalescence of oil-in-water Pickering emulsions. *J. Colloid Interface Sci.* **2011**, *361*, 170–177, doi:10.1016/j.jcis.2011.05.046.
 92. Vanapalli, S.A.; Coupland, J.N. Emulsions under shear- The formation and properties of partially coalesced lipid structures. *Food Hydrocoll.* **2001**, *15*, 507–512, doi:10.1016/S0268-005X(01)00057-1.
 93. Nandi, A.; Mehra, A.; Khakhar, D. V. Suppression of coalescence in surfactant stabilized emulsions by shear flow. *Phys. Rev. Lett.* **1999**, *83*, 2461–2464, doi:10.1103/PhysRevLett.83.2461.
 94. Nandi, A.; Khakhar, D. V.; Mehra, A. Coalescence in surfactant-stabilized emulsions subjected to shear flow. *Langmuir* **2001**, *17*, 2647–2655, doi:10.1021/la001473m.
 95. Van Puyvelde, P.; Antonov, Y.A.; Moldenaers, P. Morphology evolution of aqueous biopolymer emulsions during a weak shear flow. *Food Hydrocoll.* **2003**, *17*, 327–332, doi:10.1016/S0268-005X(02)00094-2.
 96. Padilla, P.; Toxvaerd, S.; Stecki, J. Shear flow at liquid-liquid interfaces. *J. Chem. Phys.* **1995**, *103*, 716–724, doi:10.1063/1.470105.
 97. Kaldasch, J.; Senge, B.; Laven, J. Shear thickening in concentrated soft sphere colloidal suspensions: A shear induced phase transition. *J. Thermodyn.* **2015**, *2015*, doi:10.1155/2015/153854.
 98. Yang, H.; Abbaspour, K.C. Analysis of wastewater reuse potential in Beijing. *Desalination* **2007**, *212*, 238–250, doi:10.1016/j.desal.2006.10.012.
 99. van 't Oever, R.T. Reuse of produced water into oil field application. *88th Annu. Water Environ. Fed. Tech. Exhib. Conf. WEFTEC 2015* **2015**, *8*, 5995–6001, doi:10.2175/193864715819542250.
 100. Judd, S.; Qiblawey, H.; Al-Marri, M.; Clarkin, C.; Watson, S.; Ahmed, A.; Bach, S. The size and performance of offshore produced water oil-removal technologies for reinjection. *Sep. Purif. Technol.* **2014**, *134*, 241–246, doi:10.1016/j.seppur.2014.07.037.
 101. Kwon, G.; Kota, A.K.; Li, Y.; Sohani, A.; Mabry, J.M.; Tuteja, A. On-demand separation of oil-water mixtures. *Adv. Mater.* **2012**, *24*, 3666–3671, doi:10.1002/adma.201201364.
 102. Wei, X.; Zhang, S.; Sun, Y.; Brenner, S.A. Petrochemical Wastewater and Produced Water. *Water Environ. Res.* **2018**, *90*, 1634–1647, doi:10.2175/106143018x15289915807344.
 103. Jiménez, S.; Micó, M.M.; Arnaldos, M.; Medina, F.; Contreras, S. State of the art of produced water treatment. *Chemosphere* **2018**, *192*, 186–208, doi:10.1016/j.chemosphere.2017.10.139.
 104. Pinchin, D. Subsea water treatment comes of age. *Proc. Annu. Offshore Technol. Conf.*

- 2011, 1, 376–384.
105. Cheremisinoff, P.N. Oil/water separation. *Met. Finish.* **1999**, 97, 70, doi:10.1016/s0026-0576(99)80583-2.
 106. Alther, G. Cleaning wastewater: Removing oil from water with organoclays. *Filtr. Sep.* **2008**, 45, doi:10.1016/S0015-1882(08)70057-0.
 107. Poulopoulos, S.G.; Voutsas, E.C.; Grigoropoulou, H.P.; Philippopoulos, C.J. Stripping as a pretreatment process of industrial oily wastewater. *J. Hazard. Mater.* **2005**, 117, 135–139, doi:10.1016/j.jhazmat.2004.08.033.
 108. Livingston, T.; Abbassi, B. A comparative review and multi-criteria analysis of petroleum refinery wastewater treatment technologies. *Environ. Res. Eng. Manag.* **2018**, 74, 66–78, doi:10.5755/j01.erm.74.4.21428.
 109. Husain, I.A.F.; Alkhatib, M.F.; Jami, M.S.; Mirghani, M.E.S.; Zainudin, Z. Bin; Hoda, A. Problems, control, and treatment of fat, oil, and grease (FOG): A review. *J. Oleo Sci.* **2014**, 63, 747–752, doi:10.5650/jos.ess13182.
 110. Ishak, S.; Malakahmad, A.; Isa, M.H. Refinery wastewater biological treatment: A short review. *J. Sci. Ind. Res. (India)*. **2012**, 71, 251–256.
 111. Nordvik, A.B.; Simmons, J.L.; Bitting, K.R.; Lewis, A.; Strøm-Kristiansen, T. Oil and water separation in marine oil spill clean-up operations. *Spill Sci. Technol. Bull.* **1996**, 3, 107–122, doi:10.1016/S1353-2561(96)00021-7.
 112. Smathers, C.J.; Jackson, T.; Buckwald, S.; Gonzalo, R.; McPherson, R. Technology Update: New Adsorption Media Technology Meets Water-Treatment Challenges. *J. Pet. Technol.* **2018**, 70, 18–20, doi:10.2118/0618-0018-jpt.
 113. Ashrafi, O.; Yerushalmi, L.; Haghighat, F. Wastewater treatment in the pulp-and-paper industry: A review of treatment processes and the associated greenhouse gas emission. *J. Environ. Manage.* **2015**, 158, 146–157, doi:10.1016/j.jenvman.2015.05.010.
 114. Hendricks, D. *Fundamentals of Water Treatment Unit Processes*; 1st ed.; CRC Press: Boca Raton, 2010; ISBN 9780429109034.
 115. Chaudhary, D.S.; Vigneswaran, S.; Ngo, H.H.; Shim, W.G.; Moon, H. Biofilter in Water and Wastewater Treatment. *Korean J. Chem. Eng.* **2003**, 20, 1054–1065, doi:10.1007/BF02706936.
 116. Morling, S. Why Should We Bother on Measurement in Wastewater Treatment Operation? *J. Water Resour. Prot.* **2016**, 08, 982–989, doi:10.4236/jwarp.2016.811079.
 117. Birdi, K. *Handbook of Surface and Colloid Chemistry*; Boca Raton, Fla: CRC press, 2009; ISBN 978-0-8493-7327-5.
 118. Grasso, D.; Subramaniam, K.; Butkus, M.; Strevett, K.; Bergendahl, J. A review of non-DLVO interactions in environmental colloidal systems. *Rev. Environ. Sci. Biotechnol.* **2002**, 1, 17–38, doi:10.1023/A:1015146710500.
 119. Lin, F.; Suda, J.; Yeung, A. A small point regarding DLVO coagulation conditions. *J. Colloid Interface Sci.* **2014**, 430, 113–115, doi:10.1016/j.jcis.2014.05.014.
 120. Ivanov, I.B.; Kralchevsky, P.A. Stability of emulsions under equilibrium and dynamic conditions. *Colloids Surfaces A Physicochem. Eng. Asp.* **1997**, 128, 155–175,

doi:10.1016/S0927-7757(96)03903-9.

121. Verma, S.; Prasad, B.; Mishra, I.M. Pretreatment of petrochemical wastewater by coagulation and flocculation and the sludge characteristics. *J. Hazard. Mater.* **2010**, *178*, 1055–1064, doi:10.1016/j.jhazmat.2010.02.047.
122. Wei, H.; Gao, B.; Ren, J.; Li, A.; Yang, H. Coagulation/flocculation in dewatering of sludge: A review. *Water Res.* **2018**, *143*, 608–631, doi:10.1016/j.watres.2018.07.029.
123. Shim, H.Y.; Lee, K.S.; Lee, D.S.; Jeon, D.S.; Park, M.S.; Shin, J.S.; Lee, Y.K.; Goo, J.W.; Kim, S.B.; Chung, D.Y. Application of Electrocoagulation and Electrolysis on the Precipitation of Heavy Metals and Particulate Solids in Washwater from the Soil Washing. *J. Agric. Chem. Environ.* **2014**, *03*, 130–138, doi:10.4236/jacen.2014.34015.
124. Matilainen, A.; Vepsäläinen, M.; Sillanpää, M. Natural organic matter removal by coagulation during drinking water treatment: A review. *Adv. Colloid Interface Sci.* **2010**, *159*, 189–197, doi:10.1016/j.cis.2010.06.007.
125. Sillanpää, M.; Ncibi, M.C.; Matilainen, A.; Vepsäläinen, M. Removal of natural organic matter in drinking water treatment by coagulation: A comprehensive review. *Chemosphere* **2018**, *190*, 54–71, doi:10.1016/j.chemosphere.2017.09.113.
126. Cañizares, P.; Martínez, F.; Carmona, M.; Lobato, J.; Rodrigo, M.A. Continuous electrocoagulation of synthetic colloid-polluted wastes. *Ind. Eng. Chem. Res.* **2005**, *44*, 8171–8177, doi:10.1021/ie050527q.
127. Eldemerdash, U.M.N. Using ceramic materials for enhanced wastewater treatment in industrial applications. *InterCeram Int. Ceram. Rev.* **2011**, *60*, 100–104.
128. Al-Futaisi, A.; Jamrah, A.; Yaghi, B.; Taha, R. Assessment of alternative management techniques of tank bottom petroleum sludge in Oman. *J. Hazard. Mater.* **2007**, *141*, 557–564, doi:10.1016/j.jhazmat.2006.07.023.
129. Watanabe, Y. Flocculation and me. *Water Res.* **2017**, *114*, 88–103, doi:10.1016/j.watres.2016.12.035.
130. Krupińska, I. Aluminium drinking water treatment residuals and their toxic impact on human health. *Molecules* **2020**, *25*, doi:10.3390/molecules25030641.
131. Organisation, W.H. Aluminium in Drinking-water Background. *Guidel. Drink. Qual.* **2009**, *2*, 29.
132. Yianatos, J.; Contreras, F.; Morales, P.; Coddou, F.; Elgueta, H.; Ortíz, J. A novel scale-up approach for mechanical flotation cells. *Miner. Eng.* **2010**, *23*, 877–884.
133. Kawatra, S.K.; Eisele, T.C. 1 Froth Flotation - Fundamental Principles. *Recover. Pyrite Coal Flotat. Entrain. or Flotat.* **1992**, 1–30.
134. Hoseini, S.M.; Salarirad, M.M.; Alavi Moghaddam, M.R. TPH removal from oily wastewater by combined coagulation pretreatment and mechanically induced air flotation. *Desalin. Water Treat.* **2015**, *53*, 300–308, doi:10.1080/19443994.2013.846522.
135. Biruk Gobena Evaluation of Mix-Chemical Coagulants in Water Purification Process. *Int. J. Eng. Res.* **2018**, *V7*, 431–436, doi:10.17577/ijertv7is010171.
136. Srinivasan, P.T., Viraraghavan, T., & Subramanian, K.S. Aluminium in Drinking Water.

- Water SA* **1999**, *25*, 47–55.
137. Petala, M.; Samaras, P.; Kungolos, A.; Zouboulis, A.; Papadopoulos, A.; Sakellaropoulos, G.P. The effect of coagulation on the toxicity and mutagenicity of reclaimed municipal effluents. *Chemosphere* **2006**, *65*, 1007–1018, doi:10.1016/j.chemosphere.2006.03.035.
 138. Ukiwe, L.N.; Alinnor, J.I. Assessment of Polyacrylamide and Aluminum Sulphate Coagulants in Turbidity Removal in Wastewater. *Terr. Aquat. Environ. Toxicol.* **2012**, *6*, 132–135.
 139. Li, X.; Liu, J.; Wang, Y.; Xu, H.; Cao, Y.; Deng, X. Separation of Oil from Wastewater by Coal Adsorption-Column Flotation. *Sep. Sci. Technol.* **2015**, *50*, 583–591, doi:10.1080/01496395.2014.956759.
 140. Tuan Hoang, A.; Viet Pham, V.; Nam Nguyen, D. A Report of Oil Spill Recovery Technologies. *Int. J. Appl. Eng. Res.* **2018**, *13*, 4915–4928.
 141. Olga, V.R.; Darina, V.I.; Alexandr, A.I.; Alexandra, A.O. Cleanup of Water Surface from Oil Spills Using Natural Sorbent Materials. *Procedia Chem.* **2014**, *10*, 145–150, doi:10.1016/j.proche.2014.10.025.
 142. Wolok, E.; Barafi, J.; Joshi, N.; Girimonte, R.; Chakraborty, S. Study of bio-materials for removal of the oil spill. *Arab. J. Geosci.* **2020**, *13*, 1244, doi:10.1007/s12517-020-06244-3.
 143. Delvigne, G.A.L. Droplet Size Distribution of Naturally Dispersed Oil. In *Fate and Effects of Oil in Marine Ecosystems*; Springer Netherlands: Dordrecht, 1987; Vol. 28, pp. 29–40.
 144. Delvigne, G.A.L.; Sweeney, C.E. Natural dispersion of oil. *Oil Chem. Pollut.* **1988**, *4*, 281–310, doi:10.1016/S0269-8579(88)80003-0.
 145. Li, X.; Liu, J.; Wang, Y.; Wang, C.; Zhou, X. Separation of Oil from Wastewater by Column Flotation. *J. China Univ. Min. Technol.* **2007**, *17*, 546–577, doi:10.1016/S1006-1266(07)60143-6.
 146. Krebs, T.; Schroën, C.G.P.H.; Boom, R.M. Separation kinetics of an oil-in-water emulsion under enhanced gravity. *Chem. Eng. Sci.* **2012**, *71*, 118–125, doi:10.1016/j.ces.2011.10.057.
 147. Bai, Z. shan; Wang, H. lin; Tu, S.T. Oil-water separation using hydrocyclones enhanced by air bubbles. *Chem. Eng. Res. Des.* **2011**, *89*, 55–59, doi:10.1016/j.cherd.2010.04.012.
 148. Smathers, C.; Jackson, T.; Buckwald, S.; Gonzalo, R.; McPherson, R. Removing dispersed and dissolved hydrocarbons from water using adsorption media systems with multiple regeneration processes. *Soc. Pet. Eng. - SPE Kingdom Saudi Arab. Annu. Tech. Symp. Exhib. 2018, SATS 2018* **2018**, 1–12.
 149. Loh, A.; Shankar, R.; Ha, S.Y.; An, J.G.; Yim, U.H. Stability of mechanically and chemically dispersed oil: Effect of particle types on oil dispersion. *Sci. Total Environ.* **2020**, *716*, 135343, doi:10.1016/j.scitotenv.2019.135343.
 150. Nikovska, K. Study of olive oil-in-water emulsions with protein emulsifiers. *Emirates J. Food Agric.* **2012**, *24*, 17–24, doi:10.9755/ejfa.v24i1.10594.

151. Haghghat, A.K.; Olsen, M.G.; Vigil, R.D.; Sarkar, A. Droplet coalescence and phase separation in a topical ointment: Effects of fluid shear and temperature. *Int. J. Pharm.* **2020**, *591*, 119872, doi:10.1016/j.ijpharm.2020.119872.
152. McClements, D.J. Nanoemulsions versus microemulsions: Terminology, differences, and similarities. *Soft Matter* **2012**, *8*, 1719–1729, doi:10.1039/c2sm06903b.
153. Kulkarni, S.J. An Insight into Research and Investigations on Froth Flotation. *Int. J. Sci. Res. Chem.* **2016**, *1*, 55–58.
154. Butler, E.; Hung, Y.-T.; Yeh, R.Y.-L.; Suleiman Al Ahmad, M. Electrocoagulation in Wastewater Treatment. *Water* **2011**, *3*, 495–525, doi:10.3390/w3020495.
155. Robinson, D. Oil and gas: Treatment and discharge of produced waters onshore. *Filtr. Sep.* **2013**, *50*, 40–46, doi:10.1016/S0015-1882(13)70129-0.
156. Yong, J.; Chen, F.; Yang, Q.; Bian, H.; Du, G.; Shan, C.; Huo, J.; Fang, Y.; Hou, X. Oil-water separation: A gift from the desert. *Adv. Mater. Interfaces* **2016**, *3*, 1–7, doi:10.1002/admi.201500650.
157. Daiminger, U.; Nitsch, W.; Plucinski, P.; Hoffmann, S. Novel techniques for oil / water separation. *J. Memb. Sci.* **1995**, *99*, 197–203.
158. Oller, I.; Malato, S.; Sánchez-Pérez, J.A. Combination of Advanced Oxidation Processes and biological treatments for wastewater decontamination-A review. *Sci. Total Environ.* **2011**, *409*, 4141–4166, doi:10.1016/j.scitotenv.2010.08.061.
159. Bennett, G.F.; Peters, R.W. Critical Reviews in Environmental Control The removal of oil from wastewater by air flotation : A review. *Crit. Rev. Environ. Control* **1988**, *18*:3, 189–253, doi:http://dx.doi.org/10.1080/10643388809388348.
160. Suzuki, Y.; Maruyama, T. Removal of emulsified oil from water by coagulation and foam separation. *Sep. Sci. Technol.* **2005**, *40*, 3407–3418, doi:10.1080/01496390500423755.
161. Etchepare, R.; Oliveira, H.; Azevedo, A.; Rubio, J. Separation of emulsified crude oil in saline water by dissolved air flotation with micro and nanobubbles. *Sep. Purif. Technol.* **2017**, *186*, 326–332, doi:10.1016/j.seppur.2017.06.007.
162. Tansel, B.; Pascual, B. Removal of emulsified fuel oils from brackish and pond water by dissolved air flotation with and without polyelectrolyte use: Pilot-scale investigation for estuarine and near shore applications. *Chemosphere* **2011**, *85*, 1182–1186, doi:10.1016/j.chemosphere.2011.07.006.
163. Sanchez-Salas, J.L.; Raynal Gutierrez, M.E.; Bandala, E.R. *Aerobic Treatment of Petroleum Industry Effluents*; Elsevier B.V., 2017; ISBN 9780444636768.
164. Gasim, H.A.; Kutty, S.R.M.; Isa, M.H. Anaerobic Treatment of Petroleum Refinery Wastewater. *Int. J. Environ. Chem. Ecol. Geol. Geophys. Eng.* **2012**, *6*, 512–515.
165. Umar, A.A.; Saaid, I.B.M.; Sulaimon, A.A.; Pilus, R.B.M. A review of petroleum emulsions and recent progress on water-in-crude oil emulsions stabilized by natural surfactants and solids. *J. Pet. Sci. Eng.* **2018**, *165*, 673–690, doi:10.1016/j.petrol.2018.03.014.
166. Hirasaki, G.J.; Miller, C.A.; Raney, O.G.; Poindexter, M.K.; Nguyen, D.T.; Hera, J.

- Separation of produced emulsions from surfactant enhanced oil recovery processes. *Energy and Fuels* **2011**, *25*, 555–561, doi:10.1021/ef101087u.
167. Stewart, M.; Arnold, K. Produced Water Treating Systems. In *Emulsions and Oil Treating Equipment*; 2009; pp. 107–211.
 168. Kulkarni, S.J. Coagulation for Wastewater Treatment : A Review on Investigations and Studies, article. *Int. J. Sci. Res. Sci. Technol.* **2017**, *3*, 501–505.
 169. Ghernaout, D. Advanced oxidation phenomena in electrocoagulation process: a myth or a reality? *Desalin. Water Treat.* **2013**, *51*, 7536–7554, doi:10.1080/19443994.2013.792520.
 170. Brostow, W.; Pal, S.; Singh, R.P. A model of flocculation. *Mater. Lett.* **2007**, *61*, 4381–4384, doi:10.1016/j.matlet.2007.02.007.
 171. Tsuge, H.; Li, P.; Hirofumi, O. Application of Induced Air Flotation on Water Treatment. **2004**, 1–7, doi:10.11491/apcche.2004.0.620.0.
 172. Verma, A.K.; Dash, R.R.; Bhunia, P. A review on chemical coagulation/flocculation technologies for removal of colour from textile wastewaters. *J. Environ. Manage.* **2012**, *93*, 154–168, doi:10.1016/j.jenvman.2011.09.012.
 173. Motta, A.; Borges, C.; Esquerre, K.; Kiperstok, A. Oil Produced Water treatment for oil removal by an integration of coalescer bed and microfiltration membrane processes. *J. Memb. Sci.* **2014**, *469*, 371–378, doi:10.1016/j.memsci.2014.06.051.
 174. Machín-Ramírez, C.; Okoh, A.I.; Morales, D.; Mayolo-Deloisa, K.; Quintero, R.; Trejo-Hernández, M.R. Slurry-phase biodegradation of weathered oily sludge waste. *Chemosphere* **2008**, *70*, 737–744, doi:10.1016/j.chemosphere.2007.06.017.
 175. Tansel, B.; Sevimoglu, O. Coalescence and size distribution characteristics of oil droplets attached on flocs after coagulation. *Water. Air. Soil Pollut.* **2006**, *169*, 293–302, doi:10.1007/s11270-006-3110-3.
 176. Friberg, S.E. Emulsion Thermodynamics – In from the Cold. **2018**, *2*, 7–16, doi:10.13128/substantia-37.
 177. Kuo, C.H.; Lee, C.L. Treatment of oil/water emulsions using seawater-assisted microwave irradiation. *Sep. Purif. Technol.* **2010**, *74*, 288–293, doi:10.1016/j.seppur.2010.06.017.
 178. López-Esparza, R.; Balderas Altamirano, M.A.; Pérez, E.; Gama Goicochea, A. Importance of molecular interactions in colloidal dispersions. *Adv. Condens. Matter Phys.* **2015**, *2015*, doi:10.1155/2015/683716.
 179. Kingsley Ogemdi, I. Properties and Uses of Colloids: A Review. *Colloid Surf. Sci.* **2019**, *4*, 24, doi:10.11648/j.css.20190402.12.
 180. Coulson, J.. Colloidal Dispersions. In *Coulson and Richardson's Chemical Engineering: Volume 2A: Particulate Systems and Particle Technology*; Chhabra, R., Gurappa, B., Eds.; Elsevier, 2019; pp. 693–737 ISBN 978-0-08-101098-3.
 181. Vaécha, R.; Rick, S.W.; Jungwirth, P.; De Beer, A.G.F.; De Aguiar, H.B.; Samson, J.S.; Roke, S. The orientation and charge of water at the hydrophobic oil droplet - Water interface. *J. Am. Chem. Soc.* **2011**, *133*, 10204–10210, doi:10.1021/ja202081x.

182. Trefalt, G.; Borkovec, M. Overview of DLVO Theory. *Lab. Colloid Surf. Chem. Univ. Geneva* **2014**, 1–10.
183. Ohshima, H. The Derjaguin-Landau-Verwey-Overbeek (DLVO) Theory of Colloid Stability. *Electr. Phenom. Interfaces Biointerfaces Fundam. Appl. Nano-, Bio-, Environ. Sci.* **2012**, 27–34, doi:10.1002/9781118135440.ch3.
184. Toro-Mendoza, J.; Petsev, D.N. Brownian dynamics of emulsion film formation and droplet coalescence. *Phys. Rev. E - Stat. Nonlinear, Soft Matter Phys.* **2010**, *81*, 1–11, doi:10.1103/PhysRevE.81.051404.
185. Goodarzi, F.; Zendejboudi, S. A Comprehensive Review on Emulsions and Emulsion Stability in Chemical and Energy Industries. *Can. J. Chem. Eng.* **2019**, *97*, 281–309, doi:10.1002/cjce.23336.
186. Ivanov, I.B.; Danov, K.D.; Kralchevsky, P.A. Flocculation and coalescence of micron-size emulsion droplets. *Colloids Surfaces A Physicochem. Eng. Asp.* **1999**, *152*, 161–182, doi:10.1016/S0927-7757(98)00620-7.
187. Hu, Y.T.; Ting, Y.; Hu, J.Y.; Hsieh, S.C. Techniques and methods to study functional characteristics of emulsion systems. *J. Food Drug Anal.* **2017**, *25*, 16–26, doi:10.1016/j.jfda.2016.10.021.
188. Zungur, A.; Koç, M.; Kaymak-Ertekin, F. Physical properties of olive oil in water model emulsion: Effect of aqueous and oil phase concentration and homogenization Types. *Akad. Gıda* **2015**, *13*, 22–34.
189. Cox, R.D. Fundamental emulsion science (Part 1). *Househ. Pers. Care* **2012**, *7*, 18–20.
190. Cox, R.D. Fundamental emulsion science (Part 2). *Househ. Pers. Care* **2012**, *7*, 18–20.
191. Gupta, A.; Eral, H.B.; Hatton, T.A.; Doyle, P.S. Nanoemulsions: Formation, properties and applications. *Soft Matter* **2016**, *12*, 2826–2841, doi:10.1039/c5sm02958a.
192. Gadipelly, C.; Pérez-González, A.; Yadav, G.D.; Ortiz, I.; Ibáñez, R.; Rathod, V.K.; Marathe, K. V. Pharmaceutical industry wastewater: Review of the technologies for water treatment and reuse. *Ind. Eng. Chem. Res.* **2014**, *53*, 11571–11592, doi:10.1021/ie501210j.
193. Tadros, T.F. Emulsion Formation, Stability, and Rheology. In *Emulsion Formation and Stability*; Wiley-VCH Verlag GmbH & Co. KGaA: Weinheim, Germany, 2013; pp. 1–75.
194. Sainath, K.; Ghosh, P. Stabilization of silicone oil-in-water emulsions by ionic surfactant and electrolytes: The role of adsorption and electric charge at the interface. *Ind. Eng. Chem. Res.* **2013**, *52*, 15808–15816, doi:10.1021/ie401490c.
195. Taylor, P. Ostwald ripening in emulsions. *Adv. Colloid Interface Sci.* **1998**, *75*, 107–163, doi:10.1016/S0001-8686(98)00035-9.
196. Yeung, A.; Moran, K.; Masliyah, J.; Czarnecki, J. Shear-induced coalescence of emulsified oil drops. *J. Colloid Interface Sci.* **2003**, *265*, 439–443, doi:10.1016/S0021-9797(03)00531-9.
197. Jafari, S.M.; Assadpoor, E.; He, Y.; Bhandari, B. Re-coalescence of emulsion droplets during high-energy emulsification. *Food Hydrocoll.* **2008**, *22*, 1191–1202,

- doi:10.1016/j.foodhyd.2007.09.006.
198. Paul, B.K.; Moulik, S.P. Microemulsions : An overview. *J. Dispers. Sci. Technol.* **1997**, *18*, 301–367, doi:10.1080/01932699708943740.
 199. Watcharasing, S.; Kongkowitz, W.; Chavadej, S. Motor oil removal from water by continuous froth flotation using extended surfactant: Effects of air bubble parameters and surfactant concentration. *Sep. Purif. Technol.* **2009**, *70*, 179–189, doi:10.1016/j.seppur.2009.09.014.
 200. Delmas, T.; Piraux, H.; Couffin, A.C.; Texier, I.; Vinet, F.; Poulin, P.; Cates, M.E.; Bibette, J. How to prepare and stabilize very small nanoemulsions. *Langmuir* **2011**, *27*, 1683–1692, doi:10.1021/la104221q.
 201. Rong, F.; Liu, D.; Hu, Z. Stability of oil-in-water emulsions by SDS compound. *Pet. Sci. Technol.* **2018**, *36*, 2157–2162, doi:10.1080/10916466.2018.1465970.
 202. Hunter, R. . *Zeta Potential in Colloid Science: principles and applications.*; Ottewill, R.H., Rowell, R. ., Eds.; Academic press, 1981; ISBN 9781483214085.
 203. Poli, E.; Jong, K.H.; Hassanali, A. Charge transfer as a ubiquitous mechanism in determining the negative charge at hydrophobic interfaces. *Nat. Commun.* **2020**, *11*, 1–13, doi:10.1038/s41467-020-14659-5.
 204. Roger, K.; Cabane, B. Why are hydrophobic/water interfaces negatively charged? *Angew. Chemie - Int. Ed.* **2012**, *51*, 5625–5628, doi:10.1002/anie.201108228.
 205. Strubbe, F.; Beunis, F.; Marescaux, M.; Neyts, K. Charging mechanism in colloidal particles leading to a linear relation between charge and size. *Phys. Rev. E - Stat. Nonlinear, Soft Matter Phys.* **2007**, *75*, doi:10.1103/PhysRevE.75.031405.
 206. Mishra, H.; Enami, S.; Nielsen, R.J.; Stewart, L.A.; Hoffmann, M.R.; Goddard, W.A.; Colussi, A.J. Brønsted basicity of the air-water interface. *Proc. Natl. Acad. Sci. U. S. A.* **2012**, *109*, 18679–18683, doi:10.1073/pnas.1209307109.
 207. Creux, P.; Lachaise, J.; Graciaa, A.; Beattie, J.K.; Djerdjev, A.M. Strong specific hydroxide ion binding at the pristine oil/water and air/water interfaces. *J. Phys. Chem. B* **2009**, *113*, 14146–14150, doi:10.1021/jp906978v.
 208. Gray-Weale, A.; Beattie, J.K. An explanation for the charge on water's surface. *Phys. Chem. Chem. Phys.* **2009**, *11*, 10994–11005, doi:10.1039/b901806a.
 209. Wiacek, A.; Chibowski, E. Zeta potential, effective diameter and multimodal size distribution in oil/water emulsion. *Colloids Surfaces A Physicochem. Eng. Asp.* **1999**, *159*, 253–261, doi:10.1016/S0927-7757(99)00281-2.
 210. Sun, Q. The physical origin of hydrophobic effects. *Chem. Phys. Lett.* **2017**, *672*, 21–25, doi:10.1016/j.cplett.2017.01.057.
 211. Takahashi, M. ζ Potential of microbubbles in aqueous solutions: Electrical properties of the gas - Water interface. *J. Phys. Chem. B* **2005**, *109*, 21858–21864, doi:10.1021/jp0445270.
 212. Derkach, S.R. Rheology of emulsions. *Adv. Colloid Interface Sci.* **2009**, *151*, 1–23, doi:10.1016/j.cis.2009.07.001.
 213. Deshmukh, O.S.; van den Ende, D.; Stuart, M.C.; Mugele, F.; Duits, M.H.G. Hard and

- soft colloids at fluid interfaces: Adsorption, interactions, assembly & rheology. *Adv. Colloid Interface Sci.* **2015**, *222*, 215–227, doi:10.1016/j.cis.2014.09.003.
214. Mendoza, A.J.; Guzmán, E.; Martínez-Pedrero, F.; Ritacco, H.; Rubio, R.G.; Ortega, F.; Starov, V.M.; Miller, R. Particle laden fluid interfaces: Dynamics and interfacial rheology. *Adv. Colloid Interface Sci.* **2014**, *206*, 303–319, doi:10.1016/j.cis.2013.10.010.
 215. Wang, B.; Tian, H.; Xiang, D. Stabilizing the Oil-in-Water Emulsions Using the Mixtures of Dendrobium Officinale Polysaccharides and Gum Arabic or Propylene Glycol Alginate. *Molecules* **2020**, *25*, 759, doi:10.3390/molecules25030759.
 216. Liu, S.; Wang, Q.; Ma, H.; Huang, P.; Li, J.; Kikuchi, T. Effect of micro-bubbles on coagulation flotation process of dyeing wastewater. *Sep. Purif. Technol.* **2010**, *71*, 337–346, doi:10.1016/j.seppur.2009.12.021.
 217. Biriukov, D.; Fibich, P.; Pr, M. Zeta Potential Determination from Molecular Simulations. **2020**, doi:10.1021/acs.jpcc.9b11371.
 218. Jesionowski, T. Influence of aminosilane surface modification and dyes adsorption on zeta potential of spherical silica particles formed in emulsion system. *Colloids Surfaces A Physicochem. Eng. Asp.* **2003**, *222*, 87–94, doi:10.1016/S0927-7757(03)00237-1.
 219. Ghernaout, D.; Al-ghonamy, A.I.; Naceur, M.W.; Boucherit, A.; Messaoudene, N.A.; Aichouni, M.; Mahjoubi, A.A.; Elboughdiri, N.A. Controlling Coagulation Process: From Zeta Potential to Streaming Potential. *Am. J. Environ. Prot.* **2015**, *4*, 16, doi:10.11648/j.ajeps.s.2015040501.12.
 220. Liang, Y.; Hilal, N.; Langston, P.; Starov, V. Interaction forces between colloidal particles in liquid: Theory and experiment. *Adv. Colloid Interface Sci.* **2007**, *134–135*, 151–166, doi:10.1016/j.cis.2007.04.003.
 221. Pate, K.; Safier, P. Chemical metrology methods for CMP quality. In *Advances in Chemical Mechanical Planarization (CMP)*; Elsevier, 2016; pp. 299–325 ISBN 9780081001653.
 222. Jesionowski, T.; Nowacka, M.; Ciesielczyk, F. Electrokinetic properties of hybrid pigments obtained via adsorption of organic dyes on the silica support. *Pigment Resin Technol.* **2012**, *41*, 9–19, doi:10.1108/03699421211192235.
 223. Bouyer, E.; Mekhloufi, G.; Potier, I. Le; Kerdaniel, T. du F. de; Grossiord, J.L.; Rosilio, V.; Agnely, F. Stabilization mechanism of oil-in-water emulsions by β -lactoglobulin and gum arabic. *J. Colloid Interface Sci.* **2011**, *354*, 467–477, doi:10.1016/j.jcis.2010.11.019.
 224. DeNigris, J. Top 7 reasons to consider Zeta potential for coagulant dose control Available online: <https://www.materials-talks.com/blog/2020/08/27/top-7-reasons-to-consider-zeta-potential-for-coagulant-dose-control/>.
 225. Wiacek, A.E. Effect of ionic strength on electrokinetic properties of oil/water emulsions with dipalmitoylphosphatidylcholine. *Colloids Surfaces A Physicochem. Eng. Asp.* **2007**, *302*, 141–149, doi:10.1016/j.colsurfa.2007.02.029.
 226. Fingas, M.; Fieldhouse, B.; Bobra, M.A.; Tennyson, E. The physics and chemistry of emulsions. *Work. Emuls.* **1993**, 770.

227. Matter, F.; Luna, A.L.; Niederberger, M. From colloidal dispersions to aerogels: How to master nanoparticle gelation. *Nano Today* **2020**, *30*, 100827, doi:10.1016/j.nantod.2019.100827.
228. Tcholakova, S.; Denkov, N.D.; Ivanov, I.B.; Campbell, B. Coalescence stability of emulsions containing globular milk proteins. *Adv. Colloid Interface Sci.* **2006**, *123–126*, 259–293, doi:10.1016/j.cis.2006.05.021.
229. Calgaroto, S.; Wilberg, K.Q.; Rubio, J. On the nanobubbles interfacial properties and future applications in flotation. *Miner. Eng.* **2014**, *60*, 33–40, doi:10.1016/j.mineng.2014.02.002.
230. Eom, N.; Parsons, D.F.; Craig, V.S.J. Roughness in Surface Force Measurements: Extension of DLVO Theory to Describe the Forces between Hafnia Surfaces. *J. Phys. Chem. B* **2017**, *121*, 6442–6453, doi:10.1021/acs.jpcc.7b03131.
231. Calgaroto, S.; Azevedo, A.; Rubio, J. Flotation of quartz particles assisted by nanobubbles. *Int. J. Miner. Process.* **2015**, *137*, 64–70, doi:10.1016/j.minpro.2015.02.010.
232. Tcholakova, S.; Denkov, N.D.; Lips, A. Comparison of solid particles, globular proteins and surfactants as emulsifiers. *Phys. Chem. Chem. Phys.* **2008**, *10*, 1608, doi:10.1039/b715933c.
233. Jarvis, P.; Sharp, E.; Pidou, M.; Molinder, R.; Parsons, S.A.; Jefferson, B. Comparison of coagulation performance and floc properties using a novel zirconium coagulant against traditional ferric and alum coagulants. *Water Res.* **2012**, *46*, 4179–4187, doi:10.1016/j.watres.2012.04.043.
234. Jarvis, P.; Jefferson, B.; Parsons, S.A. Floc structural characteristics using conventional coagulation for a high doc, low alkalinity surface water source. *Water Res.* **2006**, *40*, 2727–2737, doi:10.1016/j.watres.2006.04.024.
235. Jarvis, P.; Jefferson, B.; Parsons, S.A. How the natural organic matter to coagulant ratio impacts on floc structural properties. *Environ. Sci. Technol.* **2005**, *39*, 8919–8924, doi:10.1021/es0510616.
236. Ghernaout, D.; Ghernaout, B.; Kellil, A. Natural organic matter removal and enhanced coagulation as a link between coagulation and electrocoagulation. *Desalin. Water Treat.* **2009**, *2*, 203–222, doi:10.5004/dwt.2009.116.
237. Lee, C.S.; Robinson, J.; Chong, M.F. A review on application of flocculants in wastewater treatment. *Process Saf. Environ. Prot.* **2014**, *92*, 489–508, doi:10.1016/j.psep.2014.04.010.
238. Ives, K.J. Coagulation and flocculation: Part II—Orthokinetic flocculation. In *Solid-Liquid Separation*; Elsevier, 2001; pp. 130–165.
239. McClements, D.J. Critical review of techniques and methodologies for characterization of emulsion stability. *Crit. Rev. Food Sci. Nutr.* **2007**, *47*, 611–649, doi:10.1080/10408390701289292.
240. Chesters, A.K. Modelling of coalescence processes in fluid-liquid dispersions. A review of current understanding. *Chem. Eng. Res. Des.* **1991**, *69*, 259–227.
241. Marina, P.F.; Cheng, C.; Sedev, R.; Stocco, A.; Binks, B.P.; Wang, D. Van der Waals

- Emulsions: Emulsions Stabilized by Surface-Inactive, Hydrophilic Particles via van der Waals Attraction. *Angew. Chemie - Int. Ed.* **2018**, *57*, 9510–9514, doi:10.1002/anie.201805410.
242. Bishop, K.J.M.; Wilmer, C.E.; Soh, S.; Grzybowski, B.A. Nanoscale forces and their uses in self-assembly. *Small* **2009**, *5*, 1600–1630, doi:10.1002/smll.200900358.
243. Wall, S. The history of electrokinetic phenomena. *Curr. Opin. Colloid Interface Sci.* **2010**, *15*, 119–124, doi:10.1016/j.cocis.2009.12.005.
244. Ichikawa, T. Electrical demulsification of oil-in-water emulsion. *Colloids Surfaces A Physicochem. Eng. Asp.* **2007**, *302*, 581–586, doi:10.1016/j.colsurfa.2007.03.036.
245. Ghernaout, D.; Naceur, M.W.; Ghernaout, B. A review of electrocoagulation as a promising coagulation process for improved organic and inorganic matters removal by electrophoresis and electroflotation. *Desalin. Water Treat.* **2011**, *28*, 287–320, doi:10.5004/dwt.2011.1493.
246. Dagastine, R.R.; Chau, T.T.; Chan, D.Y.C.; Stevens, G.W.; Grieser, F. Interaction forces between oil-water particle interfaces - Non-DLVO forces. *Faraday Discuss.* **2005**, *129*, 111–124, doi:10.1039/b405750c.
247. Rabinovich, Y.I.; Baran, A.A. The role of structural forces in the stability of oil-in-water emulsions. *Colloids and Surfaces* **1991**, *59*, 47–57, doi:10.1016/0166-6622(91)80236-H.
248. Smith, A.M.; Borkovec, M.; Trefalt, G. Forces between solid surfaces in aqueous electrolyte solutions. *Adv. Colloid Interface Sci.* **2020**, *275*, 102078, doi:10.1016/j.cis.2019.102078.
249. Ninham, B.W. On progress in forces since the. *Adv. Colloid Interface Sci.* **1999**, *83*, 1–17.
250. Marenduzzo, D.; Finan, K.; Cook, P.R. The depletion attraction: An underappreciated force driving cellular organization. *J. Cell Biol.* **2006**, *175*, 681–686, doi:10.1083/jcb.200609066.
251. Sun, Q.; Zhang, M.; Cui, S. The structural origin of hydration repulsive force. *Chem. Phys. Lett.* **2019**, *714*, 30–36, doi:10.1016/j.cplett.2018.10.066.
252. Meyer, E.E.; Rosenberg, K.J.; Israelachvili, J. Recent progress in understanding hydrophobic interactions. *Proc. Natl. Acad. Sci. U. S. A.* **2006**, *103*, 15739–15746, doi:10.1073/pnas.0606422103.
253. Vogelmann, E.S.; Reichert, J.M.; Prevedello, J.; Awe, G.O. Hydro-physical processes and soil properties correlated with origin of soil hydrophobicity. *Ciência Rural* **2013**, *43*, 1582–1589, doi:10.1590/S0103-84782013005000107.
254. Choi, J.; Kim, G.; Choi, S.; Kim, K.H.; Han, Y.; Bradford, S.A.; Choi, S.Q.; Kim, H. Application of depletion attraction in mineral flotation: I. theory. *Minerals* **2018**, *8*, 1–15, doi:10.3390/min8100451.
255. Bolto, B.A. Soluble polymers in water purification. *Prog. Polym. Sci.* **1995**, *20*, 987–1041, doi:10.1016/0079-6700(95)00010-D.
256. Hogg, R. Bridging flocculation by polymers. *KONA Powder Part. J.* **2012**, *30*, 3–14,

- doi:10.14356/kona.2013005.
257. Luthy, R.G.; Selleck, R.E.; Galloway, T.R. Removal of emulsified oil with organic coagulants and dissolved air flotation. *J. Water Pollut. Control Fed.* **1978**, *50*, 331–346.
 258. Guzey, D.; McClements, D.J. Formation, stability and properties of multilayer emulsions for application in the food industry. *Adv. Colloid Interface Sci.* **2006**, *128–130*, 227–248, doi:10.1016/j.cis.2006.11.021.
 259. Lee, K.E.; Morad, N.; Teng, T.T.; Poh, B.T. Development, characterization and the application of hybrid materials in coagulation/flocculation of wastewater: A review. *Chem. Eng. J.* **2012**, *203*, 370–386, doi:10.1016/j.cej.2012.06.109.
 260. Dickinson, E. Flocculation of protein-stabilized oil-in-water emulsions. *Colloids Surfaces B Biointerfaces* **2010**, *81*, 130–140, doi:10.1016/j.colsurfb.2010.06.033.
 261. Juárez, J.A.; Whitby, C.P. Oil-in-water Pickering emulsion destabilisation at low particle concentrations. *J. Colloid Interface Sci.* **2012**, *368*, 319–325, doi:10.1016/j.jcis.2011.11.029.
 262. Binks, B.P. Particles as surfactants—similarities and differences. *Curr. Opin. Colloid Interface Sci.* **2002**, *7*, 21–41, doi:10.1016/S1359-0294(02)00008-0.
 263. Haase, M.F.; Grigoriev, D.; Moehwald, H.; Tiersch, B.; Shchukin, D.G. Nanoparticle modification by weak polyelectrolytes for pH-sensitive pickering emulsions. *Langmuir* **2011**, *27*, 74–82, doi:10.1021/la1027724.
 264. Low, L.E.; Siva, S.P.; Ho, Y.K.; Chan, E.S.; Tey, B.T. Recent advances of characterization techniques for the formation, physical properties and stability of Pickering emulsion. *Adv. Colloid Interface Sci.* **2020**, *277*, 102117, doi:10.1016/j.cis.2020.102117.
 265. Rayner, M.; Sjö, M.; Timgren, A.; Dejmek, P. Quinoa starch granules as stabilizing particles for production of Pickering emulsions. *Faraday Discuss.* **2012**, *158*, 139, doi:10.1039/c2fd20038d.
 266. Tan, J.; Wang, J.; Wang, L.; Xu, J.; Sun, D. In situ formed Mg(OH)₂ nanoparticles as pH-switchable stabilizers for emulsions. *J. Colloid Interface Sci.* **2011**, *359*, 155–162, doi:10.1016/j.jcis.2010.10.038.
 267. Jones, A.N. Vegetable Plants With Water Treatment Potential: a Review. **2019**, *15*, 109–123.
 268. Rubio, J.; Souza, M.; Smith, R.. Overview of flotation as a wastewater treatment technique. *Miner. Eng.* **2002**, *15*, 139–155, doi:10.1016/S0892-6875(01)00216-3.
 269. Bal, V. Coagulation behavior of spherical particles embedded in laminar shear flow in presence of DLVO-and non-DLVO forces. *J. Colloid Interface Sci.* **2020**, *564*, 170–181, doi:10.1016/j.jcis.2019.12.119.
 270. Ghernaout, D.; Ghernaout, B. Sweep flocculation as a second form of charge neutralisation-A review. *Desalin. Water Treat.* **2012**, *44*, 15–28, doi:10.1080/19443994.2012.691699.
 271. Jiang, J.Q. The role of coagulation in water treatment. *Curr. Opin. Chem. Eng.* **2015**, *8*, 36–44, doi:10.1016/j.coche.2015.01.008.

272. Polasek, P. Significance and determination of fraction of non-separable particles of impurities in water purification. *Water SA* **2014**, *40*, 89–94, doi:10.4314/wsa.v40i1.11.
273. Kulkarni, S.J. An Insight into Paint and Textile Effluent Treatment. *Int. J. Sci. Res. Chem.* **2017**, *2*, 9–12.
274. Sahu, O.; Chaudhari, P. Review on Chemical treatment of Industrial Waste Water. *J. Appl. Sci. Environ. Manag.* **2013**, *17*, doi:10.4314/jasem.v17i2.8.
275. Wang, C.; Alpatova, A.; McPhedran, K.N.; Gamal El-Din, M. Coagulation/flocculation process with polyaluminum chloride for the remediation of oil sands process-affected water: Performance and mechanism study. *J. Environ. Manage.* **2015**, *160*, 254–262, doi:10.1016/j.jenvman.2015.06.025.
276. Li, T.; Zhu, Z.; Wang, D.; Yao, C.; Tang, H. Characterization of floc size, strength and structure under various coagulation mechanisms. *Powder Technol.* **2006**, *168*, 104–110, doi:10.1016/j.powtec.2006.07.003.
277. El-Gohary, F.; Tawfik, A.; Mahmoud, U. Comparative study between chemical coagulation/precipitation (C/P) versus coagulation/dissolved air flotation (C/DAF) for pre-treatment of personal care products (PCPs) wastewater. *Desalination* **2010**, *252*, 106–112, doi:10.1016/j.desal.2009.10.016.
278. Marriaga-Cabrales, N.; Machuca-Martínez, F. Fundamentals of electrocoagulation. In *Evaluation of Electrochemical Reactors as a New Way to Environmental Protection*; Peralta-Hernández, J.M., Rodrigo-Rodrigo, M.A., Martínez-Huitle, C.A., Eds.; Research Signpost: Kerala, India, 2014; pp. 1–16 ISBN 978-81-308-0549-8.
279. Ghernaout, D. Enhanced Coagulation: Promising Findings and Challenges. *OALib* **2020**, *07*, 1–19, doi:10.4236/oalib.1106569.
280. Yeap, K.L.; Teng, T.T.; Poh, B.T.; Morad, N.; Lee, K.E. Preparation and characterization of coagulation/flocculation behavior of a novel inorganic-organic hybrid polymer for reactive and disperse dyes removal. *Chem. Eng. J.* **2014**, *243*, 305–314, doi:10.1016/j.cej.2014.01.004.
281. Ghernaout, D. Water Treatment Coagulation: Dares and Trends. *OALib* **2020**, *07*, 1–18, doi:10.4236/oalib.1106636.
282. Bache, D.H.; Johnson, C.; Papavasiliopoulos, E.; Rasool, E.; McGilligan, F.J. Sweep coagulation: Structures, mechanisms and practice. *J. Water Supply Res. Technol. - AQUA* **1999**, *48*, 201–210, doi:10.2166/aqua.1999.0022.
283. Ratnaweera, H. Meeting Tomorrow's Challenges in Particle Separation with Coagulation. *ACS Symp. Ser.* **2020**, *1348*, 207–223, doi:10.1021/bk-2020-1348.ch007.
284. Ng, M.; Liana, A.E.; Liu, S.; Lim, M.; Chow, C.W.K.; Wang, D.; Drikas, M.; Amal, R. Preparation and characterisation of new-polyaluminum chloride-chitosan composite coagulant. *Water Res.* **2012**, *46*, 4614–4620, doi:10.1016/j.watres.2012.06.021.
285. Jarvis, P.; Jefferson, B.; Gregory, J.; Parsons, S.A. A review of floc strength and breakage. *Water Res.* **2005**, *39*, 3121–3137, doi:10.1016/j.watres.2005.05.022.
286. Harif, T.; Khai, M.; Adin, A. Electrocoagulation versus chemical coagulation: Coagulation/flocculation mechanisms and resulting floc characteristics. *Water Res.* **2012**, *46*, 3177–3188, doi:10.1016/j.watres.2012.03.034.

287. Yuksel, E.; Gurbulak, E.; Eyvaz, M. Decolorization of a reactive dye solution and treatment of a textile wastewater by electrocoagulation and chemical coagulation: Techno-economic comparison. *Environ. Prog. Sustain. Energy* **2012**, *31*, 524–535, doi:10.1002/ep.10574.
288. Emamjomeh, M.M.; Sivakumar, M. Review of pollutants removed by electrocoagulation and electrocoagulation/flotation processes. *J. Environ. Manage.* **2009**, *90*, 1663–1679, doi:10.1016/j.jenvman.2008.12.011.
289. Cañizares, P.; Martínez, F.; Jiménez, C.; Sáez, C.; Rodrigo, M.A. Coagulation and electrocoagulation of oil-in-water emulsions. *J. Hazard. Mater.* **2008**, *151*, 44–51, doi:10.1016/j.jhazmat.2007.05.043.
290. Muruganandam, L.; Kumar, M.P.S.; Jena, A.; Gulla, S.; Godhwani, B. Treatment of waste water by coagulation and flocculation using biomaterials. *IOP Conf. Ser. Mater. Sci. Eng.* **2017**, *263*, doi:10.1088/1757-899X/263/3/032006.
291. Ghernaout, D. The hydrophilic/hydrophobic ratio vs. dissolved organics removal by coagulation - A review. *J. King Saud Univ. - Sci.* **2014**, *26*, 169–180, doi:10.1016/j.jksus.2013.09.005.
292. Mohammed, T.J.; Awad, E.S.; Ahmed, T.A. Oil Removal from Oilfield Produced Water , North Rumaila by Combination Coagulation- Flocculation and Microfiltration Technique. *Eng. Technol. J.* **2019**, *37*, 24–28, doi:10.30684/etj.37.2C.1.
293. Zhao, Y.X.; Gao, B.Y.; Zhang, G.Z.; Phuntsho, S.; Wang, Y.; Yue, Q.Y.; Li, Q.; Shon, H.K. Comparative study of floc characteristics with titanium tetrachloride against conventional coagulants: Effect of coagulant dose, solution pH, shear force and break-up period. *Chem. Eng. J.* **2013**, *233*, 70–79, doi:10.1016/j.cej.2013.08.017.
294. Sohrabi, Y.; Rahimi, S.; Nafez, A.H.; Mirzaei, N.; Bagheri, A.; Ghadiri, S.K.; Rezaei, S.; Charganeh, S.S. Chemical coagulation efficiency in removal of water turbidity. *Int. J. Pharm. Res.* **2018**, *10*, 188–194, doi:10.31838/ijpr/2018.10.03.071.
295. Peter, G. USING POLYALUMINIUM COAGULANTS IN WATER TREATMENT Paper Presented by : Peter Gebbie Peter Gebbie Fisher Stewart Pty Ltd USING POLYALUMINIUM COAGULANTS IN WATER. *64th Annu. Water Ind. Eng. Oper. Conf.* **2001**, 39–47.
296. Prabhakaran, G.; Manikandan, M.; Boopathi, M. Treatment of textile effluents by using natural coagulants. *Mater. Today Proc.* **2020**, *33*, 3000–3004, doi:10.1016/j.matpr.2020.03.029.
297. Spicer, P.T.; Sotiris, E.F. Coagulation and Fragmentation : Universal Steady-State Particle-Size Distribution. **1996**, *42*.
298. El Samrani, A.G.; Lartiges, B.S.; Montargès-Pelletier, E.; Kazpard, V.; Barrès, O.; Ghanbaja, J. Clarification of municipal sewage with ferric chloride: The nature of coagulant species. *Water Res.* **2004**, *38*, 756–768, doi:10.1016/j.watres.2003.10.002.
299. Jiang, J.Q. Development of coagulation theory and pre-polymerized coagulants for water treatment. *Sep. Purif. Methods* **2001**, *30*, 127–141, doi:10.1081/SPM-100102986.
300. Xu, P.; Zeng, G.M.; Huang, D.L.; Feng, C.L.; Hu, S.; Zhao, M.H.; Lai, C.; Wei, Z.; Huang, C.; Xie, G.X.; et al. Use of iron oxide nanomaterials in wastewater treatment: A review. *Sci. Total Environ.* **2012**, *424*, 1–10, doi:10.1016/j.scitotenv.2012.02.023.

301. Teh, C.Y.; Budiman, P.M.; Shak, K.P.Y.; Wu, T.Y. Recent Advancement of Coagulation–Flocculation and Its Application in Wastewater Treatment. *Ind. Eng. Chem. Res.* **2016**, *55*, 4363–4389, doi:10.1021/acs.iecr.5b04703.
302. Othman, M.N.; Abdullah, M.P.; Aziz, Y.F.A. Removal of aluminium from drinking water. *Sains Malaysiana* **2010**, *39*, 51–55.
303. Zini, L.P.; Longhi, M.; Jonko, E.; Giovanela, M. Treatment of automotive industry wastewater by electrocoagulation using commercial aluminum electrodes. *Process Saf. Environ. Prot.* **2020**, *142*, 272–284, doi:10.1016/j.psep.2020.06.029.
304. Greville, A.S. How to Select a Chemical Coagulant and Flocculant. *Albert Water Wastewater Oper. Assoc.* **1997**, *22th Annua*, 24.
305. Trinh, T.K.; Kang, L.S. Coagulation of phosphorus: effects of Al(III) species (Ala, Alb, and Alc). *Desalin. Water Treat.* **2015**, *53*, 485–492, doi:10.1080/19443994.2013.841106.
306. Yu, W.; Gregory, J.; Campos, L.C.; Graham, N. Dependence of floc properties on coagulant type, dosing mode and nature of particles. *Water Res.* **2015**, *68*, 119–126, doi:10.1016/j.watres.2014.09.045.
307. Al-Shamrani, A.A.; James, A.; Xiao, H. Destabilisation of oil-water emulsions and separation by dissolved air flotation. *Water Res.* **2002**, *36*, 1503–1512, doi:10.1016/S0043-1354(01)00347-5.
308. Ghernaout, D.; Elboughdiri, N. Electrochemical Technology for Wastewater Treatment: Dares and Trends. *OALib* **2020**, *07*, 1–17, doi:10.4236/oalib.1106020.
309. Bazrafshan, E.; Mohammadi, L.; Ansari-Moghaddam, A.; Mahvi, A.H. Heavy metals removal from aqueous environments by electrocoagulation process - A systematic review. *J. Environ. Heal. Sci. Eng.* **2015**, *13*, doi:10.1186/s40201-015-0233-8.
310. Dalvand, A.; Gholami, M.; Joneidi, A.; Mahmoodi, N.M. Dye Removal, Energy Consumption and Operating Cost of Electrocoagulation of Textile Wastewater as a Clean Process. *Clean - Soil, Air, Water* **2011**, *39*, 665–672, doi:10.1002/clen.201000233.
311. Moussa, D.T.; El-Naas, M.H.; Nasser, M.; Al-Marri, M.J. A comprehensive review of electrocoagulation for water treatment: Potentials and challenges. *J. Environ. Manage.* **2016**, *186*, 24–41, doi:10.1016/j.jenvman.2016.10.032.
312. Khandegar, V.; Saroha, A.K. Electrocoagulation for the treatment of textile industry effluent - A review. *J. Environ. Manage.* **2013**, *128*, 949–963, doi:10.1016/j.jenvman.2013.06.043.
313. Dohare, D.E.; Sisodia, T. Applications of Electrocoagulation in treatment of Industrial Wastewater : A Review. *Int. J. Eng. Sci. Res. Technol.* **2014**, *3*, 379–386.
314. Fukushima, J.; Tatsuta, H.; Ishii, N.; Chen, J.; Nishiumi, T.; Aoki, K. Possibility of coalescence of water droplets in W/O emulsions by means of surface processes. *Colloids Surfaces A Physicochem. Eng. Asp.* **2009**, *333*, 53–58, doi:10.1016/j.colsurfa.2008.09.023.
315. Kuokkanen, V.; Kuokkanen, T.; Rämö, J.; Lassi, U. Recent Applications of Electrocoagulation in Treatment of Water and Wastewater—A Review. *Green Sustain.*

- Chem.* **2013**, *03*, 89–121, doi:10.4236/gsc.2013.32013.
316. Shokri, A.; Fard, M.S. A critical review in electrocoagulation technology applied for oil removal in industrial wastewater. *Chemosphere* **2022**, *288*, 132355, doi:10.1016/j.chemosphere.2021.132355.
317. Saeedi, M.; Khalvati-Fahlyani, A. Treatment of Oily Wastewater of a Gas Refinery by Electrocoagulation Using Aluminum Electrodes. *Water Environ. Res.* **2011**, *83*, 256–264, doi:10.2175/106143010x12780288628499.
318. Ascón, E.A.A. Elimination of chemical oxygen demand from domestic residual water by electrocoagulation with aluminum and iron electrodes. *Ambient. e Agua - An Interdiscip. J. Appl. Sci.* **2018**, *13*, 1, doi:10.4136/ambi-agua.2240.
319. Mouedhen, G.; Feki, M.; Wery, M.D.P.; Ayedi, H.F. Behavior of aluminum electrodes in electrocoagulation process. *J. Hazard. Mater.* **2008**, *150*, 124–135, doi:10.1016/j.jhazmat.2007.04.090.
320. Eow, J. Electrostatic enhancement of coalescence of water droplets in oil: a review of the technology. *Chem. Eng. J.* **2002**, *85*, 357–368, doi:10.1016/S1385-8947(01)00250-9.
321. Mhatre, S.; Vivacqua, V.; Ghadiri, M.; Abdullah, A.M.; Al-Marri, M.J.; Hassanpour, A.; Hewakandamby, B.; Azzopardi, B.; Kermani, B. Electrostatic phase separation: A review. *Chem. Eng. Res. Des.* **2015**, *96*, 177–195, doi:10.1016/j.cherd.2015.02.012.
322. Eow, J.S.; Ghadiri, M.; Sharif, A.O.; Williams, T.J. Electrostatic enhancement of coalescence of water droplets in oil: a review of the current understanding. *Chem. Eng. J.* **2001**, *84*, 173–192, doi:10.1016/S1385-8947(00)00386-7.
323. Mohamad, Z.; Razak, A.A.; Krishnan, S.; Singh, L.; Zularisam, A.W.; Nasrullah, M. Treatment of palm oil mill effluent using electrocoagulation powered by direct photovoltaic solar system. *Chem. Eng. Res. Des.* **2022**, *177*, 578–582, doi:10.1016/j.cherd.2021.11.019.
324. Bałdyga, J.; Tyl, G.; Bouaifi, M. Perikinetic and orthokinetic aggregation of small solid particles in the presence of strong repulsive forces. *Chem. Eng. Res. Des.* **2018**, *136*, 491–501, doi:10.1016/j.cherd.2018.06.021.
325. Chen, L.A.; Serad, G.A.; Carbonell, R.G. Effect of mixing conditions on flocculation kinetics of wastewaters containing proteins and other biological compounds using fibrous materials and polyelectrolytes. *Brazilian J. Chem. Eng.* **1998**, *15*, 358–368, doi:10.1590/S0104-66321998000400005.
326. Kroupa, M.; Vonka, M.; Soos, M.; Kosek, J. Size and Structure of Clusters Formed by Shear Induced Coagulation: Modeling by Discrete Element Method. *Langmuir* **2015**, *31*, 7727–7737, doi:10.1021/acs.langmuir.5b01046.
327. Ghernaout, D. Brownian Motion and Coagulation Process. *Am. J. Environ. Prot.* **2015**, *4*, 1, doi:10.11648/j.ajeps.s.2015040501.11.
328. Jarvis, P.; Jefferson, B.; Parsons, S.A. Measuring floc structural characteristics. *Rev. Environ. Sci. Biotechnol.* **2005**, *4*, 1–18, doi:10.1007/s11157-005-7092-1.
329. Tzoupanos, N.D.; Zouboulis, A.I. Coagulation-Flocculation Processes in Water / Wastewater Treatment: the Application of New Generation of Chemical Reagents. In

- Proceedings of the 6th IASME/WSEAS International Conference on HEAT TRANSFER, THERMAL ENGINEERING and ENVIRONMENT; 2008; pp. 309–317.
330. Chakinala, A.G.; Gogate, P.R.; Burgess, A.E.; Bremner, D.H. Treatment of industrial wastewater effluents using hydrodynamic cavitation and the advanced Fenton process. *Ultrason. Sonochem.* **2008**, *15*, 49–54, doi:10.1016/j.ultsonch.2007.01.003.
 331. Thanekar, P.; Gogate, P. Application of hydrodynamic cavitation reactors for treatment of wastewater containing organic pollutants: Intensification using hybrid approaches. *Fluids* **2018**, *3*, doi:10.3390/fluids3040098.
 332. Hai, F.I.; Yamamoto, K.; Fukushi, K. Hybrid treatment systems for dye wastewater. *Crit. Rev. Environ. Sci. Technol.* **2007**, *37*, 315–377, doi:10.1080/10643380601174723.
 333. Mohammed, T.; Abbas, E.; Ahmed, T. Turbidity and oil removal from oilfield produced water, middle oil company by electrocoagulation technique. *MATEC Web Conf.* **2018**, *162*, 56–62, doi:10.1051/mateconf/201816205010.
 334. Adlan, M.N.; Palaniandy, P.; Aziz, H.A. Optimization of coagulation and dissolved air flotation (DAF) treatment of semi-aerobic landfill leachate using response surface methodology (RSM). *Desalination* **2011**, *277*, 74–82, doi:10.1016/j.desal.2011.04.006.
 335. Rajak, V.K.; Relish, K.K.; Kumar, S.; Mandal, A. Mechanism and Kinetics of Separation of Oil from Oil-in-Water Emulsion by Air Flotation. *Pet. Sci. Technol.* **2015**, *33*, 1861–1868, doi:10.1080/10916466.2015.1108987.
 336. Moosai, R.; Dawe, R.A. Oily wastewater cleanup by gas flotation. *West Indian J. Eng.* **2002**, *25*, 25–41.
 337. Kweiner Tetteh, E.; Rathilal, S. Evaluation of the coagulation floatation process for industrial mineral oil wastewater treatment using response surface methodology (rsm). *Int. J. Environ. Impacts Manag. Mitig. Recover.* **2018**, *1*, 491–502, doi:10.2495/ei-v1-n4-491-502.
 338. Miettinen, T.; Ralston, J.; Fornasiero, D. The limits of fine particle flotation. *Miner. Eng.* **2010**, *23*, 420–437, doi:10.1016/j.mineng.2009.12.006.
 339. Honaker, R.Q.; Ozsever, A. V.; Parekh, B.K. Selective detachment process in column flotation froth. *Miner. Eng.* **2006**, *19*, 687–695, doi:10.1016/j.mineng.2005.09.019.
 340. Moosai, R.; Dawe, R.A. Gas attachment of oil droplets for gas flotation for oily wastewater cleanup. *Sep. Purif. Technol.* **2003**, *33*, 303–314, doi:10.1016/S1383-5866(03)00091-1.
 341. Santander, M.; Rodrigues, R.T.; Rubio, J. Modified jet flotation in oil (petroleum) emulsion/water separations. *Colloids Surfaces A Physicochem. Eng. Asp.* **2011**, *375*, 237–244, doi:10.1016/j.colsurfa.2010.12.027.
 342. Tabor, R.F.; Grieser, F.; Dagastine, R.R.; Chan, D.Y.C. Measurement and analysis of forces in bubble and droplet systems using AFM. *J. Colloid Interface Sci.* **2012**, *371*, 1–14, doi:10.1016/j.jcis.2011.12.047.
 343. Edzwald, J.K. Dissolved air flotation and me. *Water Res.* **2010**, *44*, 2077–2106, doi:10.1016/j.watres.2009.12.040.
 344. Phan, C.M.; Nguyen, A. V.; Miller, J.D.; Evans, G.M.; Jameson, G.J. Investigations of

- bubble-particle interactions. *Int. J. Miner. Process.* **2003**, *72*, 239–254, doi:10.1016/S0301-7516(03)00102-9.
345. Wang, L.; Peng, Y.; Runge, K.; Bradshaw, D. A review of entrainment: Mechanisms, contributing factors and modelling in flotation. *Miner. Eng.* **2015**, *70*, 77–91, doi:10.1016/j.mineng.2014.09.003.
346. Park, H.; Wang, L. Experimental studies and modeling of surface bubble behaviour in froth flotation. *Chem. Eng. Res. Des.* **2015**, *101*, 98–106, doi:10.1016/j.cherd.2015.04.021.
347. Al-Maghrabi, M.-N. Modeling the Recovery of Froth Flotation Using Game Theory. *J. Min. World Express* **2016**, *5*, 1, doi:10.14355/mwe.2016.05.001.
348. Grattoni, C.; Moosai, R.; Dawe, R.A. Photographic observations showing spreading and non-spreading of oil on gas bubbles of relevance to gas flotation for oily wastewater cleanup. *Colloids Surfaces A Physicochem. Eng. Asp.* **2003**, *214*, 151–155, doi:10.1016/S0927-7757(02)00385-0.
349. Temesgen, T.; Bui, T.T.; Han, M.; Kim, T. il; Park, H. Micro and nanobubble technologies as a new horizon for water-treatment techniques: A review. *Adv. Colloid Interface Sci.* **2017**, *246*, 40–51, doi:10.1016/j.cis.2017.06.011.
350. Bolto, B.; Gregory, J. Organic polyelectrolytes in water treatment. *Water Res.* **2007**, *41*, 2301–2324, doi:10.1016/j.watres.2007.03.012.
351. Bhargava, A. Activated Sludge Treatment Process - Concept and System Design. *Int. J. Eng. Dev. Res.* **2016**, *4*, 890–896.
352. Ramaswamy, B.; Kar, D.D.; De, S. A study on recovery of oil from sludge containing oil using froth flotation. *J. Environ. Manage.* **2007**, *85*, 150–154, doi:10.1016/j.jenvman.2006.08.009.
353. Al-Shamrani, A.A.; James, A.; Xiao, H. Separation of oil from water by dissolved air flotation. *Colloids Surfaces A Physicochem. Eng. Asp.* **2002**, *209*, 15–26, doi:10.1016/S0927-7757(02)00208-X.
354. FAN, M.; TAO, D.; HONAKER, R.; LUO, Z. Nanobubble generation and its applications in froth flotation (part II): fundamental study and theoretical analysis. *Min. Sci. Technol.* **2010**, *20*, 159–177, doi:10.1016/S1674-5264(09)60179-4.
355. Melo, F.; Laskowski, J.S. Fundamental properties of flotation frothers and their effect on flotation. *Miner. Eng.* **2006**, *19*, 766–773, doi:10.1016/j.mineng.2005.09.031.
356. Gorain, B.K.; Franzidis, J.P.; Manlapig, E.V. FLOTATION | Flotation Cell Design: Application of Fundamental Principles. *Encycl. Sep. Sci.* **2000**, 1502–1512, doi:10.1016/b0-12-226770-2/05781-1.
357. Mesa, D.; Brito-Parada, P.R. Scale-up in froth flotation: A state-of-the-art review. *Sep. Purif. Technol.* **2019**, *210*, 950–962, doi:10.1016/j.seppur.2018.08.076.
358. Kyzas, G.Z.; Matis, K.A. The flotation process can go green. *Processes* **2019**, *7*, 1–14, doi:10.3390/pr7030138.
359. Azevedo, A.; Oliveira, H.; Rubio, J. Bulk nanobubbles in the mineral and environmental areas: Updating research and applications. *Adv. Colloid Interface Sci.* **2019**, *271*,

- 101992, doi:10.1016/j.cis.2019.101992.
360. Qi, W.K.; Yu, Z.C.; Liu, Y.Y.; Li, Y.Y. Removal of emulsion oil from oilfield ASP wastewater by internal circulation flotation and kinetic models. *Chem. Eng. Sci.* **2013**, *91*, 122–129, doi:10.1016/j.ces.2013.01.020.
361. Tao, X.; Liu, Y.; Jiang, H.; Chen, R. Microbubble generation with shear flow on large-area membrane for fine particle flotation. *Chem. Eng. Process. - Process Intensif.* **2019**, *145*, 107671, doi:10.1016/j.cep.2019.107671.
362. Sylvester, N.D.; Byeseda, J.J. Oil/Water Separation by Induced-Air Flotation. *Soc. Pet. Eng. J.* **1980**, *20*, 579–590, doi:10.2118/7886-PA.
363. Eskinlou, A.; Chegeni, M.H.; Khalesi, M.R.; Abdollahy, M.; Huang, Q. Modeling the bubble loading based on force balance on the particles attached to the bubble. *Colloids Surfaces A Physicochem. Eng. Asp.* **2019**, *582*, doi:10.1016/j.colsurfa.2019.123892.
364. Al-Dulaimi, S.L.; Al-Yaqoobi, A.M. Separation of oil/water emulsions by microbubble air flotation. *IOP Conf. Ser. Mater. Sci. Eng.* **2021**, *1076*, 012030, doi:10.1088/1757-899x/1076/1/012030.
365. Poh, P.E.; Ong, W.Y.J.; Lau, E. V.; Chong, M.N. Investigation on micro-bubble flotation and coagulation for the treatment of anaerobically treated palm oil mill effluent (POME). *J. Environ. Chem. Eng.* **2014**, *2*, 1174–1181, doi:10.1016/j.jece.2014.04.018.
366. Kyzas, G.Z.; Matis, K.A. Flotation of biological materials. *Processes* **2014**, *2*, 293–310, doi:10.3390/pr2010293.
367. Wang, H.; Yang, W.; Yan, X.; Wang, L.; Wang, Y.; Zhang, H. Regulation of bubble size in flotation: A review. *J. Environ. Chem. Eng.* **2020**, *8*, 104070, doi:10.1016/j.jece.2020.104070.
368. Nasset, J.E.; Hernandez-Aguilar, J.R.; Acuna, C.; Gomez, C.O.; Finch, J.A. Some gas dispersion characteristics of mechanical flotation machines. *Miner. Eng.* **2006**, *19*, 807–815, doi:10.1016/j.mineng.2005.09.045.
369. Finch, J.A.; Nasset, J.E.; Acuña, C. Role of frother on bubble production and behaviour in flotation. *Miner. Eng.* **2008**, *21*, 949–957.
370. Elmahdy, A.M.; Finch, J.A. Effect of frother blends on hydrodynamic properties. *Int. J. Miner. Process.* **2013**, *123*, 60–63, doi:10.1016/j.minpro.2013.04.019.
371. Shahbazi, B. Effect of Frother on Bubble-Particle Collision Probability of Fine Particles. *Am. J. Chem. Eng.* **2015**, *3*, 1, doi:10.11648/j.ajche.s.2015030202.11.
372. Ata, S.; Ng, K.Y.; Law, E.; Lim, M. Influence of particles on the formation of bubbles from a submerged capillary. *Miner. Eng.* **2014**, *66*, 47–53, doi:10.1016/j.mineng.2014.03.018.
373. Boylu, F.; Laskowski, J.S. Rate of water transfer to flotation froth in the flotation of low-rank coal that also requires the use of oily collector. *Int. J. Miner. Process.* **2007**, *83*, 125–131, doi:10.1016/j.minpro.2007.07.003.
374. Xu, Q.; Nakajima, M.; Ichikawa, S.; Nakamura, N.; Shiina, T. A comparative study of microbubble generation by mechanical agitation and sonication. *Innov. Food Sci. Emerg. Technol.* **2008**, *9*, 489–494, doi:10.1016/j.ifset.2008.03.003.

375. Eskanlou, A.; Khalesi, M.R.; Abdollahy, M.; Chegeni, M.H. Interactional effects of bubble size, particle size, and collector dosage on bubble loading in column flotation. *J. Min. Environ.* **2017**, *9*, 107–116, doi:10.22044/jme.2017.5815.1393.
376. BRATBY, J.; MARAIS, G.V.R. Dissolved Air Flotation. **1973**.
377. Palaniandy, P.; Adlan, H.; Aziz, H.; Murshed, M.; Hung, Y. *Dissolved Air Flotation (DAF) for Wastewater Treatment*; 2017; ISBN 9781315164199.
378. Yang, X.S.; Aldrich, C. Effects of impeller speed and aeration rate on flotation performance of sulphide ore. *Trans. Nonferrous Met. Soc. China (English Ed.)* **2006**, *16*, 185–190, doi:10.1016/S1003-6326(06)60033-2.
379. Ross, C.C.; Smith, B.M.; Valentine, G.E. Rethinking Dissolved Air Flotation (Daf) Design for Industrial Pretreatment. *Proc. Water Environ. Fed.* **2011**, *2000*, 43–56, doi:10.2175/193864700785155795.
380. Eskin, A.A.; Zakharov, G.A.; Tkach, N.S.; Tsygankova, K.V. Intensification dissolved air flotation treatment of oil-containing wastewater. *Mod. Appl. Sci.* **2015**, *9*, 114–124, doi:10.5539/mas.v9n5p114.
381. Ghernaout, D. The Best Available Technology of Water/Wastewater Treatment and Seawater Desalination: Simulation of the Open Sky Seawater Distillation. *Green Sustain. Chem.* **2013**, *03*, 68–88, doi:10.4236/gsc.2013.32012.
382. Woodard & Curran, I. Methods for Treating Wastewaters from Industry. In *Industrial Waste Treatment Handbook*; Elsevier, 2006; pp. 149–334.
383. Rajapakse, N.; Zargar, M.; Sen, T.; Khiadani, M. Effects of influent physicochemical characteristics on air dissolution, bubble size and rise velocity in dissolved air flotation: A review. *Sep. Purif. Technol.* **2022**, *289*, 120772, doi:10.1016/j.seppur.2022.120772.
384. Jávora, Z.; Schreithofer, N.; Heiskanen, K. Multi-scale analysis of the effect of surfactants on bubble properties. *Miner. Eng.* **2016**, *99*, 170–178, doi:10.1016/j.mineng.2016.09.026.
385. Subrahmanyam, T. V.; Forssberg, K.S.E. Fine particles processing: shear-flocculation and carrier flotation - a review. *Int. J. Miner. Process.* **1990**, *30*, 265–286, doi:10.1016/0301-7516(90)90019-U.
386. Li, P.; Tsuge, H. Water Treatment by Induced Air Flotation Using Microbubbles. *J. Chem. Eng. Japan* **2006**, *39*, 896–903, doi:10.1252/jcej.39.896.
387. Behin, J.; Bahrami, S. Modeling an industrial dissolved air flotation tank used for separating oil from wastewater. *Chem. Eng. Process. Process Intensif.* **2012**, *59*, 1–8, doi:10.1016/j.cep.2012.05.004.
388. Kyzas, G.Z.; Matis, K.A. Electroflotation process: A review. *J. Mol. Liq.* **2016**, *220*, 657–664, doi:10.1016/j.molliq.2016.04.128.
389. Sarkar, M.S.K.A.; Evans, G.M.; Donne, S.W. Bubble size measurement in electroflotation. *Miner. Eng.* **2010**, *23*, 1058–1065, doi:10.1016/j.mineng.2010.08.015.
390. Essadki, A.H.; Bennajah, M.; Gourich, B.; Vial, C.; Azzi, M.; Delmas, H. Electrocoagulation/electroflotation in an external-loop airlift reactor-Application to the decolorization of textile dye wastewater: A case study. *Chem. Eng. Process. Process*

- Intensif.* **2008**, *47*, 1211–1223, doi:10.1016/j.cep.2007.03.013.
391. Hosny, A.Y. Separating oil from oil-water emulsions by electroflotation technique. *Sep. Technol.* **1996**, *6*, 9–17, doi:10.1016/0956-9618(95)00136-0.
392. Belkacem, M.; Khodir, M.; Abdelkrim, S. Treatment characteristics of textile wastewater and removal of heavy metals using the electroflotation technique. *Desalination* **2008**, *228*, 245–254, doi:10.1016/j.desal.2007.10.013.
393. Ozkan, A.; Uslu, Z.; Duzyol, S.; Ucbeyiay, H. Correlation of shear flocculation of some salt-type minerals with their wettability parameter. *Chem. Eng. Process. Process Intensif.* **2007**, *46*, 1341–1348, doi:10.1016/j.cep.2006.10.018.
394. Chin, C.J.; Yiacoumi, S.; Tsouris, C. Shear-induced flocculation of colloidal particles in stirred tanks. *J. Colloid Interface Sci.* **1998**, *206*, 532–545, doi:10.1006/jcis.1998.5737.
395. Oyegbile, B.; Ay, P.; Narra, S. Flocculation kinetics and hydrodynamic interactions in natural and engineered flow systems: A review. *Environ. Eng. Res.* **2016**, *21*, 1–14, doi:10.4491/eer.2015.086.
396. Gui, X.; Liu, J.; Cao, Y.; Cheng, G.; Li, S.; Wu, L. Flotation process design based on energy input and distribution. *Fuel Process. Technol.* **2014**, *120*, 61–70, doi:10.1016/j.fuproc.2013.12.011.
397. Yin, W.Z.; Yang, X.S.; Zhou, D.P.; Li, Y.J.; Lü, Z.F. Shear hydrophobic flocculation and flotation of ultrafine Anshan hematite using sodium oleate. *Trans. Nonferrous Met. Soc. China (English Ed.)* **2011**, *21*, 652–664, doi:10.1016/S1003-6326(11)60762-0.
398. Roland, C.M.; Boehm, G.G.A. Shear-Induced Coalescence in Two-Phase Polymeric Systems. I. Determination From Small-Angle Neutron Scattering Measurements. *J. Polym. Sci. Part A-2, Polym. Phys.* **1984**, *22*, 79–93, doi:10.1002/pol.1984.180220108.
399. Doran, P.M. Fluid Flow. In *Bioprocess Engineering Principles*; Elsevier, 2013; pp. 201–254.
400. Zhang, J.; Xu, S.; Li, W. High shear mixers: A review of typical applications and studies on power draw, flow pattern, energy dissipation and transfer properties. *Chem. Eng. Process. Process Intensif.* **2012**, *57–58*, 25–41, doi:10.1016/j.cep.2012.04.004.
401. Hall, S.; Cooke, M.; El-Hamouz, A.; Kowalski, A.J. Droplet break-up by in-line Silverson rotor-stator mixer. *Chem. Eng. Sci.* **2011**, *66*, 2068–2079, doi:10.1016/j.ces.2011.01.054.
402. Håkansson, A. Rotor-Stator Mixers: From Batch to Continuous Mode of Operation—A Review. *Processes* **2018**, *6*, 32, doi:10.3390/pr6040032.
403. Urban, K.; Wagner, G.; Schaffner, D.; Röglin, D.; Ulrich, J. Rotor-Stator and Disc Systems for Emulsification Processes. *Chem. Eng. Technol.* **2006**, *29*, 24–31, doi:10.1002/ceat.200500304.
404. Błaszczuk, M.M.; Przybysz, Ł. A Method for the Segregation of Emulsion Inner Phase Droplets Using Imbibition Process in Porous Material. *Energies* **2021**, *15*, 110, doi:10.3390/en15010110.
405. Leiva, J.M.; Geffroy, E. Evolution of the size distribution of an emulsion under a simple shear flow. *Fluids* **2018**, *3*, doi:10.3390/fluids3030046.

406. Spicer, P.T.; Pratsinis, S.E. Coagulation and fragmentation: Universal steady-state particle-size distribution. *AIChE J.* **1996**, *42*, 1612–1620, doi:10.1002/aic.690420612.
407. Vanni, M.; Baldi, G. Coagulation efficiency of colloidal particles in shear flow. *Adv. Colloid Interface Sci.* **2002**, *97*, 151–177, doi:10.1016/S0001-8686(01)00050-1.
408. Higashitani, K.; Ogawa, R.; Hosokawa, G.; Matsuno, Y. Kinetic theory of shear coagulation for particles in a viscous fluid. *J. Chem. Eng. Japan* **1982**, *15*, 299–304, doi:10.1252/jcej.15.299.
409. Mazumdar, M.; Jammoria, A.S.; Roy, S. Effective rates of coalescence in oil–water dispersions under constant shear. *Chem. Eng. Sci.* **2017**, *157*, 255–263, doi:10.1016/j.ces.2015.11.037.
410. Fuller, G.T.; Considine, T.; Golding, M.; Matia-Merino, L.; MacGibbon, A.; Gillies, G. Aggregation behavior of partially crystalline oil-in-water emulsions: Part I - Characterization under steady shear. *Food Hydrocoll.* **2015**, *43*, 521–528, doi:10.1016/j.foodhyd.2014.07.032.
411. Mishra, V.; Kresta, S.M.; Masliyah, J.H. Self-preservation of the drop size distribution function and variation in the stability ratio for rapid coalescence of a polydisperse emulsion in a simple shear field. *J. Colloid Interface Sci.* **1998**, *197*, 57–67, doi:10.1006/jcis.1997.5217.
412. Xu, W.; Nikolov, A.; Wasan, D.T. Shear-induced fat particle structure variation and the stability of food emulsions: I. Effects of shear history, shear rate and temperature. *J. Food Eng.* **2005**, *66*, 97–105, doi:10.1016/j.jfoodeng.2004.02.041.
413. Xu, W.; Nikolov, A.; Wasan, D.T. Shear-induced fat particle structure variation and the stability of food emulsions: II. Effects of surfactants, protein, and fat substitutes. *J. Food Eng.* **2005**, *66*, 107–116, doi:10.1016/j.jfoodeng.2004.02.042.
414. Hallez, Y.; Gergianakis, I.; Meireles, M.; Bacchin, P. The continuous modeling of charge-stabilized colloidal suspensions in shear flows. *J. Rheol. (N. Y. N. Y.)* **2016**, *60*, 1317–1329, doi:10.1122/1.4964895.
415. Schroën, K.; van Dinther, A.; Stockmann, R. Particle migration in laminar shear fields: A new basis for large scale separation technology? *Sep. Purif. Technol.* **2017**, *174*, 372–388, doi:10.1016/j.seppur.2016.10.057.
416. Shashi Menon, E. Fluid Flow in Pipes. In *Transmission Pipeline Calculations and Simulations Manual*; Elsevier, 2015; pp. 149–234.
417. Guo, B.; Ghalambor, A. Transportation. In *Natural Gas Engineering Handbook*; Elsevier, 2005; pp. 219–262.
418. LaNasa, P.J.; Upp, E.L. Basic Flow Measurement Laws. In *Fluid Flow Measurement*; Elsevier, 2014; pp. 19–29.
419. Rapp, B.E. Fluids. In *Microfluidics: Modelling, Mechanics and Mathematics*; Elsevier, 2017; pp. 243–263.
420. Chern, C. Shear-induced coagulation kinetics of semibatch seeded emulsion polymerization. *Chem. Eng. Sci.* **1996**, *51*, 1079–1087, doi:10.1016/0009-2509(95)00349-5.

421. Schultz, S.; Wagner, G.; Urban, K.; Ulrich, J. High-pressure homogenization as a process for emulsion formation. *Chem. Eng. Technol.* **2004**, *27*, 361–368, doi:10.1002/ceat.200406111.
422. Tan, H.W.; Misran, M. Stability of concentrated olive oil-in-water emulsion. *Chinese J. Chem.* **2008**, *26*, 1963–1968, doi:10.1002/cjoc.200890351.
423. Wang, L.; Vigil, R.D.; Fox, R.O. CFD simulation of shear-induced aggregation and breakage in turbulent Taylor-Couette flow. *J. Colloid Interface Sci.* **2005**, *285*, 167–178, doi:10.1016/j.jcis.2004.10.075.
424. Gordillo, B.; Ciaccheri, L.; Mignani, A.G.; Gonzalez-Miret, M.L.; Heredia, F.J. Influence of turbidity grade on color and appearance of virgin olive oil. *JAOCs, J. Am. Oil Chem. Soc.* **2011**, *88*, 1317–1327, doi:10.1007/s11746-011-1787-y.
425. Mohammed, T.J.; Abbas, E.R. Turbidity and Oil Removal from Oilfield Produced Water by Coagulation - Flocculation Technique. **2017**, 1–8.
426. Prestigiacomio, A.R.; Effler, S.W.; O'Donnell, D.; Hassett, J.M.; Michalenko, E.M.; Lee, Z.; Weidemann, A. Turbidity and suspended solids levels and loads in a sediment enriched stream: Implications for impacted lotic and lentic ecosystems. *Lake Reserv. Manag.* **2007**, *23*, 231–244, doi:10.1080/07438140709354012.
427. Girgin, E.H.; Do, S.; Gomez, C.O.; Finch, J.A. Bubble size as a function of impeller speed in a self-aeration laboratory flotation cell. *Miner. Eng.* **2006**, *19*, 201–203, doi:10.1016/j.mineng.2005.09.002.
428. Schneider, C.A.; Rasband, W.S.; Eliceiri, K.W. NIH Image to ImageJ: 25 years of image analysis. *Nat. Methods* **2012**, *9*, 671–675, doi:10.1038/nmeth.2089.
429. Li, Y.; Zhu, T.; Liu, Y.; Tian, Y.; Wang, H. Effects of surfactant on bubble hydrodynamic behavior under flotation-related conditions in wastewater. *Water Sci. Technol.* **2012**, *65*, 1060–1066, doi:10.2166/wst.2012.933.
430. Zhou, Z.A. Comment on “Aqueous dispersions of nanobubbles: Generation, properties and features“ by A. Azevedo, R. Etchepare, S. Calgaroto, J. Rubio [Miner. Eng. 94 (2016) 29–37]. *Miner. Eng.* **2018**, *117*, 117–120, doi:10.1016/j.mineng.2017.12.012.
431. Hanotu, J.; Bandulasena, H.C.H.; Chiu, T.Y.; Zimmerman, W.B. Oil emulsion separation with fluidic oscillator generated microbubbles. *Int. J. Multiph. Flow* **2013**, *56*, 119–125, doi:10.1016/j.ijmultiphaseflow.2013.05.012.
432. Chau, K.W. Investigation on effects of aggregate structure in water and wastewater treatment. *Water Sci. Technol.* **2004**, *50*, 119–124, doi:10.2166/wst.2004.0703.
433. Sindhi, Y.; Mehta, M. COD Removal of Different Industrial Wastewater by Fenton Oxidation Process. *Int. J. Eng. Sci. Res. Technol. Technol.* **2014**, *3*, 1134–1139.
434. Langone, M.; Ferrentino, R.; Trombino, G.; Waubert De Puiseau, D.; Andreottola, G.; Rada, E.C.; Ragazzi, M. Application of a novel hydrodynamic cavitation system in wastewater treatment plants. *UPB Sci. Bull. Ser. D Mech. Eng.* **2015**, *77*, 225–234.
435. Rusydi, A.F. Correlation between conductivity and total dissolved solid in various type of water: A review. *IOP Conf. Ser. Earth Environ. Sci.* **2018**, *118*, doi:10.1088/1755-1315/118/1/012019.

436. Joeres, E.; Drusch, S.; Töpfl, S.; Loeffler, M.; Witte, F.; Heinz, V.; Terjung, N. Influence of oil content and droplet size of an oil-in-water emulsion on heat development in an Ohmic heating process. *Innov. Food Sci. Emerg. Technol.* **2021**, *69*, 1–10, doi:10.1016/j.ifset.2021.102638.
437. White, S.B.; Shih, A.J.-M.; Pipe, K.P. Investigation of the electrical conductivity of propylene glycol-based ZnO nanofluids. *Nanoscale Res. Lett.* **2011**, *6*, 346, doi:10.1186/1556-276X-6-346.
438. Marandi, A.; Polikarpus, M.; Jöeleht, A. A new approach for describing the relationship between electrical conductivity and major anion concentration in natural waters. *Appl. Geochemistry* **2013**, *38*, 103–109, doi:10.1016/j.apgeochem.2013.09.003.
439. Grossi, M.; Lecce, G. Di; Toschi, T.G.; Ricco, B. Fast and Accurate Determination of Olive Oil Acidity by Electrochemical Impedance Spectroscopy. *IEEE Sens. J.* **2014**, *14*, 2947–2954, doi:10.1109/JSEN.2014.2321323.
440. Zakinyan, A.R.; Kulgina, L.M.; Zakinyan, A.A.; Turkin, S.D. Electrical Conductivity of Field-Structured Emulsions. *Fluids* **2020**, *5*, 74, doi:10.3390/fluids5020074.
441. Banisi, S.; Finch, J.A.; Laplante, A.R. Electrical conductivity of dispersions: A review. *Miner. Eng.* **1993**, *6*, 369–385, doi:10.1016/0892-6875(93)90016-G.
442. Al-Malah, K.I.; Azzam, M.O.J.; Omari, R.M. Emulsifying properties of BSA in different vegetable oil emulsions using conductivity technique. *Food Hydrocoll.* **2000**, *14*, 485–490, doi:10.1016/S0268-005X(00)00028-X.
443. Zaid, A.M.; Elkanzi, E.M. Detection of hydrocarbon concentration in water using electrical conductivity. *Soc. Pet. Eng. - SPE Heal. Saf. Environ. Oil Gas Explor. Prod. Conf. 1994, HSE 1994* **1994**, 323–327, doi:10.2118/27123-ms.
444. Yan, Y.; Shan, C.; Wang, Y.; Deng, Q. Effects of Oil on Aqueous Foams : Electrical Conductivity of Foamed Emulsions. *ChemPhysChem* **2014**, *15*, 3110–3115, doi:10.1002/cphc.201402219.
445. Liu, F.; Wang, Y.; Li, X.; Zhang, Z.; Dai, X.; Wang, X.; Xin, Y.; Liu, K.; Gao, L.; Du, D.; et al. The phase inversion mechanism of the pH-sensitive reversible invert emulsion from w/o to o/w. *Open Phys.* **2020**, *18*, 380–390, doi:10.1515/phys-2020-0112.
446. Bains, U.; Pal, R. Rheology and catastrophic phase inversion of emulsions in the presence of starch nanoparticles. *ChemEngineering* **2020**, *4*, 1–15, doi:10.3390/chemengineering4040057.
447. Kwon, S.S.; Kong, B.J.; Cho, W.G.; Park, S.N. Formation of stable hydrocarbon oil-in-water nanoemulsions by phase inversion composition method at elevated temperature. *Korean J. Chem. Eng.* **2015**, *32*, 540–546, doi:10.1007/s11814-014-0234-9.
448. Posner, J.D. Properties and electrokinetic behavior of non-dilute colloidal suspensions. *Mech. Res. Commun.* **2009**, *36*, 22–32, doi:10.1016/j.mechrescom.2008.08.008.
449. Meredith, R.E.; Tobias, C.W. Conductivities in Emulsions. *J. Electrochem. Soc.* **1961**, *108*, 286, doi:10.1149/1.2428064.
450. Ali, A.; Akhtar, N. Changes in the characteristics of water-in-oil-based high internal phase emulsion containing Moringa leaves extract at various storage conditions. *Trop. J. Pharm. Res.* **2014**, *13*, 677–682, doi:10.4314/tjpr.v13i5.4.

451. Sze, A.; Erickson, D.; Ren, L.; Li, D. Zeta-potential measurement using the Smoluchowski equation and the slope of the current–time relationship in electroosmotic flow. *J. Colloid Interface Sci.* **2003**, *261*, 402–410, doi:10.1016/S0021-9797(03)00142-5.
452. Dougherty, G.M.; Rose, K.A.; Tok, J.B.H.; Pannu, S.S.; Chuang, F.Y.S.; Sha, M.Y.; Chakarova, G.; Penn, S.G. The zeta potential of surface-functionalized metallic nanorod particles in aqueous solution. *Electrophoresis* **2008**, *29*, 1131–1139, doi:10.1002/elps.200700448.
453. Mirhosseini, H.; Tan, C.P.; Hamid, N.S.A.; Yusof, S. Effect of Arabic gum, xanthan gum and orange oil contents on ζ -potential, conductivity, stability, size index and pH of orange beverage emulsion. *Colloids Surfaces A Physicochem. Eng. Asp.* **2008**, *315*, 47–56, doi:10.1016/j.colsurfa.2007.07.007.
454. Allaire, M.; Wu, H.; Lall, U. National trends in drinking water quality violations. *Proc. Natl. Acad. Sci. U. S. A.* **2018**, *115*, 2078–2083, doi:10.1073/pnas.1719805115.
455. Pourkarimi, Z.; Rezai, B.; Noaparast, M. Effective parameters on generation of nanobubbles by cavitation method for froth flotation applications. *Physicochem. Probl. Miner. Process.* **2017**, *53*, 920–942, doi:10.5277/ppmp170220.
456. Blekas, G.; Tsimidou, M.; Boskou, D. Olive Oil Composition. In *Olive Oil*; AOCS Publishing, 2006.
457. National Center for Biotechnology Information. PubChem Compound Summary for CID 133082064, Fatty acids, olive-oil. Available online: <https://pubchem.ncbi.nlm.nih.gov/compound/133082064>. (accessed on Jul 27, 2022).
458. Hutchings, I.; Shipway, P. Lubricants and lubrication. In *Tribology*; Elsevier, 2017; pp. 79–105.
459. Painmanakul, P.; Sastaravet, P.; Lersjintanakarn, S.; Khaodhiar, S. Effect of bubble hydrodynamic and chemical dosage on treatment of oily wastewater by Induced Air Flotation (IAF) process. *Chem. Eng. Res. Des.* **2010**, *88*, 693–702, doi:10.1016/j.cherd.2009.10.009.
460. Lachin, K.; Le Sauze, N.; Di Miceli Raimondi, N.; Aubin, J.; Gourdon, C.; Cabassud, M. Aggregation and breakup of acrylic latex particles inside millimetric scale reactors. *Chem. Eng. Process. - Process Intensif.* **2017**, *113*, 65–73, doi:10.1016/j.cep.2016.09.021.
461. Bremond, N.; Thiam, A.R.; Bibette, J. Decompressing emulsion droplets favors coalescence. *Phys. Rev. Lett.* **2008**, *100*, 1–4, doi:10.1103/PhysRevLett.100.024501.
462. Dukhin, S.S.; Sjöblom, J.; Wasan, D.T.; Sæther Coalescence coupled with either coagulation or flocculation in dilute emulsions. *Colloids Surfaces A Physicochem. Eng. Asp.* **2001**, *180*, 223–234, doi:10.1016/S0927-7757(00)00696-8.
463. Azzam, M.O.J.; Al-Malah, K.I.; Omari, R.M. Jojoba Oil/Water Emulsions Stabilized by BSA and Egg Proteins: A Study Using Conductivity Technique. *J. Dispers. Sci. Technol.* **2012**, *33*, 1000–1005, doi:10.1080/01932691.2011.590440.
464. Spikes, H. The History and Mechanisms of ZDDP. *Tribol. Lett.* **2004**, *17*, 469–489, doi:10.1023/B:TRIL.0000044495.26882.b5.

465. Azhari, M.A.; Suffian, Q.N.; Nuri, N.R.M. The effect of zinc dialkyldithiophosphate addition to corn oil in suppression of oxidation as enhancement for bio lubricants: A review. *ARNP J. Eng. Appl. Sci.* **2014**, *9*, 1447–1449.
466. Deliyanni, E.A.; Kyzas, G.Z.; Matis, K.A. Various flotation techniques for metal ions removal. *J. Mol. Liq.* **2017**, *225*, 260–264, doi:10.1016/j.molliq.2016.11.069.
467. Hoseinian, F.S.; Irannajad, M.; Nooshabadi, A.J. Ion flotation for removal of Ni(II) and Zn(II) ions from wastewaters. *Int. J. Miner. Process.* **2015**, *143*, 131–137, doi:10.1016/j.minpro.2015.07.006.
468. Jadhav, A.J.; Barigou, M. Bulk Nanobubbles or Not Nanobubbles: That is the Question. *Langmuir* **2020**, *36*, 1699–1708, doi:10.1021/acs.langmuir.9b03532.
469. Parker, W.J.; Monteith, H.D. Stripping of VOC's from dissolved air flotation. *Environ. Prog.* **1996**, *15*, 73–81, doi:10.1002/ep.670150210.
470. Zaleschi, L.; Teodosiu, C.; Cretescu, I.; Rodrigo, M.A. A comparative study of electrocoagulation and chemical coagulation processes applied for wastewater treatment. *Environ. Eng. Manag. J.* **2012**, *11*, 1517–1525, doi:10.30638/eemj.2012.190.
471. Saritha, V.; Karnena, M.K.; Dwarapureddi, B.K. Competence of blended coagulants for surface water treatment. *Appl. Water Sci.* **2020**, *10*, 1–11, doi:10.1007/s13201-019-1108-4.
472. Leroy, P.; Devau, N.; Revil, A.; Bizi, M. Influence of surface conductivity on the apparent zeta potential of amorphous silica nanoparticles. *J. Colloid Interface Sci.* **2013**, *410*, 81–93, doi:10.1016/j.jcis.2013.08.012.
473. Li, X.; Xu, H.; Liu, J.; Zhang, J.; Li, J.; Gui, Z. Cyclonic state micro-bubble flotation column in oil-in-water emulsion separation. *Sep. Purif. Technol.* **2016**, *165*, 101–106, doi:10.1016/j.seppur.2016.01.021.
474. Guerrini, L.; Parenti, A. Stabilization of Extra-Virgin Olive Oil. In *Products from Olive Tree*; InTech, 2016.
475. Cinelli, G.; Cofelice, M.; Venditti, F. Veiled extra virgin olive oils: Role of emulsion, water and antioxidants. *Colloids and Interfaces* **2020**, *4*, doi:10.3390/colloids4030038.
476. Ambrosone, L.; Angelico, R.; Cinelli, G.; Di Lorenzo, V.; Ceglie, A. The role of water in the oxidation process of extra virgin olive oils. *JAACS, J. Am. Oil Chem. Soc.* **2002**, *79*, 577–582, doi:10.1007/s11746-002-0525-3.
477. Palagano, R.; Valli, E.; Tura, M.; Cevoli, C.; Pérez-Camino, M. del C.; Moreda, W.; Bendini, A.; Toschi, T.G. Fatty acid ethyl esters in virgin olive oils: In-House validation of a revised method. *Foods* **2020**, *9*, 1–11, doi:10.3390/foods9070924.
478. El Riachy, M.; Hamade, A.; Ayoub, R.; Dandachi, F.; Chalak, L. Oil content, fatty acid and phenolic profiles of some olive varieties growing in Lebanon. *Front. Nutr.* **2019**, *6*, doi:10.3389/fnut.2019.00094.
479. Popoola, B.; Onilude, A.; Comfort, T. Fatty Acid Methyl Ester Analysis of Olive Oil Degraded by *Pseudomonas fluorescens*. *J. Adv. Microbiol.* **2017**, *2*, 1–7, doi:10.9734/jamb/2017/31239.

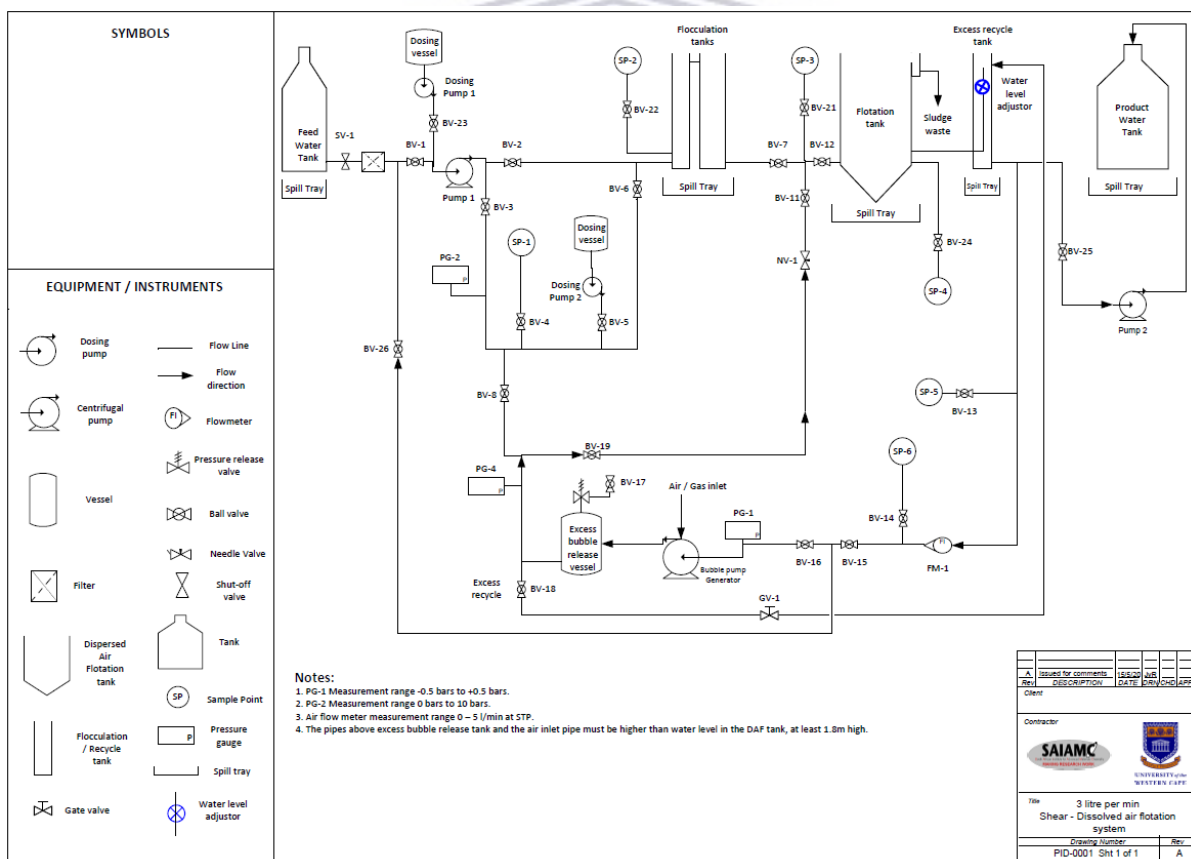
CHAPTER 7 ANNEXURES

A1. DAF shear system description

A 3 L/min hybrid DAF shear wastewater unit was designed, fabricated and commissioned at the UWC campus, to test and treat oily wastewater. The system was designed utilising a conventional DAF treatment unit with the integration of a hydrodynamic shear mixer. Various o/w wastewater sample solutions will be processed to investigate the impact of chemical and physical factors on o/w wastewater emulsions.

The unit, as highlighted in P&ID, **Figure 3.7**, in Section 3.2.7, the DAF shear system consists of two integrated units, a modified DAF treatment unit and a shear unit. The components of a modified DAF treatment unit are presented in the P&ID, **Figure 7.1** below.

Figure 7.1. P&ID, highlighting the components of the modified DAF treatment unit.



The modified DAF treatment unit consists of the following key components and described as the wastewater flows through the system:

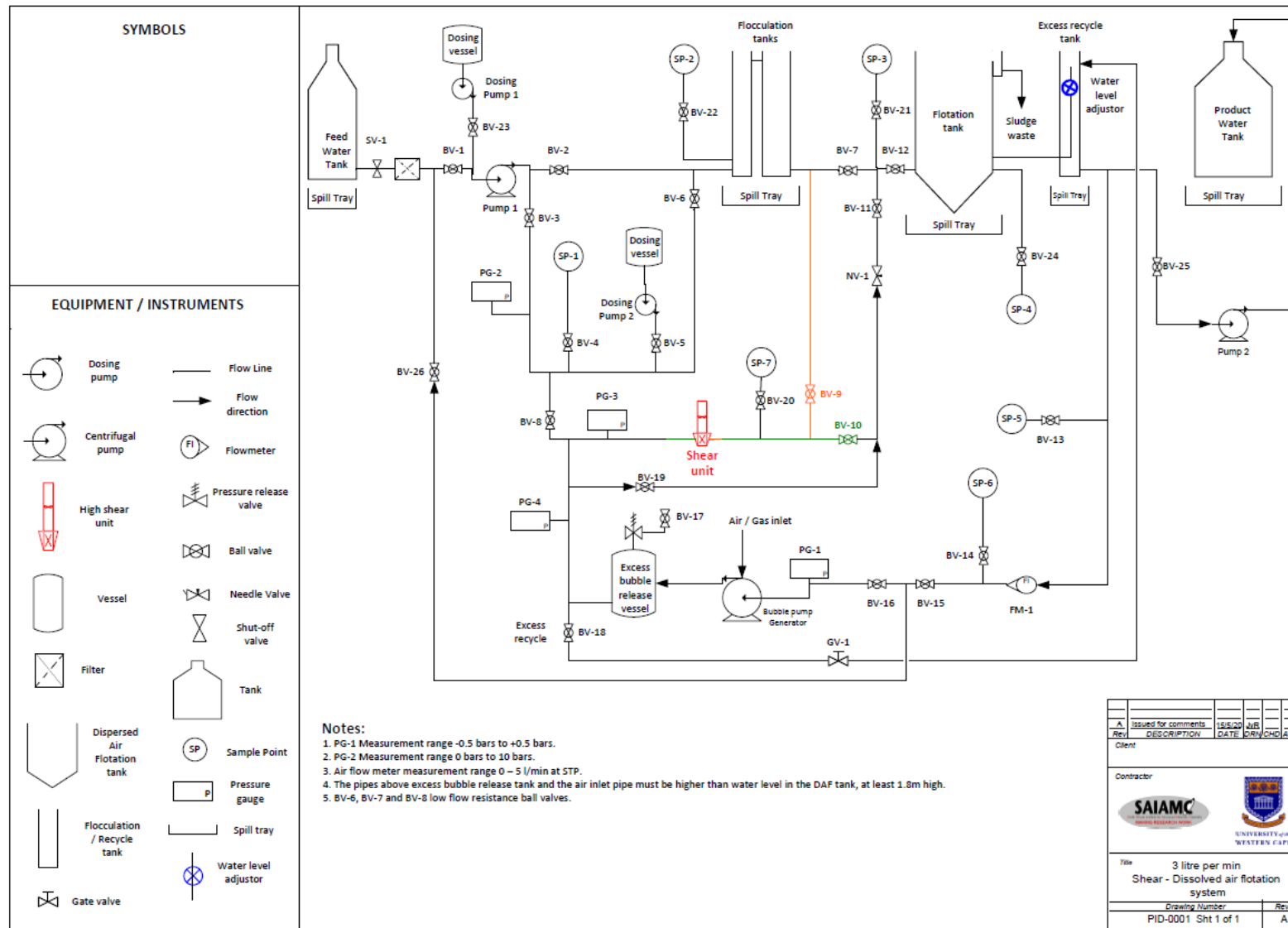
- Feed water tank, to contain the o/w emulsion prior to processing through the unit
- Screen filter, to screen any large particles or material present in the wastewater

- Pumps, to allow for efficient transfer of wastewater through the unit
- Dosing vessels with dosing pumps, to allow for the controlled dosing of chemicals such as coagulants
- Flocculation tanks, to allow for efficient mixing of chemicals downstream of the dosing pumps and to allow for the controlled flow of wastewater
- Flotation tank, to allow for dissolved air, bubbles and wastewater to mix at the contact zone. The flotation tank is also where the processed and separated oil will float to the surface.
- A rectangular DAF flotation tanks was fitted with a mechanical scraper, which removes floated sludge from the water surface.
- Excess recycle tank with water level adjustor, to contain processed water and adjust the water level of the entire system.
- Product water tank, to remove processed water from the system
- Micro-bubble pump, to create pressurised air enriched water and ensures a high efficiency of dissolving air in water (up to 90%) and increase air content of the wastewater. The bubbles are only formed when the pressure is reduced over a valve
- Excess bubble release vessel, the main functions is to release excess air sucked into the pump as large bubbles; and to provide a retention time for proper dissolution of the air into water. ~~to regulate and ensure the pressure of the system does not exceed the design pressures~~
- Needle valve before the DAF flotation tank, to release pressure and allow the air to come out of solution in the form of micro-bubbles before entering the contact zone of the DAF ~~allow for efficient and steady release of bubbles into the flotation tank.~~
- Control panel, to ensure control of the system which included controls for the pumps, the shear unit and the micro-bubble pump
- Drip trays were fabricated and placed
- Pressure gauges, to measure and ensure the system is operating at the safest and optimal parameters
- Flow meters, to measure and ensure the correct flow rate is maintained at various sections of the system
- Low flow resistance ball valves

During wastewater treatment runs, the water was first pre-treated to adjust the pH and then dosed with the appropriate amounts of coagulants. The pre-treated water was then pumped through the flocculation tanks to allow for droplet floc growth. Following the flocculation tanks, the water passed through the DAF unit where air bubbles interacted with the oil droplets to float the flocs which were removed from the surface of the water in the flotation tank DAF unit.

The components of the integrated DAF shear treatment system are presented in the P&ID, **Figure 7.2** below. This system includes the addition of the shear unit and its associated parts are highlighted in red, green and browns in **Figure 7.2**.





Rev	DESCRIPTION	ISSUED DATE	DESIGNED	APP
A	Issued for comments	15/02/20	AB	APP

Client

Contractor

SAIAMC
SPECIALISED INDUSTRIAL AUTOMATION

UNIVERSITY of the WESTERN CAPE

Title: 3 litre per min Shear - Dissolved air flotation system

Drawing Number: PID-0001 Sht 1 of 1

Rev: A

Figure 7.2. P&ID, highlighting the components of the DAF shear integrated treatment unit highlighting the two units.

The DAF shear system with its components allows for the wastewater stream to bypass or include the dosing tanks which allows for the following treatment options:

- DAF with coagulation
- DAF with shear, and
- DAF with coagulation and shear

The system allows for the following wastewater cycles post the DAF unit:

- Recycled back through the floc tanks back to the DAF unit
- Pumped through a micro-bubble pump back to the DAF unit to allow for flocs, which did not form, to be recovered improving wastewater processing
- Pumped through a micro-bubble pump and the high shear mixer back to the DAF unit
- Add wastewater to and remove processed water from the DAF unit

Samples were taken at various points throughout the process to monitor chemical and physical process of the treated wastewater.

A2. DAF shear system start up procedure

- Ensure all ball valves (BV) are in the closed position.
- Connect unit to the power mains, following which the red indicator light will go on.
- Turn the power switch to on at the control panel.
- Turn the emergency switch clock wise and the green indicator light will go on.
- Add coagulant and flocculant chemicals solutions to the dosing vessels as required.
- Open the storage tank shut off valve (SV-1).
- Open ball valves BV-2, BV-4, BV-7, BV-8, BV-13, BV-14.
- Prime pump 1 with water.
- Switch on power to the control unit panel.
- Switch on power to pump 1 and increase the motor speed to under 18Hz.
- Slowly fill up the floc tanks, DAF unit and monitor water level.
- Adjust the water level with the water level adjustor in the excess recycle tank.
- When the floc tanks and flotation tank are filled, close the wastewater feed tank and recycle for approximately ten (10) mins to get constant flow.
- Adjust water level if required by adding water from the feed water tank.

- Continually check system for leaks.
- Samples can be taken through Sample Point 2 (SP-1) by opening BV-5.

Recycle through the bubble pump

- Perform the DAF shear unit start procedure, as described above.
- Once water level in the floc tanks, flotation tank and excess recycle tank are stable, close wastewater feed tank off valve, SV-1.
- Switch off pump 1.
- Close BV-2, BV-4 and BV-7.
- Open needle valve-1 (NV-1), BV-12 and BV-16.
- Prime bubble pump.
- Switch on micro-bubble pump.
- Slowly close BV-12 and adjust pressure at pressure gauge 2 (PG-2), to between 2.5 bar.
- Pressure should not exceed 3.5 bar.
- Adjust NV-1 until small fine milky bubbles are observed in the flotation tank observation window.
- Slowly close BV-12 and adjust pressure at pressure gauge 2 (PG-2), to between 3 bar.
- Let the system recycle through the flotation tank for approximately ten (10) mins to maintain milky small bubbles and constant water flow.
- Samples were taken through SP-2 by opening BV-11.

Recycle through the bubble pump and shear mixer

- Perform the DAF shear unit start procedure, as described above, and recycle through micro-bubble pump.
- Once water levels in the floc tanks, flotation tank and excess recycle tank are stable and small bubbles are observed in the flotation tank, open BV-15, BV-17 and close BV-16.
- Adjust NV-1 until small fine milky bubbles are observed in the DAF observation window.
- Slowly close or open BV-12 and adjust pressure at pressure gauge 2 (PG-2), to between 3 bar.
- Let the system recycle through the flotation tank for approximately five (5) mins to maintain milky small bubbles and constant water flow.
- Switch on shear unit and adjust speed to 10Hz on the control panel.

- Monitor pressure at PG-2.
- Slowly close or open BV-12 to adjust pressure at PG-2 to 3 bar.
- Let the system recycle through the flotation tank for approximately five (5) mins to maintain milky small bubbles and constant water flow.
- Increase or decrease the speed at the shear mixer control and do not exceed 40 Hz on the control panel.

Adding wastewater and removing processed water from the system

- Perform the DAF shear unit start procedure, as described above, and recycle through micro-bubble pump.
- Once water level in the floc tanks, DAF unit and excess recycle tank are stable and small bubbles are observed in the DAF unit, open the wastewater feed tank, BV-2 and BV 7.
- Adjust NV-1 until small fine milky bubbles are observed in the DAF observation window.
- Slowly close or open BV-12 and adjust pressure at pressure gauge 2 (PG-2), to between 3.5 and 5 bar.
- Monitor pressure at PG-2.
- Open BV-10.
- Prime pump 1 with water.
- Switch on pump 1 and slowly increase the motor speed to 22Hz.
- Switch on pump 2 and slowly increase the speed to 15Hz.
- Adjust speed of pump 1 and pump 2 to get a constant flow of water through the unit and in and out of the unit.
- Monitor water level on the floc tanks, DAF and excess recycle tank.

The water level in the unit was adjusted through slipping a tight-fitting sleeve over the pipe in the excess recycle tank, which can be moved up or down to adjust the water level of the system. This was only done during the initial run and then the level remained constant.

There are two mechanical protections built into the system, which included:

- A cover over the moving parts of the shear mixer, and
- A pressure release valve set to 3.5 bar

A3. DAF unit emergency shut down procedure

In order to ensure a safe operating environment a shutdown procedure was developed to assist the operator if the unit operates in potentially dangerous state and operating conditions. The procedure is presented in Table 7.1 below.

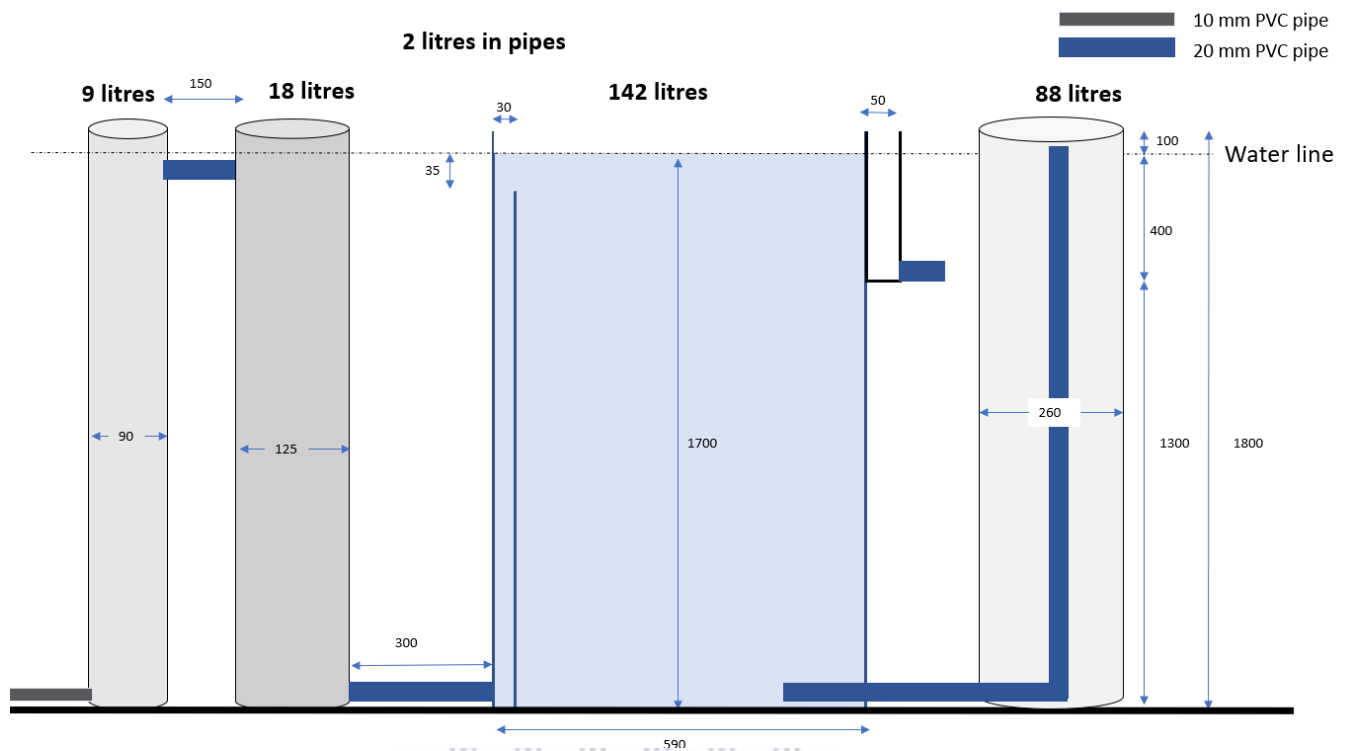
Table 7.1. DAF unit emergency shut down procedure.

TYPE OF EMERGENCY	OBSERVATION	Action
High wastewater levels	Water overflowing in the floc tanks	<ul style="list-style-type: none"> • Switch off pump 1 or reduce pump speed to below 10Hz. • Close feed water tank shut off valve, SV-1.
	Water overflowing in the DAF unit	<ul style="list-style-type: none"> • Switch off pump 1 or reduce pump speed to below 10Hz at the control panel. • Close feed water tank • Adjust water level at the water level adjuster inside the excess recycle tank.
	Water overflowing at the excess recycle tank	<ul style="list-style-type: none"> • Switch off pump 1 or reduce pump speed to below 10Hz at the control panel. • Close feed water tank • Adjust water level at the water level adjuster inside the excess recycle tank. • Open BV-9 to lower water level • Switch on Pump 2 and pump excess water to product tank.
Water leaks	Water leaks at pipes, tanks valves or pumps	<ul style="list-style-type: none"> • Switch off system immediately, with the emergency shut off switch on the control panel.
High wastewater flow rates	Water overflowing in the floc tanks	<ul style="list-style-type: none"> • Switch off pump 1 or reduce pump speed to below 10Hz at the control panel. • Close feed water tank shut off valve, SV-1.
	Water overflowing in the DAF unit	<ul style="list-style-type: none"> • Switch off pump 1 or reduce pump speed to below 10Hz.

		<ul style="list-style-type: none"> • Close feed water tank shut off valve, SV-1 • Adjust water level at the water level adjuster inside the excess recycle tank.
High pressure readings	High pressures of above 3.5 bar	<ul style="list-style-type: none"> • Release pressure through opening BV-12 or NV-1.
	High pressures of above 3.5 bar	<ul style="list-style-type: none"> • Release pressure through opening BV-12 or NV-1. • Switch off micro-bubble pump. • Switch off pump 1 at the control panel. • Switch off system at the control panel and check for blockages throughout the system.



B. DAF shear system tank sizes and volumes



Dimensioned side view of a scale model of the flocculation tanks, flotation tank and the excess recycle tank.

